Atomic negative-ion resonances

Stephen J. Buckman

Electron Physics Group, Research School of Physical Sciences and Engineering, Institute of Advanced Studies, The Australian National University, Canberra ACT 2601, Australia

Charles W. Clark

U. S. Department of Commerce, Technology Administration, National Institute of Standards and Technology, Electron and Optical Physics Division, Gaithersburg, Maryland 20899

The authors attempt to give a comprehensive discussion of observations of atomic negative-ion resonances throughout the periodic table. A review of experimental and theoretical approaches to the study of negative-ion resonances is given together with a consideration of the various schemes that are used for their classification. In addition to providing, where possible, tabulated data for the energies, widths, and symmetries of these states, the authors also attempt to highlight regularities in their behavior both within groups of the periodic table and along isoionic sequences.

CONTENTS

I. INTRODUCTION

A. Background and goals

Twenty years ago, two classic articles by George Schulz (1973a, 1973b) appeared in this journal. The sub-

 0034-6861/94/66(2)/539(117)/$16.70

ject of the first, "Resonances in electron impact on atoms," is really the same as that of the present paper, but the difference in the titles reflects the evolution of the field in the intervening years.

Up to 1973, the principal means of studying negative-ion resonances—a term denoting states in which an electron and a neutral atom are associated transiently—was by electron-atom collision processes. Since then, several alternative techniques have emerged, such as laser photodetachment spectroscopy and negative-ion–atom collisions, which yield complementary information on these states. There have also been substantial advances in experimental work on electron-atom scattering itself, which include, for instance, the development of polarized electron sources and parallel detection methods. The scope of theoretical work has expanded greatly, not only through the deployment of more powerful computational techniques—for example, the R-matrix, variational, and coordinate rotation methods—but also via the advent of new descriptive and taxonomical tools such as the hyperspherical and group-theoretic approaches.

Most of these, and other related topics, have been reviewed separately in articles to which we refer below. What has motivated us to take on the rather daunting job of updating Schulz's encyclopedic article is another, more gradual development that has been occurring in all branches of atomic physics. This is the ever-increasing number of confrontations with systems that cannot be well understood in terms of the standard independent-particle, central-field model of atomic structure and collisions. These have created a demand for alternative descriptions, in which the correlation of electronic motions can be represented in a convenient way. The need for such descriptions arises generally in the interpretation of multiple excitation phenomena, whether involving laser-atom interaction at high intensities, excitation of subvalence electrons, or multicharged ion-atom collisions. It is well known that negative ions are extremely sensitive to electron correlation effects. Thus a comprehensive understanding of negative-ion spectra may serve both to delimit the domain of applicability of the independent-electron picture and to aid the development of a more general understanding of correlated systems.

Indeed, there has recently been quite substantial progress in describing the motion of *two* electrons in a central field in terms of quantum numbers appropriate to the *pair* rather than to the individual electrons (e.g., Rau, 1983; Feagin and Macek, 1984; Klar, 1986a, 1986b; Rost and Briggs, 1991). It is possible that such treatments could unify the description of doubly excited states to the same degree that quantum-defect theory has done for singly excited states. The doubly excited states that are most effectively treated by these approaches are of a type which occur prominently as negative-ion resonances. Thus the existing experimental and computational data on resonances provide a natural basis for delineating the range of validity of new theoretical concepts in application to real atomic systems.

We have also written this article in the hope that it can serve as a central reference source of critically evaluated data on atomic negative-ion resonance properties. This is a function that, to our knowledge, is still performed only by Schulz's article. Accordingly, our review of theoretical and experimental techniques is intended primarily to summarize advances that have taken place since 1973, and especially with a view as to how they have increased the quality or comprehensiveness of experimental data. More detailed accounts of particular experimental and theoretical approaches can be found in the review articles cited in Sec. I.B.

To aid in the attainment of these two goals, we have developed a more or less uniform nomenclature for resonance states, which is based on the now widely accepted terminology for noble-gas resonances introduced by Brunt *et al.* (1976). It may seem presumptuous for us to assign names to things discovered by others, but it really is necessary to do so in cases where the same states, or several among a group of obviously related states, have been investigated by wholly different methods. We must also plead that there are only a few cases in which we have supplanted an ancient and illustrious title. There are some regularities in autodetaching spectra that seem to us to be indisputable, though their origins and implications may be still controversial. This is the reason for our assigning simple names (e.g., a_1, a_2, b_1, etc.) without hidden connotations. On the other hand, we have invested some effort in classifying resonance states in the usual terminology of atomic spectroscopy. There are few measurements that give unambiguous information on the angular momentum and parity of resonance states, and, of course, any more specific identification of a state (e.g., by electronic configuration) must be based on some theoretical model. The body of theoretical calculations, in many different approximations, that has developed over the past two decades provides a basis for confidence in many assignments, in the sense that they correctly identify the dominant configuration of the many-electron wave function. There remains a number of cases in which no theoretical consensus nor observed systematic behavior provides a clear guideline for assignment of configuration; in these instances we mention the most plausible alternatives. Other classification schemes, based on hyperspherical and group-theoretic descriptions of the motion of two electrons in a Coulomb field, are used when appropriate. One of the intellectual challenges of the study of negative-ion resonances is to meld the description of an excited electron pair, in terms of novel quantum numbers, to that of the ion core, which usually is adequately approximated by a single independent-electron configuration.

One respect in which we do not attempt to supplement Schulz's review is in the discussion of developments up to 1973. We do not discuss in detail any work that was reviewed by Schulz, unless necessary to establish a context for understanding subsequent developments. Much

pioneering work therefore goes unmentioned here, and, to attain an accurate historical perspective, one must still read Schulz's article in conjunction with our own. If broadened to include the autoionizing states of neutral atoms and positive ions, the study of resonances has had a pronounced impact on the evolution of atomic physics during the past 30 years, and its influence can be detected in the work of almost every research group in the field. It would provide a plausible unifying theme for a prospective intellectual historian of modern atomic physics.

This article proceeds as follows. We first review the basic theoretical and experimental framework for the study of atomic negative-ion resonances. We then discuss their application to specific elements in an order which approximates the completeness of understanding. These discussions include tables of "recommended" energies and lifetimes of specific resonant states, which we have derived for the most part from the experimental literature. There are instances in which no experimental information is available, and the recommended values are those obtained from theory. While this situation is not ideal, we have preferred to list such efforts rather than leave the entry blank. Finally, we review some correspondences that can be made between analogous resonances along rows and columns of the periodic table.

As a final note to this Introduction, we would like to point out that the sequel to Schulz's other (1973b) article, "Resonances in electron impact on diatomic molecules," still remains to be written (and not by us). The degree of current interest in this subject is indicated by the recent appearance of a review article in this journal on the role of resonances in molecules adsorbed on surfaces (Palmer and Rous, 1992). The relative growth in experimental and theoretical studies of electron-molecule interactions during the past 19 years indeed probably exceeds that of electron-atom processes. However, the difficulty of presenting a coherent picture of developments at the frontiers of the field is probably no greater now than it was then. Schulz's two papers are an enduring testimony of his unique grasp of atomic and molecular physics, which our present work hopes to emulate, but does not pretend to duplicate.

B. Recent review articles in related areas

Since the Schulz reviews of 1973, there have been many publications of a general nature on the subject of atomic negative-ion resonances, although none of these have involved a systematic study of resonances throughout the periodic table. In many cases they represent published invited conference contributions and, as such, are usually limited to a broad overview or to a discussion of recent, topical experimental and/or theoretical progress. Nonetheless, we have found these articles to be of immense benefit in constructing this paper and have used all of them as reliable, comprehensive sources of reference material, for which we express our gratitude to the individuals responsible.

We have listed separately under the Reference section some papers published since the Schulz review that might be described as "review articles." We strongly recommend that these articles be read in conjunction with the present, as in many cases they contain considerably more detail for specific topics.

A resonance is no more than an excited state of a negative ion, and it does not make sense to try to describe it in isolation from the rest of the spectrum of the system—in particular, the ground state and metastable excited states. Comprehensive reviews have been given elsewhere of ground states (Hotop and Lineberger, 1975, 1985) and metastable excited states (Bunge *et al.*, 1982; Nicolaides *et al.*, 1989) of negative ions. When necessary, we use information from these reviews and the original literature whence they were derived, but we have made no attempt to critically evaluate data for states other than resonances.

II. THEORETICAL FRAMEWORK

A. Overview

The properties of negative-ion resonances are, for the most part, governed by electron correlation phenomena.

Contrast, for example, the elementary description of doubly excited states of a neutral atom (or positive ion) with that of a negative ion. If we begin with a simple independent-electron configuration with the label $X^{q+}nln'l'$, where X^{q+} is a positively charged ion core, then there is a clear distinction between $q=1$ (a negative ion) and $q \geq 2$. For $q \geq 2$, the outermost of the two external electrons ($n'l'$) sees a positively charged ion core, and its motion will tend to be dominated by the long-range Coulomb interaction. Thus, in the absence of electron correlation, an infinite number of resonances will occur, which are Rydberg states converging on the limit $X^{q+}nl$. Although effects of electron correlation are of great significance in the quantitative study of doubly excited states of neutrals and positive ions, the independent-electron picture gives a reasonable zeroth-order description and has provided the most widely used interpretive frameworks (configuration interaction, quantum-defect theory). We must generally expect to see long series of doubly excited states in these systems, which are essentially Rydberg in character.

For $q=1$, on the other hand, the innermost electron effectively screens the ionic charge, so the outer electron moves in a potential that can support only a finite number of bound states (unless the residual atom can maintain a permanent electric dipole moment due to l degeneracy, as for the case of H^-); and, indeed, the dominant contributions to that potential (e.g., the polarizability of the residual atom) derive from electron correlations. There is no long-range Coulomb field to support Rydberg series of the same character as for $q \geq 2$. The long series of resonances observed in negative ions, most prominent-

ly in hydrogen and the inert gases (see, e.g., Fig. 18), must thus derive from an alternative mechanism. They necessarily involve two electrons moving at large distances from the residual ion, and it must be assumed that the electrons are correlated in some specific fashion. In particular, a configuration in which the two electrons are on opposite sides of and comparable distances from the ion (the "Wannier ridge" configuration) gives rise to a long-range Coulomb field that might support a Rydberg-like series of resonances. This mechanism was proposed by Fano (1980) and was widely adopted as an interpretive framework for the observations that followed it (Buckman *et al.*, 1983a). However, recent theoretical work (Richter and Wintgen, 1990; Ezra *et al.*, 1991) suggests that an alternative electronic configuration is more plausible; these results are discussed in Sec. II.E.

1. Idealizations: parent, grandparent, shape, and Feshbach resonances

The distinction between the multiply excited states of neutrals and negative ions is reflected in the existence of two broad classification schemes for resonances, the "parent" and "grandparent" models, a terminology introduced by Schulz (1973a). In the parent model, the $X^{q+}\ nln'l'$ resonance is viewed in terms of an $n'l'$ electron bound to a $X^{q+}\ nl$ parent state; this is an appropriate description of, e.g., the $2p^5 3sns$ resonances observed in photoabsorption by Na $2p^6 3s$. In the grandparent model, on the other hand, $X^{q+}\ nln'l'$ is described as an $(nln'l')\alpha$ electron pair bound to the X^{q+} parent state, where α denotes a set of quantum numbers that specify the two-electron coupling. This turns out to be the appropriate description, for example, for many of the $2p^5 nln'l'$ resonances observed in electron scattering by Ne. In light of the remarks of the previous paragraph, the grandparent model is the more appropriate framework within which to view the Wannier ridge resonances.

A division of classifications of wider use in physics is that made between "shape" and "Feshbach" resonances. The classical description of a shape resonance in scattering depicts the projectile tunneling through a potential barrier, remaining confined within the barrier for the lifetime of the resonance, and tunneling out again. The mechanism for a Feshbach resonance involves the capture of the projectile via deposition of its energy into some internal degree of freedom of the target, and its release when it reacquires enough energy to escape. In electron scattering by an N-electron atom, the principal distinction between these two types is that a shape resonance can be produced by the barrier structure formed by the repulsive centrifugal potential and the attractive atomic mean field; such a barrier is essentially a property of the unperturbed target atom. A Feshbach resonance, in contrast, is an excited state of a distinct $N+1$-electron complex, the negative ion, with its own dynamics, distinct from those of the target. Feshbach resonances observed thus far in electron-atom collisions appear to fall into the two categories identified by Taylor (1970): one, in which an incident electron is bound to an excited state of the target; the other, in which it is trapped in a potential barrier associated with an excited state. Despite expectations that resonances might be seen in electron-atom scattering that would be similar to the compound-nucleus resonances of nuclear physics (Herzenberg, 1988), there are no cases known to date in which an electron incident upon a target atom is captured by sharing its energy with a large number of target electrons, even at high collision energies.

All these classifications are idealizations, and it is not surprising to find that they are of mixed utility in practice. Although an atomic mean field may yield a barrier structure that can support a shape resonance, the resonance energy and width may depend sensitively on correlated interaction of the electron and the target. Conversely, a Feshbach resonance may derive from a simple potential barrier structure provided by an excited state of the target, and would be manifested as a shape resonance in an experiment on electron scattering by that excited state. It is our view that, of these two general schemes, classification by parentage is of greater utility in understanding atomic negative-ion resonances than is the shape/Feshbach distinction. For example, one prominent family of resonances, which we discuss in detail later, the b states, is well characterized by the grandparent scheme, but its members can appear as either shape or Feshbach resonances in different elements (see Sec. VI.B). In such a case we feel it is more useful to identify the basic symmetry and underlying dynamics of the negative-ion complex than to focus on its relationship to the spectrum of the target.

To date, all atomic negative-ion resonances that have been analyzed in depth have been described in terms of a complex of, at most, three excited electrons outside a tightly bound residual ion core (or, in a few cases, like $O^-\ 2s2p^6$, as core-excited states). A variety of classification schemes for states of two highly excited electrons have been developed (see, e.g., Lin, 1986); some limited work has been done towards categorizing triply excited states (van der Burgt and Heidemann, 1985; van der Burgt *et al.*, 1986; Watanabe and Lin, 1987; Komninos *et al.*, 1988), but this subject is in a fairly rudimentary state.

2. Practical approaches to the characterization of resonances

There are two more or less independent, though interacting, directions taken by theoretical analyses of atomic negative-ion resonance phenomena: one predominantly computational, the other predominantly modelistic.

On the computational side, a good deal of effort has been directed during the past two decades towards the development of general methods for the calculation of

atomic structure and collision phenomena, based on approximate numerical solution of the many-electron Schrödinger equation. Most such efforts have been applied primarily to calculating energy levels and photoionization of neutral atoms and positive ions, or electron collisions with positive ions, but they have yielded significant information on negative-ion resonances in simple systems. Nicolaides (1972) distinguished three principal approaches to resonance computation: (a) computation of the wave functions of continuum states, from which resonance parameters are inferred via the analysis of scattering matrices or eigenphase shifts; (b) direct calculation of complex energies of decaying states, by treating the resonance as an eigenfunction of a non-Hermitian system; (c) computations that treat resonances more or less like ordinary bound states and neglect interactions with the continuum as a first approximation. Despite significant theoretical developments and expansion of the scope of many-electron calculations, this distinction remains appropriate.

The main progress made in the first of these approaches has been due to implementation of general electron collision methods, such as the R-matrix, close-coupling, random-phase, and many-body perturbation-theory approximations, though there are some applications in which the specific nature of negative-ion resonances has played a key role, such as eigenchannel analysis and effective-range description of photodetachment. These methods are capable, in principle, of describing all observable phenomena, such as differential angular and partial excitation cross sections, and their principal mode of comparison with experimental data is in reference to such observables. By and large, the only spectroscopic information on the character of resonances that emerges from such calculations concerns their angular momenta and parity, so that it is possible, for example, to identify an Ar^- resonance as having $^2F^\circ$ symmetry, but not to attribute it unambiguously to either $3p^5 4s 3d$ or $3p^5 4p^2$ configurations. This should not be viewed as a deficiency of the collisional approach, since spectroscopic assignments are attempts to account for phenomena within the framework of a restrictive model, which may be inadequate in application to complex systems. Nevertheless, spectroscopic assignment is a major focus of this paper, since it has been found to provide a useful taxonomy for relating resonances in different systems and for understanding propensity rules for the channels of excitation and decay.

The second general computational approach, direct calculation of resonance parameters, casts the problem into a form where only square-integrable wave functions are determined, and which therefore leads immediately to spectroscopic assignments analogous to those applied to bound states. The most widely used such approach during the past decade has involved the application of a complex-coordinate rotation to the many-electron Hamiltonian, which is then treated by (more or less) conventional electronic structure methods. In this review we shall emphasize the direct computation of resonances by this approach and by the third method described in the following paragraph. This is not because they represent a viewpoint that is more useful or important than those of the collisional approaches, but rather because they are more specifically tied to the analysis of resonance phenomena.

The third approach consists of *ad hoc* calculations of resonances, which do not incorporate any mechanisms for interacting with continuum channels. Such calculations represent resonance states by diagonalizing the Hamiltonian in a finite basis of N-electron configuration-state functions constructed from square-integrable orbitals; such a basis may be chosen more or less arbitrarily or may be optimized, for example, by solving the multiconfiguration Hartree-Fock equations. The basis is always constructed so as to exclude functions that could mimic continuum states, thereby imposing a somewhat imprecisely defined form of projection operator. Despite its unsure theoretical foundations, this class of methods has been quite successful in determining resonance energies. It should be noted that the resonances of highest "visibility" in experiments tend to be those that are relatively long-lived, reflecting weak interactions with the continuum. In such cases we are entitled to hope that the interaction of the resonance with any reasonable approximation to the physical continuum would not have dramatic effects; and so the exclusion of continuum interaction by approximate methods should not lead to major qualitative errors.

The second general class of theoretical approaches involves the development of general dynamical models that may not necessarily facilitate quantitative calculations. Examples are the group-theoretic description of doubly excited states (Ezra and Berry, 1982, 1983a, 1983b, and references therein; Herrick, 1983, and references therein; Makarewicz, 1989; Dimitrieva and Plindov, 1990; de Prunelé, 1991), the generalized Wannier theory (Rau, 1983; Feagin, 1984; Feagin and Macek, 1984; Fano and Rau, 1986), the identification of special classes of classical orbits (Klar, 1986a, 1986b, 1987a, 1987b) various adiabatic methods such as the hyperspherical expansion (Fano, 1983a, 1983b), and the quasimolecular picture (Rost and Briggs, 1991). All these approaches are the outgrowth of observations of suggestive patterns in resonance spectra, which do not appear to derive naturally from the independent-particle model, and whose origins therefore might be revealed by the identification of an appropriate system of collective coordinates. Of the above-mentioned methods, the group-theoretic and Wannier models are devised to describe only certain classes of resonances and do not provide a platform for systematic quantitative improvement of approximate calculations. They have nevertheless been of key importance and, in particular, have led to a classification scheme for two-electron resonances that has been widely adopted (see Sec. II.F). The adiabatic methods, on the other hand, do offer a framework within which calculations can be im-

proved in a systematic fashion. However, this has actually been done in relatively few cases. In its earliest implementations, the hyperspherical method did not offer impressive quantitative accuracy and was not competitive with standard computational methods for calculating low-lying resonances. However, it did provide useful qualitative insights, and technical advances now seem to have made it a powerful quantitative technique for calculating high-lying doubly excited states. These methods all deal with states in which two electrons move in the field of a frozen residual ion core, usually a bare proton or a closed shell (the hyperspherical representation can be generalized to the description of any number of electrons, but to date has had limited application in this respect).

B. Computational approaches

Methods for *ab initio* calculations of properties of negative-ion resonances for the most part involve approximate solution of the nonrelativistic, many-electron Schrödinger equation. As such, they do not differ in a fundamental way from the methods employed generally in the theory of atomic structure and collisions. However, the computational description of a negative-ion resonance is usually more difficult in practice than is that of a corresponding state of a neutral atom or positive ion. Specific manifestations of these difficulties will be discussed below; their common origin lies in the fact that resonances are weakly bound (or low-energy shape resonances) with respect to some parent state, and so they are described by diffuse orbitals. With any method there is thus the problem of representing a wave function over large regions of configuration space. Thus, although the spectra of noble-gas negative-ion resonances have been studied extensively in a variety of experiments, we are unaware of any calculations of resonances above the second excited configuration of the neutral atom; the same observation applies to most other species.

We deal first with methods that describe electron-atom scattering, in which resonances appear as incidental phenomena, and then discuss methods that are specifically targeted at determining resonance parameters.

1. Computations of electron-atom scattering

An ideal resonance in a single channel manifests itself in scattering through a phase shift of the form

$$\delta_r = \tan^{-1}\left[\frac{\Gamma}{2(E_0 - E)}\right], \tag{1}$$

where $E_0 - i\Gamma/2$ is the complex energy of the resonance. The phase shift increases by π as the collision energy increases through E_0. This result comes from the assumption that all energy dependence of the S matrix derives from the presence of a single pole at the complex energy of the resonance. In practice, allowance is usually made for a smoothly varying background energy dependence, and resonance parameters are determined by a fit of computed phases to a form $\delta = \delta_0 + \delta_r$, where δ_0 is a simple polynomial function of the energy (see, e.g., Fig. 1 of Ojha *et al.*, 1982).

However, this ideal is often not closely approached in practice. Most negative-ion resonances occur in regions where more than one channel is open. In addition, they are often found near thresholds, which impose their own constraints upon the permissible behavior of phase shifts.

A generalization of Eq. (1) to multichannel scattering, under similar basic presumptions (an isolated resonance, far from thresholds), has been given by Hazi (1979), who showed that the *eigenphase sum* behaves in a manner analogous to that of the single-channel resonance phase shift:

$$\Delta = \sum_i \delta_i = \Delta^\circ + \tan^{-1}\left[\frac{\Gamma}{2(E_0 - E)}\right], \tag{2}$$

where the sum runs over all open channels, δ_i are the eigenphases of the S matrix, and Δ° is a smoothly varying background contribution. The individual eigenphases are given by $\delta_j = \ln(s_j)/2i$, where s_j is the jth eigenvalue of S; the eigenphase sum can be found more directly via $\Delta = \ln[\det(S)]/2i$. An alternative has been given by Macek (1970). This result is widely used to characterize resonances in electron-molecule scattering, where multichannel shape-type resonances are frequently encountered, but it tends to be employed only in a qualitative fashion in the interpretation of atomic negative-ion resonances (see, e.g., Scott *et al.*, 1984b), where additional complexities are introduced by excitation thresholds. In cases where only a few channels are open, specific information on the nature of resonances can be gleaned from analysis of individual eigenphases. We discuss this issue in Sec. VI.B.

We examine the effect of a threshold in the context of a simple example, single-channel scattering of the partial wave l by a short-range potential. At threshold, $E = 0$, the radial wave function $f_l(r)$ at large distances r must take the form

$$f_l(r) \to a r^l + r^{-(l+1)}, \tag{3}$$

where a is a constant determined by the potential. Away from threshold, however, $f_l(r)$ is given by

$$f_l(r) = \cos(\delta) j_l(kr) - \sin(\delta) y_l(kr); \tag{4}$$

in order for Eqs. (3) and (4) to be consistent, we must have

$$k^{2l+1}\cot(\delta) \to \text{const as } E \to 0.$$

A deeper analysis shows that, under fairly general conditions, $k^{2l+1}\cot(\delta)$ must be analytic in E near threshold (Blatt and Jackson, 1949; this is drastically modified when a long-range potential of any sort is present). The suppression of the phase shift forced by the presence of a threshold will usually retard its growth through the full π

radians specified by Eq. (1). An example of this is shown in Fig. 1(a), which depicts d-wave electron scattering by Ar, as computed in the continuum Hartree-Fock approximation. There is a resonance in this channel, with a complex energy of $0.41-i0.31$ a.u. Such a resonance is also present when correlation effects are included via the random-phase approximation (see Amusia and Cherepkov, 1975). Its complex energy can be inferred from fitting [Fig. 1(b)] the computed phase shifts to the appropriate low-energy expansion based on Eq. (4) and using these parameters to solve (numerically) for the resonance condition $\cot(\delta)=i$. This type of behavior is often encountered in low-energy shape resonances, such as the b states of the alkalis and alkaline earths. Formalisms for characterizing multichannel resonances in the vicinity of thresholds have been developed by Nesbet (1980a, 1980b) and by Bae and Peterson (1985, 1986) and have been applied, respectively, to the description of electron scattering by He and various photodetachment pheneomena.

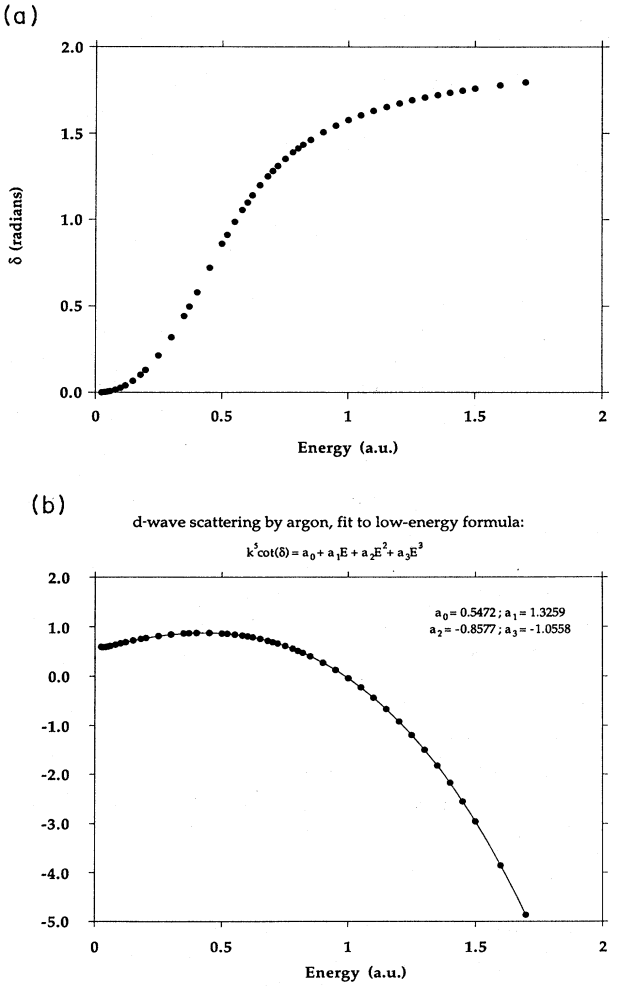

FIG. 1. Behavior of the d-wave phase shift for electron scattering by argon: (a) characteristic low-energy shape resonance behavior (continuum Hartree-Fock approximation, present work); (b) fit of the phase shift of (a) to the Blatt-Jackson formula.

A variety of approximations have revealed resonances in electron-atom scattering that are relevant to this paper. We defer detailed discussion of their results to the sections describing the specific elements to which they have been applied, but comment briefly on the principal methods, roughly in order of their complexity.

Single-channel approximations. These describe the collision in terms of an electron moving in the field of a fixed atomic target state. Thus they are capable of yielding only shape-type resonances, i.e., those that can be produced by a one-electron effective potential, and cannot give any account of inelastic processes. A variety of forms for the electron-target interaction have been employed; the best, from a fundamental point of view, account for exchange symmetry at the Hartree-Fock or Dirac-Fock level and represent the effects of target polarizability through an *ad hoc* polarization potential. These methods have had reasonable success in reproducing low-energy shape resonances in the alkalis and alkaline earths. We use examples from one such method, the continuum Hartree-Fock approximation, for illustrative purposes in various parts of this paper, since we think it is useful to know whether a resonance is found within a simple self-consistent-field description. The implementation of these methods is not a very challenging task by modern standards of computation, and they should be viewed as a special case of the close-coupling approximation described next. Some relevant examples of this general approach can be found in Robinson (1969), Hunt and Moiseiwitsch (1970), Bui and Stauffer (1975), Walker (1975), Bui (1977), Rescigno, McCurdy, and Orel (1978), Sin Fai Lam (1980, 1981), Kurtz and Jordan (1981), and Yuan and Zhang (1989).

Close-coupling approximation. In this class of methods the wave function of the $N+1$ electron system is expanded as

$$\Psi(\mathbf{r}_1,\mathbf{r}_2,\ldots,\mathbf{r}_{N+1})=\mathcal{A}\sum_k \Phi_k(\mathbf{r}_1,\mathbf{r}_2,\ldots,\mathbf{r}_N)f_k(\mathbf{r}_{N+1}) , \quad (5)$$

where the index k labels a set of fixed eigenstates Φ_k of the N-electron target, $\mathcal{A}$ is an operator that effects appropriate antisymmetrization of the $N+1$ electron wave functions, and the f_k are scattering orbitals to be determined. The eigenstates Φ_k are usually approximated by Hartree-Fock or configuration-interaction wave functions; about 20 such states have been included in the largest calculations yet reported, but most of the results reviewed here were obtained with two to four target states in the expansion. Integro-differential equations for the f_k are obtained by requiring that $\langle\Psi|H-E|\Psi\rangle$ be stationary with respect to variations of all f_k, where H is usually the nonrelativistic many-electron Hamiltonian, occasionally supplemented by relativistic corrections or potentials that represent core polarization, and E is the total collision energy. This approach goes beyond the single-channel approximation by accounting for correla-

tion between electron and target to some extent and by allowing for inelastic processes. It has been very successful in describing low-energy electron scattering by the alkalis. Much of the early theoretical work reviewed by Schulz (1973a), particularly on H^- resonances, was done in the close-coupling approximation. Some examples of work reviewed in this paper are those of Norcross and collaborators (Moores and Norcross, 1972, 1974, and numerous other references up to Taylor and Norcross, 1986), Rountree and Henry (1972), Ormonde *et al.* (1973), and Le Dourneuf (1976).

The R-matrix method. This is among the most widely used methods for computation of atomic collision phenomena, due to its intensive development and application at the Queen's University of Belfast over the past two decades; during the past five years or so, it has also become the principal vehicle of a major program for computing stellar opacities (Berrington *et al.*, 1987). It is based on enclosing the $N+1$ electron system within a sphere of radius r_0 and imposing a fixed logarithmic derivative boundary condition on the wave functions on its surface. The many-electron Hamiltonian is diagonalized within the sphere using standard configuration-interaction techniques. Only one electron is allowed to move in the region $r > r_0$. The wave function in that region takes the form of Eq. (5) and is determined by close-coupling equations of motion and a boundary condition at $r = r_0$ that is determined by the eigenfunctions within the sphere. This allows for a much more flexible representation of the wave function than can be provided by the close-coupling expansion, which is restricted to a few states of the target atom. This approach has been highly developed by Burke and collaborators and applied by them to numerous elements, which are discussed in Sec. IV. One respect in which R-matrix calculations of negative-ion resonances differ from those of neutrals and positive ions is that the magnitude of r_0 can be significantly larger in order to accommodate diffuse excited states of the target. For example, a recent calculation (Pathak *et al.*, 1988, 1989) of H^- resonances converging to the $H(n=5)$ threshold uses $r_0 = 83a_0$, vs $r_0 \leq 10a_0$ typically used elsewhere. This increases the size of the calculation significantly, since the number of states within the R-matrix volume that is needed to span a given range of energy is proportional to r_0^2. An alternative approach has recently been introduced by Greene and collaborators (e.g., Kim and Greene, 1989), which represents explicitly only two or three electrons, moving in a model potential that is adjusted to give a good account of the spectrum of a parent or grandparent ion.

We note briefly two other general methods that have given results on atomic negative-ion resonances: the Kohn *variational method* and its modifications, applied by Nesbet and collaborators to He, the alkalis, and first-row elements (reviewed in Nesbet, 1980b); and *many-body perturbation theory* (Chase and Kelly, 1972; Radojevic *et al.*, 1987; Johnson *et al.*, 1989). The latter of these has found wide application in studies of photoionization of neutral atoms and positive ions, but has had relatively little application to negative-ion systems to date.

2. Direct computations of resonance parameters

The familiar description of a resonance as a discrete state embedded in a continuum carries with it the implication that the resonance should be characterized by some localized wave function. This concept is difficult to realize in a rigorous fashion in practice, since, for systems with more than two electrons, the continuum can only be defined in the context of some approximate model. Nevertheless, a variety of techniques have been deployed to calculate such wave functions.

There exist two standard frameworks within which a resonance has a well-defined meaning as a "discrete state": the Feshbach projection approach and its variants, and complex-coordinate methods. It is not our purpose here to provide a critical or historically correct review of these methodologies, which have wide applicability; general reviews are given by Temkin and Bhatia (1985), and by Reinhardt (1982) and Junker (1982a) for the Feshbach and complex-scaling methods, respectively. We restrict our discussion to general background and specific applications to negative-ion resonances.

a. Use of projection operators

The basic idea of the Feshbach projection operator technique is to make explicit the notion of a resonance as a "discrete state embedded in a continuum," by deriving an equation of motion for the component of the wave function that is orthogonal to the continuum. The method, originally introduced in a general context with envisaged applications in nuclear physics (Feshbach, 1962), has been adapted to the specific requirements of many-electron atomic calculations (Hahn *et al.*, 1962; Temkin and Bhatia, 1985) and has provided very accurate results for two-electron systems.

This method proceeds by the definition of projection operators Q and $P = 1 - Q$, which effect the required partition of the wave function. For a two-electron system with a single continuum associated with a target state $|\phi_0\rangle$ (as in electron-hydrogen scattering below the first inelastic threshold, so that $\phi_0 = \phi_{1s}$), then $Q = Q_1 Q_2$ with $Q_i = 1 - |\phi_0(\mathbf{r}_i)\rangle\langle\phi_0(\mathbf{r}_i)|$. One then determines the spectrum of a transformed Hamiltonian,

$$QHQ\Psi_n = \varepsilon_n \Psi_n \ , \tag{6}$$

which has no projection onto the continuum. If there exist any discrete eigenvalues ε_n, they correspond to zeroth-order resonance energies: they are equal to the discrete-state energies to which the resonances would converge if the interaction with the continuum were turned off. Computation of the resonance width and its shift due to interaction with the continuum involves ad-

ditional computations that we shall not discuss here; they are often carried out by use of perturbation theory (Temkin and Bhatia, 1985).

The major task for any practical resonance calculation is accurate solution of Eq. (6) for a many-electron atom. Since Eq. (6) is subject to the Rayleigh-Ritz variational principle, it is usually solved by basis set expansions, e.g., using Hylleraas-type functions. Bhatia and Temkin (1974) used this approach to calculate the three lowest resonances of H^-. This method would appear to have the potential to compute resonance energies of such states to very high accuracy.

A general formalism for extension of this method to targets with more than one electron has been presented by Temkin and Bhatia (1985). The approach would necessarily involve the use of an approximate $|\phi_0\rangle$, and it has not yet been extensively applied. One such computation is that of the lowest $^2P^\circ$ resonance of He^- (Bhatia and Temkin, 1981). This has also been investigated by a related hole-projection method developed by Chung (1972, 1979, 1981). Although the Feshbach method has been important in providing benchmark calculations for low-lying resonances of the simplest systems, it has not been used in cases where many continua are present, nor has it yet been applied to targets with more than two electrons.

b. Complex-coordinate methods

Siegert (1939) treated the problem of compound states in nuclear scattering by an implicit assumption that the scattering amplitudes would be analytic functions of the energy, so that the sharp maximum in a cross section observed at real collision energies could be attributed to a singularity at a complex energy near the real axis. In the case of s-wave scattering by a short-range, spherically symmetric potential $V(r)$, Siegert demonstrated that a singularity in the cross section occurs at a complex energy ε for which

$$\frac{\partial\phi}{\partial r}=ik\phi \quad \text{at } r=r_0 \ , \tag{7}$$

where ϕ is the reduced radial wave function, $k=\sqrt{2\varepsilon}$, and r_0 is a value of the radius beyond which $V(r)=0$. (We express Siegert's general result in the atomic units appropriate for electron scattering.) For such a potential, Eq. (7) is satisfied for any $r_1>r_0$, so there is no ambiguity associated with the arbitrariness of r_0. Imposing the boundary condition (7) upon the Schrödinger equation thus presents us with an eigenvalue problem for a complex energy $\varepsilon=E_0-i\Gamma/2$. The singularity in the scattering amplitude at this energy gives rise to the usual Breit-Wigner form of the resonant scattering cross section, so Γ admits interpretation as the width of the resonance.

Considered as an ordinary eigenvalue problem, Eq. (7) presents a difficulty in that the boundary condition depends upon the eigenvalue being sought. Furthermore, in application to atomic systems with long-range forces, the independence of (7) upon r_0 can only be attained in the limit $r_0\to\infty$. Unfortunately, the wave function ϕ grows exponentially with r, so one cannot use standard variational techniques to obtain approximate solutions.

A way around this difficulty was proposed by Nuttall (1972) and applied by Bardsley and Junker (1972) to the calculation of the position and width of the $2s^2\ ^1S$ resonance of H^-. Nuttall noted that if the radius r were also regarded as a complex variable, then ϕ could be made to converge at larger $|r|$: in particular, if $k=|k|e^{-i\beta}$, and $r=\rho e^{+i\alpha}$, then ϕ would be square integrable for $\alpha>\beta$. Thus the application of a complex-scaling transformation to a many-electron system leads one to a variational principle for the wave function that is quite similar to that which applies to ordinary bound states. Bardsley and Junker (1972) applied this to a two-electron trial function composed of about 50 Slater-type orbitals, obtaining results for H^- $2s^2\ ^1S$ that agreed well with other determinations. This work demonstrated that, with some modification, standard techniques for the calculation of atomic structure could be applied to the calculation of resonances.

However, the prevailing view of resonance computation by complex-coordinate scaling involves a perspective differing somewhat from the Siegert theory. It derives from the fundamental work of Combes, Simon, and collaborators (Aguilar and Combes, 1971; Balslev and Combes, 1971; Simon, 1972, 1973; see also Reinhardt, 1982), who obtained rigorous results for complex-coordinate scaling in a general system of N particles intereacting via Coulomb forces. If all particle coordinates are scaled by a factor $e^{i\theta}$, the transformed Hamiltonian $H(\theta)$ may support discrete eigenfunctions with complex energies $\varepsilon e^{-i\phi}$, provided that $\theta>\phi/2$. The complex energies are independent of θ, and they correspond to resonances.

This framework offers an obvious means for actual computation of resonance energies: diagonalization of $H(\theta)$ in an appropriate basis of many-electron wave functions composed of square-integrable orbitals. Since all necessary matrix elements are identical, except for a scaling factor, to those required for ordinary bound-state calculations, there exist many computer codes that can be trivially adapted to implement this procedure. Doolen *et al.* (1974) performed the first calculation of this type, using a Hylleraas-type wave function of up to 95 terms to obtain the energy and width of the H^- $2s^2\ ^1S$ resonance. They observed a phenomenon that has occurred in all subsequent work that utilizes basis set expansions: the complex energies are found to be θ dependent, but for a sufficiently large basis there exists a value of θ at which the energy is stationary with respect to small variations $\delta\theta$.

Numerous calculations of negative-ion resonances by complex-scaling methods have been performed. In particular, Ho and collaborators (Ho, 1983, 1992, and references therein) have performed extensive calculations of

H^- resonances. Low-lying resonances in He^- and the p- and d-wave shape resonances in electron scattering by the alkaline earths have been investigated by several independent groups; these are discussed in the relevant sections. Complex-rotation calculations of the b and c resonances of Ne^- have recently been reported by Bentley (1991).

c. Bound-state calculations ignoring continuum interaction

A large number of calculations of resonance energies have been performed by the use of conventional bound-state techniques, in which the interaction with the continuum has been eliminated in a nonrigorous fashion. Such methods are occasionally referred to as "stabilization" techniques. For the most part, we discuss such calculations under the specific element headings, since their principal interest consists of their results rather than their underlying procedure.

The basic idea of this approach has been articulated by Hose and Taylor (1983) in a more general context. A resonance results from a transient localization of the wave function in some finite region Ω of configuration space. If viewed in a time-independent framework, a stationary state of energy E in the vicinity of the resonance energy E_r will be characterized by a wave function that behaves like that of a free particle at large distances from Ω, i.e., a standing wave. If we normalize the wave function by requiring the standing wave to have unit amplitude at large distances, then the wave function within Ω will vary smoothly with E, *except* for an overall normalization constant: that is, the shape of the wave function within Ω will be insensitive to changes in energy around $E=E_r$, but its overall amplitude there will show a pronounced maximum. Thus, if one attempts successive approximations to the resonance wave function by diagonalizing the Hamiltonian with a larger and larger set of basis functions that are all confined to Ω, one can expect one of the eigenfunctions to converge to a reasonable facsimile of the resonance solution in that region (except for an overall normalization constant). On the other hand, if one adds to the basis functions that extend outside Ω, this procedure will become unstable; each additional function will result in a change of the entire spectrum, as the wave function propagates further outward at an uncontrolled energy.

We note a few examples of this approach that indicate how it has worked in practice. Weiss and Krauss (1970) performed a superposition-of-configurations calculation of the resonances of Ne^- and Ar^-, of which the dominant configurations are, respectively, $2p^5 3s^2\,^2P^\circ$ and $3p^5 4s^2\,^2P^\circ$. These states decay by interaction with the $np^6\varepsilon p$ continuum. By including in the basis only configurations of the type (e.g., for Ne^-) $2p^5 nln'l'$ with $n, n' > 2$, Weiss and Krauss obtained stable solutions. Addition of $2p^6 np$ functions would have resulted in the above-mentioned instability. In effect, Weiss and Krauss were enforcing orthogonality to the $np^6\varepsilon p$ continuum. We report in this paper calculations of a similar character, except they are performed in a multiconfiguration Hartree-Fock (MCHF) approximation in which all orbitals are determined self-consistently. In such a case the resulting core orbitals define a continuum that is not identical to that of the neutral atom at the same level of approximation. Nevertheless, judicious choice of configuration-state functions leads to stable results. Lipsky *et al.* (1977), in a calculation that has endured as a benchmark for computations of doubly excited states, computed all resonances of H^- below the $H(n=2)$ and $H(n=3)$ thresholds by the simple expedient of diagonalizing the Hamiltonian in a basis of product states in which one electron was in an $n=2$ (or $n=3$) hydrogenic orbital, and the other in a hydrogenic orbital with $n=2$ (or 3) through 10. Exclusion of configurations of the type $1snl$ enabled these results to converge, on values that show reasonable agreement with experiment. Finally, in perhaps the most ambitious work of this type, Komninos *et al.* (1987) performed MCHF calculations of doubly excited S states of H^- and He^- for principal quantum numbers between 3 and 10. Again, by excluding configurations with single (H^-) or double (He^-) $1s$ occupancy, they obtained convergence and got reasonably good agreement with experimental values.

C. Hyperspherical coordinate representations

Hyperspherical coordinates were introduced into atomic physics by Fock (1958), who was concerned with the analytic structure of the wave function of a three-body Coulomb system in the region of three-particle coalescence. For the case of infinite nuclear mass, which is all we shall discuss here, the hyperspherical coordinates may be taken to be

$$\begin{aligned} R &= \sqrt{r_1^2 + r_2^2}\ , \\ \alpha &= \arctan(r_2/r_1)\ , \\ \theta_{12} &= \arccos\left[\frac{\mathbf{r}_1\cdot\mathbf{r}_2}{r_1 r_2}\right]\ , \end{aligned} \tag{8}$$

where r_1, r_2 are the two electron-nuclear radii, plus three Euler angles that describe the overall orientation of the two-electron system. Note that in this system, R is the only coordinate with the dimension of length, and it characterizes the root-mean-square size of the system; the others are dimensionless angles, with the "mock angle" α characterizing the relative proportions of r_1, r_2 at fixed R. This scheme is extensible to an N-electron system, in which it leads to an equation for the kinetic-energy operator T:

$$T = -\frac{1}{2}\left[\sum_{i=1}^{3N}\frac{\partial^2}{\partial x_i^2}\right] = -\frac{1}{2}\left[\frac{\partial^2}{\partial R^2} + \frac{3N-1}{R}\frac{\partial}{\partial R} - \frac{\Lambda^2}{R^2}\right]\ , \tag{9}$$

where Λ^2 is an operator in the physical and mock angles (which we shall collectively call Ω) obtained by generalization of Eq. (8). Furthermore, the net Coulomb potential energy of such a system is given by $V=C(\Omega)/R$. This potential is displayed in Fig. 2 as a function of the two relevant angles α, θ_{12} in the two-electron system. Thus in the limit $R\rightarrow 0$, the kinetic energy dominates the Hamiltonian, and the many-electron wave function takes the limiting form

$$\Psi\rightarrow R^{\nu}\Theta(\Omega)\ , \tag{10}$$

where $\Theta(\Omega)$ is an eigenfunction of Λ^2 with eigenvalue λ^2, and

$$\nu=1-3N/2+\sqrt{\lambda^2+(1-3N/2)^2}\ . \tag{11}$$

The characteristic exponent ν depends only upon the symmetry of the wave function and is indeed identical to that which would describe a system of free particles with the same symmetry. As shown by Fock, the effect of the Coulomb potential becomes manifest in the development of the expansion that begins with Eq. (10) and it induces terms that are powers of $R\ \ln(R)$, which are not present in the analogous expansion for a free-particle system. It is believed that the Fock expansion converges for all relevant physical values of the parameters (Macek, 1967; Morgan, 1986, and references therein); it has long been known that explicit representation of the logarithmic terms must be included in finite basis set expansions in order to get highly accurate values of the energies of two-electron systems (Frankowski and Pekeris, 1966).

An obvious consequence of Eqs. (9) and (10) is the presence of a potential "barrier" $\Lambda^2/2R^2$ analogous to the centrifugal barrier in one-electron systems, from which qualitative properties of many-electron wave functions can be inferred. This was first applied to an analysis of resonances by Macek (1968), who found that a hyperspherical representation of wave functions yielded novel qualitative information on the $^1P^{\circ}$ autoionizing series of He converging to the He^+ ($n=2$) ionization limit. These series had been analyzed by Cooper *et al.* (1963) in terms of a configuration-interaction expansion, in which it was found that the observed resonances could be placed in two series, called "+" and "−" because they

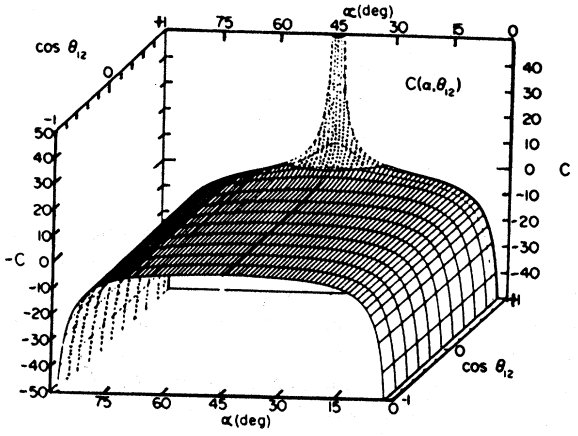

FIG. 2. Function $C(\alpha,\theta_{12})$ for a pair of electrons in the field of a proton. The point $\alpha=45°, \theta_{12}=180°$ corresponds to the Wannier saddle. From Lin (1974).

were fairly well described by a superposition of configurations $2snp\pm 2pns$. The "−" series has a much smaller oscillator strength and decay width than the "+". Cooper *et al.* showed a plot of the two-electron wave functions for each series (constructed from an appropriately symmetrized product of hydrogenic wave functions) in the r_1, r_2 plane; these showed that the nodal lines of the wave functions for the "+" series were approximately lines of constant R, whereas the "−" series exhibited nodal lines roughly along $\alpha=$const. This behavior, which suggests an approximate separability of the equations of motion in R and α, was also found in a representation constructed from more accurate, close-coupling wave functions by Macek (1966). To try to account for this suggested approximate separability of the equations of motion, Macek (1968) introduced the adiabatic hyperspherical expansion, in which the net wave function is expanded as

$$\Psi=R^{-5/2}\sum_{\mu}\phi_{\mu}(R;\Omega)F_{\mu}(R)\ , \tag{12}$$

where $\phi_{\mu}(R;\Omega)$ is an eigenfunction of the angular operators in the two-electron Hamiltonian at fixed R, i.e.,

$$U(R,\Omega)\phi_{\mu}(R;\Omega)=\left[\frac{\Lambda^2}{2R^2}+\frac{C(\Omega)}{R}\right]\phi_{\mu}(R;\Omega)=[U_{\mu}(R)-15R^{-2}/8]\phi_{\mu}(R;\Omega)\ . \tag{13}$$

(Our notation differs somewhat from that of Macek; the factor $15R^{-2}/8$ simplifies subsequent equations.) Applying the Schrödinger equation to the expansion (12) then yields

$$\left[-\frac{1}{2}\frac{\partial^2}{\partial R^2}+U_{\mu}(R)\right]F_{\mu}(R)=EF_{\mu}(R)+\sum_{\nu}\left[P_{\mu\nu}(R)\frac{\partial F_{\nu}(R)}{\partial R}+Q_{\mu\nu}(R)F_{\nu}(R)\right]\ , \tag{14}$$

where

$$P_{\mu\nu}(R)=\left\langle \phi_\mu \left| \frac{\partial}{\partial R}\phi_\nu \right\rangle \right. ,$$
$$Q_{\mu\nu}(R)=\frac{1}{2}\left\langle \phi_\mu \left| \frac{\partial^2}{\partial R^2}\phi_\nu \right\rangle \right. . \quad (15)$$

Thus the $U_\mu(R)$ play the role of adiabatic potentials, analogous to those which arise in the Born-Oppenheimer approximation for molecular potential curves. To the extent that $P_{\mu\nu}$ and $Q_{\mu\nu}$ can be neglected, we obtain a set of uncoupled equations for the evolution of the wave function in each adiabatic channel μ. This approach was taken by Macek (1968), who found that the "$-$" series was characterized by a larger characteristic exponent at small R than that of the "$+$" series. Thus the hyperspherical "centrifugal barrier" effectively suppresses the overlap of the "$-$" wave functions with the He ground state, which results in the diminution of the oscillator strengths and widths of this series.

This result had pronounced intellectual impact, in that it demonstrated that a qualitative aspect of the absorption spectrum could be associated with a quantum number (the characteristic exponent of the hyperradial function) that derived explicitly from a collective description of electron motion, and which was distinct from the usual quantum numbers that arise in the central-field model of atomic structure. However, it is not obvious why this should be so. The Born-Oppenheimer separation of nuclear and electronic degrees of freedom in a molecule is predicated upon the disparity in the speeds of motion of the electrons and nuclei, which is encapsulated in a "small" parameter $(m/M)^{1/4}$ that can be used to develop a perturbative description of coupling between electronic and nuclear modes. No such small parameter is evident in the hyperspherical representation of many-electron systems, which would justify treating the motion in Ω as "fast" compared to motion in R. Nevertheless, an approximate separability of these two modes is apparent in a variety of atomic states. A review of general developments in this subject to 1982 has been given by Fano (1983a, 1983b), and subsequent work has been discussed by Lin (1986).

Lin (1984) has proposed a classification of adiabatic hyperspherical channels in terms of the supermultiplet quantum numbers introduced by Herrick and collaborators (Herrick and Sinanoglu, 1975; Kellman and Herrick, 1980). Although the scheme does not have universal applicability, it appears to be appropriate in many cases of interest and has become widely accepted. This scheme is reviewed in Sec. II.F. In the following discussion, the hyperspherical channel index μ should be understood to refer to the complex $\{N,K,T,A,L.S,\pi\}$, where these symbols are defined in Sec. II.F. Note, in particular, that in this context N is the principal quantum number of the one-electron eigenenergy to which $U_\mu(R)$ converges as $R\rightarrow\infty$.

Application of the adiabatic hyperspherical approach to a negative-ion resonance was first made by Lin (1974, 1975), who treated H^- resonances around the H ($n=2$) threshold. This calculation gave insight into the mechanism of $^1P^\circ$ photoabsorption resonances, as indicated in Fig. 3. The adiabatic potential curve labeled "$sp+$", analogous to that which governs the "$+$" series in He, is insufficiently deep to support a bound state, but it does exhibit a potential barrier around $R=20a_0$. This gives rise to a shape resonance in the "$+$" channel, which lies above $H(n=2)$. The "$sp-$" potential curve holds a very weakly bound state that corresponds to the Feshbach resonance just below $H(n=2)$. These resonances have been calculated by other techniques, in many cases with superior quantitative accuracy (see Sec. IV.A), but the adiabatic hyperspherical technique provides a framework within which the underlying physics is revealed in the form of an effective potential for a collective coordinate.

In its earlier applications the adiabatic hyperspherical method did not give results of impressive quantitative accuracy, primarily because Eq. (13) was solved by expanding ϕ_μ in eigenfunctions of Λ^2, which are Jacobi polynomials in the angles Ω. The advantage of this basis (or of any other R-independent basis) is that the matrix elements of Λ^2 and C need be computed only once, since the operator U then has a simple parametric dependence upon R. It is evident that if any finite R-independent basis is used to solve this equation, the potentials $U_\mu(R)$ must all tend to 0 as $R\rightarrow\infty$, since the left-hand side of (13) would then be proportional to R^{-1} times a bounded operator. In fact, the $U_\mu(R)$ must always converge to eigenenergies $-Z^2/N_\mu^2$ of the residual one-electron atom. This convergence problem could be postponed to relatively large values of R by choosing a suitably large basis (Klar and Klar, 1980). However, a more effective approach, first implemented by Lin (1981), is to incorporate eigenfunctions of the one-electron Hamiltonian into the basis. Although this increases the amount of compu-

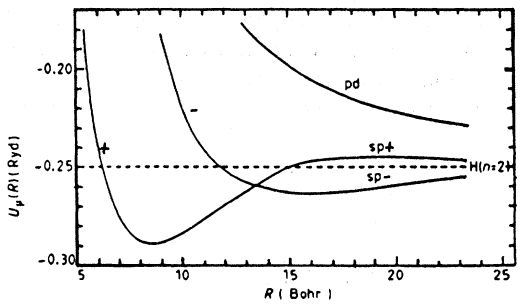

FIG. 3. Adiabatic hyperspherical potential curves for $^1P^\circ$ channels of H^- as calculated by Lin (1975a, 1975b). "$sp+$," "$sp-$," and "pd" label the three possible channels of $^1P^\circ$ symmetry associated with $H(n=2)$, which are approximately described as $2s\varepsilon p+2p\varepsilon s$, $2s\varepsilon p-2p\varepsilon s$, $2p\varepsilon d$, respectively. The crossing between "$sp+$" and "$sp-$" is avoided, contrary to the impression given here; subsequent, more accurate calculations (Klar and Klar, 1980) exhibit a pronounced avoided crossing of these curves.

tational work required to generate the potentials $U_\mu(R)$, it has brought the quantitative accuracy of the hyperspherical approach to a level that is competitive with alternative techniques.

The superficial simplicity of the adiabatic hyperspherical approach is lost at higher energies, where a large number of channels open up and numerous crossings of the adiabatic potential curves occur (Fig. 4). However, it has recently been found that the effect of curve crossings is not of essential significance in many cases of interest. Fukuda *et al.* (1987) and Koyama *et al.* (1986, 1989) investigated ^1S and $^1P^\circ$ resonances of H^- for values of N up to 9. They were able to justify diabatic connection of potential curves in the vicinity of curve crossings by using a Landau-Zener approximation to estimate nonadiabatic transition probabilities for electron wave packets with energies corresponding to the eigenfunctions of the connected potential. Their results were found to agree well with those of complex rotation (Ho, 1986), and multiconfiguration Hartree-Fock (Nicolaides and Komninos, 1987) calculations. Sadeghpour and Greene (1990) and Sadeghpour (1991) carried out a similar approach up to $H(n=12)$ and found, in addition, that the photoabsorption spectrum of H^- is dominated by resonances in the lowest "+" channel for each value of N.

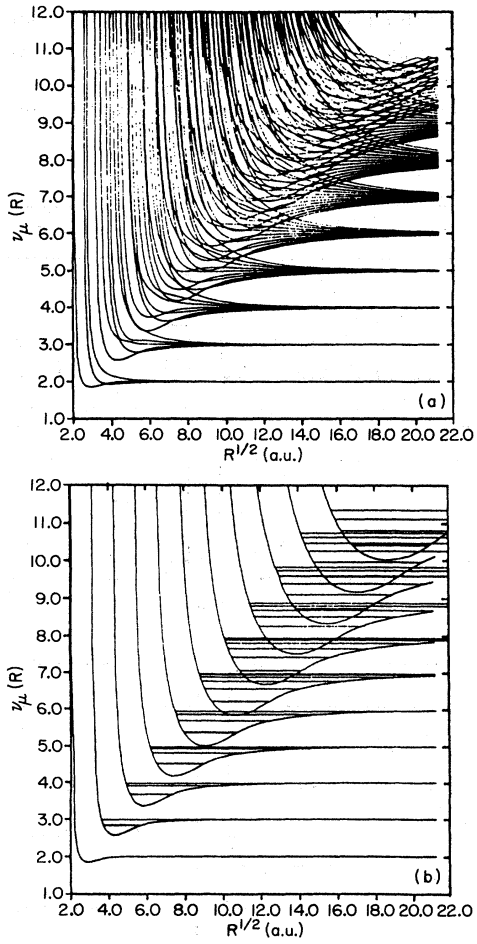

FIG. 4. Adiabatic hyperspherical potential curves for $^1P^\circ$ channels of H^-, converging to the limits $H(n=2)$ through $H(n=12)$, as a function of $\sqrt{R}$. The energy scale is represented in terms of the effective principal quantum number $\nu_\mu(R)=\sqrt{-2U_\mu(R)}$ shown in (a) are all $^1P^\circ$ adiabatic potentials in this energy region, and in (b) are the adiabatic potentials of only the lowest "+" channels converging to each hydrogenic threshold, with level positions in each potential as indicated. From Sadeghpour and Greene (1990).

The adiabatic hyperspherical approach has been applied to systems with more than two electrons at two different levels of approximation: one in which two electrons move outside an ionic core, which is represented by an effective potential; and one in which the hyperspherical formalism is extended to treat more than two electrons explicitly. Examples of the first approach that are germane to this review are the calculations of Lin (1983c) on Li^-, Christensen-Dalsgaard (1988) on the alkalis, and Watanabe (1982) and Le Dourneuf and Watanabe (1990) on He^-. The last-mentioned work is particularly noteworthy in that the adiabatic potentials for He^- are found to exhibit strong similarities to those of H^-, and it is possible to classify many of the He^- resonances in terms of the quantum numbers used for two-electron systems.

Relatively few calculations of systems with more than two electrons have been performed within the hyperspherical framework. Clark and Greene (1980; Greene and Clark, 1984) undertook hyperspherical calculations of three-electron states of ^2S and $^2P^\circ$ symmetry in H^{2-} and Li. Watanabe *et al.* (1982) computed the metastable negative-ion state He^- $2p^3\,^4S^\circ$ in the adiabatic hyperspherical approximation. However, we are unaware of any calculations performed within this framework to date on negative-ion *resonances* with more than two active electrons. Some experimental data have accumulated on He^- resonances for which a three-electron hyperspherical approach might be advantageous (Heideman, 1988). The hyperspherical description of atomic systems with more than three electrons is in a very rudimentary stage and has not yet been developed into a practical vehicle for calculations. Nevertheless, it has offered qualitative insights of some interest. For example, Cavagnero (1984) has suggested that the strong $2s^2$-$2p^2$ interaction in the ground state of Be is mediated by level crossing of adiabatic potential curves at small values of the four-electron hyperradius R.

D. Quasimolecular models

The experimental observation of long series of two-electron resonances of similar character suggests that one ought to be able to identify characteristic channels in which two-electron excitation takes place ("channel" refers to an identification of eigenstates in terms of all relevant quantum numbers except the energy, and an eigenchannel is equivalent to a "normal mode"). A prin-

cipal attraction of the hyperspherical coordinate approach is that it identifies *collective coordinates,* which correspond to some extent to the two-electron eigenchannels. In particular, as discussed above, it has been found possible in many cases to identify eigenchannel properties in terms of the quantum numbers $\{\mu\}$ obtained by diagonalizing the Hamiltonian at fixed value of $R=\sqrt{r_1^2+r_2^2}$. The remaining dynamics is then encapsulated in an effective potential $U_\mu(R)$ that governs the motion of the system in the coordinate R.

An alternative set of collective coordinates has been identified by Feagin and Briggs (1986, 1988) and by Rost and Briggs (1991, and references therein) that is applicable to a Coulomb system of three particles, two of which are identical. We discuss these coordinates in the particular case of H^-; any other three-body system is described by straightforward scaling of the units of energy and length. With ρ_1,ρ_2 the positions of the two electrons (of unit mass) and ρ_3 that of the proton (of mass M), we define

$$\begin{aligned}\mathbf{R}&=\rho_2-\rho_1\\ \mathbf{r}&=\rho_3-(\rho_2+\rho_1)/2\ .\end{aligned}\tag{16}$$

We let $\mathbf{R}$ define the quantization axis for the "body frame" of the three-particle system, which is obtained from a space-fixed frame by Euler rotations. For fixed values of total angular momentum L and projection M, the wave function in the space-fixed frame, $\Psi_{LM}(\mathbf{r},\mathbf{R})$, can be represented by an expansion in body-frame wave functions $\Psi_{Lm}(\mathbf{r},R)$, with $0\le m\le L$, where m is the azimuthal quantum number associated with the azimuthal motion of $\mathbf{r}$ in the body frame. One then proceeds by an adiabatic expansion of the body-frame wave functions,

$$\psi_L^t(\mathbf{r},R)=R^{-1}\sum_{i,m}f_{im}^L(R)\Phi_{im}^t(\mathbf{r},R)\ ,\tag{17}$$

in which the motion in $\mathbf{r}$ will be taken to be fast in comparison to that in R and will generate effective potentials for the channel functions $f_{im}^L(R)$. The indices in Eq. (17) have the usual molecular interpretation: L is the total angular momentum of the system; m and t equal 0 and 1, respectively, the azimuthal quantum number and inversion symmetry of the body-frame adiabatic wave function Φ; and i, an adiabatic channel index.

A key advantage of this method is that the adiabatic wave functions Φ are eigenfunctions of the two-center Coulomb Hamiltonian

$$h=-\frac{1}{2\nu}\nabla_r^2-\frac{1}{r_1}-\frac{1}{r_2}\ ,\tag{18}$$

where ν is a reduced mass, and the vectors $\mathbf{r}_1,\mathbf{r}_2$ are given by $\mathbf{r}\pm\mathbf{z}R/2$, where $\mathbf{z}$ is the unit vector along the body-frame symmetry axis. The Schrödinger equation obtained from (18) is separable in prolate spheroidal coordinates,

$$\lambda=\frac{r_1+r_2}{R}\ ,\quad \mu=\frac{r_1-r_2}{R}\ ,\tag{19}$$

so that the adiabatic wave functions Φ have a well-defined structure characterized by quantum numbers n_λ,n_μ. These provide adiabatic channel indices with implicit information about the internal symmetry of the wave function at all values of R. Furthermore, the adiabatic potentials that emerge from this treatment can be related to those of the H_2^+ molecule by a simple scaling transformation.

Figure 5 shows adiabatic potential curves for various states of H^- as computed by this approach and by the adiabatic hyperspherical method. Note that the coordinate R has completely different meanings in these two sets of curves. There are some qualitative similarities in these potentials, such as the existence of a barrier in the "+" or $2p\sigma_u$ channels of $^1P^o$ symmetry, but there are noticeable differences in detail, particularly in the distribution of curve crossings. Energies of doubly excited states computed in the adiabatic approximation by this method exhibit good agreement with results obtained by other methods, particularly at high energies (Rost and Briggs, 1991).

This model therefore casts the two-electron problem

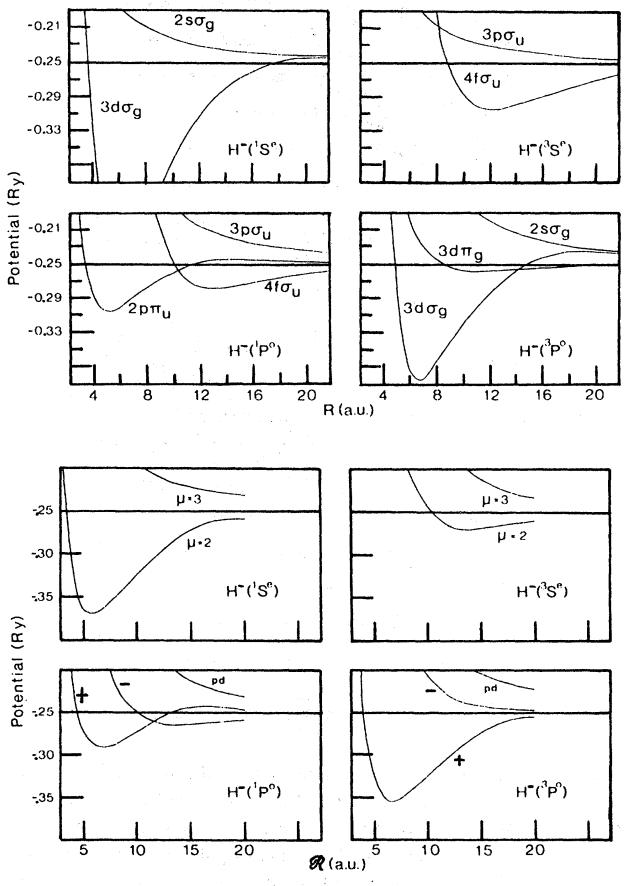

FIG. 5. Adiabatic potential curves for H^- near $H(n=2)$, for $LS\pi$ symmetries as indicated. Top frames: as computed in the molecular model; bottom frames: from adiabatic hyperspherical calculations. From Feagin and Briggs (1988).

into a molecular framework in a natural fashion. It appears to explain the essential physics that underlies the quasimolecular aspects of doubly excited spectra, which hitherto had been discussed within the context of group theory or approximate atomic models.

E. The Wannier ridge resonances

Wannier (1953) presented a theory of the threshold behavior of electron-impact ionization based on classical mechanics. Semiclassical versions of this theory were derived by Peterkop (1971) and Rau (1971), and there have been many subsequent theoretical and experimental investigations of its validity (for reviews, see Sec. VII.A). Although it would be an exaggeration to say that this theory is universally accepted, it has become the primary focus for all discussions of processes involving two electrons near the threshold for double escape from the field of an ion (electron-impact ionization, double photoionization, and double photodetachment). The Wannier theory postulates that double escape at threshold proceeds through a highly specific region of configuration space, in which the two electrons travel outward on opposite sides of ($\theta_{12}\approx\pi$) and comparable distances from ($r_1\approx r_2$ or $\alpha\approx\pi/4$) the ion. This region of configuration space appears as a *ridge* or saddle in the hyperspherical potential surface for the two-electron system: at fixed R, this trajectory is stable with respect to small variations of θ_{12} and unstable in a (see Fig. 2). The physical underpinning of this argument is that if one electron lags the other, it will be captured in the field of the ion at large distances, and single ionization of the leading electron will ensue.

We discuss this situation from the perspective of classical mechanics. If we use the coordinates

$$\begin{aligned}\mathbf{R}&=(\mathbf{r}_1+\mathbf{r}_2)/2\\ \rho&=(\mathbf{r}_2-\mathbf{r}_1)\ ,\end{aligned} \tag{20}$$

the Hamiltonian takes the form

$$H=\frac{P_R^2}{2(2m)}+\frac{P_\rho^2}{2(m/2)}-\frac{Z}{|\mathbf{R}-\rho/2|}-\frac{Z}{|\mathbf{R}+\rho/2|}+\frac{1}{\rho}\ , \tag{21}$$

where m is the electron rest mass.

The solution $\mathbf{R}=0$ is allowed by classical mechanics, although it is unstable (Richter and Wintgen, 1990). In this case the Hamiltonian for ρ takes the form

$$H_\rho=\frac{P_\rho^2}{2(m/2)}-\frac{4Z-1}{\rho}\ , \tag{22}$$

which is the hydrogenic Hamiltonian for a particle of mass $m/2$ in the field of a charge $4Z-1$. By naive quantization of Eq. (22), we obtain the spectrum (in atomic units)

$$E_n=-\frac{4(Z-1/4)^2}{n^2}\ , \tag{23}$$

where $n=1,2,\ldots$. Thus the basic Wannier model of threshold escape of two electrons also gives Rydberg-type series of resonances converging on the threshold.

A more rigorous derivation, yielding a formula similar to Eqs. (23) has been carried out by Macek and Feagin (1985) utilizing a WKB approximation of the wave functions. They obtain

$$E_n=-\frac{4(Z-1/4-\sigma/4)^2}{(n-d)^2}\ , \tag{24}$$

where σ is a screening constant that is much less than unity, and d can be interpreted as a quantum defect: it is related to the phase of the WKB wave functions at the boundary R_0 of the "Coulomb zone" in which the Wannier treatment is valid.

The possible existence of a series of negative-ion resonances which arise as a consequence of motion on the Wannier ridge seems to have been first mentioned by Fano (1980), and this idea was used by Buckman *et al.* (1983a, 1983b) to interpret long resonance series observed in electron scattering by He below the first ionization threshold. These measurements are discussed in detail in Sec. IV.B. However, they have promoted a substantial amount of theoretical activity, which is worthy of some comment.

The energies of such a Rydberg series of doubly excited resonances can be approximated by variations to the Rydberg formula that take into account the mutual screening of the core by the two electrons and that assume that the two excited electrons are equidistant from the core. Heddle (1976b, 1977) and Read (1977) developed such a modified Rydberg formula, and it, along with several other variants (Rau, 1983; Lin and Watanabe, 1987), does a reasonable job at fitting the energies of the observed resonances in He^- and many other systems. These semiempirical formulas and the results derived from them are discussed in detail in the next section and in Sec. IV.B.

Feagin and Macek (1984; Macek and Feagin, 1985) have also shown the existence of a Rydberg series of resonances converging on the first ionization threshold by extrapolating Wannier continuum wave functions, which describe two-electron escape, to the energy region just below the ionization threshold. They derive the modified Rydberg formula (24), which agrees with that of Rau (1983). However, they point out that, in order for this formula to fit the experimental data of Buckman *et al.*, unreasonably large values of σ must be used. They also obtain an equation for the partial widths of these resonance states which is based on an argument that the observed average intensity, $\langle I_n\rangle$, for these resonances, can be related to the Wannier threshold law at high n. That is

$$\langle I_n\rangle=\frac{\Gamma_n}{E_{n+1}-E_n}\underset{n\to\infty}{\approx}E_n^{1.127}\ , \tag{25}$$

where Γ_n is the partial width. From this they show that the partial widths of these states should vary as $n^{-5.254}$

for large n. This disagrees with the result of Rau (1983, 1984c), who obtains an $n^{-6.254}$ variation based on the normalization of a Coulomb function in six dimensions.

The ridge resonances in He^- and H^- were also calculated by Komninos *et al.* (1987). In particular, they calculated the energies of He^- states of ^2S symmetry up to $n=10$ based on a multiconfiguration Hartree-Fock approach, which includes the effects of both angular and radial correlations. The energies they obtain are in good agreement with experiment, and probability plots indicate localization of the excited electrons on the Wannier ridge. These results are discussed in more detail in Sec. IV.B.

Recently, a rather different picture of "Wannier ridge resonances" was put forward (Richter and Wintgen, 1990; Ezra *et al.*, 1991; Rost *et al.*, 1991), though it has been applied primarily to doubly excited states of neutrals rather than negative ions. These papers report studies of trajectories of two-electron systems, as computed in classical mechanics, and their implications for quantum-mechanical spectra using methods due to Gutzwiller (1990). Richter and Wintgen (1990) find that the Wannier configuration described by Eq. (22) is highly unstable and that it therefore cannot be associated with quantum-mechanical resonances. On the other hand, they find that a two-electron orbit first identified by Langmuir (1921) is stable for $Z=2$ (though apparently not for $Z=1$) and that it therefore ought to describe a series of Rydberg-type resonances in He. Langmuir's two-electron orbit has the two electrons always at equal distances from the nucleus, so that $\alpha=\pi/4$; but the configuration is relatively localized in R, the dominant mode of motion being an oscillation in θ_{12} about the value of π. Thus the motion of the two electrons about the nucleus resembles the bending mode of vibration of a triatomic molecule. Quantum-mechanical calculations of doubly excited states of He that have been regarded as Wannier ridge resonances (Ezra *et al.*, 1991) show wave-function clustering about the classical Langmuir orbit.

F. Classification schemes, techniques, and nomenclature

A number of semiempirical techniques have been developed as an aid in the study of negative-ion resonances. The earliest methods involved extrapolation either along isoelectronic sequences or along states of equal ionization and were developed to enable determinations of ionization potentials and electron affinities. They have not proven particularly useful for predicting accurate resonance energies and can give little insight to the classification of the states concerned. Other, somewhat more successful techniques have involved the comparison of resonance spectra with the spectra of both singly and doubly excited states of similar or isoelectronic atoms (e.g., Kuyatt *et al.*, 1965; Swanson *et al.*, 1973). From such comparisons some educated guesses as to the configuration of the resonance states involved have been made.

However, as Read *et al.* (1976) have pointed out, the complete classification of any spectral feature involves the assignment of both a configuration and an appropriate coupling scheme. In the cases of helium and atomic hydrogen, this task is relatively straightforward, and the classification of the lower-lying ($n=2$) resonances march almost hand in hand with their observation, both as a result of the detail of the experimental observations and of the availability of accurate wave-function information. Similar progress has followed in the description of the higher-lying ($n=3,4$) resonances, and these are discussed in some detail in Sec. IV.B and in the latter parts of this section.

It is perhaps appropriate, however, to describe briefly a classification scheme that has proved successful in the description of the resonance spectra observed in the heavier rare gases, a group of atoms for which there is a substantial body of high-quality experimental evidence. Almost without exception, the early experimental papers on these gases noted the occurrence of a number of resonance pairs that appeared to be split in energy by an amount that was comparable to the spin-orbit splitting in the ion core. At the time of the Schulz review, the lowest few resonances in the rare gases had been assigned configurations, and it was generally believed that these states consisted of two excited s electrons attached to the spin-orbit–split ion core. Spence and Noguchi (1975) made a comparison between the resonances observed in the hydrogen halides and in their isoelectronic rare-gas counterparts and proposed configurations for a number of the higher-lying features in the rare-gas spectra of Sanche and Schulz (1972a). In assigning these configurations, they relied on an earlier conclusion (Spence, 1974) that the two excited electrons are in their most stable configuration in the field of the positive-ion core when they have the same principal quantum number n and similar angular momentum l.

These ideas were expanded significantly by Read *et al.* (1976), who proposed a coupling scheme for the rare-gas resonances and provided detailed configurations and terms arising from this scheme. This coupling scheme has as its physical basis the notion, based largely on the observed correspondence between the energy separation of the resonance pairs and the ion core splitting, that the coupling between the two excited electrons and the ion core is weak compared to the coupling between the electrons themselves. Read *et al.* (1976) propose that the two excited electrons couple together to form a total angular momentum **L** and total spin **S** and that the coupling between the total angular momentum of the core **j** and **L** is stronger than that between **j** and **S**, which is also stronger than that between **L** and **S**. They propose a **jLS** coupling scheme of the following form for the two electrons with spins $\mathbf{s}_{1,2}$ and orbital angular momenta $\mathbf{l}_{1,2}$,

$$\begin{aligned} \mathbf{l}_1+\mathbf{l}_2&=\mathbf{L}\ , \\ \mathbf{s}_1+\mathbf{s}_2&=\mathbf{S}\ , \\ \mathbf{j}+\mathbf{L}&=\mathbf{K}\ , \\ \mathbf{K}+\mathbf{S}&=\mathbf{J}\ . \end{aligned} \tag{26}$$

The interaction between the external electrons and the ion core has the effect of splitting the **SL** term into states of (generally) different energy and total angular momentum **J**. Read *et al.* provide tabulated examples of the values of **J** obtained from the *LS* terms ^{1,3}S, $^{1,3}P$, $^{1,3}D$ when coupled to an ion core with angular momentum between $\frac{1}{2}$ and 2. In an associated paper (Brunt *et al.* 1976) this classification scheme, which is usually referred to as the "external coupling" or "grandparent" classification scheme, was applied to the rare-gas resonances, as observed in metastable atom excitation functions. Assignments were made to classes of resonances observed in each of the heavier rare gases, neon through xenon, and each of these classes was designated by an alphabetical letter. In general, we have attempted in this paper to use this nomenclature when discussing resonances in the rare gases or, where appropriate, in other systems. Following Read *et al.*, the letters *a*–*f* correspond to the following configurations in the rare gases:

$$\begin{aligned} a&\equiv np^5\,{}^2P^{\circ}_{1/2,3/2}(n+1)s^2\,{}^1S\ , \\ b&\equiv np^5\,{}^2P^{\circ}_{1/2,3/2}(n+1)s(n+1)p^3P^{\circ}\ , \\ c&\equiv np^5\,{}^2P^{\circ}_{1/2,3/2}(n+1)s(n+1)p\,{}^1P^{\circ}\ , \\ d&\equiv np^5\,{}^2P^{\circ}_{1/2,3/2}(n+1)p^2\,{}^1S\ , \\ e&\equiv np^5\,{}^2P^{\circ}_{1/2,3/2}(n+1)p^2\,{}^1D\ , \\ f&\equiv np^5\,{}^2P^{\circ}_{1/2,3/2}(n+2)s^2\,{}^1S\ . \end{aligned} \tag{27}$$

In the above notation, contrary to usual spectroscopic practice, the final term designation refers to the coupling scheme appropriate to the outer two electrons. Only for ^1S external coupling (i.e., and *a*, *d*, and *f* resonances) has it been possible to identify the total angular momentum of the resonant states with any confidence. In all other cases there exists multiplet structure, little of which has been specifically identified to date.

Because of the ubiquitous occurrence of resonances similar to the *a* and *b* cases identified above, we have used this notation to label such states in a variety of elements. As discussed in Sec. VI, the complex of two electrons, coupled either as ^1S or $^3P^{\circ}$ and attached to a positive-ion core, exhibits a propensity to form a resonance that is largely unaffected by the details of the core. This is about the strongest generalization that can be made about negative-ion resonances in different elements. The *c*, *d*, *e*, and *f* features occur with notable similarity in the noble gases, but we have not found many other systems in which these classifications are useful.

Several other semiempirical techniques have proved beneficial as an aid in the classification of negative-ion resonances. Firstly, Heddle (1976b) and Read (1977) proposed a modification to the Rydberg formula in order to parametrize the energies of two-electron configurations. Read considered configurations of the type [core] *nlnl'*, in which the two electrons mutually screen each other from the charge of the core (Z) such that they each experience an effective charge of $(Z-\sigma)$, where σ is a screening constant. The effect of core penetration by either of the two Rydberg electrons is accounted for by the quantum defect δ_{nl}, and the energy of the two-electron configuration is given by

$$E_{nlnl'}=I-\frac{R(Z-\sigma)^2}{(n-\delta_{nl})^2}-\frac{R(Z-\sigma)^2}{(n-\delta_{nl'})^2}\ , \tag{28}$$

where I is the ionization potential or the core energy, R is the Rydberg constant (equal to $\frac{1}{2}$ a.u.), and σ is considered to be identical for each electron, with $\sigma=0.25$ indicating a highly correlated motion of the two Rydberg electrons (Read, 1977). Note that this formula differs by a factor of 4 from that of Eq. (24), if similar values of the screening constant and quantum defects are used. For each electron the value of δ_{nl} is that which is appropriate for the parent configuration [core]*nl*. Read demonstrated that, particularly for those configurations of the type [core]$ns^2\,{}^1S$, the modified Rydberg formula does extremely well in predicting the energies of negative-ion resonances and doubly excited states and the electron affinities of many stable negative ions. Although it appears to be less accurate in predicting the energies of other terms such as [core]$nsnp(^{1,3}P^{\circ})$ and $np^2(^3P,{}^1D,{}^1S)$ (i.e., there is a greater variation required in σ to enable the term energies to be reproduced), it is considered to be a useful tool in aiding the classification of negative-ion resonance states and has been used as such by many workers in the field. A similar approach was employed by Heddle (1977) to group resonances observed in optical excitation functions for helium. The application of these techniques will be discussed in many of the following sections.

Another technique that has proved quite successful as an aid to classifying resonances into groups or families is a graphical method developed by Spence (1977). He noted that a scheme used by Maria *et al.* (1973) for expressing the frequency of Rydberg states in structurally related molecules in terms of the ionization potential may be applicable to many Feshbach resonances which are essentially two electrons in Rydberg-like orbitals. He proposed that the energies of resonances of similar configurations in different rare-gas atoms could be accurately predicted by a simple relation, $E=AI+B$, where I is the ionization potential and A and B are arbitrary parameters independent of the atomic species. This formula, when fitted to the measured energies of Sanche and Schulz (1972a) and Brunt *et al.* (1976) for families of resonance features in the heavy rare gases (not He), indicated that, of 46 resonances, the predicted energies are different from the measured energies by less than 40 meV

in all but three cases. The striking feature of this form of analysis is the ability to easily group resonance features into families of similar configuration. It has been used more recently by Dassen *et al.* (1983) as an aid to the classification of resonances in the region of the rare-gas doubly excited states and also by Johnston (1983) in his work on the alkalis. These applications will be discussed in detail in later sections.

An alternative two-electron classification scheme has been proposed by Lin (1983d, 1984, 1986, 1987), which builds on earlier work by both Herrick and collaborators (Sinanoglu and Herrick, 1973; Herrick and Sinanoglu, 1975; Herrick *et al.*, 1980; Herrick, 1983). By analysis of configuration-interaction wave functions, Sinanoglu and Herrick (1973; Herrick and Sinanoglu, 1975) discovered an approximate constant of motion for states of two-electron systems in which both electrons occupy hydrogenic orbitals of the same principal quantum number N:

$$\mathbf{B}=\frac{\mathbf{A}_1-\mathbf{A}_2}{\sqrt{-2E}}\ , \tag{29}$$

where $E=-Z^2/2N^2$ is the usual hydrogenic energy, and $\mathbf{A}_i$ is the Runge-Lenz operator for electron i, defined as

$$\mathbf{A}=\mathbf{P}(\mathbf{R}\cdot\mathbf{P})-\mathbf{R}(\mathbf{P}^2-R^{-1}) \tag{30}$$

with $\mathbf{R}=Z\mathbf{r}$, $\mathbf{P}=\mathbf{p}/Z$. As is well known, the vector that is the equivalent of Eq. (30) in classical mechanics is directed along the semimajor axis of the ellipse of the Kepler orbit, so that the approximate conservation of Eq. (29) expresses a tendency for the two electrons to maintain a constant relative orientation. Since $\mathbf{L}^2$ and $(\mathbf{B}\cdot\mathbf{L})^2$ commute with $\mathbf{B}\cdot\mathbf{B}$ ($\mathbf{L}$ being the net orbital angular momentum operator), they may be simultaneously diagonalized. Their eigenvalues can be expressed in terms of L and two additional integer quantum numbers K and T, with

$$\begin{aligned}&0\le T\le \min(L,N-1)\ ,\\ &\pm K=N-T-1,N-T-3,\ldots,0 \text{ or } 1\ .\end{aligned} \tag{31}$$

T can be interpreted as the projection of $\mathbf{L}$ onto the axis $\mathbf{r}_1-\mathbf{r}_2$, and K is proportional to $-\langle r_< \cos\theta_{12}\rangle$, where $r_<$ is the radius of the inner electron. These quantum numbers therefore primarily characterize the angular correlations of the wave function. It was found that many doubly excited spectra fit the "supermultiplet" pattern that derives from these quantum numbers (Herrick, 1983). Furthermore, the spectra resemble to some degree the ro-vibrational spectrum of a linear triatomic molecule. This resemblance gave rise to a variety of studies in which doubly excited states were given a "molecular" interpretation.

Lin (1983d) drew attention to another quantum number, A, which is not independent of k and T but which provides a more direct indication of the radial correlation in the two-electron wave function. A can take the values 0, ±1 and is defined by

$$\begin{aligned}A&=\pi(-1)^{S+T} \text{ for } K>L-N\\ &=0 \text{ otherwise}\ ,\end{aligned} \tag{32}$$

where S is the total spin and π the parity of the state. Empirical analysis of wave functions has shown that states with $A=0$ reside in the "valleys" of the hyperspherical potential surface (i.e., the regions near $\alpha=0°$, $\alpha=90°$ in Fig. 2) and therefore have relatively weak radial correlations. States with $|A|=1$ can have significant wave-function amplitude in the vicinity of the saddle point $\alpha=45°$. Those with $A=1$ typically have an antinode near the saddle, and those with $A=-1$ have a mode. The $A=\pm1$ states correspond, respectively, to in-phase and out-of-phase stretching vibrations of the two excited electrons. Mølmer and Taulbjerg (1988) have shown that A, as defined by Lin, is the eigenvalue of the operator $P_{12}S_{xy}$, where P_{12} interchanges electron coordinates and S_{xy} is a reflection in the plane perpendicular to the intrinsic symmetry axis of the state.

Under this scheme doubly excited states are conventionally designated by the symbol

$${}_n(K,T)_N^{A\ 2S+1}L^{\pi}\ , \tag{33}$$

where N and n are principal quantum numbers of the inner and outer electron, respectively. As noted above, this scheme has been used often in the description of the doubly excited spectrum of neutral helium [see, for example, Lin (1986) and references therein]. Recently, Lin and Watanabe (1987) and Le Dourneuf and Watanabe (1990) applied this classification scheme to the spectrum of He^- resonances. In both cases, the latter involving the description of the resonance series in terms of a double Rydberg formula, the agreement with experiment is good. Rau (1983) has also developed a pair Rydberg formula for predicting the energies of He^- resonances and has provided a review of alternative schemes (Rau, 1991). Details of this work are presented and discussed in Sec. IV.B. This scheme has also been applied to the rich doubly excited resonance spectrum of H^- (Fukuda *et al.*, 1987; Pathak *et al.*, 1988; Sadeghpour and Greene, 1990; Ho, 1992).

As discussed in Sec. II.E, an alternative set of quantum numbers, deriving from a quasimolecular description of the Coulomb three-body problem, has been presented by Feagin and Briggs (1986, 1988; Rost and Briggs, 1991). These can be presented in the same form as the electronic states of the molecular ion H_2^+: either in terms of the united-atom limit (e.g., $1s\sigma_g$); in terms of the separated-atom limit (n_1n_2m), where n_1,n_2 are parabolic quantum numbers and m is the projection of the electronic angular momentum upon the internuclear axis; or in terms of an intermediate molecular-orbital system $(n_\lambda n_\mu m)$, where n_λ,n_μ are the quantum numbers of the adiabatic wave function in prolate spheroidal coordinates. Rost and Briggs (1991) present a table that summarizes the relationships between these designations and the $(K,T)^A$ description for $N=1-6$.

III. EXPERIMENTAL TECHNIQUES

In this section we attempt to give an overview of the experimental techniques that are available for the study of temporary negative ions. We do not wish to detail the specifics of all the many techniques that have been applied to this field, but rather to highlight those advances and new techniques that have been developed since the comprehensive reviews by Schulz. Detailed descriptions of the major techniques may be found in the review articles of Schulz (1973a, 1973b), Andrick (1973), Risley *et al.* (1974), Golden (1978), Read (1983), and references therein. We have also relied heavily on these articles for much of the reference data.

A. Electron-atom scattering

Electron-impact spectroscopy has provided the majority of the recent information on atomic negative-ion resonances. While few entirely new approaches have been developed in the past decade, many of the existing experimental techniques have been refined such that low-energy electron beams with energy spreads less than 25 meV (full width at half maximum, FWHM) can now be readily obtained. In fact, several recent experiments have demonstrated that sub-10-meV resolution is possible for gas-phase electron spectroscopy, both through the application of conventional techniques (Rohr and Linder, 1976; Jung, 1980; Jung *et al.*, 1982; Williams, 1985, 1988) and through new developments (Kennerly *et al.*, 1981; Wallbank *et al.*, 1983).

Negative-ion resonances formed by electron impact are generally studied by detecting reaction products in one or more of the decay channels energetically available to the compound state. Some of the many possible decay routes and the resultant detected particles are shown in Fig. 6. Such studies involve the measurement of either the total or differential scattering cross section (or a quantity proportional to these) for the above reaction products as a function of the incident electron energy. Many of the experiments involving the measurement of a total cross section are performed by studying the passage of an electron beam through a gas cell and detecting those electrons that are *not* scattered by the gas; this is the so-called transmission technique.

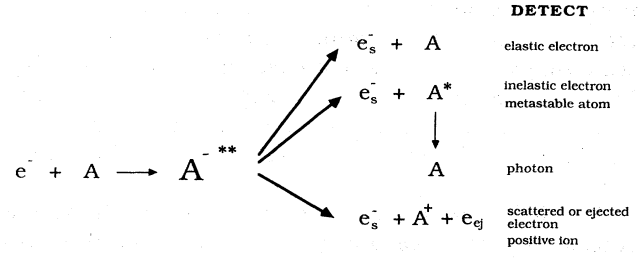

FIG. 6. Some possible decay modes for negative-ion resonances excited by electron impact.

1. Transmission studies

Electron transmission experiments, in which the attenuation of a beam of electrons by a gas sample in a scattering cell of known length is measured, have formed the basis of accurate total-cross-section measurements since the pioneering work of Ramsauer (1921). The study of sharp (< 100 meV) structure in the energy dependence of such cross sections due to the presence of negative-ion resonances requires the use of some form of energy selection of the incident electron beam prior to the scattering cell. A number of devices have been developed for this purpose. Schulz and Fox (1957) used a retarding potential analyzer for the study of metastable atom excitation functions in helium with an energy resolution of about 100 meV. The Ramsauer technique was further developed by Golden and Bandel (1965), who demonstrated that an energy resolution of 20–100 meV is achievable with this method. However, the use of the conventional transmission measurement was found to be limited in the study of resonance effects, because the resonance structure is generally only weakly apparent in the (usually) large nonresonant total cross section.

A major advance was the development of the transmitted-current derivative technique (Sanche and Schulz, 1972a), which was first applied in conjunction with the trochoidal monochromator transmission apparatus developed by Stamatovic and Schulz (1968, 1970). This technique makes use of a small (5–60 mV) ac signal applied to the walls of the collision cell with respect to the entrance and exit electrodes. Subsequent phase-sensitive detection of the transmitted current results in a signal that is proportional to the derivative of the total cross section dQ_T/dE, rather than to Q_T, and thus highlights even very small changes in the total cross section. This technique was used extensively by Schulz and his co-workers to provide the bulk of the early information on atomic and molecular negative-ion resonances (see Sanche and Schulz, 1972a, 1972b, 1972c; Schulz, 1973a, 1973b, and references therein). In the years since the Schulz review, its application has mainly been in the study of molecular systems (see Burrow, 1985), although several investigations on atomic resonance effects have been carried out with this technique and it has been used for the study of metal vapors and some transient atomic species (e.g., Spence and Chupka, 1974; Spence and Inokuti, 1974; Burrow and Comer, 1975; Spence, 1975a, 1975b; Burrow *et al.*, 1976; Johnston and Burrow, 1982). These will be discussed in later sections. While there have been no major technological advances in this area in the past decade, some effort has been invested in modeling the operation of trochoidal monochromators with a view to optimizing their performance (McMillan and Moore, 1980).

A related technique, which in many aspects is very similar to the transmission technique but which actually detects the scattered electrons, is the trapped-electron method, first used by Schulz (1958). These experiments usually consist of a trochoidal electron monochromator

and a collision volume lined with a circular collecting electrode to which is applied a small potential W. Those electrons that undergo an inelastic collision and have a resultant energy less than eW will be trapped by the potential well in the collision volume and confined by the axial magnetic field until, as a result of collisions, they migrate to the collecting electrode. Thus, as the incident electron energy is increased above an atomic threshold, with the well depth W fixed, the collected current is proportional to the total excitation cross section for that state. A modification to this technique by Knoop and Brongersma (1970) involved modulating the well depth W by an amount ΔW and measuring the ac component of the collected current in phase with the modulation frequency. This has the added sensitivity that it results in the detection of only those electrons with an energy of $e(W \pm \Delta W)$.

This technique has been used in a number of studies to measure excitation and ionization cross sections for a variety of atomic and molecular targets, some of which have revealed resonance effects and which are discussed in later sections. A novel extension to the technique was proposed and applied by Spence (1975a, 1980), who developed a method to enhance and separate those features in a trapped-electron spectrum that were due to negative-ion resonances from those due to inelastic excitation of the neutral atom. This technique proved particularly useful in the detection and classification of resonances in the autoionizing region of neon and, by inference, the heavier rare gases. As outlined above, the conventional trapped-electron technique detects only those electrons that have been *inelastically* scattered. The current of inelastically scattered electrons is detected synchronously with a modulated voltage, ΔW, applied to the trap depth W. The output is proportional to the inelastic cross section at an energy above threshold corresponding to the depth W of the trap. In such a spectrum, features associated with doubly excited states are strongly present compared to those associated with negative-ion resonances, as the latter can only be detected as a result of a two-electron decay into the continuum, with one of the electrons having an energy corresponding to the well depth. Spence was able to enhance the visibility of the resonance states in this experiment by noting that a portion of the elastically scattered signal also reaches the detector but is not measured, as its magnitude does not depend on the modulation voltage ΔW. Instead of modulating W, he modulated the incident energy and detected a signal with two components, the first being the *derivative* with respect to the incident energy of the elastically scattered signal and the second being a spectrum of the inelastically scattered electrons similar to the previous method. He was able to demonstrate that, for helium, the negative-ion features in the region of 56–60 eV were enhanced by about a factor of 40 by using this technique, presumably as a result of the preferential decay of these states into the elastic channel rather than the continuum.

Spence also noted that the position of the negative-ion resonances in the trapped-electron spectrum depended on the well depth W, while the position of the doubly excited neutral states was independent of W. Thus, by collecting spectra with variations in W of several hundred millivolts, he was able to chart those features that shifted correspondingly; and these could be ascribed, with some certainty, to negative-ion resonance states. These results are discussed in Sec. IV.D.

Various other derivative techniques that employ only electrostatic fields have been used for high-resolution resonance studies. Golden *et al.* (1972) make a comparison between the retarding potential difference method and the retarded energy modulation method. Schowengerdt and Golden (1974) combined both of these techniques in a double modulation spectrometer, which realized an energy resolution of 29 meV with good signal-noise characteristics, and resolution as high as ~ 10 meV with a poorer signal-noise ratio. Data obtained with this technique will be discussed in a later section. Jost and Ohnemus (1979) combined a parallel-plate energy selector and associated electron optics with a scattering cell to measure the absolute total collision cross section for Hg. Their energy resolution of 100 meV enabled the observation of many resonance features below 12 eV. Similar experiments with a hemispherical energy selector ($\Delta E \sim 30$ meV) have been conducted in the rare gases (Jost *et al.*, 1983).

Several other recent, novel electron monochromator designs have been used in conjunction with scattering cells to obtain transmission resonance spectra with observed widths of 30 meV or less. Grisenti and Zecca (1982) have obtained low-energy electron beams with an energy resolution of less than 25 meV at a current of 1 nA in a linear electron gun by utilizing the dispersion due to chromatic aberration in an electrostatic lens system. Paske *et al.* (1981) have developed a digital difference technique that gives similar results to the retarded energy modulation technique without the need for energy modulation, phase-sensitive detection, or a highly monochromatic incident electron beam. They obtained an energy resolution of 30 meV at an incident energy of 20 eV.

Transmission experiments, in particular those that measure the derivative of the transmitted current, are arguably the most sensitive means of detecting the presence of narrow negative-ion resonances. However, because these experiments only detect those electrons that have *not* undergone collisions (with the exception of the trapped-electron method, which detects inelastically scattered electrons), all information about the energy and scattering angle of those that have undergone collisions is lost. As a result, transmission experiments cannot provide conclusive evidence leading to the unambiguous classification of negative-ion resonances or their decay modes.

Such information can, however, be obtained from measurements where the presence, or otherwise, of a resonance is determined by detecting particles that directly arise from the decay of the resonant state. Reaction

products such as electrons, photons, metastable atoms, and positive ions, and their angular distributions and/or polarizations, can all be used in a detailed study of resonance excitation. Experiments in which *scattered* particles are detected are usually (but not exclusively) performed in a beam-beam geometry.

2. Crossed-beam studies

The past decade has witnessed a marked increase in the variety of experiments used to study resonance effects. In addition to the detection of the directly ejected or autodetached electrons, a number of intermediate and final states involved in the decay process have been probed by the detection of metastable atoms (see, for example, Brunt *et al.*, 1976, 1977a; Keesing, 1977; Buckman *et al.*, 1983a, 1983b; Koch *et al.*, 1984; Newman *et al.*, 1985), decay photons (see, for example, Kisker, 1972a; Heddle *et al.*, 1973, 1977; Heddle, Keesing, and Kurepa, 1974; Heddle, Keesing, and Watkins, 1974; Heddle 1976, 1977; Brunt *et al.*, 1977b, 1977c; Wolcke, 1983; van der Burgt *et al.*, 1985a, 1985b), and dissociation fragments of molecular negative ions (Huetz and Mazeau, 1981).

Much of the wealth of new data derived from crossed-beam and beam-gas cell techniques is without doubt due to improvements in electron optical and spectrometer design as well as data-acquisition and analysis techniques. The manifestation of negative-ion resonances as sharp structures in the energy dependence of electron-scattering cross sections has maintained interest in the quest for stable, highly monochromatic, variable-energy electron beams. Most of the experimental work in this field is performed with conventional energy analyzers and electron optical techniques. The majority of the energy analyzers in use are still the dispersive devices such as the 180° hemispherical or the 127° cylindrical electrostatic deflection analyzers. Little use has been made of either magnetic or combination crossed magnetic- and electric-field analyzers, because of the difficulty in shielding the electron paths external to the analyzer from stray B fields, the difficulties faced in construction, and, often, the lack of compatibility of magnetic devices with high-vacuum conditions. Another variety of dispersive device, the time-of-flight analyzer, has also seen little use in the study of atomic negative-ion resonances, because the energies involved are generally too high to exploit the high resolution which this technique can provide at very low energies. Time-of-flight spectroscopy has, however, been successfully applied in electron-molecule collisions (see, for example, Raith, 1976 and Kennerly *et al.*, 1979).

a. Developments in electron-energy analyzers

Considerable effort has been invested in approaches to improve the performance of electrostatic analyzers. Where a large angular scattering range is not of prime importance, the size of energy analyzers can be increased in order to reduce the effects of surface nonuniformities and improve energy resolution (Brunt *et al.*, 1977e). These authors also reduced the effects of field nonuniformities at the entrance and exit of an 180° hemispherical analyzer by use of a series of empirically designed fringe-field correcting hoops and virtual entrance and exit apertures. They found a marked improvement in the achievable energy resolution over a similar system with real defining apertures. Nevertheless, there are many examples of spectrometers with real apertures that have achieved an energy resolution of 25 meV or better (see, for example, Jost, 1979b; Jung *et al.*, 1982; Weyhreter *et al.*, 1983; Williams, 1985).

Many articles offering a comparison of electrostatic energy analyzers have been written. They are generally characterized by a "figure of merit," such as the ratio of the analyzer transmission to its resolution, $T/(\Delta E/E_0)$, where E_0 is the mean pass energy (Aksela *et al.*, 1970); the product of the entrance area A and solid angle Ω, or "etendue," $\varepsilon = A\Omega$ (Heddle, 1971a); the luminosity L, which is the product of the transmission, entrance area, and entrance solid angle; or a criterion that aims for a workable compromise between transmitted current and energy resolution (Read *et al.*, 1974). While such criteria are extremely useful in assessing the relative performance of a particular analyzer, it is generally only a part of the overall electron optical system, and its design and successful operation, of course, depend critically on the other elements of the system. Read *et al.* (1974) used a computer code to determine the optimum physical dimensions and operating conditions for double focusing analyzers (cylindrical mirror and hemispherical deflector) that would maximize the transmitted current for a given energy resolution. This design study included the effects of Boersch energy spreading, space charge, and lens and analyzer aberrations. They concluded that the hemispherical deflector was the superior device, and, provided careful design criteria are followed (such as the elimination of stray B fields), it is generally favorable to use a large analyzer with small, well-defined virtual apertures.

Jost (1979b) proposed a novel spectrometer design that produced spherical equipotentials in the region of the electron-beam trajectories from a series of nonspherical electrodes. The principal advantage of this device was its ease of construction, and a prototype yielded an energy resolution of less than 25 meV with an unspecified beam current.

In addition to those references already mentioned, there are many other articles on the design and optimization of energy analyzers (see, for example, Kuyatt and Simpson, 1967; Sar-El, 1970; Risley, 1972; Steckelmacher, 1973; Roy *et al.*, 1975b; Imhof *et al.*, 1976; Eland, 1978; Poulin and Roy, 1978; Jost, 1979a; Boesten, 1985, and references therein). An excellent general review article by Granneman and Van der Wiel (1979) on electron optics, energy analyzers, and particle detectors is also recommended.

b. Developments in electron optics

Regardless of the form of energy analysis used, optimum performance almost always necessitates the use of electron lenses at the input and output of the analyzer. As the absolute resolution of an electrostatic analyzer, ΔE, is proportional to the pass energy E_0, the resolution may be improved greatly by operating with a low value of E_0. However, the entrance to the energy selector of an electron monochromator is perhaps the most critical region in the system (Read *et al.*, 1974). The size, angular spread, and aberrated radius of the electron beam must be carefully controlled at this point, and a multielement energy-changing lens is usually required to transport the beam from the (generally) higher-energy region of the electron source to the selector entrance. Similar lens systems are also required to transport and accelerate/decelerate the energy-analyzed electron beam to the scattering region.

Perhaps the most significant contributions to the design of electron optical systems in recent years have been the publication of extensive tables of calculated lens parameters for a large variety of two- and three-element cylinder, aperture, and slit lenses (Harting and Read, 1976) and the development of personal-computer-based ray tracing programs such as SIMION (Dahl and Delmore, 1988) and LENSYS (Heddle, 1991) for quick evaluation of electron optical systems of various geometries. The Harting and Read book represents a compilation and extension of the many lens calculations undertaken by the Manchester group (see Harting and Read for references) and is an invaluable asset to any experimental electron spectroscopist. This volume, and Heddle's book, also contains comprehensive introductions to the terminology and parameters used in lens design. Many other sources of calculated lens parameters for two- and three-element lenses also exist (e.g., Heddle, 1969; Klemperer and Barnett, 1971; Grivet, 1972; Natali *et al.*, 1972).

One disadvantage in the use of three-element lenses, particularly when used as zoom lenses (Cross *et al.*, 1967), is that it is difficult to maintain a constant image position and magnification over a wide zooming range. In general, if it is required to maintain n individual properties of an image, then $n-1$ independent voltage ratios will be required (Read, 1983). Design criteria for lenses of more than three elements can be found in the literature (e.g., Heddle, 1971b; Kurepa *et al.*, 1974; Chutjian, 1979; Fink and Kisker, 1980; Kisker, 1982). Recently Martinez and co-workers (Martinez and Sancho, 1983; Martinez *et al.*, 1983) applied a new version of the charge-density method (Read *et al.*, 1971) to calculate the focal properties, aberrations, and energy-scanning capabilities for a range of four-element cylinder lens configurations. Read (1983) has given design parameters for a three-cylinder lens with a movable midplane that can be used to maintain the required focal properties over a wider energy range than a fixed four-cylinder lens. Heddle and Papadovassilakis (1984) give experimental evidence of the ability of a five-element cylinder lens to maintain constant magnification over a wide range of overall voltage ratio.

While there have certainly been major advances in the design and application of energy analyzers and electron optical systems, no conventional high-resolution system has yet achieved those beam currents predicted by calculation, even when effects such as space charge and lens aberrations are accounted for. In fact, as has been discussed previously by Read (1983), the experimentally achieved electron-beam currents are generally a factor of 5–10 lower than those predicted by calculation. Read has postulated that this may be due to factors such as surface patch fields or a non-Maxwellian initial energy distribution in the electron gun. Other possible detrimental influences, particularly at the very high-energy resolutions obtained in recent experiments, may be the stability of power supplies at the mV level and, more importantly, the effects of stray-field broadening (Read, 1975).

Many other factors have contributed in part to the improvements in resolution and sensitivity of electron spectrometers in recent years. Prominent among these is the increased attention devoted to the maintenance of clean ultrahigh vacuum and uniform surface conditions. In most cases the latter has been attained by the use of turbomolecular pumping systems and extensive high-temperature bakeout. Jung *et al.* (1982) heat their spectrometer during operation to 100 °C to help preserve clean surface conditions. While many of the procedures used in different laboratories have almost entered the realm of folklore, it is clear that the maintenance of high resolution requires rigorous attention to *all* experimental details.

3. New techniques

There have been several new and elegant experimental techniques developed in the past decade that have made, or indicate the potential to make, a significant contribution to the study of atomic negative-ion resonances.

A high-resolution spectrometer based on a photoionization electron source has been developed and used at the Joint Institute for Laboratory Astrophysics (JILA). The experimental arrangement for this spectrometer is shown in Fig. 7 and described in detail by Gallagher and York (1974) and Kennerly *et al.* (1981). A beam of metastable $6s5d\,^1D_2$ barium atoms formed in a dc discharge at the exit of an oven is photoionized within the cavity of a He-Cd laser. The uv wavelength of 3250 Å (3.815 eV) results in the production of photoelectrons with an energy of 17 meV. These electrons are extracted from the photoionization region, accelerated, and focused by an electrostatic lens system onto the supersonic target beam of interest. The energy width of the electron beam so formed is limited mainly by the potential gradient established across the photoionization region by the slow-moving photoions and the Doppler broadening due to the relative motion of the photoions and electrons.

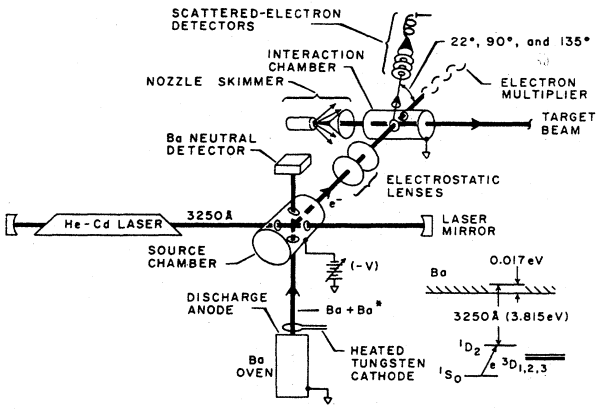

FIG. 7. Schematic of the experimental arrangement of Kennerly *et al.* (1981).

In measurements conducted with this system by Kennerly *et al.* (1981) on resonances in elastic scattering from Ar, N_2, and He, the widths of the observed features were dominated by Doppler broadening in the target gas beam. However, they could deduce that source widths of ≤ 2 meV at a beam current of 1×10^{-11} A are achievable with this system. In a series of impressive measurements on the He^- $1s(2s^2)\ ^2S$ resonance, they were able to routinely achieve an instrumental width of 5 meV at a beam current of 5×10^{-12} A. While these measurements, which will be discussed in Sec. IV.B, represent perhaps the most accurate determination of the ^2S resonance width and the *s*- and *p*-wave phase shifts at the resonance energy, it appears unlikely that the method could be used for a study of weaker, higher-lying features unless a significant increase in beam current could be achieved. A similar source that utilizes electrons produced by photoionization of argon by synchrotron radiation has recently been developed by Field *et al.* (1988, 1991) and applied to electron-molecule scattering.

Another promising area which has not yet been fully explored by high-resolution resonance studies has been the development of high-brightness, solid-state sources of polarized electrons. Several experiments (Heindorff *et al.*, 1973; Albert *et al.*, 1977; Wolcke *et al.*, 1983) have demonstrated the advantages to be gained from conducting resonance excitation with beams of spin-polarized electrons, even at relatively low intensity and energy resolution. This work is discussed in later sections. The new era of polarized electron sources that use photoemission from a GaAs crystal are capable of producing several microamps of beam current with an energy resolution of about 100 meV. Recently, Feigerle *et al.* (1984) demonstrated that by cooling the Ga As crystal to 77 K, an energy width of about 30 MeV is attainable with a beam current of 1 μA. Such high-resolution versions of these sources have not yet been specifically used for the investigation of resonance effects, but the advantages to be gained from their use are obvious. Indeed, regardless of the degree of polarization of the beam, these sources can provide, at an energy resolution of 30 meV, up to an order of magnitude more beam current than conventional combinations of thermionic emitters and electrostatic analyzers. One other possibility yet to be extensively explored for obtaining high-energy resolution is the use of a GaAs source as the input to a dispersive energy analyzer.

Yet another exciting development in electron spectroscopy has been the recent successes in the use of multi- or position-sensitive detectors. In a typical high-resolution electron spectrometer, the information collected through the exit aperture (real or virtual) of a dispersive energy analyzer represents only a small fraction of the total signal available at the image plane. It would be an obvious advantage to be able to gather the signal from discrete positions across the whole image plane simultaneously and thus span a significantly wider range of scattered electron energies. A number of systems have been developed in the past to improve the efficiency of conventional analyzers (see Granneman and Van der Wiel, 1983 and Hicks *et al.*, 1980 for a general discussion), but the most efficient seems to be that of Hicks *et al.* (1980, 1982), which uses a charge-coupled device as an image scanner. In this apparatus, electrons arriving at the image plane of a large (10 cm mean radius) hemispherical deflector are detected and amplified by channel plates and then accelerated onto a phosphor screen. The photon image from the phosphor is then transferred by an optical system to the charge-coupled device, which integrates the charge generated by the photon input to its 256 discrete channels and transfers the information to a data-acquisition system This apparatus has demonstrated that an improvement in efficiency of at least a factor of 100 over conventional spectrometers is possible. Furthermore, energy-loss measurements in CO (Wallbank *et al.*, 1983) show that it is capable of an energy resolution of 7 meV.

To our knowledge such a system has not yet been used in the study of atomic negative-ion resonances. The increase in sensitivity obtained in recent measurements of vibrational excitation functions in N_2 (Reddish *et al.*, 1984) indicates that its application to atomic systems would be of great benefit. The attainment of higher resolution in conventional spectrometers is almost always achieved at the expense of signal, and this ultimately restricts the range of experiments that is possible. Multidetectors may well provide the key to overcoming these problems.

Another emerging area that holds some promise is that of electron scattering in laser fields. A number of experiments in which both electron and photon excitation have been combined to study negative-ion resonances have been carried out. These have involved either discrete excitation (e.g., Hanne *et al.*, 1985; Zetner *et al.*, 1986) or free-free excitation (Langendam and Van der Wiel, 1978; Langhans, 1978; Weingartshofer *et al.*, 1983; Andrick and Bader, 1984; Bader, 1986). With the exception of the work in mercury (Hanne *et al.*), most of these studies have highlighted the substantive effect that resonances can have on the free-free cross section, but have not shed

any extra light on the assignments of the resonances concerned. The experiments of Langendam and Van der Wiel are somewhat different and will be discussed in more detail in Sec. IV.D.2.

B. Photodetachment spectroscopy

An area in which significant contributions have been made since the Schulz (1973a, 1973b) review is the field of negative-ion laser photodetachment. This field, which was in its formative stages in 1973, expanded rapidly during the 1970's mainly as a result of advances in both laser and negative-ion beam technology.

The first observation of resonance structure in a negative-ion photodetachment cross section was made by Lineberger's group at JILA (Patterson *et al.*, 1974) in a series of experiments to determine the electron affinities of alkali negative ions. In these experiments, and subsequent measurements by this group where resonances were observed (Slater *et al.*, 1978), a 2–2.5-keV negative-ion beam from a hot cathode discharge source is crossed with light from a tunable dye laser. A variety of reaction products including positive ions, neutrals, and electrons can be detected with this system as a function of laser frequency. A schematic of the apparatus is shown in Fig. 8 . For a single photodetachment process, several final channels may be available, depending on the energy of the detaching photon. In the case of the alkalis, with electron affinities in the range of 0.62–0.47 eV, the onset of neutral production at the photodetachment threshold corresponds to wavelengths in the range 2.0–2.64 μm, which is outside the range of available dye-laser systems. However, the energy required to leave the neutral alkali atom in its first excited state following photodetachment can be achieved with conventional dye lasers; thus the electron affinities can be accurately measured by detecting the production of the $n\,^2P$ excited states. In these experiments on the alkalis, both flash-lamp-pumped and argon-ion-pumped dye lasers were utilized, and, in the case of the Rb^- measurements, laser linewidths of ~ 0.5 cm^{-1} were used for high-resolution studies in the vicinity of the $5\,^2P_{1/2}$ excited-state threshold. While the principal aim of these experiments was the determination of the alkali electron affinities, the photodetachment cross sections for the heavier alkali ions (Cs^- and Rb^-) were dominated near the neutral excited-state thresholds by doubly excited states of the negative ion (resonances). These results are discussed in some detail in Sec. IV.C. A similar experiment with significantly higher photon resolution (~ 0.1 cm^{-1}) has been conducted in Rb^- by Frey *et al.* (1978) and is also discussed in Sec. IV.C.

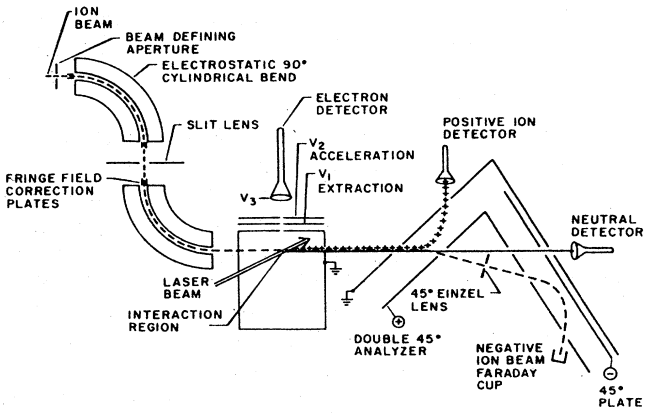

FIG. 8. Schematic of the laser photodetachment apparatus used by Slater *et al.* (1978).

A more recent development in the laser photodetachment (LPD) field has been the study of photodetachment of H^-. In a series of experiments at the Los Alamos Meson Physics Facility, Bryant and co-workers (Bryant *et al.*, 1977; Hamm *et al.*, 1970; Clark *et al.*, 1980) crossed a beam of relativistic H^- ions (800 MeV) with pulsed light from a nitrogen (Bryant *et al.*, 1977) or Nd:YAG (Hamm *et al.*, 1979) laser. By changing the angle of intersection of the two beams, the photon energy in the ion rest frame can be continuously varied according to the equation

$$E_{h\nu}=\gamma E_{\rm lab}(1+\beta\cos\alpha)\ ,$$

where α is the angle between the beams, $\beta=v/c$ for the H^- ions, $\gamma=(1-\beta^2)^{-1/2}$, and $E_{\rm lab}$ is 3.678 eV for the nitrogen laser and 4.65 eV for the Nd:YAG laser. For the LAMPF H^- beam with $\beta=0.842$, this results in a tunable photon energy range of 1.8 to 11.5 eV and 1.63 to 15.6 eV for the nitrogen and Nd:YAG lasers, respectively. Photodetached electrons resulting from the interaction are removed from the ion beam downstream from the interaction region by application of a small magnetic field and are identified by virtue of both their energy and temporal relationship to the laser pulse. Resonances in the smoothly varying photodetachment cross section are detected when the process proceeds via an excited state of H^-, and the energy of the resonance (by necessity of $^1P^\circ$ symmetry) is given by the photon energy at the resonance minus the binding energy of H^- (0.754 eV) in its ground state. This technique has been used to study H^- resonances in the vicinity of neutral excited states of H up to $n=6$, and these results are discussed in Sec. IV.A.

Photodetachment spectroscopy has also been used by the SRI group to study resonances in a range of atomic negative ions including, among others, He^- (Peterson *et al.*, 1983, 1985) and Ca^- (Peterson, 1992). These are discussed in more detail in later sections.

C. Collisions of negative ions with atoms

Heavy-particle collisions have also proved very useful in the study of the spectra of various negative ions, particularly for many reactive species such as the halogens and atomic hydrogen and oxygen, where there is only sparse information from electron-scattering experiments. In general, those experiments that have proven the most

informative have involved the collision of fast (1–10 keV) negative-ion beams with thermal atomic and molecular beams. Less energetic collisions do not appear to produce excited negative-ion states.

The negative-ion beams are usually produced in a gas discharge source such as a duoplasmatron ion source (Aberth and Peterson, 1967). They are then extracted and momentum analyzed before being focused onto the atomic beam of interest. Electrons that result from the collision are energy analyzed, typically in a dispersive electrostatic analyzer (e.g., Edwards *et al.*, 1971; Cunningham and Edwards, 1973, 1974) or by time-of-flight techniques (e.g., Fayeton *et al.*, 1978). These electrons can result from a number of different collision processes, but only those involving excitation of some sort, of either the beam or target species, will lead to structure in the yield of electrons as a function of energy. In particular, if the collision results in the formation of doubly excited states in either the beam, as a result of direct excitation,

$$A^- + B \rightarrow A^{-**} + B \rightarrow A^{(*)} + B + e^- ,$$

or the target,

$$A^- + B \rightarrow A + B^{-**} \rightarrow A + B^{(*)} + e^- ,$$

as a result of charge exchange plus excitation, then the electron spectrum should show structure corresponding to the energy of these excited negative-ion states.

The energy resolution in most of these experiments has been better than 100 meV, and the absolute accuracy of the energy calibration as high as 20 meV.

IV. REVIEW OF SPECIFIC RESULTS BY ELEMENT

A. Hydrogen

As the simplest possible negative-ion system, H^- has been treated in numerous theoretical calculations and has been subjected to a variety of modelistic descriptions. Early experimental studies have been less prolific, due mainly to the technical difficulties associated with *e-H* scattering and with H^- photodetachment in the resonance region (around Ly-α wavelengths). At the time of Schulz's 1973 review, three H^- resonances had been clearly observed experimentally in the region of the $n=2$ excited states (e.g., in the transmission experiments of Sanche and Burrow, 1972), and there was evidence for many more structures in the vicinity of the $n=3$ excited-state thresholds (e.g., in the optical excitation functions of McGowan *et al.*, 1969).

The amount of experimental work on this system increased dramatically in the late 1970s and early 1980s, due to the development of a relativistic ion-beam apparatus that enabled photodetachment studies to be carried out with laser techniques (Bryant *et al.*, 1977—see Sec. III.B), and due to the improvement of H atom sources to enable high-resolution electron-impact studies (Slevin and Sterling, 1981). Both experimental and theoretical studies have advanced beyond the point at which a spectroscopic description of the H^- spectrum in terms of isolated resonances is either feasible or desirable. For example, Ho and Callaway (1986) give a table of over 150 resonances converging to the $n=4$, 5, and 6 thresholds of H. In the period immediately following the Schulz review, there were a number of further observations of resonances in H^-. In the light of the recent experimental advances, we shall not summarize all of these, but recommend the articles of both Williams (1976a, 1976b) and Risley (1980) as excellent reviews of work carried out in the 1970s.

The lowest-lying resonance in H^- is the $2s^2\ ^1S$ state, which, combined with the effects of other resonances, was first observed experimentally by Schulz in 1964. This resonance lies below the first excited state of neutral hydrogen (10.200 eV) and thus can only be observed in the elastic channel in electron-scattering measurements or in the ejected electron spectra resulting from an ion-atom collision. There is excellent agreement for the energy of this resonance between high-resolution elastic differential cross-section measurements (9.557±0.010 eV—Williams, 1976a; 9.549±0.013 eV—Warner *et al.*, 1990), high-resolution electron transmission experiments (9.558±0.010 eV—Sanche and Burrow, 1972), and in studies of the energy spectra of ejected electrons following collisions of H^- and He, Ar and N_2 (9.59±0.030—Risley *et al.*, 1974). However, the two determinations of the width of this state differ slightly, with Williams measuring a value of 45±5 meV while Warner *et al.* find it to be 63±8 meV.

On the theoretical side there have been many calculations of both the energy and the width of the $2s^2\ ^1S$ resonance using a variety of techniques: for example, the Feshbach projection operator (Bhatia and Temkin, 1974; Temkin and Bhatia, 1985, and references therein); complex rotation (e.g., Bardsley and Junker, 1972; Bain *et al.*, 1974; Doolen *et al.*, 1974; Ho, 1977; Wendoloski and Reinhardt, 1978); and close-coupling approaches (e.g, Burke *et al.*, 1967; Taylor and Burke, 1967; Seiler *et al.*, 1971; Morgan *et al.*, 1977). The results of these range in value between 9.54 and 9.59 eV for the position and 40 and 54 meV for the width, both of which are in good general accord with the experiments.

Also located below the 2*s*-2*p* excitation thresholds are the $2s2p\ ^3P^\circ$ and $2p^2\ ^1D$ resonances. These have been clearly observed in a range of experiments similar to those described above. The most accurate experimental estimates for the energy of the $^3P^\circ$ state are from Williams (1976a, 9.735±0.010 eV), Warner *et al.* (1986, 9.736±0.013 eV), and Sanche and Burrow (1972, 9.738±0.010 eV). Clearly there is good accord between these measured values for the position, and a similar level of agreement is observed for the width (5–6 meV) of this state. Theoretical estimates (Burke *et al.*, 1967; Taylor and Burke, 1967; Seiler *et al.*, 1971; Mercouris and Nicolaides, 1991) range between 9.74 and 9.77 eV for the position and 6 and 8 meV for the width of the state. The

^1D resonance position has been accurately measured by Sanche and Burrow and Warner *et al.*, who find energies of 10.128±0.010 eV and 10.115±0.013 eV, respectively. They are also in good accord as to the width of this state with values of 7.3±2 meV and 6.0±2 meV, respectively. The calculations appear to generally overestimate both the energy (10.12–10.16 eV) and the width (8–9 meV) for this state. Figure 9 shows an example of electron elastic-scattering determinations of the resonances below the $n=2$ thresholds.

Several other resonances were predicted, by calculation, to exist below the threshold for the first excited state of neutral hydrogen. They are the $2p^2\ ^1S$ and the $2s2p\ ^1P^\circ$ and a ^3S state. There is some evidence for the $2p^2\ ^1S$ state in the elastic measurements of Warner *et al.* (1986) at a scattering angle of 54° where the contribution from the ^1D resonance is minimal, and Sanche and Burrow place the $2s2p\ ^1P^\circ$ resonance, observed in electron transmission at 10.128±0.010 eV. The former is in good general agreement with the predicted energy (Burke *et al.*, 1967; Taylor and Burke, 1967; Seiler *et al.*, 1971) of 10.178 eV, while the latter is some 50 meV below the range of predicted theoretical values (10.177–10.185 eV).

Autodetaching states of H^- have been observed, both below and above the $H(2p)$ threshold, in collisions of energetic H^- $(1s^2\ ^1S)$ with rare-gas atoms (Risley, 1972; Risley *et al.*, 1974; Risley and Geballe, 1974). These experiments, in which the autodetached electrons are detected over a range of scattering angles with a typical energy resolution of 50 meV, provide evidence for four excited states of H^-, three below and one above the $H(2p)$ threshold. Those observed below the threshold were classified as $2s^2\ ^1S$ (9.59±0.03 eV), $2s2p\ ^3P^\circ$ (9.76±0.03 eV), and $2p^2\ ^1D+2s2p\ ^1P^\circ$ (10.18±0.03 eV), all of which are in reasonable to good agreement with the values from high-resolution electron scattering. Risley *et al.* (1974) also contains an excellent summary of work in this area, both experiment and theory, prior to 1974.

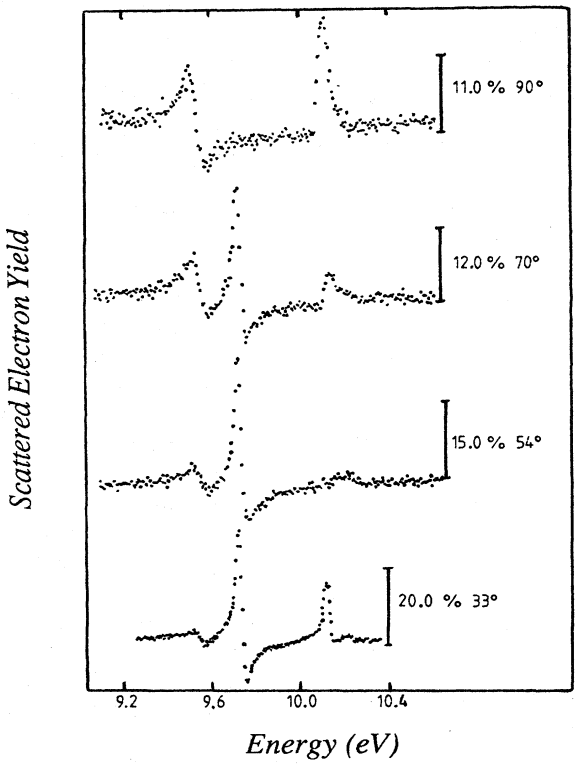

FIG. 9. Elastic electron scattering below the $n=2$ threshold of hydrogen at various scattering angles (from Warner *et al.*, 1986).

H^- resonances have also been observed in electron-molecular hydrogen scattering experiments. In these experiments (Huetz and Mazeau, 1981) the resonant states are observed in the decay of short-lived molecular negative-ion resonances:

$$e^-_{\text{inc}}+H_2\rightarrow H_2^-\rightarrow H(1s)+H^-(2l2l')$$
$$\rightarrow 2\ H(1s)+e^-_{ej}\ .$$

They observe five features in excitation functions of the nuclear continuum at various energy-loss values which they attribute to atomic negative-ion resonances. In general, the energies they assign are in good agreement with other measurements performed with higher resolution. They also tentatively assign a structure at 10.18±0.04 eV as $2p^2\ ^1S$, which appears to be in good agreement with the observation of Warner *et al.* (1986), covered later in this review.

Without doubt, most interest in this energy region has centered on the threshold behavior of the cross sections for the $2s$ and $2p$ excited states and the predicted $2s2p\ ^1P^\circ$ shape resonance just above the thresholds for these excited states. Damburg and Gailitis (1963) predicted that the cross sections for these states would be finite at threshold. This was first shown experimentally by Chamberlain *et al.* (1964), who measured the yield of Ly-α photons following electron-impact excitation of $H(2p)$. By unfolding the energy resolution of their apparatus from the measured spectrum, they were able to show good agreement with the predicted cross section of Damburg and Gailitis. The existence of a $2s2p\ ^1P^\circ$ shape resonance above the threshold for the $2s$ and $2p$ levels was first predicted in a three-state close-coupling calculation by Taylor and Burke (1967). Shortly after this the first observation of this resonance was made by Williams and McGowan (1968) and McGowan *et al.* (1969) in an experiment where the optical excitation function for the $2p$ state was measured with an energy resolution of 0.07 eV. They found a resonance at threshold, in good agreement with the calculated position of 10.214 eV but with a width that appeared slightly larger than the calculated value of 0.015 eV. They also observed several subsidiary maxima in the near-threshold cross section, which were explained in an accompanying paper (Marriott and Rotenberg, 1968) as interference effects between resonant and nonresonant scattering. In a subsequent, similar experiment performed with the same energy resolution but

with considerably higher statistical accuracy, Williams and Willis (1974) observed only one $^1P^\circ$ resonance above the $2p$ threshold and suggested that its true width was less than that calculated by Taylor and Burke.

In parallel with the electron-scattering investigations of this resonance, there has been considerable interest in its detection in both photoabsorption and photodetachment experiments on H^-. It will be strongly coupled to the H^- $1s^2\ ^1S$ ground state, and its predicted energy indicates that it should appear in the photoabsorption cross section at a wavelength of 1129.5 Å [10.976 eV, equivalent to the predicted energy of 18 meV above the $H(2p)$ threshold at 10.204 eV plus the electron affinity of H^-, 0.754 eV]. Macek (1967) calculated the peak photoabsorption cross section for H^- in the vicinity of this resonance to be 1.5×10^{-16} cm^2, which is about 25 times the background photoionization cross section. Using this calculation as a base, Ott *et al.* (1975) searched for the $2s2p\ ^1P^\circ$ shape resonance of H^- in a plasma emission experiment. They found no obvious indication of any structure between the wavelengths of 1105 and 1135 Å. This negative result was explained by a series of calculations by Broad and Reinhardt (1976) and Wendoloski and Reinhardt (1978), who indicated that the resonance structure would be much weaker than expected due to a smaller oscillator strength for the transition and the effects of processes such as Stark broadening and molecular background. In a subsequent plasma experiment, similar to that of Ott *et al.* but presumably with higher sensitivity, Behringer and Thoma (1978) were able to demonstrate clearly the presence of this resonance at the predicted energy.

However, the experiments that have shed the most light on this particular resonance are the H^- photodetachment measurements of Bryant and collaborators (e.g., Bryant *et al.*, 1977). These experiments, which have been described in detail in Sec. III.B, involved a measurement of the photodetachment cross section at incident photon energies between 10.90 and 11.10 eV, with respect to the H^- ground state. They reveal two clear resonance features (see Fig. 10). The first is a sharp $^1P^\circ$ Feshbach resonance at a photon energy of 10.93 eV, which, with respect to the ground state of the H atom, is at 10.176 eV, in excellent agreement with calculated values (Burke and Taylor, 1966; Taylor and Burke, 1967; Seiler *et al.*, 1971). The second is a broad shape resonance feature at a photon energy of 10.980 eV [10.226 with respect to $H(1s)$], which places it above the $H(2p)$ threshold as predicted. In these measurements it has an apparent width of 22±3 meV. Subsequent measurements in this energy region (MacArthur *et al.*, 1985) give a more accurate value for the energy of the Feshbach resonance of 10.1722±0.0006 eV.

Resonances between the $n=2$ and $n=3$ thresholds of neutral hydrogen have been observed in a number of experiments. Semiresolved structure was first seen in this energy region in the measurements of McGowan *et al.* (1969) and, subsequently, by Koschmieder *et al.* (1973).

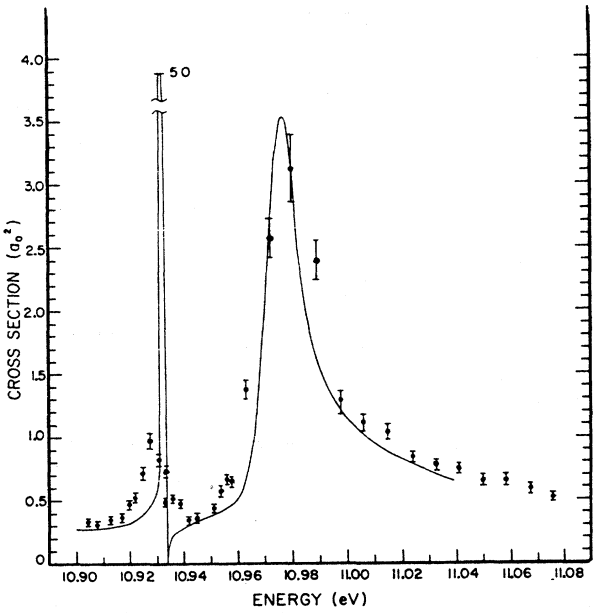

FIG. 10. Photodetachment cross section for H^- in the region of the $n=2$ threshold (from Bryant *et al.*, 1977).

Spence (1975a) identified a lone structure in a transmission experiment at an energy of 11.86±0.03 eV, which he classified as a ^1D resonance. A substantial amount of the current information on resonances in this region has come from a wonderful series of electron-scattering experiments by Williams (1988) with sub-10-meV energy resolution. These experiments, which measured the absolute excitation cross section for both $H(2s)$ and $H(2p)$ from threshold to about 12 eV, give a beautiful illustration of the finite excitation cross section at threshold and the effect of the shape resonance on the near-threshold cross section (see Fig. 11). These data and recent inelastic electron differential cross-section measurements by Warner *et al.* (1990) are in excellent agreement with one another and with the close-coupling calculation of Callaway (1982) for the positions and widths of 13 H^- resonances below the $n=3$ threshold. This calculation includes a basis set of 18 states, seven of which are exact hydrogenic functions (all states up to $n=3$ plus the $4f$) and the remaining 11 are pseudostates. In particular, the level of agreement shown between the experimental (Williams, 1988) and the calculated $2s$ and $2p$ total cross sections is remarkable (Fig. 12). In some cases the two experiments are entirely complementary, as features that do not appear in the high-resolution integral cross-section measurements are present at certain scattering angles in the lower-resolution (typically 25 meV) differential measurements. In other cases, particularly at higher energies approaching the $n=3$ threshold, neither experiment is capable of identifying all of the resonances that are predicted by Callaway (1982). More recent calculations by

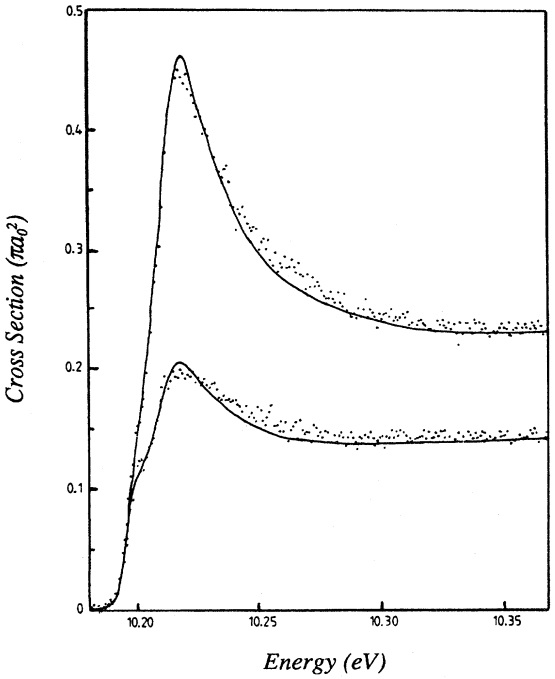

FIG. 11. Near-threshold excitation cross sections for H(2s) and H(2p). From Williams (1988).

Callaway (1990) of differential angular cross sections and spin asymmetry parameters yield information that could provide more detailed classification of these resonances.

There have recently been several other theoretical investigations of resonance energies in this region. Pathak *et al.* (1988) calculated the positions of a host of resonances converging on the $n=2$, 3, and 4 neutral thresholds in a 15-state R-matrix approach. They found excellent agreement with the experimental values discussed above for resonances below the $n=2$ and 3 thresholds.

In a series of photodetachment experiment of the type mentioned above, Hamm *et al.* (1979) observed resonance structure much closer to the $n=3$ threshold. They measured two pronounced dips in the photodetachment cross section at photon energies of 12.650 and 12.837 eV. They interpreted these structures as the first two members of a $^1P^\circ$ Feshbach resonance series that converges on the $n=3$ neutral thresholds. They further predict, based on their experimental observations of the widths and q values for these resonances and agreement with various calculations (Chung, 1972; Oberoi, 1972; Morgan *et al.*, 1977; Greene, 1980c), that these resonances belong to a "+" Feshbach series; i.e., they are states where the two excited electrons reside at approximately equivalent distances from the core, and the wave function is approximately even under radial exchange. These states are likely to be less stable against autodetachment than the "−" states, where the two electrons have different radial separations.

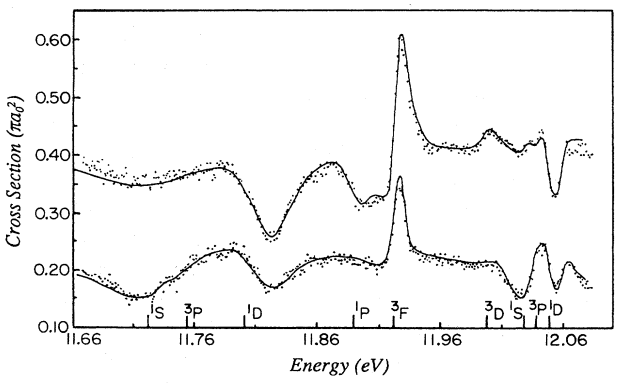

FIG. 12. Excitation cross sections for production of H(2s) and H(2p) between the $n=2$ and $n=3$ thresholds (from Williams, 1988).

In a more recent and extremely impressive investigation of resonances in the photodetachment cross section, Harris *et al.* (1990; Harris, Bryant, *et al.*, 1990) observed series of resonances converging on the $n=5$, 6, 7, and 8 neutral hydrogen thresholds. By monitoring the yield of excited neutral hydrogen, they observed structures due to resonances formed in the process

$$H^- + \gamma \rightarrow H^{-**} \rightarrow H^*(\leq n) + e^- .$$

The excited states are detected by detaching the excited electron in a strong electric field whose strength is successively reduced to enable observation of selectively higher excited states. The high-energy photons are obtained from the fourth harmonic of a Nd:YAG laser. Harris *et al.* stress the importance of selectively isolating the excited final states of neutral hydrogen in observing any resonance structure. This is apparently due to the preferential decay of resonances with principal quantum n to excited neutral states with $(n-1)$.

They observe a total of 13 resonance features converging on these thresholds with an absolute uncertainty in position of 1 meV and an energy resolution of about 8 meV (Fig. 13). The observed structures are mainly dips in the photodetachment continuum, but, as they indicate some asymmetry, an extensive fitting process to sets of Fano profiles has been applied to accurately extract their energies and widths. Furthermore, by combining the modified Rydberg formula (Read, 1977), which gives the energy of the lowest resonance in a series, with a recursion formula (Gailitis and Damburg, 1963) to give the energies of subsequent resonances, they obtain excellent agreement (within a few meV) with the experimental data for almost all of the observed structures. This high level of agreement led them to conclude that the observed series of resonances, which are the lowest "+" series, dominate the spectrum. There is also good agreement with the calculated values of Ho and Callaway (1986), Pathak *et al.* (1988, 1989), Koyama *et al.* (1989), and Ho (1990) for the widths of the lowest-lying member of each series converging on the $n=5$, 6, and 7 thresholds. It is interesting to note that the members of each series be-

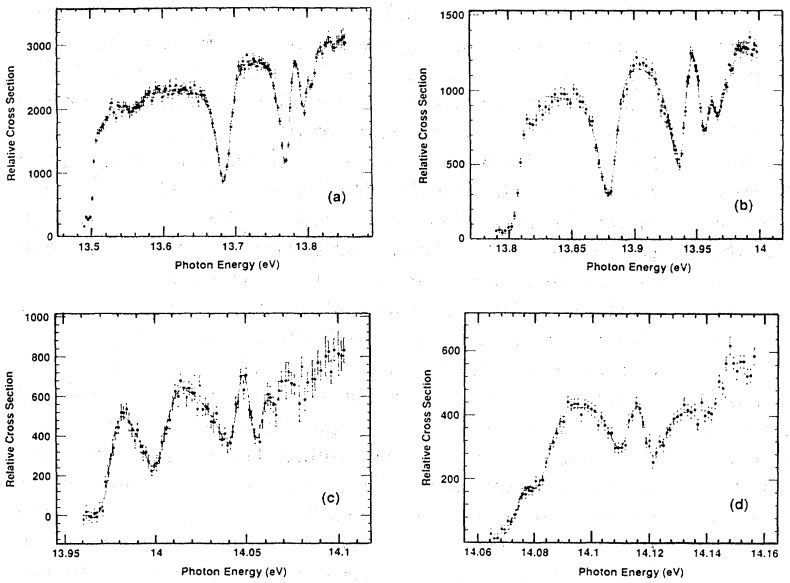

FIG. 13. Partial photodetachment cross sections for H^- showing production of neutral hydrogen in (a) $n \geq 4$; (b) $n \geq 5$; (c) $n \geq 6$; and (d) $n \geq 7$ (from Harris *et al.*, 1990.

come progressively narrower and thus progressively more stable against autodetachment. It also appears that the lowest member of each series may become somewhat broader as n increases, although this trend is marginal.

In a concurrent theoretical study, Sadeghpour and Greene (1990) calculated adiabatic hyperspherical potential curves for highly excited states of H^- converging on neutral excited states with $n \leq 12$. They demonstrate that the resonances observed in the above experiments are in fact associated with the lowest "+" state within each n manifold and propose that their dominance in the photodetachment cross section is evidence of a new selection rule involving the approximate conservation of the bending vibrational quantum number v (see Sec. II). They also use a similar combination of modified Rydberg formula and recursive relation to fit both the experimental resonance positions and those calculated by Ho and Callaway (1986; Ho, 1990) and find excellent agreement for both the screening parameter σ and the quantum defect μ, derived from these fits. It is also of interest to note that plots showing comparisons of the observed experimental resonance positions, expressed as the energy below the double detachment thresholds, with those calculated from the above formula indicate that the lowest resonance in each series is a ridge resonance, while the subsequent resonances become increasingly planetary in nature. Sadeghpour (1991) elaborates upon these selection rules and demonstrates that the experimental spectra of Harris *et al.* that converge to each n can be fit well by a two-channel quantum-defect theory, in which the open channel is taken to be the "+" channel associated with $n-1$. This supports the idea that the dominant autodetachment channel for these resonances is that associated with the closest threshold. This result has also been found by Chrysos *et al.* (1992), who have computed partial widths of $^1P^\circ$ resonances converging to the $n=3$, 4, and 5 thresholds.

Ho (1992) has calculated the positions of the $^1P^\circ$ resonance series converging on the $n=3-9$ hydrogen thresholds, as observed in the experiments of Hamm *et al.* (1979), Cohen *et al.* (1987), and Harris *et al.* (1990; Harris, Bryant, *et al.*, 1990). In general, he finds excellent agreement with both the experimental resonance energies and those from the calculations discussed above. At higher values of n there are some differences between his calculated and the measured widths, although most of these cases involve resonance widths that are less than the experimental resolution and are thus subject to some additional uncertainty (Harris, Bryant, *et al.*, 1990).

Recommended values for the energies, widths, and classifications of negative-ion resonances in H^-, including those in the $(KT)^A$ coupling scheme, are given in Table I.

We now discuss the effects of external fields.

There have been many studies, particularly in recent years, on the effects of external electric and magnetic fields on highly excited atomic Rydberg states. In contrast, there has been little work done in this area on transient excited states of negative ions, and the bulk of this effort has been concentrated on H^- (e.g., Gram *et al.*, 1978; Wendoloski and Reinhardt, 1978; Bryant *et al.*, 1983; Lin, 1983a, Cohen *et al.*, 1987). There have also been several investigations of resonance excitation in the rare gases in the presence of laser fields, and this work is discussed further in Sec. IV.D.

The effect of external fields on the low-lying H^- resonances has been extensively reviewed (Bryant, 1980; Bryant *et al.*, 1981; Smith *et al.*, 1985; Lin, 1986), and, as the ramifications of this work are somewhat peripheral to the main thrust of the present review, we shall only

briefly summarize the salient features.

Gram *et al.* (1978) studied the effects of external electric fields of between 1.2×10^6 and 5.5×10^7 V/m on both the shape and Feshbach $^1P^\circ$ resonance near the $n=2$ neutral excited-state threshold. They found quite different behavior, the Feshbach resonance splitting into three components at low-field strengths which then disappeared, at differing values as the field strength was raised to around 2×10^4 V/m. They did note that the two outermost components of this resonance showed characteristics of a linear Stark shift while the middle component appeared to be due to the quadratic Stark shift. On the other hand, the shape resonance was essentially unaffected at similarly low values of the external field strength and appeared to decrease in strength and broaden considerably for fields in excess of 5×10^7 V/m. Gram *et al.* postulated several possible explanations for this observed behavior and noted that it was qualitatively very similar to that calculated by Wendoloski and Reinhardt (1978).

This experimental work prompted calculations by Callaway and Rau (1978), using the stabilization method (see Sec. II), of the positions of H^- resonances and their behavior under the influence of an electric field. They note that the near degeneracy of the $^1P^\circ$ resonance and the second member of the ^1S resonance series [$^1S(2)$] lead to a linear Stark effect that is responsible for the behavior observed by Gram *et al.* (1978). They interpret the "triplet" observed by Gram *et al.* as features due to the $^1S^e$ ($M=0$) and $^1P^\circ$ ($M=0$ and $M=\pm1$), the $^1S^e$ resonance being excited as a result of the Stark mixing in the external field. Their results were in good qualitative agreement with the observations of Gram *et al.*

These earlier experimental studies were extended by Bryant *et al.* (1983), who increased the range of the electric-field strength covered to 1.3×10^8 V/m and introduced polarized laser photons as a means of probing the resonance structure, in particular, that of the Feshbach triplet. These studies confirmed the earlier measurements and demonstrated that the two outer components of the split Feshbach resonance have $M=0$ while the inner is due to $M=\pm1$. Based on the simple model of Stark mixing, they also interpret the two lower resonance as the $M=0$ and $M=\pm1$ branches, respectively, of the $^1P^\circ$ Feshbach resonance, with the upper feature being due to the $^1S^e$ resonance.

TABLE I. Recommended energies, widths, and classifications for negative-ion resonances in hydrogen. Energies are expressed relative to the 1*s* ground state of *H*. Experimental values are from Warner *et al.* (1986, 1990), Williams (1976a, 1976b, 1988), Cohen *et al.* (1987), and Harris *et al.* (1990; Harris, Bryant, *et al.*, 1990). Figures in parentheses following the energies and widths represent the uncertainty in the least significant digit. Those following the classifications indicate the recursion number calculated by Ho (1992).

Classification	$(KT)^A$	Energy (eV)	Width (meV)	Comments
$2s^2\,^1S$	$(10)^+$	9.557(10)	63(8)	
$2s2p\,^3P^\circ$	$(10)^+$	9.735(10)	5(2)	
$2p^2\,^1D$	$(10)^+$	10.115(13)	6(2)	
$2s2p\,^1P^\circ$	$(10)^-$	10.1722(6)		Feshbach resonance
$2s2p\,^1P^\circ$	$(01)^+$	10.226(2)	22(3)	Shape resonance
^1S	$(20)^+$	11.722(9)	37(8)	
^1D	$(20)^+$	11.807(9)	45(8)	
$3s3p\,^1P^\circ(1)$	$(20)^-$	11.902(6)	33(10)	Electron scattering
		11.900(7)	27.5(0.8)	Photodetachment
$^3F^\circ$	$(20)^+$	11.925(2)	4(2)	
^3D	$(20)^-$	11.997(5)	10(3)	
^1S	?	12.029(5)	9(3)	
$^3P^\circ$	$(20)^+$	12.036(4)	10(4)	
^1D		12.049(4)	7(3)	
$3s3p\,^1P^\circ(4)$		12.082	1.6(0.3)	Photodetachment
$5s5p\,^1P^\circ(1)$		12.9316(3)	21.5(5)	
$5s5p\,^1P^\circ(4)$		13.0166(3)	14.1(7)	
$5s5p\,^1P^\circ(7)$		13.0377(11)	14.3(7)	
$6s6p\,^1P^\circ(1)$		13.1270(3)	13.0(3)	
$6s6p\,^1P^\circ(4)$		13.1837(2)	10.5(3)	
$6s6p\,^1P^\circ(10)$		13.2015(1)	8.4(3)	
$6s6p\,^1P^\circ(?)$		13.2086(1)	1.4(1)	
$7s7p\,^1P^\circ(1)$		13.2482(7)	12.4(14)	
$7s7p\,^1P^\circ(3)$		13.2914(7)	4.9(9)	
$7s7p\,^1P^\circ(7)$		13.3016(2)	0.9(2)	
$8s8p\,^1P^\circ(1)$		13.326(10)	3.1(1)	
$8s8p\,^1P^\circ(?)$		13.3590(2)	1.39(4)	
$8s8p\,^1P^\circ(?)$		13.3629(3)	1.13(6)	

At field strengths in excess of 4×10^7 V/m, Bryant *et al.* (1983) observe a further feature at energies below the split Feshbach resonance. They believe that this is due to a ^1D Feshbach resonance which, although normally not accessible from the H^- ground state by single photoabsorption, can be excited in the presence of a strong external field via its mixing with the nearby $^1P^\circ$ states. Its apparent energy is in good accord with a calculation by Burke (1968). They also propose that this resonance may be split into two components, presumably $M=0$ and ±1 components. They also observe that the upper branch of the Feshbach resonance may not, in fact, be quenched at high electric fields, as there is experimental evidence for a small shoulder on the shape resonance at electric-field strengths above 4×10^7 V/m which gradually becomes consumed by the broadening shape resonance as the field strength is further increased.

There is some uncertainty as to the relative positions of the zero-field $^1P^\circ$ and $^1S(2)$ resonances. The Los Alamos experiments are consistent with the $^1P^\circ$ lying below the ^1S as the calculation of Callaway and Rau indicates is the case, the difference in the calculated energy being 2.3 meV. However, the calculation of Callaway (1978), which was undertaken to investigate this question (among others), indicates the $^1P^\circ$ is 0.6 meV above the ^1S. The more recent calculation of Pathak *et al.* (1989) predicts that the $^1S(2)$ lies 1 meV *above* the $^1P^\circ$.

The shape resonance itself was shown, in this latter series of measurements, to initially narrow for the low-field strengths where the Feshbach resonance begins to quench, and then to broaden considerably until, at 1.3×10^8 V/m, it had a width of approximately 60 meV, up from the zero-field value of about 20 meV, but still showed no sign of quenching.

In a more recent series of experiments, Cohen *et al.* (1987) studied the effects of strong ($0-2.36\times10^8$ V/m) external electric fields on the $^1P^\circ$ Feshbach resonance at an energy of 12.650 eV in the H^- photodetachment cross section below the $n=3$ thresholds. They observed this feature to gradually broaden as the field strength was increased until it was quenched at the maximum field strength.

A recent theoretical paper by Mercouris and Nicolaides (1991) presents results on the width of the $2s2p\ ^3P^\circ$ resonance of H^- in both ac and dc electric fields. They note that this resonance is much less sensitive to a dc field than is the $^1P^\circ$ shape resonance.

B. Helium

1. Resonances below the first ionization potential

The negative-ion resonance spectrum of helium has been the subject of the most extensive experimental and theoretical investigation of any element in the periodic table. It was, in fact, the $He^-\ 1s(2s^2)\ ^2S$ resonance that was the first such state positively observed and identified in an electron-scattering experiment by Schulz (1963). Since that pioneering observation, resonances in the helium atom have been studied in an impressive variety of electron-scattering experiments where the energy dependence of reaction products such as electrons (elastic and inelastically scattered and transmitted), decay photons, and metastable atoms has been measured. Recently there have also been observations of resonance states, which by virtue of their parity or angular momenta are inaccessible by electron-impact excitation, during the photodetachment of metastable helium ions.

The abundance of experimental interest and the relative ease of describing the e^-+He scattering process have also resulted in significant theoretical interest in the spectroscopy of He^- and in the mechanisms responsible for the formation of the negative-ion states. In fact, as has already been demonstrated in Sec. II, several new methods including group-theoretic and classical Wannier techniques have been adopted to describe many of these He^- features in terms of two excited electrons in a highly correlated state.

The logical place to begin any discussion on He is with the well-established, lowest-lying $1s(2s^2)\ ^2S$ resonance at 19.37 eV, which is observable only in elastic electron scattering. Since its first observation, much effort has been devoted to the determination of its energy and width and to the value of the scattering phase shifts at the resonance energy. These parameters have been used extensively for the absolute calibration of the energy and width of high-resolution electron beams and as a means of calibrating absolute electron-scattering cross sections. The extent of the interest shown in their determination can be gauged from Fig. 14, which documents the many experimental and theoretical investigations of the width of this resonance over the past 20 years. It is interesting to note that the most recent, and most accurate, estimate of the width by Kennerly *et al.* (1981) is in excellent agreement with the first experimental determination made by Simpson and Fano (1963).

This resonance has been discussed in much detail in many papers and review articles, and we do not wish to dwell further upon it here other than to record what we believe to be the best current estimates for its energy and width. The first high-accuracy (uncertainty <10 meV) measurement of the resonance energy was performed by Cvejanovic *et al.* (1974), who measured the relative position of the (fitted) ^2S resonance center to that of the (fitted) center of the cusp at the 2^3S threshold in elastic scattering at 19.819 eV. Their value of 19.367 ± 0.009 eV was higher than most previous values, including that of Mazeau *et al.* (1973), who determined an energy of 19.345 ± 0.009 eV from the relative position of the resonance to the 2^1S threshold. Cvejanovic and Read (1974) derived a value of 19.361 ± 0.009 eV from their measurements of threshold excitation in He. The 2^2S resonance is present in these measurements through a secondary process, and its energy was again determined from its position relative to the 2^3S threshold. The most accurate

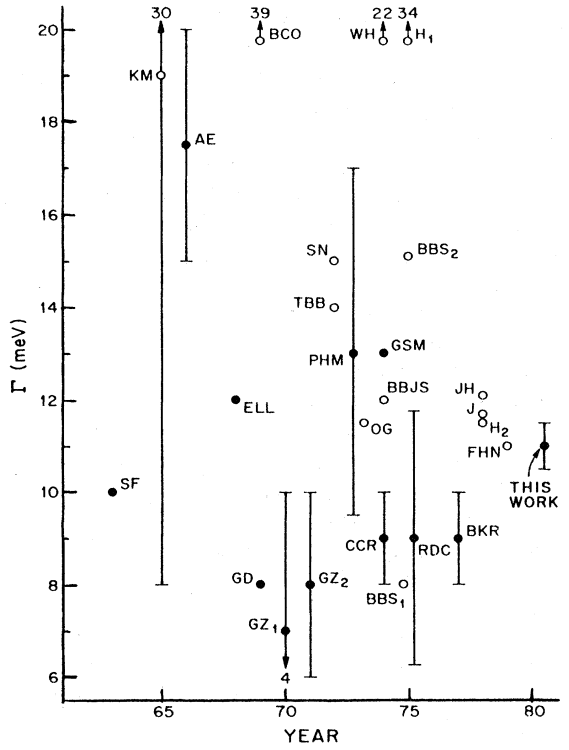

FIG. 14. Published results for the natural width of the $1s2s^2\,{}^2S$ resonance (see Kennerly *et al.*, 1981, for details of references).

measurement to date is that of Brunt *et al.* (1977c), who used a technique similar to that of Cvejanovic *et al.* (1974), but with improved sensitivity, to obtain a resonance energy of 19.366±0.005 eV.

The width of this resonance, as noted above, has recently been accurately determined in an experiment by Kennerly *et al.* (1981). The details of this experiment have been discussed in Sec. III.A, the essential improvements over previous measurements being the use of near-threshold laser photoionization as a source of monochromatic electrons ($\Delta E \sim 2$ meV) and a reduction in the Doppler broadening of the resonance profile through the use of a supersonic atomic beam. This technique yielded a resonance width of 11.0±0.5 meV, a value which is slightly higher than most other recent measurements. Kennerly *et al.* believe that this difference is possibly due to the presence of finite background levels in the other measurements, all of which assumed the background to be zero. Also shown in Fig. 14 are theoretical estimates for the width of this resonance, most of which are in good agreement with the above experimental value. The most recent theoretical estimate of the width of this resonance, 11.7 meV, by Fon *et al.* (1989), is in excellent agreement with the experimental value. A complete discussion of both experimental and theoretical comparisons can be found in Kennerly *et al.* and Brunt *et al.* (1977c). In our general classification nomenclature this state is an *a*-type resonance.

One of the earliest observations of this resonance, that of Kuyatt *et al.* (1965), also indicated the presence of a weak feature on the high-energy side of the ^2S resonance at an energy of about 19.45 eV, which they tentatively classified as $He^-\ 1s(2s2p)\ ^2P$. Further observations of a structure at this energy were made by Gibson and Dolder (1969) and Golden and Zecca (1970). In the latter case five weak, narrow structures were observed in the energy interval between the ^2S resonance and the 2^1S threshold. These structures were not observed in the transmission experiments of Sanche and Schulz (1972) under normal operating conditions, but a feature that shifted in energy relative to the 2^2S resonance could be produced in the neighborhood of 19.45 eV by detuning their apparatus. They concluded that the structures were an artifact of the experiment and most likely represented an echo of the ^2S resonance formed by electrons losing energy on collision with an aperture. Golden *et al.* (1974) repeated the measurements of Golden and Zecca (1970) with improved signal to noise and resolution and confirmed the earlier results. Further, they estimated the width of the resonance at 19.45 eV to be 0.4 meV and argued that it was not observed by Sanche and Schulz (1972) because of their lower-energy resolution.

In a specific attempt to resolve this situation, Andrick and Langhans (1975) studied the differential elastic electron yield at a scattering angle of 10° in a crossed-beam geometry. The energy resolution in these measurements was about 40 meV (including Doppler broadening), and the relative statistical error was less than 0.01%. While acknowledging the increased sensitivity that is possible with transmission experiments employing the derivative technique, Andrick and Langhans concluded that their results were not consistent with either the resonance width or classification proposed by Golden *et al.* (1974) and that, if additional resonances do exist in this energy region, the widths of these states must be smaller than 10 μeV. They further conclude that when comparing spectra from apparatus of comparable sensitivity, the presence of a structure is less significant than the absence, a point with which we concur. They postulate that these structures are due to some (unspecified) experimental error.

The high-resolution elastic-scattering measurements of Brunt *et al.* (1977c) and Kennerly *et al.* (1981) also covered the energy region where these additional structures had been observed. These measurements covered a wide range of scattering angles (33°–100°, 22°–135°, respectively), and although both were of high resolution (17 and 5 meV) and high relative statistical accuracy (0.1% and 1.4%), neither showed any evidence of these additional resonances. Kennerly *et al.* place upper limits of 10 and 50 μeV, respectively, on the widths of any *s*- or *p*-wave resonances in this region. There has also been no substantive theoretical evidence for the existence of these features. On the contrary, several specific searches for resonances (in addition to the ^2S) below the 2^3S threshold (e.g., Sinfailam and Nesbet, 1972; Temkin *et al.*, 1972;

Berrington, Burke, and Sinfailam, 1975) found no evidence for additional ^2P resonances. Given the weight of these recent, specific experimental and theoretical studies, it would appear that the structures observed between the 2^2S resonance and the 2^3S threshold are most likely artifacts of the experiments concerned.

The energy region between the $n=2$ and $n=3$ excited states of He contains several generally rather broad resonances. These states have been observed in a variety of experiments in which scattered electrons and metastable atoms have been detected. The earlier work (e.g., Kuyatt *et al.*, 1965; Chamberlain, 1967; Ehrhardt *et al.*, 1968; Pichanick and Simpson, 1968) has been reviewed by Schulz (1973a). Andrick *et al.* (1975), Pichou *et al.* (1976), and Phillips and Wong (1981) have measured the yield of inelastically scattered electrons from threshold to several eV above for the $n=2$ states of He. The lowest-lying resonance occurs at 20.40 eV (Pichou *et al.*, 1976; Phillips and Wong, 1981); and from the angular behavior observed in these and earlier excitation functions, it is undoubtedly of overall P symmetry with a width of about 400 meV. This resonance has also been observed in metastable excitation functions (Brunt *et al.*, 1977a; Keesing, 1977; Buckman *et al.*, 1983a), although its apparent energy in this decay channel (2^3S) is somewhat lower (20.27 eV), and its apparent width (~ 0.8 eV) much larger, than the values obtained from the electron-scattering experiments. Brunt *et al.* classify this state as He^- $1s(2s2p\ ^3P)\ ^2P$, which in our nomenclature is a b-type resonance. The classification scheme favored by Brunt *et al.* assumes that two excited electrons, in well-defined valence states of the negative ion, couple externally to the positive-ion core to form the resonance state—the so-called grandparent scheme. To aid in the classification of the observed features in their metastable excitation function, they used the modified Rydberg formula (MRF) of Read (1977) to predict the energies of resonances of the type [core]$nln'l'$. For the configuration $(2s2p\ ^3P)\ ^2P$, the MRF predicts an energy of 20.192 eV, in reasonable agreement with experiment. The experimental estimates for the width of this state vary quite dramatically. The most reliable value is probably that from the differential scattering experiments (e.g., Andrick *et al.*, 1975; Phillips and Wong, 1981) where the resonance appears as a symmetric structure above a small nonresonant background contribution.

A number of calculations have also been performed on this state. The earlier R-matrix (see, for example, Burke *et al.*, 1969; Fon *et al.*, 1978) and variational (Oberoi and Nesbet, 1973; Nesbet, 1975) calculations determined the resonance energy to be 20.45 eV and 20.17 eV, respectively, and concluded from its width and dominant presence in the 2^3S excitation function that it was a $^2P^\circ$ shape resonance associated with the 2^3S state. In the early 1980s, however, several investigators concluded that this state was, in fact, a Feshbach resonance. The saddle-point and quasiprojection operator methods of Chung (1981) give energies of 20.536 and 20.495 eV, respectively, for this state. The quasiprojection was also used by Bhatia and Temkin (1981) to give an energy of 20.52 eV, while Junker's (1982a, 1982b) study using the complex stabilization method resulted in an energy of about 20.4 eV. Junker also performed a computation of p-wave scattering by He $2\ ^3S$ and found no shape resonance. Komninos *et al.* (1983) calculated the energy and width of this resonance using a two-term multiconfigurational Hartree-Fock approach which included correlation effects. They obtained an energy of 20.26 eV and a width of 600 meV. The most recent 19-state R-matrix calculation (Fon *et al.*, 1989) indicates a width of about 500 meV. There is thus good accord between theory and experiment on the position of this resonance, but some uncertainty as to its width. The assignment of Feshbach character to this state was based on the fact that it is bound with respect to He $2\ ^1S$ and that a projection of its wave function onto target channels indicates that it is predominantly (He $2\ ^1S)2p$ rather than (He $2\ ^3S)\varepsilon p$. However, in light of what is now known regarding the b resonances in the heavier noble gases, we feel that this issue deserves reexamination, and we comment upon it in Sec. VI.B. In brief, we believe that the appropriate coupling scheme for this resonance should be written $1s\,2s\varepsilon p(^3P^\circ)$, and that it is indeed essentially a shape resonance analogous to the $1s^22s\varepsilon p(^3P^\circ)$ b feature of Li^-.

At a slightly higher energy Ehrhardt and Willmann (1967) observed the next prominent He^- resonance feature in the excitation function of the 2^3S state. This resonance, at 21.0 eV, was classified, from its angular behavior, as having overall ^2D symmetry and was also observed by Pichanick and Simpson (1968) in metastable production. Its position and classification were confirmed in the excitation functions of Andrick *et al.* (1975) and Phillips and Wong (1981). Brunt *et al.* (1977a) associate a prominent feature in their metastable excitation function with the ^2D resonance, but note that the asymmetry of this feature in their high-resolution study is probably due to the opening of the 2^3P and 2^1P channels, and they decline to assign an energy to it. They do calculate through the MRF that the $1s(2p^2\ ^1D)\ ^2D$ resonance occurs at 20.583 eV.

Phillips and Wong (1981) also proposed the existence of a further resonance of ^2P symmetry in the region of the ^2D resonance. This observation was based on the behavior of the excitation function for the 2^3S state in the vicinity of 20.8 eV. To support this proposal, they examined, as a comparison, the two-electron configurations $1s^2\ 2s2p$ and $1s^2\ 2s^2$ in Be. In order to obtain correspondence with the He^- states, they assigned the Be ground state to the energy of the He^- ^2S resonance and divided the energy above this ground state of the Be excited states by 4 to correct for the difference in core charge. This model predicts the He^- $1s(2s2p^{1,3}P)\ ^2P^\circ$ states at 20.1 and 20.7 eV, respectively. Given the classification of the lower resonance as the triplet (in grandparent coupling) member of this configuration (Brunt *et al.*, 1977a), the resonance proposed by Phillips and Wong is presum-

ably the $1s(2s2p\ ^1P)\ ^2P^\circ$ state of He^-, a *c* resonance in our notation. Although they make no observation of such a state, Brunt *et al.* had calculated its energy with the MRF to be 20.606 eV. While the spectra of Phillips and Wong can be interpreted as suggesting a further ^2P resonance near 20.8 eV, the situation is complicated by the position and width of other nearby He^- resonances. There is also no definitive theoretical evidence for the existence of this state, despite specific searches conducted by Junker (1982b) and Nesbet (1982). Indeed, the evidence for *c* resonances is, in general, rather sketchy throughout the periodic table. As discussed in Sec. VI, they are invariably quite broad features, usually situated near excitation thresholds, and there are some uncertainties regarding their classification. For example, one would expect the spectrum of Li^- $1s^2\ 2s2p$ to provide a closer correspondence to the He^- spectrum than does that of Be, but there is no evidence for a $2s2p\ ^1P^\circ$ feature there (see Sec. IV.C.2).

Also found in this energy region is the $1s2p^2\ ^4P$ state of He^-, which, although not accessible by electron-impact excitation from the ground state, has been observed in the photodetachment of metastable He^- $(1s2s2p\ ^4P^\circ)$ by Peterson and co-workers (Peterson *et al.*, 1983, 1985). In these experiments a metastable He^- beam is formed by electron-capture collisions of a He^+ beam in an alkali vapor oven. The process

$$He^-\ (1s2s2p\ ^4P^\circ)+h\nu\rightarrow He(2^3P)+\varepsilon p$$

was studied near threshold by extending the operation of a Kr^+ laser-pumped cw dye laser into the infrared region above 1000 nm. The yield of neutral He atoms produced in the photodetachment collision was measured by detection of the secondary electrons ejected on their collision with a metal surface. Peterson *et al.* (1985) determined the ^4P shape resonance to lie 12.3 meV above the 2^3P threshold at 20.963 eV and to have a width of about 8 meV (Fig. 15). They also determined the electron affinity of $He(2^3S)$ to be 77.5 MeV. These values are in excellent accord with the calculations of Hazi and Reed (1981) and Bunge and Bunge (1984) and with the hyperspherical coordinate treatment of Watanabe (1982).

Before discussing the next group of resonances in the vicinity of the $He(n=3)$ excited states, some mention should be made of the sharp structures observed at the excitation thresholds of the 2^3S, 2^1S, and 2^3P states, particularly, but not exclusively, in differential electron-scattering experiments. Structure, in the form of a narrow peak, has been observed at threshold in the electron excitation function for the 2^3S state by Ehrhardt and Willmann (1967), Ehrhardt *et al.* (1968), Pichou *et al.* (1976), and Phillips and Wong (1981). It is attributed to the rapid rise of the ^2S contribution to the 2^3S excitation due to the proximity of the ^2S resonance, and its shape and width appear to be limited by apparatus resolution (Pichou *et al.*, 1976). It has also been observed in elastic-scattering measurements (Cvejanovic *et al.*, 1974; Andrick *et al.*, 1975; Brunt *et al.*, 1977c), where it appears as a cusp; in metastable excitation functions (Brunt *et al.*, 1977a; Keesing, 1977), where it manifests itself as a break or shoulder in the near-threshold cross section; and in transmission experiments (e.g., Golden *et al.*, 1974). There is excellent qualitative agreement between the above observations and the theoretical calculations of Nesbet (1975) and Berrington *et al.* (Berrington, Burke, and Robb, 1975; Berrington, Burke, and Sinfailam, 1975). Similar behavior is observed near the threshold of the 2^1S state in elastic, inelastic, and metastable excitation functions. Berrington *et al.* performed an eigenphase sum analysis in this energy region, and their calculations indicated a virtual state near the 2^1S threshold. Again, the experimentally observed features are in excellent qualitative agreement with theory, particularly for the cusp in elastic scattering (see Nesbet, 1975) and for the threshold feature observed in the metastable channel (see Brunt *et al.*, 1977a). Cusp behavior has also been observed at the 2^3P threshold but has not been reproduced in either the variational or *R*-matrix calculations.

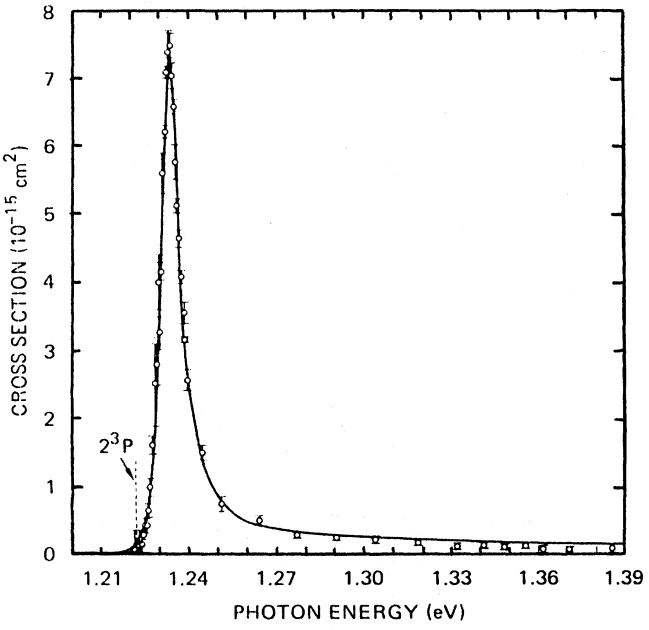

FIG. 15. He^- photodetachment cross section near the 2^3P threshold. The solid line represents a least-squares fit to the experimental data of a modified Wigner threshold law.

The energy region spanning the $n=3$ thresholds is rich in sharp resonance structure. Since the Schulz (1973a) review, high-resolution studies in the metastable atom channel (Brunt *et al.*, 1977a; Keesing, 1977; Buckman *et al.*, 1983a), in the photon channel (Heddle, 1976, 1977; Brunt *et al.*, 1977b), and in the inelastic electron channel (Pichou *et al.*, 1976; Andrick, 1979) have all shed further light on the nature of these autodetaching states.

The first strong feature observed in this region in all of the above excitation functions is at 22.44 eV (Andrick, 1979) and was first tentatively classified by Kuyatt *et al.*

(1965) as He^- $1s(3s^2\ ^1S)\ ^2S$ by analogy with the $n=2$ resonance features at lower energies. This classification was confirmed by Ehrhardt and Willmann (1967), Ehrhardt *et al.* (1968), and Andrick *et al.* (1968) in differential electron excitation functions for the $n=2$ levels. In the metastable excitation functions of Brunt *et al.* (1977a) and Buckman *et al.* (1983a), this feature was assigned an energy of 22.450 eV, while Keesing determined an energy of 23.434 eV. In the UV photon excitation function of Brunt *et al.* (1977b), this feature occurs at 22.47 eV. The MRF (Brunt *et al.*, 1977a) predicts an energy of 22.543 eV for this state with a screening parameter value of $\sigma=0.25$.

Although many other resonances had been observed in this energy region prior to the Schulz review, the only other state that had been classified was one of overall ^2P symmetry at 22.6 eV (Andrick *et al.*, 1968). This and many other resonances were observed in the high-resolution studies of metastable excitation by Brunt *et al.* (1977a). These authors also advance tentative classifications for many of the observed features based on predictions from the MRF. In addition to the $1s(3s^2\ ^1S)\ ^2S$ resonance at 22.45 eV, they assign classifications to features at 22.64 eV $[1s(3s3p\ ^3P^\circ)\ ^2P^\circ]$, 22.70 eV $[1s(3p^2\ ^1D)\ ^2D]$, 22.74 eV $[1s(3s3p\ ^1P^\circ)\ ^2P^\circ]$, and 22.88 eV $[1s(3p^2\ ^1S)\ ^2S]$. This work prompted Nesbet (1978) to extend the earlier variational calculations of Oberoi and Nesbet (1973), which did not adequately predict the structure observed by Brunt *et al.* Nesbet computed total cross sections for excitation of both 2^3S and 2^1S metastable states with an expanded variational wave function and explicit consideration of states with total symmetry ^2S, $^2P^\circ$, and ^2D. The results of this calculation in the vicinity of the $n=3$ levels of He are shown in Fig. 16 along with the experimental excitation function from Brunt *et al.* The qualitative agreement between the two spectra is remarkably good. However, thee are some differences in the classifications proposed by Nesbet and by Brunt *et al.* for these states. Specifically, in addition to the resonances of the grandparent type. Nesbet established the existence of another class of resonance states that are not associated with He^- valence shells but are formed by the attachment of an electron in the polarization potential associated with a neutral excited state. Nesbet found examples of such states at the thresholds of the $3^{1,3}S$ states of He, and, as will be highlighted in later sections, there is evidence for the presence of these so-called nonvalence states in many other atomic systems.

The major differences in the classifications are for the two nonvalence features at 22.74 and 22.88 eV, which Nesbet classifies as $1s(3s\ \bar{p})\ ^2P^\circ$ and $1s(3s\ \bar{s})\ ^2S$, respectively. There is good correspondence between the theory and the experimental classifications for the overall symmetry of all the other resonances in this region. Another interesting comparison can be made between the experimental values for the $n=3$ resonance energies and those from the hyperspherical coordinate analysis of Watanabe *et al.* (1982). They identify all the features observed by Brunt *et al.* (1977a) and calculated by Nesbet (1978), and their calculated energies are in good agreement with both of the above. In addition, they find resonances of overall $^2F^\circ$ and ^2G symmetry at 22.836 and 23.014 eV. It is possible that these states are the features U and V observed, but not classified, by Brunt *et al.* at 22.99 and 23.05 eV. Such states would not appear in the calculation of Nesbet because of the high angular momenta involved.

Freitas *et al.* (1984) have extended earlier R-matrix calculations (e.g., Berrington, Burke, and Robb, 1975; Berrington, Burke, and Sinfailam, 1975) to include the first 11 helium target states in the expansion of the total wave function and have investigated the eigenphase sums for the symmetries ^2S, $^2P^\circ$, ^2D, $^2F^\circ$, and ^2G in the vicinity of the $n=2$ and 3 excited-state thresholds in helium. They find a wealth of resonance structures in these symmetries between 22.0 and 22.5 eV but refrain from assigning a single configuration to each due to the presence of strong configuration mixing. However, their calculations are in excellent agreement with the metastable excitation functions of Brunt *et al.* (1977a) and Buckman *et al.* (1983a) and further indicate that the higher-lying features U and V may be $^2F^\circ$ and ^2G resonances, respectively.

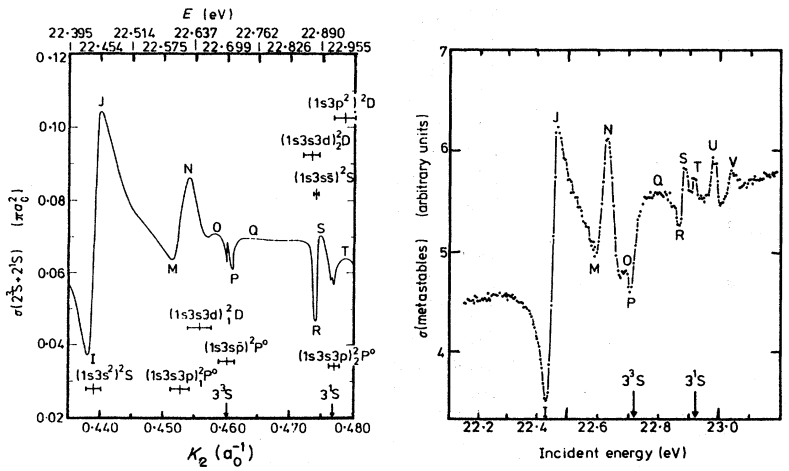

FIG. 16. Comparison of a variational calculation of the $2\,^3S+2\,^1S$ total cross section (a) and the measured metastable excitation function (b). From Nesbet (1978).

The calculations of Freitas *et al.* also indicate that there are two classes of resonance in this energy region. Firstly, Freitas and co-workers, like Nesbet, find several narrow features that are associated with the threshold of a neutral excited state—the "nonvalence" or intershell resonances. Resonances in the second class are broader and, in general, not closely associated with any threshold, but are mixtures of configurations, such as $1s\,3l3l'$. These are the states classified by Read and Brunt *et al.* (1977a) as grandparent or intrashell (Herrick *et al.*, 1980) doubly excited resonances.

Le Dourneuf and Watanabe (1990) have used the adiabatic hyperspherical formalism to classify the He^- ($n=3$) resonances in terms of the normal modes of a triatomic molecule (see Sec. II.F). They obtain the resonance energies after a comparison of the normal modes for He^{-**} with those of H^-, taking into account the effect of the perturbation due to the core electrons. Their resonance energies are in good agreement, both with experiment and with the other calculations described above.

A discrepancy that existed between the calculated and experimental widths for these $n=3$ resonances (see Nesbet, 1978) was resolved by Andrick (1979), whose high-resolution differential electron excitation functions for the 2^3S state enabled separation of the overlapping resonance profiles by appropriate choices of scattering angle (Fig. 17). While not in complete concurrence with the theoretical values, these experimental widths do show the same trend of increasing with increasing energy.

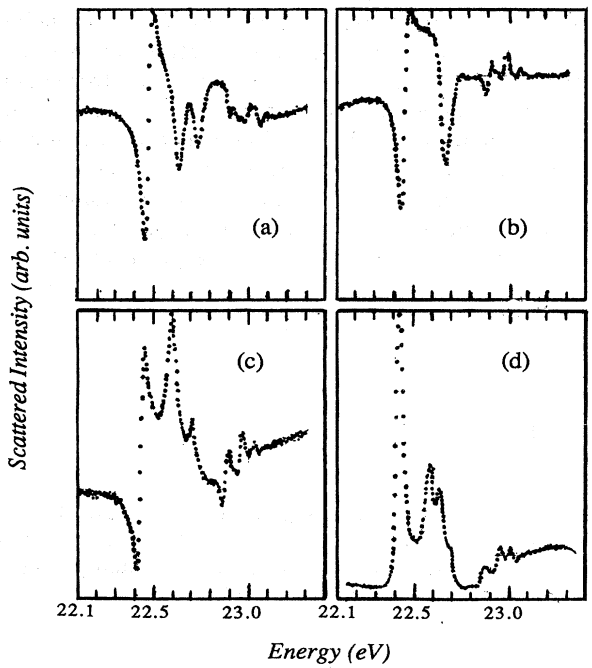

FIG. 17. Differential electron excitation functions for the $2\,^3S$ state at (a) 54.5°, *d* wave vanishes; (b) 90°, *p* wave vanishes; (c) 125.5°, *d* wave vanishes; and (d) 140°, all partial waves present (from Andrick, 1979).

The majority of these states in the region of the $n=3$ thresholds were also observed by Heddle (1976a) in a series of optical excitation functions for the $n^{1,3}S$ states and were classified with the assistance of an expression similar to the modified Rydberg formula. There is good general agreement between this work and the above experimental and theoretical studies, although there are some discrepancies in the energies of assigned features. A summary of the recommended positions, widths, and classifications for the $n=3$ resonances is given in Table II.

The higher-lying reaches of the He^- resonance spectrum were observed in several of the early experimental measurements [see Schulz (1973a) for a summary], although no attempts were made to classify the observed features. The first detailed studies were made by Heddle and co-workers (see Heddle, 1976, 1977, and references therein), who carried out optical excitation functions for many singly excited helium states with principal quantum number $n=3$–6 and identified many features up to

TABLE II. Recommended energies, widths, and classifications of resonances in He^- below the first ionization potential. Energies are expressed relative to the $1s^2$ ground state of atomic He. Unless otherwise specified, values are from Brunt *et al.* (1977a) and Buckman *et al.* (1983a). Figures in parentheses represent the uncertainty in the least significant digit.

Classification	Energy (eV)	Width (meV)	Comments
$1s2s^2\,^2S$	19.366(5)	11.0(5)	Width: Kennerly *et al.*
$1s2s2p\,^2P$	20.400(30)	~400(100)	Pichou *et al.*
$1s2p^2\,^4P^e$	20.963(1)	8.0(4)	Patterson *et al.*
$1s2p^2\,^2D$	21.000(3)	–	Andrick *et al.*
$1s(3s^2\,^2S)$	22.440(10)	35	"
$1s3s3p\,^2P$	22.600(10)	42	
$1s3s3d\,^2D$	22.660(10)	47	
$1s3s\,p\,^2P$	22.740(10)	23	Nesbet
$1s3s\,s\,^2S$	22.880(10)	18	"
$1s3p^2\,^2D$	22.930(10)	20	
^2F	22.990(10)	20	Freitas *et al.*
^2G	23.050(10)	32	"
	23.443(5)		
	23.518(10)		
	23.579(10)		
	23.667(5)		
	23.860(5)		
	23.907(10)		
	23.952(10)		
	23.983(10)		
	24.088(10)		
	24.144(15)		
	24.176(10)		
	24.216(10)		
	24.261(15)		
	24.288(10)		
	24.307(15)		
	24.340(15)		
	24.367(15)		
	24.387(15)		

$n=7$ and 8, although attempts at classification were only tentatively made for features above $n=5$. Resonances near the $n=4$ singly excited states were also observed in the metastable excitation functions of Keesing (1977) and Brunt *et al.* (1977a), the latter offering tentative classifications for four features at 23.45 eV $[1s(4s^2\ ^1S)\ ^2S]$, 23.53 eV $[1s(4s4p\ ^3P^\circ)\ ^2P^\circ]$, 23.57 eV $[1s(4p^2\ ^1D)\ ^2D]$, and 23.67 eV $[1s(4p^2\ ^1S)\ ^2S]$. Brunt *et al.* also observed weak features at 23.86 and 23.96 eV but offered no classification for them.

The most extensive study of these features and others with principal quantum numbers up to $n=7$ was made by Buckman *et al.* (1983a), once again in measurements of metastable atom excitation. These experiments trace the occurrence of resonances belonging to the four prominent symmetry classifications observed in the $n=3$ and $n=4$ manifolds, i.e., the ^2S, $^2P^\circ$, ^2D, and ^2S, respectively (see Buckman *et al.* and Andrick, 1979), from $n=3$ to $n=7$, although for $n=6$ and 7 the $^2P^\circ$ states were not observed (Fig. 18). We note that in discussing these high-lying states it is certainly more appropriate to use the two-electron classification scheme of Lin (1984). Under this scheme these states are classified ${}_n(n-1)_n^+\ ^1S$. In the interest of brevity, we shall retain the more conventional notation for these states in the following discussion but stress that, particularly for high values of n, this is not the most accurate description of these doubly excited states.

Buckman *et al.* note several aspects of these resonance multiplets that lead them to conclude that some of the observed features are formed as a result of a highly correlated two-electron motion. Firstly, they note that the Rydberg formula, when applied to a normal, unperturbed series of neutral atomic excited states, predicts that the energy span of a multiplet of states corresponding to a given n is proportional to $(n-\delta_{nl})^{-3}$ for high values of n, as is the energy separation of neighboring multiplets.

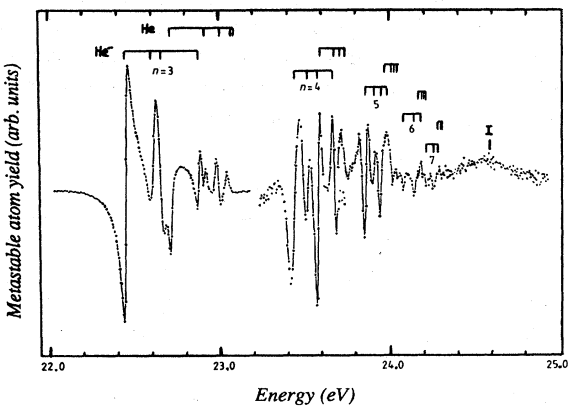

FIG. 18. Metastable atom $(2\,^3S+2\,^1S)$ excitation function extending from 22.0 eV to the He^+ threshold. The energies of the prominent He^- resonances are indicated along with those of the *ns*, *np*, and *nd* states of He for $n=3$–7. In each spectrum a sloping background has been subtracted and the zero suppressed (from Buckman *et al.*, 1983a).

If, as is the case in He, the atomic multiplets do not overlap at low values of n, then they will also not do so for high values of n. Buckman *et al.* observe that for the He^- features, the gap between successive multiplets decreases as n increases until they begin to overlap for $n \geq 8$. They also note that when applied to the lowest ^2S member of each multiplet, the usual Rydberg formula gives values of the quantum defect δ_{nl} that increase essentially linearly with n; this is in marked contrast to the behavior generic to atomic Rydberg series, for which δ_{nl} converges to a constant as $n \to \infty$ (see also Read, 1983).

Buckman *et al.* also apply the modified Rydberg formula (Read, 1977—see Sec. II.F) to the lowest ^2S member of each multiplet, with the quantum defect for the ns^2 configuration being approximated by a weighted mean of the δ_{nl} obtained from the Rydberg formula for the configurations $1sns\ ^1S$ and $1sns\ ^3S$ of neutral He. With a value of 0.25 chosen for the screening parameter σ, which corresponds to the situation in which the two electrons reside at or near the Wannier ridge (with $r_1 \approx r_2$) in a highly correlated state, this formula predicts binding energies for the ^2S terms that are within 1.6% of the experimental value for $n=2$ and 9.5% for $n=7$.

The existence of such high-lying resonance states had been proposed by Fano (1980), who drew an analogy between double electron excitation near the ionization potential and the behavior of a Rydberg electron in a strong magnetic field. He proposed that the electron-scattering analog to the quasi-Landau resonances in the magnetic-field problem may well have been observed in the higher reaches of the optical excitation functions of Heddle (1976, 1977). As this work, and much of the other theoretical contributions to correlation effects in electron scattering, is based on Wannier's (1953) treatment of the unstable motion of a pair of electrons along a potential ridge, Buckman *et al.* have referred to the observed feature as "Wannier ridge" resonances.

Following the work of Buckman *et al.* (1983a), there have been several semiempirical calculations using Rydberg-like formulas for the energies of these higher-lying states, as well as a number of calculations using correlated wave functions and the R-matrix technique. The 19-state R-matrix calculation of Fon *et al.* (1989) extends the earlier R-matrix calculations (Freitas *et al.*, 1984) to the $n=4$ region. While there is still excellent agreement with experiment in the $n=3$ region, the agreement with experiment for the metastable cross section in the region of the $n=4$ excited states is not as good. This may in part be due to cascade contributions in the experimental spectrum. However, the agreement for the positions and assignments of most of the resonances in this region are nonetheless remarkably good. For the most part, the generalized Rydberg formulas (see, for example, Rau, 1983; Feagin and Macek, 1984; Lin and Watanabe, 1987; Dmitrieva and Plindov, 1988, 1989; Read, 1990) show good agreement with the experimental resonance energies for the ridge states. Rau (1983) derived an equa-

tion for the energies of a Rydberg series of bound states in a six-dimensional Coulomb potential. This equation is algebraically similar to the MRF, although it is conceptually different in that it arises from considering the two electrons as a single entity rather than as individual contributors with their own, possibly different, quantum numbers. Rau's Bohr-Rydberg equation has the form

$$E_n = I - \frac{[Z_0(Z-\sigma)]^2}{2(n+5/2-\delta)^2} ,$$

where $Z_0 = 2\sqrt{2}(Z-0.25)$, Z being the charge of the core, σ the screening constant, δ a quantum defect, and I the ionization potential. The energies calculated from this formula show excellent agreement with the experimental values (see table below). Lin and Watanabe (1987) have calculated the screening constant used in the double Rydberg formula using intrashell configuration-interaction states. They determine the dependence of the screening constant σ on the bending rovibrational quantum numbers (Lin, 1986—see Sec. II), and their calculated energies for the He^- resonances ("$ns^2\ ^2S$") also show excellent agreement with the experimental values.

Feagin and Macek (1984) extrapolated Wannier continuum wave functions for two-electron escape to energies just below the ionization potential and obtained a Rydberg series of resonances. However, in order to reproduce the experimental energies of Buckman *et al.*, they required unphysical magnitudes for the parameters in their double Rydberg formula. They do not provide tabulated values for these states, but it is apparent that their widths and energy spacings are smaller than those observed experimentally. They also found that the partial widths of these states should vary as $n^{-5.254}$, not n^{-6} as calculated by Rau and noted experimentally by Buckman *et al.* in terms of the variation in intensity of these states. Subsequent experiments (Buckman and Newman, 1987) show a slightly different variation in the intensity as a function of n, but it should be stressed that such measurements are not definitive as an indicator of partial widths.

Rost and Briggs (1988) derived, using molecular coordinates, an analytic diabatic potential for vibrational excitation in a symmetric state of a two-electron atom. From this approach they have determined a Rydberg formula for calculating the energies of the eigenstates of this potential which correspond to the energies of ns^2 doubly excited states. This formula provides results that are in excellent agreement with experiment (Buckman *et al.*, 1983a; Buckman and Newman, 1987) for n greater than about 5.

Read (1990) has recently extended his double Rydberg formula in a specific investigation of Wannier ridge intrashell states. His revised expression, which is based both on the earlier modified Rydberg formula and on the expression of Dmietrieva and Plindov (1988, 1989), includes a double electron quantum defect which is energy dependent. In particular, this quantum defect decreases as the principal quantum number increases, a result of higher angular momentum components contributing to the "$ns^2\ ^2S$" configuration.

In the extension to the experiment of Buckman *et al.*, Buckman and Newman (1987) have traced the occurrence of these resonances to $n=8$ and 9. The energies they assign to their observed features are in excellent agreement with those of Buckman *et al.* up to $n=7$ and with those calculated from the various modified Rydberg expressions (see table below).

The first quantum-mechanical calculations on these highly excited states were reported by Komninos *et al.* (1987). They have performed a multiconfiguration Hartree-Fock (MCHF) calculation on the ^1S and ^2S states of H^- and He^-, respectively, for a range of principal quantum numbers $n=3-10$. The multiconfigurational wave functions used in this calculation contain both angular and radial correlations. Their calculated energies for the ^2S states of He^- are in good agreement with the experimental results of Buckman *et al.* and Buckman and Newman, and conditional probability plots for a selection of these states show localization around the classical Wannier point.

In the table below we reproduce experimental values for the "$ns^2\ ^2S$" ridge resonances together with values calculated using several of the semiempirical forms of the modified Rydberg formula, correlated wave-function expansions, and R-matrix techniques.

		Theory				
n	Experiment	a	b	c	d	e
3	22.451			22.432	22.774	22.439
4	23.435			23.408	23.578	23.434
5	23.850	23.857	23.865	23.843	23.879	–
6	24.080	24.087	24.095	24.077	24.090	–
7	24.217	24.223	24.230	24.213	24.219	–
8	24.307	24.310	24.316	24.301	24.304	–
9	24.387	24.369		24.361	24.362	–

The experimental values are from Buckman *et al.* (1983a) and Buckman and Newman (1987); theory: a—Rau (1983); b—Lin and Watanabe (1987); c—Komninos *et al.* (1987); d—Rost and Briggs (1988); e—Fon *et al.* (1989).

The agreement, especially for high values of n, is remarkably good and may be interpreted as strongly supporting the notion that many of these features are exam-

ples of highly correlated, ridge-riding states.

Further discussions of the implications of both the experimental and theoretical work in this area can be found in the review articles of Fano (1983a, 1983b), Fano and Rau (1985), Read (1983), and Macek and Watanabe (1987).

Recommended values for the energies, widths, and classifications of He^- resonances below the first ionization potential are given in Table II.

2. Resonances in the autoionizing region of He

In addition to the wealth of resonance structure observed below the first ionization potential in He, resonances have also been observed in the energy region of the doubly excited autoionizing states between 57 and 66 eV. The first such measurement was in the transmission experiment of Kuyatt *et al.* (1965), who observed two weak features at 57.1 and 58.2 eV. Fano and Cooper (1965) classified these as states of He^- in which all three electrons were excited to the $n=2$ shell, $2s^2\,2p\ ^2P^\circ$ and $2s2p^2\ ^2D$, respectively. In addition, they suggested that two other states with the configurations $2s2p^2\ ^2S$ and $2p^3\ ^2P^\circ$ should also exist.

In the years preceding the Schulz (1973a) review, the $2s^22p\ ^2P^\circ$ and $2s2p^2\ ^2D$ resonances were observed in a trapped-electron experiment by Burrow and Schulz (1969), in transmission by Golden and Zecca (1970) and Sanche and Schulz (1972a), in electron-energy loss by Kuyatt *et al.* (1965) and Simpson *et al.* (1966), and by Quemener *et al.* (1971) in a measurement of the yield of He^+ following high-resolution electron impact. The energies of these two resonances in the transmission experiments (57.16±0.05 and 58.25±0.05 eV, respectively; Sanche and Schulz, 1972a) were in excellent agreement with the ionization measurements of 57.15±0.04 and 58.23±0.04 eV.

In a study of post-collision-interaction (PCI) effects in the autoionization of He, Hicks *et al.* (1974) also investigated the $^2P^\circ$ and ^2D resonances in a number of different decay channels. Measurements of the yield of elastically scattered electrons at scattering angles of 90°, 54°, and 40° confirmed the symmetries of these resonances. Their energies were accurately determined by a novel calibration technique involving the excitation of the 2^1P state of He. They used a double-scattering process involving excitation of the He^- $1s2s^2\ ^2S$ resonance at 19.367 eV to provide an energy calibration in the region above the ionization potential. In this fashion they determined the energies of these resonances to be 57.22±0.04 and 58.30±0.04 eV, respectively. Hicks *et al.* found no evidence of any further resonances in the energy range from 56 to 66 eV.

In a series of recent experiments, Heideman and coworkers made a comprehensive study of resonances and their effects in the excitation of helium autoionizing states. They proposed (van der Burgt and Heideman, 1985; van der Burgt *et al.* 1986) that, by analogy with the situation near the $n=3$ excited-state thresholds of He, it may be possible that two classes of resonances, the so-called intrashell and the intershell or nonvalence resonances, also exist in the autoionizing region. The two strong, triply excited features discussed above are clearly examples of intrashell resonances. They argued that intershell resonances, if they exist, would presumably be formed by an electron being weakly bound in the polarization potential associated with a doubly excited state and that these resonances would only give rise to structures in the excitation functions for high-n neutral excited states, as these states are favored in the decay of autoionizing levels near threshold because of the effects of PCI. On the other hand, the intrashell resonances are expected to decay strongly and preferentially to the low-n neutral excited states, a process that has been demonstrated experimentally by Roy *et al.* (1978a, 1978b), who investigated the relative decay strength of the He^- $2s^22p\ ^2P^\circ$ resonance into various neutral excited states with principal quantum number $2\le n\le 8$. Spence (1980) used a similar scheme in neon to separate structure due to negative-ion states from that due to neutral autoionizing states.

The first observation of an additional resonance in this energy region was by Baxter *et al.* (1979), who measured the excitation function for the $He^{**}(2s2p)^3P^\circ$ autoionizing state in the energy range from 61 to 64 eV. A structure observed at 62.90±0.05 eV is attributed to a negative-ion resonance at or near the threshold of the $He^{**}(2s3s)^1S$ state. Van der Burgt *et al.* (1985a) proposed the existence of a resonance at 59.90 eV, which they observed in both the ejected electron spectrum of the $He^{**}(2s2p)^3P^\circ$ state and the electron excitation function for the 2^3S singly excited state at a scattering angle of 10°. By comparison of the measured width (0.4±0.1 eV) of this resonance with the calculation of Ormonde *et al.* (1974) for the predicted He^- $(2s2p^2)\ ^2S$ state (0.3 eV), and its relatively strong decay to the $He^{**}(2s2p)\ ^3P^\circ$ state, van der Burgt *et al.* tentatively classified this feature as He^- $(2s2p^2)\ ^2S$. However, they also add the caveat that great care must be exercised when interpreting such structures in the autoionizing region.

To investigate their hypothesis on both the existence and decay modes of intra- and intershell resonances in the autoionizing region of He, van der Burgt and others (van der Burgt and Heideman, 1985; van der Burgt *et al*, 1986) carried out a comprehensive series of excitation function measurements for the $n^{1,3}l\,(2\le n\le 6;0\le l\le 2)$ singly excited states of He. For the $2^{1,3}S$ states, these measurements comprised inelastic electron excitation functions, while for all other states, optical excitation function measurements were made.

In the excitation functions for the $n=2$ levels, prominent structure is observed due to the ^2P and ^2D intrashell resonances at 57.22 and 58.30 eV, but there is little evidence of further resonance excitation. However, in the $n=3,4,5\ ^3S$ excitation functions, a strong peak, the relative intensity of which increases with increasing n, is seen

at the threshold of the $He^{**}(2p^2)\ ^1D$ autoionizing level at 59.90 eV (Fig. 19). Their observations indicated that this feature is clearly influenced by PCI and, in contrast to their earlier tentative classification of it as $2s2p^2\ ^2S$, an intrashell resonance, they classify it as a shape or intershell resonance associated with the ^1D state with an approximate configuration of $He^-\ (2p^2\ \bar{s})\ ^2D$.

Similar structure is observed at 58.30 eV in the 4,5 ^1D and 3,4 ^1P excitation functions (Fig. 20) and at 57.8 eV in the 4,5 ^3P excitation functions (Fig. 21). Based on the higher-n excitation function, van der Burgt *et al.* (1986) propose that, in addition to the $2s2p^2\ ^2D$ He^- state at 58.30 eV, an intershell resonance of undetermined symmetry also occurs at this energy, presumably due to the polarization potential associated with the $He^{**}(2s2p)\ ^3P^\circ$ state. The strong peak observed near 57.8 eV in the excitation function for the 4,5 ^3P states is, they propose, due to another intershell resonance of the configuration $(2s^2\bar{p})\ ^2P$ at the threshold of the $He^{**}(2s^2)\ ^1S$ autoionizing level.

Further evidence of intershell resonances is found at 62.94 eV at the threshold of the $He^{**}(2s3s)\ ^1S$ state and at 63.50 eV at the threshold of the $He^{**}(2p3p)\ ^1D$ state. Van der Burgt *et al.* (1986) tentatively classify the former as $He^-\ (2s3s\bar{p})\ ^2P^\circ$. They offer no classification for the latter. To further support their proposal for the existence of this class of intershell resonance in the autoionizing region of He, van der Burgt *et al.* have investigated the polarizabilities of the doubly excited states of He by using the surface density plots of Lin (1982a), the expectation being that those states that have a small amplitude outside the Wannier region (see Lin, 1982a, 1982b, 1984; Le Dourneuf and Watanabe, 1984) have a high polarizability. They find that those doubly excited states, which they propose as supporting intershell resonances, all have a small surface charge amplitude outside the Wannier region. A comprehensive summary of much of the recent work on triply excited states is given in a recent review paper by Heideman (1988).

The $2s^22p\ ^2P^\circ$ and $2s2p^2\ ^2D$ resonances at 57.22 and 58.30 eV have also been studied in a recent series of experiments in which their effect on the electron-impact excitation cross section for the $3\ ^3D$ state was measured by Batelaan *et al.* (1991). These experiments involved the detection, and the measurement of the polarization, of photons arising from the $3\ ^3D$-$2\ ^3P$ decay as a function of incident electron energy. While the experiments do not shed any new light on the energy or widths of these

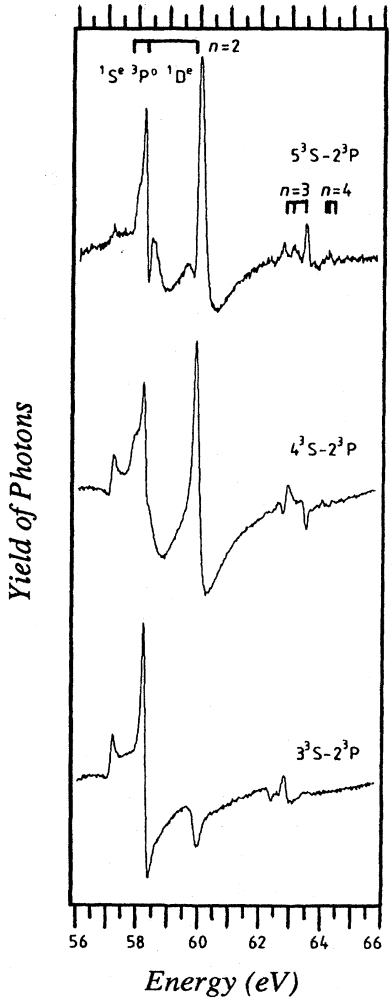

FIG. 19. Optical excitation functions for the $n=3,4,5\ ^3S$ levels of He in the energy region of the doubly excited autoionizing states (from van der Burgt *et al.*, 1986).

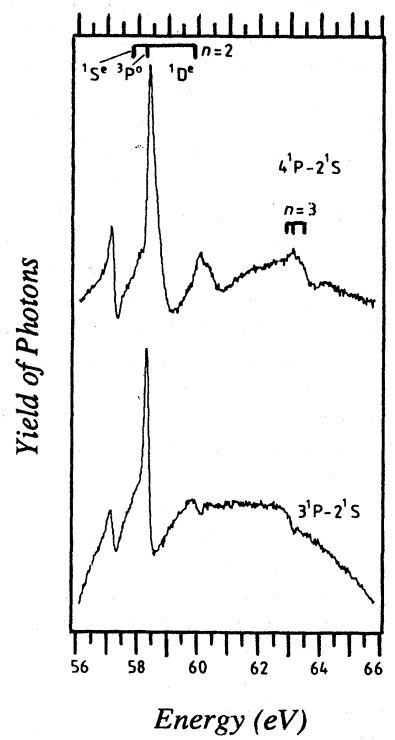

FIG. 20. Optical excitation functions for the $n=3,4\ ^1P$ and $n=3,4,5\ ^1D$ levels of He in the energy region of the doubly excited autoionizing states (from van der Burgt *et al.*, 1986).

TABLE III. Recommended energies, widths, and classifications for resonances in He^- above the first ionization potential. Energies are expressed relative to the $1s^2$ ground state of atomic He. Figures in parentheses represent the uncertainty in the least significant digit.

Classification	Energy (eV)	Width (meV)	Comments
$2s^2 2p\ ^2P^\circ$	57.22(4)	0.07(1)	Hicks *et al.*
			Width: van den Brink
$2s^2 p\ ^2P^\circ$	57.80		van der Burgt *et al.*
$2s2p^2\ ^2D$	58.30(4)		Hicks *et al.*
$2p^2 s\ ^2D$	59.90	0.4(1)	van der Burgt *et al.*
$2s3s\ p\ ^2P$	62.94		van der Burgt *et al.*
	63.50		"

states, they do illustrate significant interference effects between direct and resonance excitation of the $3\ ^3D$ state in this energy region.

The recommended energies, widths, and classifications for He^- resonances in the region of the He doubly excited states are given in Table III.

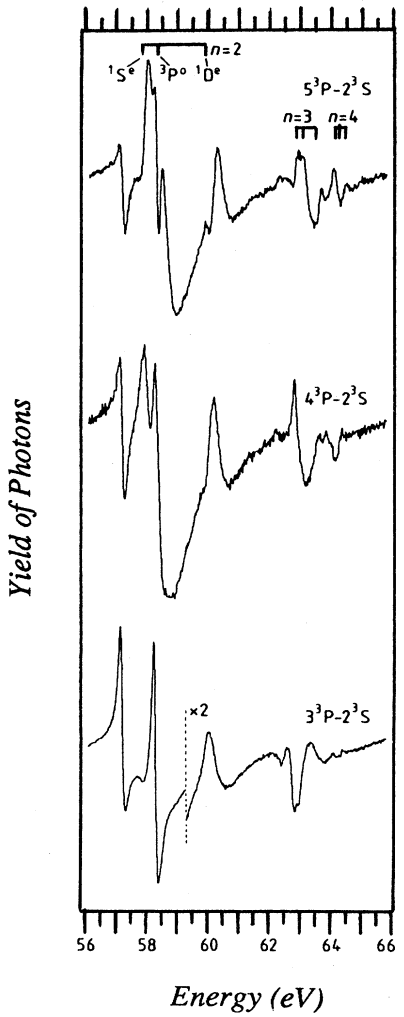

FIG. 21. Optical excitation functions for the $n = 3,4,5\ ^3P$ levels of He in the energy region of the doubly excited autoionizing states (from van der Burgt *et al.*, 1986).

C. The alkali metals

The alkali negative-ion resonances have been studied in electron-scattering, electron-transport, and laster photodetachment experiments. The amount of experimental data available, particularly from the electron-scattering area, is not extensive when compared with the rare gases, a consequence, no doubt, of the difficulties these elements pose when used in conjunction with high-resolution electron beams. On the theoretical side, calculations employing multconfigurational Hartree-Fock, close-coupling, variational, and relativistic R-matrix techniques have been applied. In addition, in the low-energy region, effective-range theory has been used in order to extrapolate scattering phase shifts to energies below 0.1 eV. Relatively few autodetaching features have been observed in the energy region below the ionization potentials of these atoms, and, indeed, little is known about the higher-lying resonances within a few eV of the ionization limit. Because many of the autodetaching states appear to be common to all of the alkali group, we start with a detailed discussion of sodium rather than lithium, which is perhaps the logical choice as an example of the alkali metals, as the latter has been the subject of little investigation. Any differences that occur or, in the heavier alkalis, any more extensive information that becomes available, will be discussed in appropriate detail.

1. Sodium

The autodetaching states of Na^- have been studied in electron scattering by Gehenn and Reichert (1972), Andrick *et al.* (1972), Eyb and Hofmann (1975), Johnston and Burrow (1982), and Johnston (1983) and in photodetachment studies by Patterson *et al.* (1974). The stable ground state of Na^- ($3s^2\ ^1S^\circ$) is bound with respect to Na ($3s$) by 0.543 eV (Patterson *et al.*, 1974). The lowest-lying autodetaching state was predicted by several calculations (Norcross, 1971; Karule, 1972; Moores and Norcross, 1972; Sinfailam and Nesbet, 1973) to be a shape resonance with the configuration $3s3p\ ^3P^\circ$, i.e., in our notation, a b resonance, at an energy of about 1.0 eV. However, the first direct experimental observation of this feature was only made in recent years in an electron transmission experiment (Johnston and Burrow, 1982), although an earlier theoretical analysis of electron swarm data (Nakamura and Lucas, 1978a, 1978b) resulted in a derived momentum-transfer cross section which exhibited a pronounced low-energy shape resonance at about 0.13 eV, in good agreement with the close-coupling calculation of Norcross (1971).

The measurement of Johnston and Burrow (Fig. 22), which is proportional to the derivative of the total scattering cross section, reveals the low-energy shape resonance to be located at 0.08 ± 0.02 eV, in excellent agreement with the value of 0.083 eV obtained from both the variational calculation of Sinfailam and Nesbet (1973) and the effective-range-theory analysis of Fabrikant

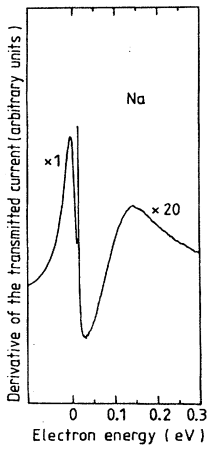

FIG. 22. Derivative of the transmitted current as a function of impact energy for Na (from Johnston and Burrow, 1982).

(1982). Sinfailam and Nesbet also calculate a width of 0.085 eV for this resonance. As the transmission experiment cannot provide definitive information on the configuration of the autodetaching states, Johnston (1983) has analyzed this feature with the aid of the modified Rydberg formula (MRF) of Read (1977). He finds that the configuration $3s3p$ and energy of 0.08 eV result in a value for the screening parameter $\sigma=0.21$, close to the recommended value of 0.25 (Read, 1977). In addition, Johnston applied the approach of Kurtz and Jordan (1981) for estimating the depth of the potential barrier formed by the combination of the long-range polarization potential and the centrifugal potential. This potential in the lth partial wave is given by

$$V(r)=\frac{l(l+1)}{2r^2}-\frac{\alpha}{2r^4}\ , \tag{34}$$

where α is the dipole polarizability. The barrier height is given by

$$V_{\max}=\frac{l^2(l+1)^2}{8\alpha}\ . \tag{35}$$

Johnston notes a striking correspondence between the p-wave barrier height calculated from this equation for sodium (0.085 eV) and the b resonance energy. He also notes that the values calculated for other partial waves (and other alkali atoms) show some correspondence with the energies of other observed features. The particular relevance of the correspondence with the sodium b resonance is that this rather simple approach may be an indicator that this feature is a shape resonance of the nonvalence type formed as a result of the electron being attached in the polarization potential of the ground state, which for the alkalis is very strong. Similar features found by Nesbet (1978) in helium and proposed by Buckman *et al.* (1983b) in the heavier rare gases have already been discussed. The correspondence of this feature in these and other atoms is discussed in Sec. VI.D.

For the higher-lying resonance features, near and above the threshold for excitation of the $3^2P_{1/2,3/2}$ states, experimental information is available from transmission spectroscopy (Johnston, 1983), electron scattering (Andrick *et al.*, 1972; Gehenn and Reichert, 1972; Eyb and Hofmann, 1975), and laser photodetachment measurements (Patterson *et al.*, 1974). At energies close to the 3^2P excitation thresholds (2.102, 2.104 eV), the variational calculation of Sinfailam and Nesbet and the four-state ($3s$-$3p$-$4s$-$3d$) close-coupling calculation of Moores and Norcross both predict resonances in the $^1P^\circ$ and ^1D channels, as well as cusp activity in the $^1P^\circ$ channel. Andrick *et al.* and Eyb and Hofmann have measured the energy dependence for elastically scattered electrons in the neighborhood of the 3^2P thresholds over a wide range of electron-scattering angle, and the structure they observed is in good agreement with the calculation of Moores and Norcross (1972; Fig. 23). However, no conclusive information about the predicted resonances in this region can be drawn from the electron-scattering data, as the threshold structure is strongly influenced by the cusp in the $^1P^\circ$

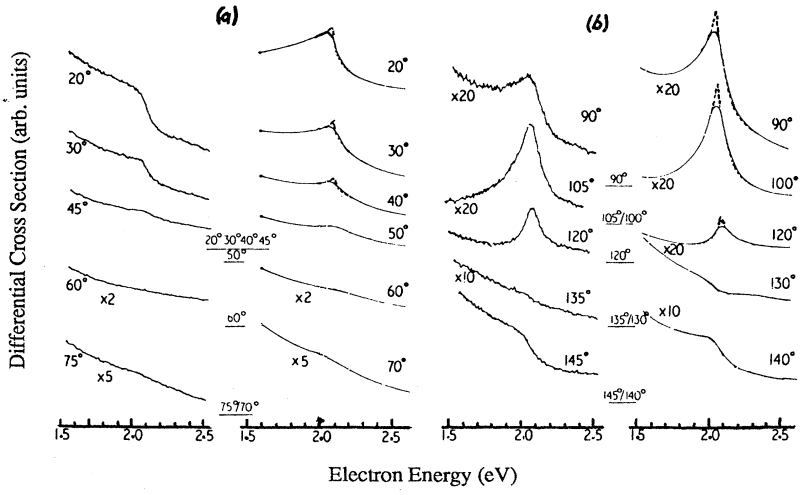

FIG. 23. Experimental (left) and theoretical (right) differential elastic cross sections for electrons scattered from Na near the 3^2P thresholds. The dashed lines are the calculations of Moores and Norcross (1972); the smooth solid lines are the result of folding the theory with the experimental resolution function (from Eyb and Hofmann, 1975).

channel (Eyb and Hofmann, 1975). Moreover, unlike the heavier alkali atoms (see following sections), the laser photodetachment (LPD) measurements of Patterson *et al.* do not show any evidence of resonance structure near the 3^2P thresholds, but only the existence of a Wigner cusp.

In measurements of the transmitted current in Na, Johnston observes a strong broad feature near the 3^2P thresholds (Fig. 24). This observation in itself provides no clue as to the nature of the feature, but Johnston has drawn on other experimental and theoretical work to support a classification. He rejects the configuration $3s3p\,^1P^\circ$ on two grounds. Firstly, such a state would be quite broad due to its strong coupling to the ground state, a notion which is not consistent with the laser photodetachment measurements in Cs^- and Rb^- (Patterson *et al.*, 1974; Slater *et al.*, 1978), where the $^1P^\circ$ resonance is observed with a width of about 1 meV. Secondly, the screening parameter σ calculated from the MRF for such a configuration is 0.38, a value not consistent with the examples provided by Read (1977). Calculations by both Patterson *et al.* and Moores and Norcross (1974) indicate a configuration of $np(n+1)s$ for this resonance in the heavier alkalis ($n=5$ for Rb^-, 6 for Cs^-) with a sizable admixture of $np(n-1)d$. Johnston points out that both these configurations ($3p4s$ and $3p3d$) in Na give rise to a plausible value of σ from the MRF.

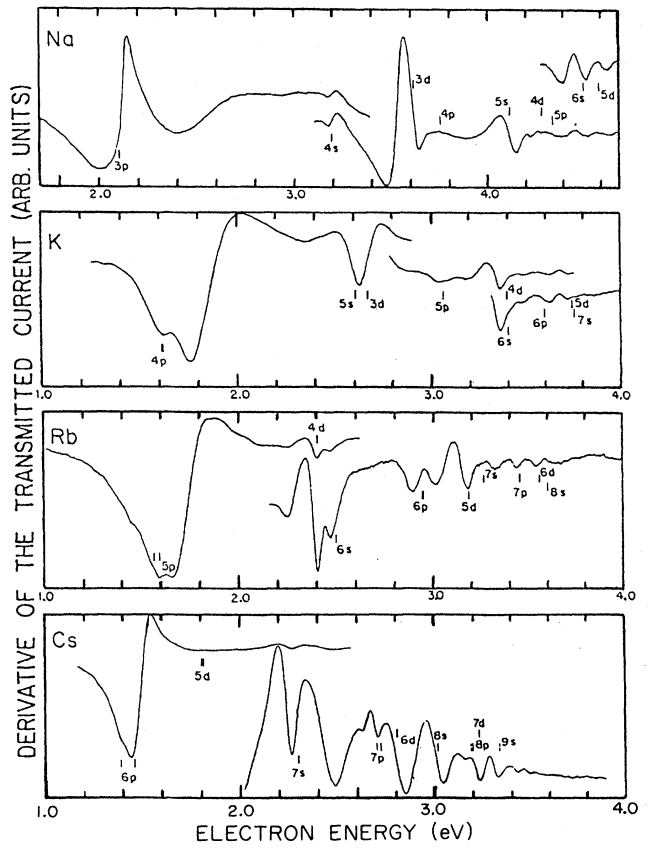

FIG. 24. Derivative of the transmitted electron current as a function of energy for Na, K, Rb, and Cs. The positions of atomic excited states are indicated by small vertical lines (from Johnston, 1983).

Johnston proposes that the ^1D term has the configuration $3p^2$ and supports this classification, over alternatives such as $3s3d$ or $3d^2$, on the basis of the MRF screening parameters. Such a configuration also gives rise to ^1S and ^3P terms. Moores and Norcross (1974) calculated the $3p^2\ ^3P$ term to lie about 60 meV below the 3^2P states, but it would not be observable in electron scattering because of parity considerations. Johnston further proposes that the $3p^2\ ^1S$ term lies above the 3^2P thresholds but is not observed, as it will decay strongly to these states and consequently be very broad.

No estimate of the widths of the $^1P^\circ$ and ^1D resonances can be given for Na^-, due mainly to the effect of the cusp in the $^1P^\circ$ channel, although the width of the observed threshold feature in electron scattering can certainly serve as an upper limit on the width of the ^1D resonance. For resonances above the 3^2P thresholds, the only experimental evidence available comes from the transmission experiments of Johnston (Fig. 24). He observes a feature at 2.57 eV, which is not predicted by any of the theoretical calculations. However, several calculations (Burke and Mitchell, 1973; Moores, 1976; Scott *et al.*, 1984b) for the heavier alkalis predict a $^3F^\circ$ resonance above the first inelastic threshold. Johnston observes such structures in K^-, Rb^-, and Cs^- and shows, by application of Spence's (1977) graphical classification method (see Sec. II.F), that these three structures extrapolate to the center of the broad feature in Na^- at 2.57 eV, prompting the tentative classification of this resonance as a ^3F term. Furthermore, based on the strength of the decay of this state to the inelastic channel, as measured in a series of trapped-electron experiments (Johnston, 1983), and on the values of calculated screening parameter from the MRF, Johnston favors a configuration of $3p3d$ for this state.

The next feature in Johnston's transmission spectrum is a narrow resonance at 3.20 eV (Fig. 24), just above the $4s$ excited state. There is no additional experimental information to assist in the classification of this feature. However, the multiconfigurational Hartree-Fock calculation of Fung and Matese (1972) produces a ^1S state of Na^- at 3.04 eV, just below the $4s$ threshold. On this basis Johnston tentatively classifies this resonance as $4s^2\ ^1S$. Further support for this classification comes once again from the MRF, which gives a screening parameter of 0.29 for such a configuration.

The feature at 3.53 eV in Johnston's transmission spectrum has been classified as a ^1D resonance, as graphical extrapolation techniques indicate it belongs to the same family of resonance as a feature in potassium at 2.60 eV, for which angular electron-scattering data exist (Eyb, 1976). Johnston tentatively classifies this state as $4s3d\ ^1D$. This is supported to some extent by his trapped-electron measurements, which indicate a strong decay of this resonance into the $4s$ channel.

Two further features were observed by Johnston at

TABLE IV. Recommended energies, widths, and classifications for resonances in Na^-. The energies are expressed relative to the $3s\,^2S$ ground state of atomic Na. Values are from Johnston and Burrow (1982) or Johnston (1983).

Classification	Energy (eV)	Width (meV)	Comments
$3s3p\,^3P^\circ$	0.08		
$3p4s\,^1P^\circ + 3p^2\,^1D$	2.10		
$3p3d\,^3F^\circ$	2.57		
$4s^2\,^1S$	3.20		
$4s3d\,^1D$	3.53		
?	4.11		
?	4.49		

4.11 and 4.49 eV, but the lack of any other experimental or theoretical information has not enabled a firm assignment to be made for either of these resonances.

Recommended parameters for the autodetaching states of Na^- are given in Table IV.

2. Lithium

As mentioned previously, there have been few studies of the autodetaching states of Li^-, particularly experimental studies. In fact, to our knowledge, there has been no definitive observation of a negative-ion resonance in lithium, although the LPD measurements of Bae and Peterson (1985) have demonstrated the existence of a virtual state below the 2^2P° excited states. On the theoretical side, electron-scattering calculations utilizing the close-coupling approximation (Burke and Taylor, 1969), the scaled Thomas-Fermi model potential (Norcross, 1971), and variational techniques (Sinfailam and Nesbet, 1973) have been applied to the identification of resonance effects. In addition, Fung and Matese (1972) have performed MCHF calculations, and Moores and Norcross (1974) have calculated Li^- photodetachment cross sections using configuration-interaction wave functions for the initial state and close-coupling scattering wave functions for the final state. Stewart *et al.* (1974) used a model potential to compute the energies of 11 resonances in the vicinity of the $2p$ and $3s$ states of Li. Lin (1983c) computed the energies of eight resonances using an adiabatic hyperspherical treatment.

The lowest energy feature in the electron-scattering calculations, the $1s^2\,(2s2p)\,^3P^\circ$ b resonance, has been shown to occur at an energy of about 0.06 eV (Burke and Taylor, 1969; Norcross, 1971; Sinfailam and Nesbet, 1973; Fabrikant, 1982) with a width of about 0.06 eV. These calculations also indicate the existence of $2p3s\,^1P^\circ$ and $2p^2\,^1D$ resonances near the 2^2P thresholds. The photodetachment calculations also show a strong, sharp feature at the 2^2P threshold, which is attributed (Moores and Norcross, 1974) to a combination of cusp and resonance effects. In the experiment of Bae and Peterson (1985), a 3-keV Li^- beam is directed coaxially with the light from a Kr^+ laser-pumped dye laser, and Li atoms formed by photodetachment are detected by detecting the secondary electrons they eject on striking a low work-function conductive plate. The absolute photodetachment cross section so measured is in excellent agreement with that of Moores and Norcross near the 2^2P° threshold, and the structure they observe in this region is well fitted by a parametric expression derived from multichannel scattering theory (Nesbet, 1980a) including the effects of a virtual state. Their fitting procedure yields the energy of the virtual state to be 55 ± 10 meV below that of the $2^2P^\circ_{1/2}$ state, i.e., at an energy of 1.793 eV.

The calculations of Fung and Matese (1972) were done in a MCHF formalism that only reveals states that are bound with respect to their parents. Thus they did not find the lowest b or c resonances near the 2^2P threshold. However, seven resonances were found near the $3s$ and $3p$ states, which would appear to have the term designations $3s^2$, $3s3p\,^3P^\circ$ and $^1P^\circ$, $3s4s\,^3S$, $3p^2\,^1D$ and ^1S, and $3p4s\,^3P^\circ$ and $^1P^\circ$ [these designations are not proposed by the authors, but are inferred by us from the subsequent work of Stewart *et al.* (1974) and Lin (1983c)]. The model potential calculations of Stewart *et al.* yield all the resonances found by Fung and Matese, at energies that agree to within 0.001 Rydberg, plus five additional resonances, apparently associated with the $3p$ parent state. This method is of the stabilization type, and it did not produce the lowest b or c features. Lin treated Li^- by using a model potential similar to that of Stewart *et al.* to represent the electron-core interaction, and by describing the outer electrons in the adiabatic hyperspherical approximation. He shows adiabatic potential curves for several symmetries (Fig. 25). No discussion of the b or c resonances is given; however, it is of interest to note in Fig. 25 that the $^3P^\circ$ adiabatic potential curve that converges to Li $2s$ as $R\to\infty$ could possibly support a shape resonance, whereas no such possibility is apparent in the

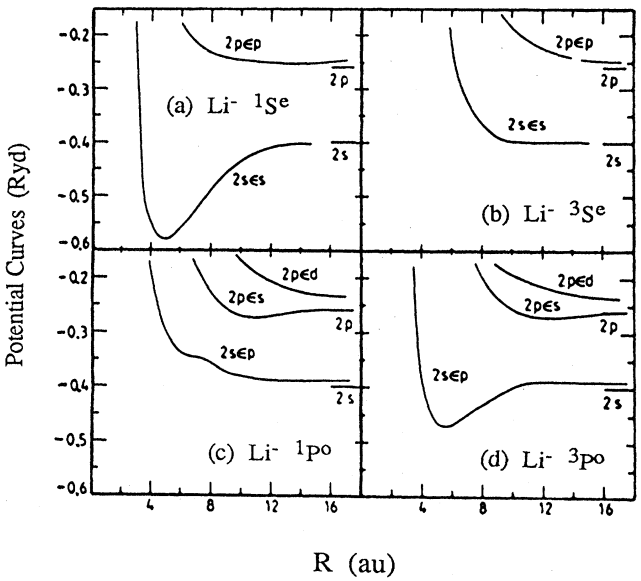

FIG. 25. Adiabatic potential curves for the Li^- $^1S^e$, $^3S^e$, $^1P^\circ$, $^3P^\circ$ channels converging to the $n=2$ limits of Li (from Lin, 1983c).

TABLE V. Recommended energies, widths, and classifications of resonances in Li^-. The energies are expressed relative to the $2s\,^2S$ ground state of atomic Li. There are no experimental values available.

Classification	Energy (eV)	Width (meV)	Comments
$2s2p\,^3P^\circ$	0.06	0.06	
$2p3s\,^1P^\circ + 2p^2\,^1D$	1.85		
$^1S, ^3P, ^3S$	3.11–3.34		
$^1D, ^1S, ^3P, ^1P$	3.70–3.78		

$^1P^\circ$ curve. Lin reproduces many of the results of Stewart *et al.* and also reports some resonances in the vicinity of the 4^2S state.

A summary of the Li^- autodetaching states is given in Table V.

3. Potassium

The situation in potassium is somewhat brighter due to information being available from both electron-scattering and photodetachment measurements, as well as from various theoretical treatments.

The low-lying *b* resonance, which in potassium will have the configuration $4s4p\ ^3P^\circ$, apparently occurs at a lower energy than the corresponding state in Na^- and Li^-. Sinfailam and Nesbet (1973) calculate its energy to be 2.4 meV, while Moores finds the $^3P^\circ$ phase shift to go through $\pi/2$ radians at about 20 meV. Kaulakys (1982) has calculated the position and width of this resonance from experimental data (Stoicheff *et al.*, 1981) on self-broadening of $K(ns)$ and $K(nd)$ Rydberg series. These resonance parameters, which can be related to the oscillating components of the linewidths and shifts as a function of n, were found to be 1.7 meV and 0.47 meV, respectively. Fabrikant's (1982, 1986) effective-range-theory extrapolation of K-phase shifts results in a value of 19 meV for the resonance energy and 16 meV for the width. These low-energy phase shifts are obtained by extrapolating phase shifts from calculations (Karule, 1965, 1972) at higher energies and are supported by favorable comparisons with various experimental data. The data are, firstly, information on the broadening and shift of Rydberg levels by alkali atom perturbers and, secondly, the widths and shifts of the free-electron spin-resonance frequencies which result from collisions of Rydberg atoms with alkali metals. However, no such resonance could be observed in the transmission apparatus of Johnston and Burrow (1982). Given the predicted low energy, this is perhaps not surprising.

Information on the *c* and other resonances near the 4^2P thresholds from electron-scattering experiments (Eyb and Hofmann, 1975; Eyb, 1976; Johnston, 1982) is again clouded by the strong cusp activity in the $^1P^\circ$ channel. We can only note the good agreement between the elastic differential cross-section measurements of Eyb and Hofmann and the three-state close-coupling calculation of Moores (1976), which predicts both ^1D and $^1P^\circ$ resonances and a $^1P^\circ$ cusp in the near-threshold region. Strong, sharp structure is observed in the LPD cross section near the opening of the 4^2P channel (Patterson *et al.*, 1974; Slater *et al.*, 1978). This structure, which has the form of a downward step at each of the fine-structure thresholds, is interpreted, by comparison with Rb^- and Cs^-, as the $4p5s\ ^1P^\circ$ state of K^-. In the case of potassium, these resonances are very loosely bound to the parent 4^2P states, and the resonance profile in the photodetachment cross section does not fully develop before the new channels open.

A strong feature observed by Johnston in electron transmission at an energy of 1.86 eV (Fig. 24) has been classified by him as $4p3d\ ^3F^\circ$ (see Sc. VI.C.1). This assignment is well supported by both theoretical work in K (Moores, 1976) and the use of the graphical technique to extrapolate theoretical (Scott *et al.*, 1984a, 1984b) and experimental (Gehenn and Reichert, 1977) information in Cs.

At 2.4 eV Eyb observes a small feature in the elastic-scattering cross section for scattering angles above 60° (Fig. 26). This feature is not observed by Johnston in transmission and apparently not by Eyb in the excitation functions for the 4^2P levels. Considering the intensity and relatively small width in the differential measurements, it is somewhat surprising that it is not observed in transmission, given the high sensitivity of this technique. From its observed angular distribution, Eyb suggests that this resonance is an S state. However, Johnston maintains that such a classification is not consistent with his graphical analysis scheme across the alkalis. The most plausible configuration for such a state is $5s^2\ ^1S$, and the

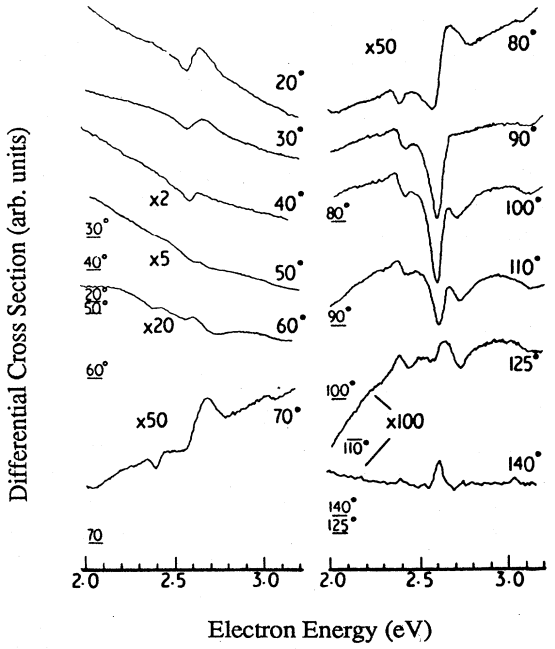

FIG. 26. Experimental elastic differential cross sections for electrons scattered by K (from Eyb, 1976).

TABLE VI. Recommended energies, widths, and classifications for resonances in K^-. The energies are expressed relative to the $4s\,^2S$ ground state of atomic K. Unless otherwise specified, the values are from Johnston and Burrow (1982) or Johnston (1983).

Classification	Energy (eV)	Width (meV)	Comments
$4s4p\,^3P^\circ$	~0.01(?)		Calculation
$4p5s\,^1P^\circ + 4p^2\,^1S$	1.61		Various experiments
$4p3d\,^3F$	1.86		
	2.4	~50	Eyb
$5s4d\,^1D$	2.60–2.63	60	
P or F	2.68		
	3.08		
	3.34		
	3.70		

graphical extrapolation of similar features in Na^- and Rb^- predicts such a state at 2.6 eV in K^-. A strong structure exists at this energy in the measurements of both Eyb and Johnston, but the differential data indicate that this is a D state. As a result, Johnston does not identify a $5s^2\,^1S$ state in K and raises the possibility that the 2.4-eV structure observed by Eyb is an artifact. Clearly, more experimental work in this energy region would be desirable.

As we have alluded to above, the strongest feature in the higher reaches of the potassium spectrum is observed by both Eyb and Johnston at an energy of 2.60 and 2.63 eV, respectively. Johnston has tentatively classified it as $5s4d\,^1D$ (see Sec. IV.C.1). Eyb also observes another state at 2.68 eV at angles where the resonance at 2.6 eV disappears. From its angular behavior, he concludes that it is a P or F state. Structure is also observed by Eyb in the vicinity of 2.6–2.7 eV in the 4^2P excitation functions, but it is thought to be strongly influenced by threshold effects at the opening of the 5^2S (2.607 eV) and 3^2D (2.670 eV) neutral excited states, which are strongly coupled to the 4^2P° level. Higher-energy features (at 3.08, 3.04, and 3.07 eV) have been observed by Johnston, but he offers no classification for them. A summary of the K^- autodetaching states is given in Table VI.

4. Rubidium

The autodetaching states of Rb^- (ground state $5s^2\,^1S$, binding energy 0.4859 eV—Frey *et al.*, 1978) have been investigated experimentally by electron scattering (Johnston and Burrow, 1982; Johnston, 1983) and photodetachment (Patterson *et al.*, 1974; Frey *et al.*, 1978). Theoretical studies by Rabin and Rebentrost (1982), Kaulakys (1982), and Fabrikant (1982, 1986) have been devoted exclusively to the study of the low-lying b resonance.

Johnston and Burrow found evidence for the $5s5p\,^3P^\circ$ resonance at an energy of less than 50 meV, but could not clearly resolve the structure from the wings of the electron-energy distribution in their transmission experiment. From the analysis of the shift and broadening of Rb Rydberg spectra, Rabin and Rebentrost predicted an energy and width for this state of 1.7 and 0.5 meV, respectively. Kaulakys (1982) analyzed the same experimental data and obtained values of 1.3 and 0.4 meV for the energy and width, while Fabrikant's phase-shift extrapolation via effective-range theory gave 23 and 25 meV, respectively, for these resonance parameters.

Rubidium is the first member of the alkali series for which unambiguous information concerning the resonances near the first excited states is available from high-resolution LPD measurements. In the experiment of Patterson *et al.* (1974), a ground state Rb^- beam is photodetached by radiation from a tunable dye laser, and the neutral atoms so formed are detected as a function of laser wavelength (see Sec. III.B). They observed the photodetachment cross section to vanish over a small wavelength range just below the $5^2P_{1/2}$ threshold at 1.560 eV (Fig. 27) and attributed this structure in the cross section to the existence of an autodetaching state that is optically connected to the Rb^- ground state. A similar feature is located below the $5^2P_{3/2}$ threshold (1.590 eV), but does not result in a vanishing cross section because of the newly opened $5^2P_{1/2}$ nonresonant continuum channel. These features can be explained by the existence of a resonance in the $^1P^\circ$ channel just below the respective excited-state thresholds. The width of the lower resonance is about 0.15 meV and that of the upper resonance about 1 meV, the lower feature lies about 0.5 meV below the $^2P_{1/2}$ threshold. The configuration of these states is believed to be $5p6s\,^1P^\circ$.

In a more recent experiment, Frey *et al.* (1978) have

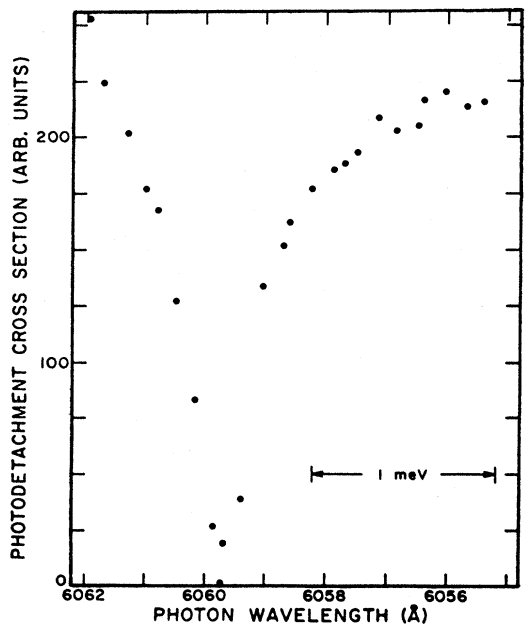

FIG. 27. Rb^- photodetachment cross section near the Rb ($5\,^2P_{1/2}$) channel opening (from Patterson *et al.*, 1974).

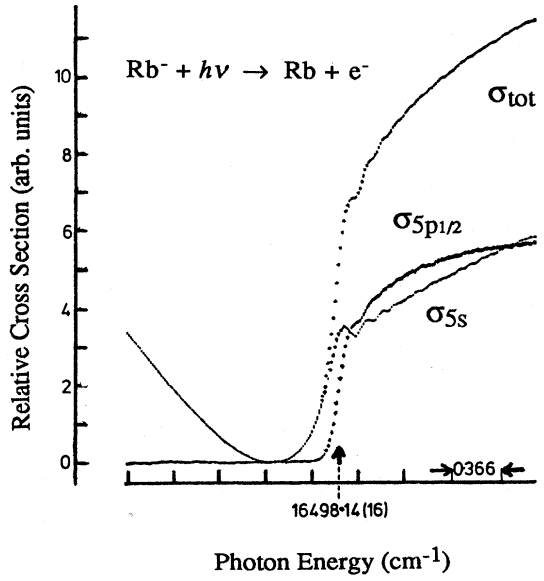

FIG. 28. Total and partial cross sections for the photodetachment of Rb^- near the $5^2P_{1/2}$ threshold, which is indicated by the broken arrow (from Frey *et al.*, 1978).

conducted a series of elegant high-resolution (0.1 cm^{-1}) measurements of Rb^- photodetachment in the region of the $5^2P_{1/2}$ threshold. They measured both the total photodetachment cross section, by detecting neutral atoms, and the partial Rb(5*s*) cross section, by measuring the yield of 1.56 eV electrons produced in the photodetachment process. Both the total and partial 5*s* cross sections show a strong resonance below the $5^2P_{1/2}$ threshold (Fig. 28) with a width similar to that quoted above. In addition, above the $5^2P_{1/2}$ threshold, extremely sharp structure ($\sim$10 μeV) is evident in the 5*s* cross section. The origin of this structure is unknown, although Frey *et al.* postulate that it may be evidence of a new threshold effect.

TABLE VII. Recommended energies, widths, and classifications for resonances in Rb^-. The energies are expressed relative to the $5s\ ^2S$ ground state of atomic Rb. Unless otherwise specified, the values are from Johnston and Burrow (1982) or Johnston (1983).

Classification	Energy (eV)	Width (meV)	Comments
$5s5p\ ^3P^\circ$	<0.05		Various experiments
$5p6s\ ^1P^\circ$	1.559	0.15	Patterson *et al.*
$5p6s\ ^1P^\circ$	1.588	1	"
$5p^2\ ^1S + 5p^2\ ^1D$	1.58		
$5p4d\ ^3F^\circ$	1.74		
$6s5d\ ^1D$	2.40		
$7s^2\ ^1S$	2.45–2.50		
	2.93		
	3.15		
	3.52		

Once again there is no definitive experimental information for the existence of other resonance configurations in the vicinity of the 5^2P thresholds. The transmission experiments of Johnston (1983) show a broad feature in this energy range (Fig. 24), but individual contributions (^1P, ^1D, ^1S, and ^1P cusp) cannot be resolved.

The only available evidence for resonances above the 5^2P thresholds is once again the experimental work of Johnston. As there is no supporting information from other experimental or theoretical work, Johnston has relied heavily on the graphical technique to classify these features into groups observed in the other alkali atoms. The energies of these states, and, in some cases, their tentative classifications, are shown together with the other Rb^- resonances in Table VII.

5. Cesium

The stable ground state ($6s^2\ ^1S$) of the cesium negative ion is bound by 0.472 eV (Slater *et al.*, 1978) with respect to the ground state of the neutral cesium atom ($6s\ ^2S$). As for sodium and potassium, a relatively large amount of information is available on the autodetaching states of Cs^-. Experimental electron-scattering investigations include transmission studies (Johnston and Burrow, 1982; Johnston, 1983) and differential elastic-scattering and optical excitation function measurements (Gehenn and Reichert, 1977). In addition, low-energy data are available from swarm experiments (Postma, 1969a, 1969b, 1969c; Nighan and Postma, 1972; Saelee and Lucas, 1979) and measurements of electron thermal conductivity (Stefanov, 1978). In the energy region near the 6^2P excited states, the LPD measurements of Patterson *et al.* (1974) and Slater *et al.* (1978) provide further experimental information. Theoretical treatments include the effective-range, phase-shift analysis of Fabrikant (1982), and two-state close-coupling calculations of Burke and Mitchell (1973), and the relativistic *R*-matrix method of Scott *et al.* (1984a, 1984b).

The transmission experiments of Johnston and Burrow do not exhibit a *b* resonance in cesium at energies above 0.1 eV. On the other hand, several independent swarm experiments predict a broad low-energy maximum in the Cs momentum-transfer cross section (Q_M). Nighan and Postma analyzed the electron-transport data of various groups and derived a Q_M that has a strong, broad maximum at about 0.25 eV. Saelee and Lucas analyzed their own electron drift-velocity data to obtain a Q_M with a very broad maximum at about 0.15 eV. Stefanov's analysis of electron thermal-conductivity data also leads to a pronounced structure in Q_M at about 0.2 eV. The swarm and transmission results are thus inconsistent concerning the presence of a resonance; however, it should be noted that the independent swarm analyses yield vastly different results, as indicated in Fig. 29. The relativistic *R*-matrix calculation by Scott *et al.* (1984b) exhibits a maximum ($\sim$1 radian) in the eigenphase sum in the $J=1$ odd-parity channel at around 0.1 eV, which may be con-

sistent with a low-energy shape resonance. However, the authors do not identify it as such. There are no structures visible in the $J=0$ or 2 odd-parity channels, which would also be associated with a $^3P^\circ$ resonance, that suggest its presence at low energies.

The absence of a b resonance in the data of Johnston and Burrow could be due either to the insensitivity of the transmission experiment to reasonably broad structures, or to the possibility that this feature is not strongly manifested in the *total* cross section. However, there is a significant body of theoretical evidence suggesting that the b state of Cs^- is *bound,* or that it lies at very low energies ($\sim$0.01 eV). Fabrikant (1982, 1986) has performed several phase-shift analyses using effective-range theory. His first extrapolation of higher-energy phase shifts used a value for the Cs dipole polarizability of 449 a.u., derived from wave functions of Karule (1965). The analysis indicated that the b state was bound by 27 meV. However, as noted by Fabrikant, this value of the polarizability is about 10% larger than the accepted experimental value (403$\pm$8 a.u., from Molof *et al.*, 1974), so it would give a more attractive long-range potential than is actually present. Fabrikant's subsequent analysis using this lower

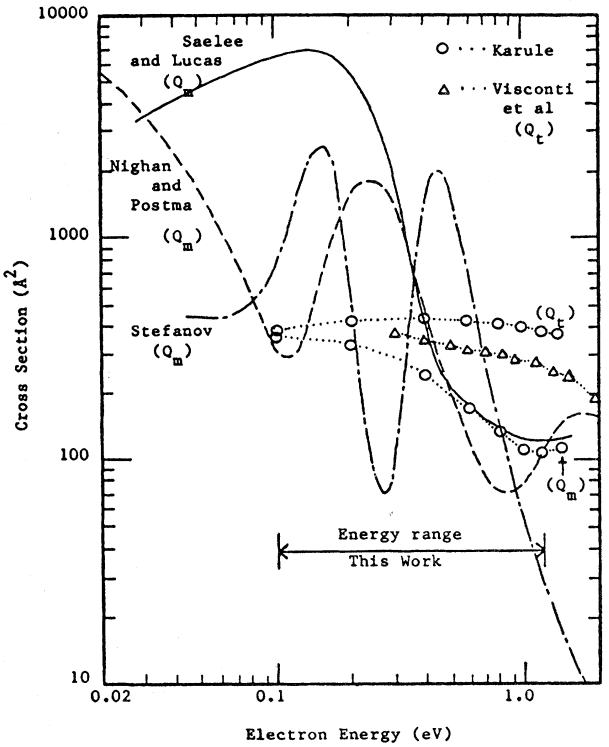

FIG. 29. Summary of low-energy cross sections for electron scattering by Cs, from Johnston (1983). Q_m and Q_t denote momentum transfer and total cross sections, respectively. The experimental results of Nighan and Postma (1972), Saelee and Lucas (1979), and Stefanov (1978) come from an analysis of swarm data; those of Visconti *et al.* (1971) are from atomic beam recoil measurements. Karule's (1965) results are calculated. The arrow indicates the energy range of electron transmission measurements of Johnston.

value of the polarizability produced a shape resonance in the $^3P^\circ$ channel at about 12 meV. A calculation by Krause and Berry (1986) gives a b state that is bound by 12 meV, but this result is well outside the range of accuracy claimed by those authors.

Following the discovery that the b state of Ca^- was stable, several groups addressed the question of whether the corresponding states in the heavier alkalis were also bound. We discuss these results in Sec. VI.B. Froese, Fischer, and Chen (1989) have performed an extensive MCHF calculation that predicts the b state of Cs^- to be bound, by between 1 and 10 meV. Greene (1990), using a frame transformation approach that is very successful in reproducing experimental photodetachment data, finds all states of the $6s6p\ ^3P^\circ$ term to be bound, a energies of 32, 25, and 11 meV for $J=0$, 1, and 2, respectively. On the other hand, a recent relativistic scattering calculation by Thumm and Norcross (1991) finds all these states to be resonances at energies of 1.8, 5.6, and 12.8 meV, respectively. All these results are at the limits of accuracy that can reasonably be claimed for calculations, but they do strongly suggest that the b resonance, if it is not bound, is at a much lower energy than has been investigated by direct methods. Our tabulated value thus indicates a conservative upper bound on the energy of this resonance. Thumm and Norcross also identify a series of $6p^2\ ^3P_{0,1,2}$ resonances within several hundred meV (below) the $6p_{1/2}$ threshold.

At energies near the $6^2P_{1/2,3/2}$ excited-state thresholds (1.386, 1.455 eV), angular electron-scattering data (Gehenn and Reichert, 1977) indicate the presence of several strong structures, as do the transmission data of Johnston. The energy resolution in the experiment of Gehenn and Reichert (60 meV FWHM) does not enable them to clearly identify individual features at each of the thresholds; but a strong feature(s) occurs at the $^2P^\circ_{1/2}$ threshold, and there is an indication of structure at the $^2P^\circ_{3/2}$ threshold, although this is masked somewhat by a further, strong feature at 1.49 eV (Fig. 30). The feature(s) observed at the $^2P^\circ_{1/2}$ threshold are again not thought to be due to a single resonance but to a superposition of resonance and cusp effects, the c-type resonance ($6s6p\ ^1P^\circ$) perhaps making the dominant contribution to the observed intensity. This state is clearly observed in the LPD experiments of Patterson *et al.* (1974) and Slater *et al.* (1978; see also Fig. 31). These authors measure widths of about 1 meV and 3–4 meV for the resonances below the $^2P^\circ_{1/2}$ and $^2P^\circ_{3/2}$ thresholds, respectively. They have also performed close-coupling ($6s$-$6p$-$6d$) calculations that indicate that the dominant resonance configuration is $6p7s$ with a strong admixture of $6p5d$.

The structure observed by Gehenn and Reichert at 1.49 eV in their elastic differential scattering experiments has an angular dependence consistent with a resonance in the f wave. To verify that this feature was not associated with the 6^2P° thresholds, these authors made simultaneous measurements of elastic scattering at $\theta=135^\circ$ and of the photon yield from the $6^2P^\circ_{1/2}$ and $6^2P^\circ_{3/2}$ excited

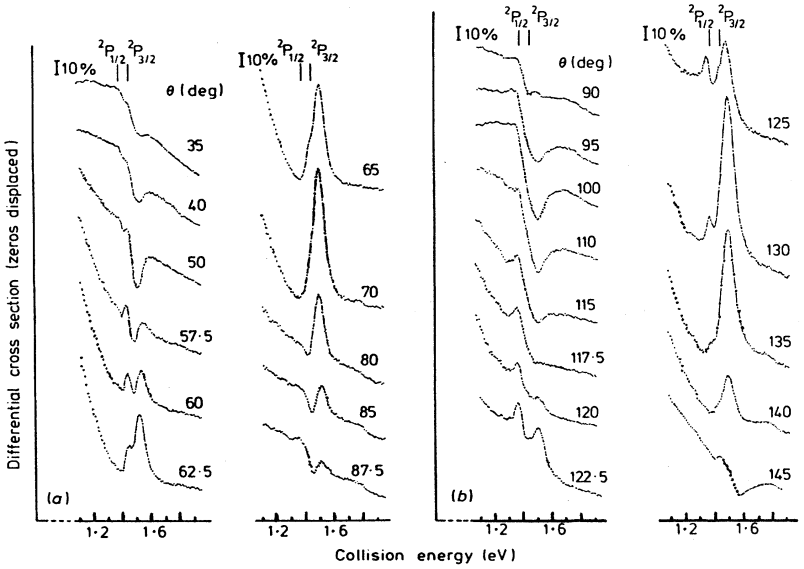

FIG. 30. Energy dependence of the elastic differential cross section for cesium. The positions of the 6^2P thresholds are shown at the top (from Gehenn and Reichert, 1977).

states at wavelengths of 894.6 and 852.3 nm, respectively. The photon excitation functions clearly show the resonance to be above both excited-state thresholds. The two-state close-coupling calculation of Burke and Mitchell (1973) reveals a $^3F^\circ$ shape resonance at 1.7 eV with a width of 0.4 eV. The inclusion of additional target eigenstates ($6s, 6p, 5d$) in the relativistic R-matrix calculations of Scott *et al.* (1984a, 1984b) has the effect of moving this resonance, which has the configuration $6p5d$, to an energy just above the $^2P_{1/2}$ threshold, in good agreement with Gehenn and Reichert. Recent experimental work (Reichert, 1986) has provided further support for the classification of this resonance. The measured circular polarization of the $6^2P_{1/2}$ resonance radiation emitted following excitation by spin-polarized electrons agrees well with a calculation that assumes the collision is dominated by a $^3F^\circ$ resonance at 1.50 eV.

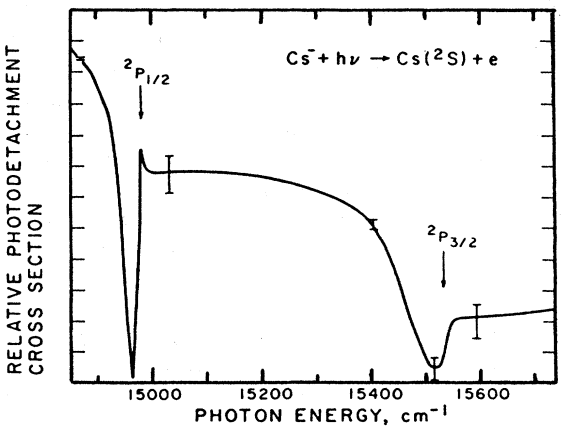

FIG. 31. Cs^- photodetachment ground-state partial cross section in the vicinity of the 6^2P thresholds (from Slater *et al.*, 1978).

The elastic angular distributions of Gehenn and Reichert show a further very weak structure at about 1.8 eV on which they make no comment (Fig. 30). We note that this feature is in the vicinity of the 5^2D excited states (1.798, 1.810 eV) and that Scott *et al.* (1984b) find evidence of resonance activity in the d wave in this energy region, their calculations indicating the presence of a $6p5d\ ^3D^\circ$ resonance.

At energies above 2 eV, the only available experimental data are once again provided by Johnston (1983; see also Fig. 24). As the R-matrix calculations do not extend beyond 2 eV, and as there is no other theoretical information available, one can only rely on a comparison with the other alkali metals for some insight as to the nature of the high-energy features. Johnston observes resonances at energies of 2.20–2.30, 2.68, 2.83–2.93, and 3.26 eV, but only offers a classification for the first of these states. Based on a graphical extrapolation of resonances in Na^-, K^-, and Rb^-, the nature of the K^- resonance having been determined unambiguously by angular scattering data, he tentatively classifies the structure at 2.2–2.3 eV as a D resonance with a possible configuration of $6s5d$. Johnston does point out, however, that the energy of this feature is higher than that predicted by the extrapolation of 0.1–0.2 eV, an amount which is unusually large for this technique when applied to the alkalis. Scott *et al.* do find a $6s5d\ ^3D$ resonance in their calculation, but at a very low energy (<0.5 eV). The nature of this resonance, and of those at higher energies, thus remains in doubt.

In conclusion, it is worth noting (again) that the calculations of Scott *et al.* (1984b) indicate the existence of a number of polarization-type resonances that arise when an electron is captured at very large distances in the long-range field associated with an excited state of the atom. In this case the state in question is the 6^2P, and

TABLE VIII. Recommended energies, widths, and classifications for resonances in Cs^-. The energies are expressed relative to the $6s\ ^2S$ ground state of atomic Cs. Unless otherwise specified, the values are from Johnston and Burrow (1982) or Johnston (1983).

Classification	Energy (eV)	Width (meV)	Comments
$6s6p\ ^3P^\circ$	<0.15		No firm experimental evidence: may be bound
$6p7s\ ^1P^\circ + 6p5d\ ^1P^\circ$	1.38	1	Patterson *et al.* and Slater *et al.*
"	1.45	3–4	
$6p^2\ ^1S$, $6p^2\ ^1D$	1.39		Various experiments
"	1.45		"
$6p5d\ ^3F^\circ$	1.49	~80	Gehenn & Reichert
$6p5d\ ^3D^\circ$(?)	1.80		"
$6s5d\ ^1D$	2.2–2.3		
	2.68		
	2.83–2.93		
	3.26		

these resonances appear in the calculation ostensibly as a result of the inclusion of the 5^2D states, which are strongly coupled to the 6^2P.

A summary of observed and calculated Cs^- states is given in Table VIII.

D. The noble gases

It is appropriate to consider the heavier rare gases neon, argon, krypton, and xenon separately to helium, as the spectrum of negative-ion resonances observed for these atoms reflects the significant differences in the nature of their positive ion-cores from that of helium. The ion core of these atoms, unlike helium, is split by the spin-orbit interaction, with the result that the $np^5\,(^2P^\circ_{3/2})$ and $np^5\,(^2P^\circ_{1/2})$ core terms are separated by 97, 177, 666, and 1307 meV for neon ($n=2$), argon ($n=3$), krypton ($n=4$), and xenon ($n=5$), respectively. This, together with the fact that the above ion cores have different parity and angular momenta to that of helium, results in the need for a different coupling scheme to describe the observed resonances. Furthermore, few similarities exist between the observed neutral spectra for the above gases and that of helium, and as such helium cannot generally be used as a guide for these atoms.

As a result of the ease with which these gases can be formed into target beams or cells, and their inherent inert nature, many high-resolution electron-scattering experiments have been conducted in recent years. There have, however, only been sporadic contributions from other fields, such as ion-atom collisions, and, unfortunately, relatively little theoretical work.

There are many similarities in the resonances observed within this group of atoms, but each, in general, has specific information to add to the overall picture, so it is not possible to use one as a general example. Systematic variations of resonances within the rare gases are discussed in some detail in Sec. VI.

1. General remarks on collision channels

Before reviewing specific details of resonances observed in electron scattering by the noble gases, it is helpful to recall some symmetry considerations that are generally applicable to electron-atom collisions. All experiments to date have dealt with electron scattering by the $np^6\ ^1S_0$ ground state. This implies that the initial state of the electron-atom system is characterized by the quantum numbers $lJ\pi$, where l is the initial orbital momentum of the electron; and the total angular momentum $J=l\pm 1/2$ and parity $\pi=(-1)^l$ are the only quantum numbers that are strictly conserved in the collision. This imposes significant constraints upon the nature of the resonances that can be observed: there is only one incident collision channel for each value of $J\pi$. Thus, for example, a resonance that is characterized by the configuration $np^5\,n's^2$ can only be excited by a p wave incident on the ground state, and one with a configuration $np^5\,n'sn'p$ only by an s or a d wave. For making qualitative statements about resonances in Ne and Ar, it is also appropriate in most cases to regard the total angular momentum $L=l$ and spin $S=\frac{1}{2}$ to be conserved quantities (though even for such light atoms the angular distribution of scattered electrons at resonance energies can exhibit pronounced effects of spin-orbit interaction: for example, the strong appearance of the a resonances in elastic electron scattering at 90°, which could not take place under strict LS conservation). These facts restrict the possible classifications of the low-lying resonances. They also allow for the existence of doubly excited metastable negative-ion states. For example, the $np^5\,(n+1)s\,(n+1)p\ ^4S_{3/2}$ state cannot autodetach into the $np^6\varepsilon l$ channel if LS coupling is valid. Such a state would thus be metastable if its energy were less than that of the $np^5\,(n+1)s\ ^3P^\circ_2$ state. This is apparently the case for Ar^-, but no cases are known to date in any other of the noble gases (Bae *et al.*, 1985).

All the heavy noble gases have two metastable states, $np^5\ (n+1)s\ ^3P^o_{2,0}$, which are sufficiently long-lived for a variety of atomic physics experiments: there have been numerous studies of photoabsorption in beams of metastable noble gases. To date, no experimental results on resonances in electron scattering by these metastable states have been reported. Calculations suggest that a number of resonances observed in scattering by the ground state would also play a role in scattering by the metastables (Taylor *et al.*, 1985). The low-energy cross sections that have been computed to date show strong similarities to those for electron scattering by ground-state alkali atoms.

2. Neon

Negative-ion resonances have been observed in Ne in a large number of electron-impact experiments in which a range of scattered particles, including elastic and inelastic electrons, photons, and metastable atoms, have been detected. Theoretical interest in these problems has been limited by the complexity of the correct neon target representation and the difficulty involved in accounting for spin-orbit effects. Despite these problems, some considerable success has been achieved through the R-matrix method in elucidating the spectroscopic classification of the lower-lying resonances and the contributions they make to near-threshold excitation cross sections.

The first observations of a Ne^- resonance were made in 1963 by Schulz and by Simpson and Fano in elastic electron scattering. Shortly after this, Simpson (1964) and Kuyatt *et al.* (1965) observed *two* sharp structures in electron transmission studies near 16 eV. These features were found to be separated by about 95 meV and were the first observation of a large class of resonances in the rare gases which are thought to be formed by two excited electrons being strongly coupled external to the positive-ion core and interacting only weakly with the core. Their signature is an energy separation that is closely related to that of the spin-orbit–split grandparent ion core states. Simpson and Fano (1963) classified these states as $Ne^-\ 2p^5\ (^2P^o_{3/2,1/2})\ 3s^2\ (^1S)$. In the years following these measurements, and up until the review by Schulz (1973a), there were many other studies of low-lying Ne^- resonances carried out in electron scattering and transmission (Andrick and Ehrhardt, 1966; Reichert and Deichsel, 1967; Sanche and Schulz, 1972a), metastable atom production (Olmsted *et al.*, 1965; Pichanick and Simpson, 1968), and decay photon observation (Sharpton *et al.*, 1970). These results have been discussed by Schulz (1973a). In the years since the Schulz review, further observations have been made in many of the same final channels, although with such improved resolution and sensitivity that considerably more structure has been resolved and, to some extent, identified.

Because of their energies, some 0.6 eV below the first excited $(2p^5\ 3s)$ configuration of neon, the two lowest-lying resonances in Ne^- can only be observed in electron scattering in the elastic channel. Such measurements have been performed by Eyb (1968), Kisker (1972b), Heindorff *et al.* (1973), Roy *et al.* (1975b), and Brunt *et al.* (1977c), with the measurement of Heindorff *et al.* including the spin-polarization analysis of the scattered electrons. The measurements of Brunt *et al.* constitute the most accurate determination of the energy of these resonances, the experimental energy scale having been determined by a combination of methods involving the known spectroscopic energies of the $2p^5\ 3s\ ^3P^o_2$ metastable level of neon and the energy of the 2^2S resonance in helium. These experiments (Fig. 32), conducted with an energy resolution of 14–20 meV, give the energies of the $^2P^o_{3/2,1/2}3s^2$ resonances as 16.111 and 16.208±0.008 eV, in good agreement with other values (Kisker, 1972b; Sanche and Schulz, 1972a, 1972b, 1972c). They also determine the widths of both the $3s^2$ resonances to be 1.3±0.4 meV, in excellent agreement with the measurements of Roy *et al.* (1.4–1.8 meV) and Eyb (1.4 meV). The measured spin polarization of electrons elastically scattered from neon (at 90°) in the region of these resonances shows distinct maxima and minima corresponding to the excitation of the $^2P^o_{3/2,1/2}$ resonances, respectively (Heindorff *et al.*, 1973). These states, the Ne^- *a* resonances, have also been observed recently in the free-free cross section for e^--Ne scattering in the presence of a laser field (Bader, 1986).

The few calculations of the Ne^- *a* resonances are all in reasonable agreement with experiment. The energy of the center of gravity of the $2p^5\ 3s^2$ resonance pair was

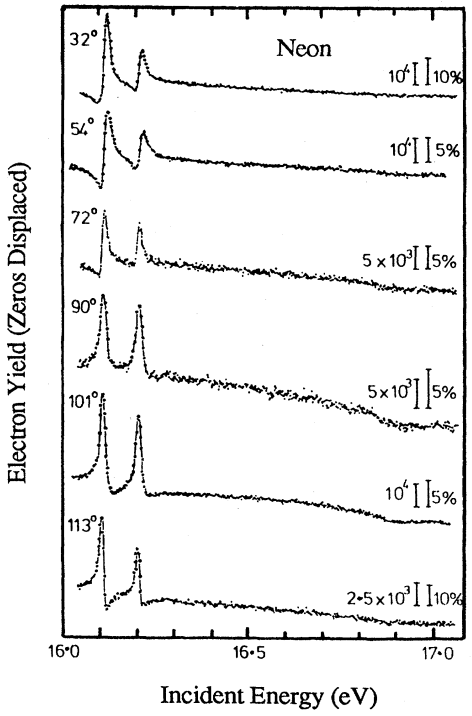

FIG. 32. Elastic electron-scattering spectra for neon at a range of scattering angles (from Brunt *et al.*, 1977c).

calculated by Weiss and Krauss (1970), using a superposition-of-configurations technique; this result agreed with the experimental value to within about 0.1 eV. Similar results using a MCHF method were obtained by Clark (1984, 1986). Analysis of the dominant configurations in these calculations indicates that the $2p^5 3s^2$ classification is appropriate and that the structure of the external electron pair is similar to that of the ground state of Na^- (see Sec. VI.A). The resonance energy and width were calculated by an R-matrix method by Noro *et al.* (1979) and by Clark and Taylor (reported in Clark, 1984). Both energies agree with the experimental value to within about 0.04 eV. The width reported by Noro *et al.* is 0.9 meV, whereas that of Clark and Taylor is 3 meV.

Spence and Noguchi (1975), in their analysis of Rydberg Feshbach resonances in the hydrogen halides, drew many comparisons with the higher reaches of the noble-gas resonance spectra observed by Sanche and Schulz, and made the first detailed attempt to classify the rare-gas resonances by considering them as two excited electrons external to the positive-ion core in a configuration such that their mutual screening of the core charge is maximized. This so-called grandparent scheme was expanded upon in the mid 1970s when several high-resolution observations of these and other resonances were made. Read *et al.* (1976) proposed an external coupling scheme appropriate to the grandparent resonance picture, and a number of semiempirical techniques, including the modified Rydberg formula (Heddle, 1977; Read, 1977) and a graphical approach (Spence, 1977), were introduced to aid in the classification of the higher-lying resonances. These techniques have been discussed in some detail in Sec. II.F.

High-resolution studies of the resonances above the $2p^5$ $3s$ neutral excited-state thresholds have been carried out by measuring the yield of UV photons resulting from the decay of the $2p^5$ $3s$ ($J=1$) states of neon (Raible *et al.*, 1974; Brunt *et al.*, 1977d), excitation functions for the $2p^5$ $3s$ ($J=0,2$) metastable states of neon (Brunt *et al.*, 1976; Buckman *et al.*, 1983b), and elastic electron differential scattering at a range of angles in the energy region from 16.5 to 17.5 eV (Brunt *et al.*, 1977c). Several calculations have also been performed in this energy region utilizing the R-matrix (Noro *et al.*, 1979; Clark and Taylor, 1982; Taylor *et al.*, 1985) and distorted-wave (Sawada *et al.*, 1971) approaches, all within the framework of LS coupling.

The near-threshold metastable and UV excitation functions of Brunt *et al.* (1976, 1977d) and Buckman *et al.* are dominated by resonance features at 16.907 and 16.950 eV, respectively (Fig. 33). Structure is also observed at about 16.9 eV in elastic-scattering measurements (Brunt *et al.*, 1977c). These features have been classified as one or more of the resonances associated with a $2p^5$ $(^2P^\circ_{3/2,1/2})$ $(3s3p)^3P^\circ$ coupling scheme and are therefore, in our nomenclature, b resonances. Noro *et al.* (1979) performed an R-matrix calculation that gave a b resonance, which they identified with this coupling scheme. Clark and Taylor (1982) carried out an eigenchannel analysis of electron-scattering calculations in this energy region. The calculations were made with the R-matrix method, and, although performed in LS coupling, they reproduced the general features observed in the metastable and UV excitation functions (i.e., the singlet and triplet channels) reasonably well. Their analysis confirmed the classification for the b resonances of Brunt *et al.* (1976, 1977d). In a later paper, Taylor *et al.* (1985) calculated total scattering cross sections for excitation of the $3s$ and $3p$ states of neon from the ground state as well as cross sections for elastic, inelastic, and superelastic scattering from the $3s$ level. In particular, the relative agreement between their cross section for the excitation of the $3s$ $^3P_0$ state and the metastable excitation function of Buckman *et al.* (1983b) is excellent up to about 2 eV above threshold.

In the grandparent or external coupling scheme of Read (1976), the configuration $3s3p$ can also couple to give a $^1P^\circ$ term, and this has been associated with the broad feature labeled c in the work of Brunt *et al.* (1976,

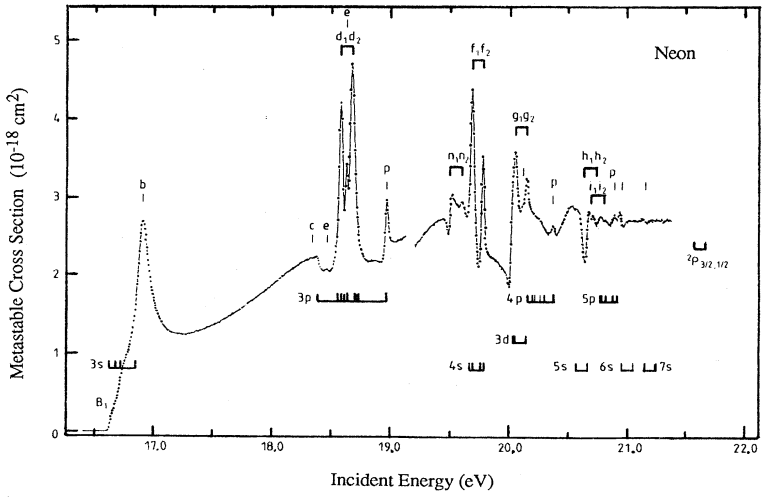

FIG. 33. Metastable atom excitation function for neon. A linear function has been subtracted from the higher-energy part of the spectrum and its vertical scale has been expanded. The positions of observed resonances are indicated by the lines above the spectra, while those below indicate the energies of the excited states of neutral neon (from Buckman *et al.*, 1983b).

1977d) at an energy of about 18.35 eV. On coupling with the Ne^+ core, five different states are possible, and all can decay to the 3*s* levels of neon by emission of a *p*-wave electron (Read *et al.*, 1976) and minimal rearrangement, raising the expectation that they would be rather broad features, in line with the experimental observation. In neon this resonance does not fully develop before the opening of the $2p^5\ (^2P_{3/2})\ 3p\,(J=1)$ level at 18.382 eV, where a sharp decrease in the metastable yield is noted, consistent with a Wigner cusp or step (Buckman *et al.*, 1983b).

The classification of this feature is also supported by the eigenchannel analysis of Clark and Taylor (1982), but, somewhat surprisingly, the analogous resonance in argon has been classified differently by Ojha *et al.* (1982). This will be discussed in more detail in the next section. Noro *et al.* (1979) classified the *c* feature as a $3s3p\ ^3P^\circ$ state, but their reason for doing so is unclear. This matter is discussed further in Sec. VI.C. It should be noted that in all these calculations, the resonances appear in all *terms* of the relevant resonance *configurations.* For example, the configuration labeled $2p^5\ (^2P^\circ)\ (3s3p)^3P^\circ$ gives rise to six spectroscopic terms $^{2,4}S$, P, D; a *b* resonance has been found in all collision channels with these *LS* values [only the ^2S and ^2D channels occur in electron scattering by the ground state of Ne; all are present in scattering by the lowest metastable state (Taylor *et al.*, 1985)]. This is consistent with the picture of these resonances as a well-defined two-electron complex in the field of a positive ion: the dynamics of the system are governed by the external coupling of the two electrons, with electron-core interactions giving rise only to multiplet structure. Such a picture contrasts with the alternative, a one-electron description, in which the properties of the resonance are determined by the coupling of an outer electron to the core; this latter description applies, for example, to the shape resonances in the halogens discussed in Sec. VI.D. Thus it should be kept in mind that the experimentally observed "resonances" attributed to non-^1S externally coupled pairs are probably an unresolved composite of states with different total angular momenta and different collision strengths. The experimentally determined energies and widths of these features therefore will usually not describe the properties of individual resonances. The calculations of Clark and Taylor show that the ^2S and ^2D terms of the *b* resonance are separated by energies that are smaller than their widths, so that the *c* feature is not associated with a term of the externally coupled $^3P^\circ$ configuration.

In a recent complex dilated double-configuration Hartree-Fock calculation, Bentley (1991) has confirmed the grandparent nature of the *b* and, to a lesser extent, the *c* resonance. He demonstrates how the two outer electrons that constitute the resonance in the grandparent scheme are almost completely isolated from the core orbitals and have little effect upon them. Some question remains about the nature of the *c* resonance in this approximation, as Bentley was unable to obtain convergence for a calculation using a single-configuration approximation to the $^1P^\circ$ grandparent state. Attempts to describe the *c* feature in similar terms to those used by Ohja *et al.* for argon (outlined briefly above) were not successful; so there still remains some uncertainty as to the nature of the *c* resonance in neon.

Located immediately above the *c* resonance in neon (and in the heavier noble gases) is a group of strong resonances in the region of the thresholds of the $2p^5\ 3p$ manifold (see Fig. 33). In neon these features have been observed with high resolution in the transmission experiments of Sanche and Schulz (1972a), in metastable excitation by Brunt *et al.* (1976) and Buckman *et al.* (1983b), and in optical (vuv) excitation functions by Brunt *et al.* (1977d). The two dominant resonances in this region at 18.578 and 18.670 eV (Brunt *et al.*—in excellent agreement with the energies of Sanche and Schulz) were classified as $2p^5\ (^2P_{3/2,1/2})\ 3p^2\ ^1S$ by Brunt *et al.* (1976) and Read *et al.* (1976), although the first such classification was made for the analogous pair of resonances in krypton by Spence and Noguchi (1975).

Read *et al.* point out that within their grandparent coupling scheme the configuration $3p^2$ can result in ^1S, ^1D, and ^3P terms and, on coupling to the ion core, these terms will be further split into 2, 6, and 13 *jLSJ* states, respectively. With the exception of the resonance pair mentioned above, only three other resonance features are observed in neon in the energy region of the 3*p* excited states. One of these, between the d_1d_2 pair, was assigned the configuration $3p^2\ ^1D$, and a further weaker resonance located below the d_1 feature by Buckman *et al.* (1983b) has also been given this tentative assignment, the ^1D classification being favored over ^3P as the widths of the latter are expected to be broader (Read *et al.*, 1976). So, while this region is of particular interest with regard to the application of the external coupling scheme, the combination of the widths of the resonances and the relatively small ion core splitting in neon results in little conclusive information being available. However, we shall return to this region in more detail in the heavier noble gases.

The applicability of the grandparent scheme in the rare gases was brought into question by a series of experiments in which resonant free-free transitions were observed between the $3s^2$ resonances and higher-lying resonances in the d_1d_2 resonance region discussed above. These experiments (Langendam and Van der Wiel, 1978) indicated a series of nine resonances at energies between 18.6 and 18.75 eV, which were all classified as nonvalence resonances associated with neutral $2p^5\ 3p$ parent states. This classification, based on close correspondences with neutral-state thresholds and the imposed even parity of any such states produced by photoexcitation, was in conflict with the classification of Read *et al.* (1976). However, subsequent experiments of this type were not able to confirm the earlier results, and they thus remain in some doubt.

At an energy of 18.964 eV (Brunt *et al.*, 1976) a strong,

narrow, and rather interesting feature is observed in the metastable excitation function (18.95 eV in transmission—Sanche and Schulz). As there is no apparent partner associated with this resonance, and as Spence's (1977) graphical analysis indicates that it belongs to a family of similar features in the heavier gases, it was considered by Brunt *et al.* (1977d) not to be of the grandparent type. Rather, they proposed that this family of states, all of which are located very close to the np^5 $(^2P^\circ_{3/2,1/2})$ $(n+1)p$ $(J=0)$ levels, are possibly *nonvalence* or *polarization* resonances of the type suggested by Nesbet (1978) at the 2^1S and 2^3S thresholds in helium. In the case of neon, this resonance is situated near the $(^2P^\circ_{3/2,1/2})$ $3p$ $(J=0)$ state at 18.966 eV. That it lies below this state in energy is supported by its relatively narrow width and the fact that optical excitation functions for the $3p$ state (Kisker, 1972a; Brunger *et al.*, 1987) show no evidence of a strong, near-threshold resonance.

At higher energies many additional resonances, including several resonance pairs, were observed in the experiments of Sanche and Schulz (1972a) and Brunt *et al.* (1976). Brunt *et al.* proposed tentative classifications for some of these features, as did Spence (1977) in the application of his graphical technique to both of the above data sets. They proposed that the resonance pairs observed at 19.961–19.778 eV (f_1f_2) and 20.05–20.15 eV (g_1g_2) were possibly [core]$4s^2$ and [core]$3d^2$, respectively, with the most likely term being ^1S. Buckman *et al.* (1983b) measured metastable excitation functions with improved resolution and sensitivity. They observed all of the features found in the transmission experiment of Sanche and Schulz and offered tentative classifications for many of them. They observed a resonance pair (n_1n_2) at 19.498–19.598 eV that is below the f_1f_2 pair, and subsequently reassigned this pair the configuration $4s^2\ ^1S$, the f_1f_2 pair as $3d^2\ ^1S$, and the g_1g_2 pair as $4p^2\ ^1S$. Higher-energy pairs h_1h_2 and i_1i_2 were also observed, but no definitive classification was offered. These resonances and others mentioned above are shown in Fig. 33.

In addition to these resonance pairs, several other strong single-resonance features were observed. Two of these, at 20.369 and 20.890 eV, lie very close to the thresholds of the $(^2P^\circ_{1/2})4p$ and $5p$ $(J=0)$ states of neon and were proposed by Buckman *et al.* as further examples of nonvalence resonances.

Recommended energies, widths, and classifications for the autodetaching states of neon are given in Table IX.

TABLE IX. Recommended energies, widths, and classifications of resonances in Ne^- below the first ionization potential. The energies are expressed relative to the $2p^6\ ^1S$ ground state of atomic Ne. Unless otherwise specified, the values are from Brunt *et al.* (1976, 1977c) and Buckman *et al.* (1983b). Figures in parentheses represent the uncertainty in the least significant digit.

Classification	Energy (eV)	Width (meV)	Comments
$2p^5(^2P^\circ_{3/2})3s^2(^1S)$	16.111(8)	1.3(4)	*a*
$2p^5(^2P^\circ_{1/2})3s^2(^1S)$	16.208(8)	1.3(4)	*a*
$2p^5(^2P^\circ_{3/2,1/2})3s3p(^3P^\circ)$	16.906(10)	117	*b*
$2p^5(^2P^\circ_{3/2,1/2})3s3p(^1P^\circ)$	18.35(100)		*c*
$2p^5(^2P^\circ_{3/2,1/2})3p^2(^1D)$	18.464(15)		
$2p^5(^2P^\circ_{3/2})3p^2(^1S)$	18.580(10)	30	
$2p^5(^2P^\circ_{3/2,1/2})3p^2(^1D)$	18.626(15)	25	
$2p^5(^2P^\circ_{1/2})3p^2(^1S)$	18.672(10)	50	
$[2p^5(^2P^\circ_{1/2})3p]_0+\varepsilon s$	18.965(10)	22	
$2p^5(^2P^\circ_{3/2})4s^2(^1S)$	19.498(15)		
$2p^5(^2P^\circ_{1/2})4s^2(^1S)$	19.598(15)		
$2p^5(^2P^\circ_{3/2})3d^2(^1S)$	19.686(10)	42	
$2p^5(^2P^\circ_{1/2})3d^2(^1S)$	19.778(10)	23	
$2p^5(^2P^\circ_{3/2})4p^2(^1S)$	20.054(10)	60	
$2p^5(^2P^\circ_{1/2})4p^2(^1S)$	20.150(10)	60	
$[2p^5(^2P^\circ_{1/2})4p]_0+\varepsilon s$	20.369(15)		
	20.636(15)		
	20.737(15)		
	20.693(15)		
	20.798(15)		
$[2p^5(^2P^\circ_{1/2})5p]_0+\varepsilon s$	20.890(20)		

3. Argon

The negative-ion resonance spectrum of argon is, in general, similar to that of neon, although the increased spin-orbit splitting in the ion core (177 meV) results in less overlapping of many of the resonance features and a correspondingly richer spectrum. Once again these features have been mainly studied in electron-impact experiments with a small input from ion-atom collisions. Theoretical treatments of Ar^- resonances have been made by quasi-bound-state methods and by R-matrix calculations.

The lowest-lying (a) resonances are the pair $(^2P^\circ_{3/2,1/2})4s^2\ ^1S$ that are below the energy of the first excited $(4s)$ state of argon and are thus only observable, in electron-scattering experiments, in the elastic channel. The body of available work on these two features is similar to that for neon, except that these features have also been observed in ion-atom collisions. Measurements prior to 1972 are summarized in Schulz's review. Since 1972 accurate determinations of the energies of these states have been made by Weingartshofer *et al.* (1974) and Brunt *et al.* (1977c). The latter experiment, with an energy resolution of 20 meV, gives energies of 11.098 and 11.270±0.010 eV, slightly higher than that of Weingartshofer *et al.* (11.07, 11.242±0.01 eV, with an energy resolution of <30 meV) but in excellent agreement with the transmission experiment of Sanche and Schulz (1972a). Most of the discrepancy with Weingartshofer *et al.* can be attributed to these authors' using a lower value of the He^- 2^2S resonance energy as a calibration energy. Both Weingartshofer *et al.* and Brunt *et al.* performed a phase-shift analysis of their data to extract values for the widths of these resonances. Their respective values of 3–4 and 2.5±0.5 meV are in

reasonable agreement. Edwards (1975a, 1975b, 1976) observed the autodetachment spectra of these resonances in collisions of Ar with O^-, H^-, and D^-; measurements of the electron angular distributions provided information on the M_J populations of these resonances as produced in atomic collisions, which supports the (noncontroversial) assignment of their J values.

Weiss and Krauss (1970) computed the average-of-configuration energy of the a resonances, using a superposition-of-configurations approach. Their result agrees with the experimental value given here to within 100 meV. They made note of the similarity of the 4s orbital with that of K^- $3p^6 4s^2$. These resonances have also been studied in two calculations using the R-matrix approach (Ojha *et al.*, 1982; Scott *et al.*, 1982). The calculation of Ojha *et al.* was performed in the LS-coupling approximation, while that of Scott *et al.* included, for the first time in such a calculation, the effects of spin-orbit interaction. The resultant energies and widths for the $(^2P^\circ_{3/2,1/2})4s^2\ ^1S$ resonances are in reasonable agreement with the experimental values cited here.

These resonances have also been observed in the cross section for free-free radiative transitions in experiments in which high-resolution electron-argon scattering is carried out in the presence of a laser field (e.g., Langhans, 1978; Bader, 1986).

At energies above the lowest excited state of argon [$3p^5$ 4s ($J=2$) at 11.548 eV], negative-ion resonance features have again been observed in electron scattering and transmission, and in metastable atom and vuv photon excitation functions. Yet again the metastable channel has proven to be an extremely sensitive means of studying these features, and we use it as an example of the argon resonance spectrum in Fig. 34. In the work of Brunt *et al.* (1976) and Buckman *et al.* (1983b), four features are clearly observed in the region of the 4s manifold of neutral excited states. Sanche and Schulz (1972a) observed two features in this region at 11.71 and 11.91 eV and classified them as $3p^5$ 4s4p resonances. As in neon, Brunt *et al.* extended this classification, associating the four observed states at 11.631, 11.675, 11.785, and 11.845 eV with the $^3P^\circ$ term of this configuration. Two of these features were also observed in optical (vuv) excitation functions at 11.664 and 11.845 eV (Brunt *et al.*, 1977d). The R-matrix calculation of Ojha *et al.* (1982) is in accord with the classification of these states as b resonances.

Between the 4s and 4p neutral excited states a broad, strong resonance is observed in the metastable excitation function and in inelastic excitation functions for the 4s levels (Buckman *et al.*, 1981; Wong, 1981; Bass *et al.*, 1987). Brunt *et al.* (1976) classified this feature at an energy of about 12.7 eV as $(^2P^\circ_{3/2,1/2})4s4p\,(^1P^\circ)$, analogous to the c resonance in neon, and this classification was supported by Buckman *et al.* However, this classification is not confirmed by the R-matrix calculation of Ojha *et al.* They find that the c feature receives a significant contribution from channels of overall $^2F^\circ$ symmetry, which is inconsistent with a p^5sp' configuration. They do not report results of a specific eigenchannel analysis, but assign the c feature to a mixture of the externally coupled configurations $4s3d\ ^1D$ and $4p^2\ ^1D$.

This feature has also been studied in inelastic electron excitation functions for the individual states of the 4s manifold by Buckman *et al.* (1981), Wong (1981), and Bass *et al.* (1987). All of these measurements indicate an apparent preferential decay of the resonance to the 4s levels with a $^2P^\circ_{3/2}$ ion core: that is, to the $3p^5$ $(^2P^\circ_{3/2})4s$ ($J=2$ and $J=1$) states. They also indicate an enhanced decay to these final states at intermediate (30°–60°) scattering angles. It is difficult, on the basis of this experimental evidence, to be conclusive in assigning a configuration to this structure. We believe the terms of the $4p^2\ ^1D$ configuration proposed by Ohja *et al.* are those observed experimentally at higher energies (and discussed in some detail below). Both of the alternate

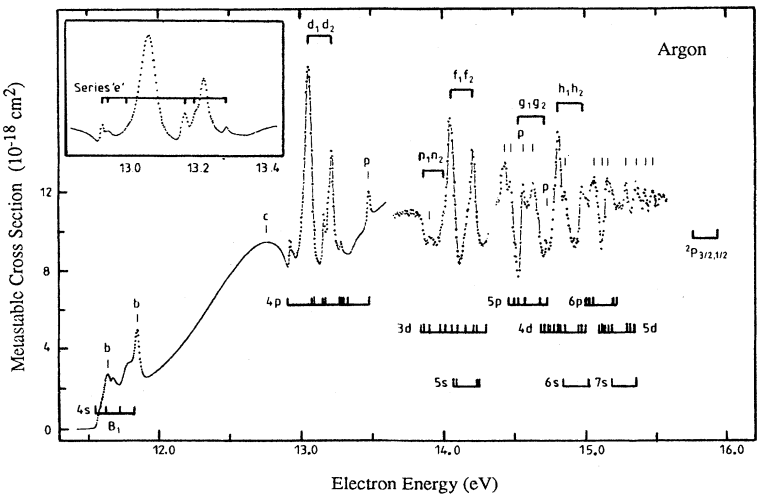

FIG. 34. Metastable atom excitation function for argon. The two upper parts of the spectrum have had a background function subtracted, and the vertical scale has been expanded. The inset shows the region around the d_1d_2 resonances in greater detail (from Buckman *et al.*, 1983b).

configurations [$4s4p(^1P^\circ)$ and $4s3d\ ^1D$] possess a large number of possible terms, and a consideration of probable decay modes based on angular momenta and parity arguments does not clearly favor one over the other. It is thus not possible to conclude that all of the resonance strength observed in this region is due to a series of c-type resonances. It is more likely that it arises from a combination of the $4s4p\ ^1P^\circ$ and $4s3d\ ^1D$ configurations. We discuss this issue somewhat further in Sec. VI.E.

The region above this broad resonance, in the vicinity of the $3p^5 4p$ manifold, is of great interest and importance in the discussion of the nature of the rare-gas negative-ion resonances. Unlike neon, many resonance features have been observed in this region in recent high-resolution experiments, and the experiments themselves cover a wide range of final channels, enabling a critical evaluation of the proposed resonance classifications. In both the transmission experiments of Sanche and Schulz and the metastable atom excitation functions of Brunt *et al.*, six features are observed in this energy region. Two of these dominate the spectrum and are separated in energy by an amount approximately equal to the ion core splitting. These features, analogous to the d resonances in neon, have been classified as $(2P^\circ)4p^2\ ^1S$ by Read *et al.* (1976). As both of the above experiments represent total cross sections, it is not possible to unambiguously determine the configurations of the observed features. The application of the classification scheme of Read *et al.*, particularly to the higher-lying resonances, was based on information for similar two-electron configurations in the alkaline earths and the predictions of semiempirical approaches such as the modified Rydberg formula or graphical analysis. However, in the case of the resonances near the $np^5\ (n+1)p$ excited states of the heavier noble gases, information is also available from further experiments where the angular behavior of the autodetached electrons is studied, enabling, in principle, a more detailed investigation of proposed classification schemes. These experiments include the differential elastic-scattering measurements of Hammond (1982) and the differential excitation functions for the argon $3p^5 4s$ levels (Buckman *et al.*, 1981; Wong, 1981; Bass *et al.*, 1987) mentioned previously.

When studied in elastic scattering, the $3p^5$ $(^2P^\circ_{3/2,1/2})4p^2\ (^1S)$ resonances, which have odd parity, are formed from and decay into the target atom plus a $p_{1/2,3/2}$ electron. Hammond's studies for argon, covering an angular scattering range from 32° to 112°, show no intensity of these features ($d_1 d_2$) at 90°, in accord with an outgoing p-wave electron. The conclusions that can be drawn from the inelastic electron excitation functions are not quite so straightforward, as the angular momentum of the ion core of the final state must also be considered. The measurements of Buckman *et al.* and Bass *et al.* involved measuring excitation functions for all four of the $3p^5\ 4s$ levels for a range of scattering angles between 10° and 90°. The interpretation of these excitation functions depends rather heavily on the coupling scheme adopted for the description of the argon excited states. Buckman *et al.* used jj coupling, and their analysis of the decay modes of the $d_1 d_2$ pair was reasonably consistent with the classification of Read *et al.* The few inconsistencies that they noted, particularly concerning the decay of the d_1 resonance, may well be indicative of the inadequacies of the jj-coupling description or of configuration mixing in the resonant state. It is also apparent in the spectra of Buckman *et al.*, Wong, and Bass *et al.* that there is a clear preference, within the constraints imposed by the external classification scheme, for decay routes that preserve the nature of the ion core. This is particularly true for the $d_2(^2P^\circ_{1/2})$ resonance, which shows little or no intensity in the excitation functions for the $3p^5(^2P^\circ_{3/2})$ $4s\ (J=2)$ excited state (Fig. 35). These considerations will be discussed and illustrated in further detail in the next section.

In addition to the remaining four resonances observed in this energy region by Sanche and Schulz and Brunt *et al.*, three more narrow and relatively weak new features were observed in the high-resolution metastable atom experiment of Buckman *et al.* (1983b; see also Fig. 34). Read *et al.* had classified three of the remaining four resonances as possible candidates for the

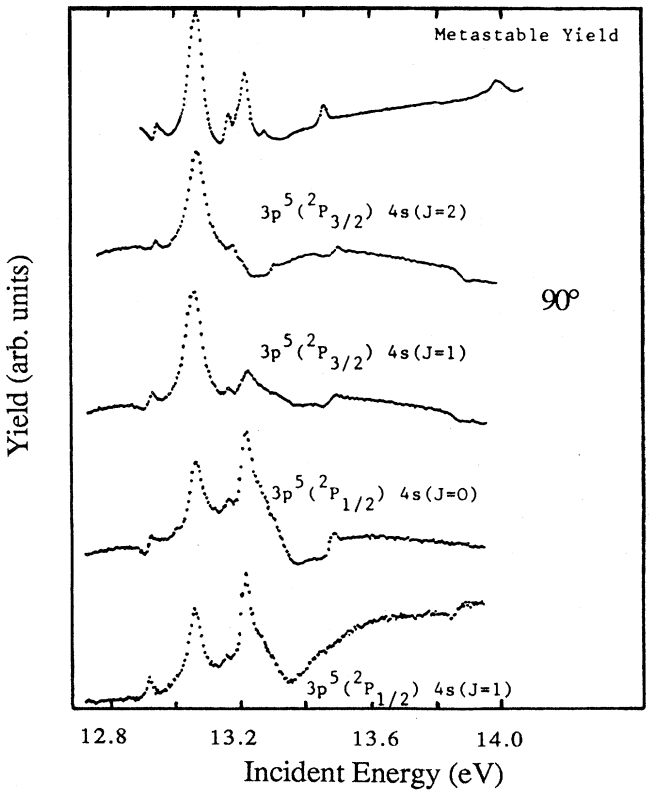

FIG. 35. Inelastic electron excitation functions for the four $3p^5 4s$ levels of argon at a scattering angle of 90° and in the energy range from 12.8 to 14.0 eV. The top spectrum is the metastable atom excitation function over the corresponding energy range (from Bass *et al.*, 1987).

configuration $4p^2\ ^1D$. On the basis of their energies and widths, the three new resonances were also classified as $4p^2\ ^1D$ by Buckman *et al.*, bringing the total number of *e* resonances in argon to six, consistent with the predictions of the external coupling scheme. However, observations in both elastic and inelastic electron excitation functions are not entirely supportive of these classifications. In general, these experiments have only managed to identify the three stronger *e* features initially observed by Brunt *et al.* These features, if their classification is correct, should decay to the elastic channel by emission of a *p*- or *f*-wave electron. The elastic-scattering experiments of Hammond support this proposition for the resonance e_i but apparently not for the other two resonances, although the sensitivity of this channel to these weak features is very low. Once again, in the inelastic excitation functions (Buckman *et al.*, 1983b; Bass *et al.*, 1987), the expected behavior of these states is difficult to predict because of spin-orbit effects; however, the behavior of the observed resonance features is generally consistent with the classification of Read *et al.*

TABLE X. Recommended energies, widths, and classifications of resonances in Ar^- below the first ionization potential. The energies are expressed relative to the $3p^6\ ^1S$ ground state of atomic Ar. Unless otherwise specified, the values are from Brunt *et al.* (1976, 1977c) and Buckman *et al.* (1983b). Figures in parentheses represent the uncertainty in the least significant digit.

Classification	Energy (eV)	Width (meV)	Comments
$3p^5(^2P^\circ_{3/2})4s^2(^1S)$	11.098(10)	2.5(5)	*a*
$3p^5(^2P^\circ_{1/2})4s^2(^1S)$	11.270(10)	"	*a*
$3p^5(^2P^\circ_{3/2,1/2})4s4p\,(^3P^\circ)$	11.631(8)		*b*
	11.675(8)		
	11.785(8)		
	11.845(8)	40	
$3p^5(^2P^\circ_{3/2,1/2})4s4p\,(^1P^\circ)$	12.7(1)		*c*
$3p^5(^2P^\circ_{3/2,1/2})4p^2(^1D)$	12.925(10)	17	
	12.942(10)		
	12.99(1)		
$3p^5(^2P^\circ_{3/2})4p^2(^1S)$	13.055(8)	52	
$3p^5(^2P^\circ_{3/2,1/2})4p^2(^1D)$	13.162(8)	23	
	13.190(10)		
$3p^5(^2P^\circ_{1/2})4p^2(^1S)$	13.216(8)	43	
$3p^5(^2P^\circ_{3/2,1/2})4p^2(^1D)$	13.282(8)	27	
$[3p^5(^2P^\circ_{1/2})4p]_0+\varepsilon s$	13.479(8)	25	
$3p^5(^2P^\circ_{3/2})3d^2(^1S)$	13.864(15)		
	13.907(15)		
$3p^5(^2P^\circ_{3/2})4p^2(^1S)$	14.006(15)		
$3p^5(^2P^\circ_{3/2})5s^2(^1S)$	14.052(10)	52	
$3p^5(^2P^\circ_{1/2})5s^2(^1S)$	14.214(10)	45	
	14.434(20)		
	14.478(20)		
$3p^5(^2P^\circ_{3/2})5p^2(^1S)$	14.530(15)	60	
$[3p^5(^2P^\circ_{3/2})5p]_0+\varepsilon s$	14.566(20)		
	14.634(20)		
$3p^5(^2P^\circ_{1/2})5p^2(^1S)$	14.711(20)		
$[3p^5(^2P^\circ_{1/2})5p]_0+\varepsilon s$	14.735(20)		
$3p^5(^2P^\circ_{3/2})6l^2(^1S)$	14.811(20)		
	14.859		
$3p^5(^2P^\circ_{1/2})6l^2(^1S)$	14.983		
	15.064		
	15.120		
	15.160		
	15.288		
	15.364		
	15.429		
	15.477		

The remaining resonance in this energy region is the strong, sharp feature labeled *p* in Fig. 34 at 13.475 eV, 5 meV below the energy of the $3p^5\ (^2P^\circ_{1/2})4p\ (J=0)$ level of argon. This resonance, which is analogous to those discussed previously in neon, has been classified as a "nonvalence" resonance formed by the attachment of an electron in the polarization potential associated with a neutral excited state. In this case, and in all other similar cases in the noble gases, the excited states concerned have the same spin and parity as the ground state. Thus excitation observed in elastic scattering will involve *s* waves in both entrance and exit channels. The elastic-scattering measurements of Hammond (1982) confirm this prediction. The inelastic-scattering measurements are again not conclusive because of the uncertainty in describing the coupling of the excited states concerned. However, they do indicate that decay paths that involve a flip of the core spin, in this case to the $(^2P^\circ_{1/2})4s\ (J=2)$ level, are not favored.

At higher energies in argon, four further resonance pairs have been observed (Buckman *et al.*, 1983b) as well as many other single-resonance features (Sanche and Schulz, 1972a, 1972b, 1972c; Buckman *et al.*). The energies and widths of these resonances, along with those discussed above, are given in Table X together with suggested classifications.

The total cross section for electron scattering by Ar, as viewed on an extended energy scale between 0 and 300 eV, is dominated by a broad resonance, about 10 eV wide, centered at a collision energy of about 15 eV (see Fig. 32). This is presumably a $3p^6\varepsilon d$ shape resonance, which results from a "double-well" structure in the effective potential for a *d* wave. This resonance was used as an illustrative example in Sec. II and is discussed further in Sec. VI.D. It has counterparts in Kr and Xe, but not in Ne.

4. Krypton

In many respects, krypton offers the best opportunity for an appraisal of coupling schemes used to describe resonance behavior in the noble gases. Firstly, it possesses a relatively large spin-orbit splitting in the ion core (666 meV), and, as a result, the lower-lying excited states are well separated, as are many of the *b*, *c*, *d*, and *e* resonances. Secondly, as we descend the group-VIII elements of the periodic table, it becomes more appropriate to apply *jj* coupling in the description of the excited states of the atom. While the above may ease the task of

analyzing the lower-lying resonances, it renders, however, the interpretation of features near the ionization limit rather difficult, as many of the excited-state manifolds and resonance pairs begin to overlap. A further advantage in the analysis of the Kr^- spectrum is that many final channels have been investigated in a wide range of experiments. In particular, electron excitation functions for all four of the $5s$ excited states, and for some of the states in the $5p$ manifold, assist in the classification of the observed resonances.

Krypton is the first atom in the rare-gas sequence in which the higher-lying a resonance (a_2) is located above the first neutral excited state. In fact, this resonance lies above both the $4p^5\ (^2P^\circ_{1/2})5s$ $(J=2)$ and $(J=1)$ excited states but below the $4p^5\ (^2P^\circ_{3/2})5s$ $(J=0)$ and $(J=1)$ states, and, consequently, it has been observed in a range of both elastic- and inelastic-scattering experiments. These include transmission experiments and excitation functions for uv photons and metastable atoms. In the elastic electron excitation functions (Weingartshofer *et al.*, 1974; Heindorff *et al.*, 1976; Hammond, 1982), these resonances $[4p^5\ (^2P^\circ_{3/2,1/2})5s^2\ (^1S)]$ display quite different intensities at most scattering angles, with the $^2P^\circ_{3/2}$ state being considerably stronger. As is the case in the other noble gases, these resonances decay into the ground state by emission of a p-wave electron. However, the a_2 resonance in Kr can also decay into either of the $(^2P^\circ_{3/2})$ $4s$ levels and, in particular, into the $(^2P^\circ_{3/2})$ $4s$ $(J=1)$ level by emission of an s-wave electron, resulting in a lower intensity in the elastic channel (Fig. 36). This resonance is also noticeably broader than the a_1 resonance, reflecting a shorter lifetime against autodetachment as a result of the larger number of possible decay routes.

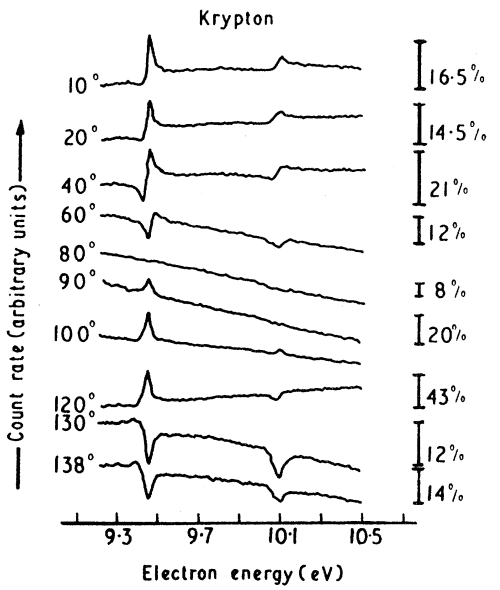

FIG. 36. Elastic electron scattering from krypton in the energy range from 9.3 to 10.5 eV showing the variation of intensity with scattering angle of the $4p^5 5s^2$ resonance pair (from Weingartshofer *et al.*, 1974).

Weingartshofer *et al.* locate these resonances at 9.47 and 10.107 ± 0.01 eV, in good agreement with the earlier measurements of Kuyatt *et al.* (1965) but somewhat lower than the energies given by Sanche and Schulz (1972a, 1972b, 1972c) in their transmission measurements. As in the case of argon, the energies quoted by Weingartshofer *et al.* may be too low by up to 50 meV as a result of the calibration energy used for the $2\ ^2S$ resonance in helium. Weingartshofer *et al.* also conducted a phase-shift analysis on the a_1 resonance from which they determined a width of about 8 meV. They note that the a_2 resonance is broader but do not give a value for its width. In their work on metastable excitation functions, Brunt *et al.* (1976) also performed simultaneous measurements for elastically scattered electrons and located the a_1 and a_2 resonances at 9.484 and 10.123 eV, respectively.

Perhaps the most accurate determination of the energy of this resonance comes from the threshold electron spectrum of Jureta *et al.* (1978). These types of experiment collect low-energy inelastically scattered electrons with high efficiency, and, when a negative-ion feature is near a neutral excited state into which it can autodetach, such a feature will appear in the threshold spectrum. This is the case in the threshold electron spectrum of krypton, where the decay of the a_2 resonance into the $(^2P^\circ_{3/2})5s$ $(J=1)$ neutral excited state results in emission of an electron of energy less than 100 meV, which can be detected, albeit with diminished efficiency, by the threshold electron detector. The measurement of Jureta *et al.* places the a_2 resonance at 10.119 ± 0.005 eV.

A MCHF calculation in LS coupling by Clark (1984) gives energies for the a resonances that agree with the experimental values to within 100 meV. These results are described in more detail in Sec. VI.A. We are not aware of other theoretical calculations of Kr^- resonances.

At higher energies the a_2, b, c, d, and e resonances have been observed in a wide variety of experiments including metastable excitation functions (Brunt *et al.*, 1976; Buckman *et al.*, 1983b), vuv photon excitation functions (Brunt *et al.*, 1977d), differential electron excitation functions (Swanson *et al.*, 1973; Buckman *et al.*, 1981; Hammond, 1982; Phillips, 1982; Bass *et al.*, 1987), and in the transmission experiments of Sanche and Schulz. As mentioned earlier, the a_2 resonance, according to its classification as $(^2P^\circ_{1/2})5s^2\ ^1S$, can decay into the $(^2P^\circ_{3/2})5s$ $(J=2)$ level by emission of a d-wave electron or into the $5s$ $(J=1)$ level by s-wave emission (Swanson *et al.*, 1973; Brunt *et al.*, 1977d), although both of these routes involve a change of the core angular momentum. These expectations are confirmed by the experimental evidence. Firstly, the near-threshold differential excitation functions for the $J=2$ and $J=1$ levels measured by Swanson *et al.* and Phillips indicate a much stronger decay of the a_2 feature to the $J=1$ level than to the $J=2$. Secondly, measurements at several

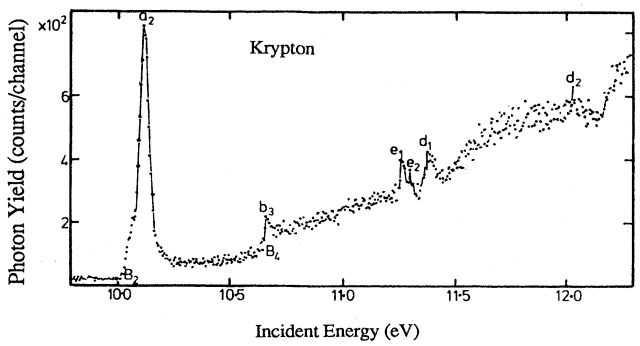

FIG. 37. Excitation function for the uv-emitting levels of krypton (from Brunt *et al.*,1977d).

scattering angles (30°,55°,90°-Phillips, 1982) support the decay scheme

$$(^2P^\circ_{1/2})5s^2\ ^1S \Longrightarrow (^2P^\circ_{3/2})5s\ (J=1)+\varepsilon s\ .$$

In addition to these measurements, the metastable (Brunt *et al.*, 1976; Buckman *et al.*, 1983b) and vuv photon (Brunt *et al.*, 1977d) excitation functions, which at energies below 10.56 and 10.64 eV represent total scattering measurements of the $J=2$ and $J=1$ levels, respectively, also indicate that decay of the a_2 resonance to the $J=1$ level is favored (Figs. 37 and 38). These excitation functions, in which the a_2 resonance is present as a strong, symmetric feature, indicate that it occurs at an energy of 10.125 eV and has a width of about 40 meV. It should be stressed, however, that it is uncertain as to what extent these results are affected by other nearby resonances.

Evident, also, in the $J=2$ excitation functions is another resonance at an energy (10.027 eV—Brunt *et al.*, 1976) lower than the a_2 feature. Brunt *et al.* classified this as a b resonance with configuration $4p^5(^2P^\circ_{3/2})5s5p\,(^3P^\circ)$ and an estimated width of 130 meV.

The $4p^5\,(^2P^\circ_{1/2})5s$ $(J=0)$ and $(J=1)$ levels of krypton occur at 10.562 and 10.644 eV, respectively. The inelastic electron excitation functions for these states at a scattering angle of 45° (Swanson *et al.*, 1973) indicate the presence of strong threshold resonances. Similar, but higher, resolution ($\sim$33–35 meV) measurements by Phillips (1982) indicate the presence of some structure at these thresholds, but it is considerably weaker than that observed by Swanson *et al.* Two features are observed in the metastable atom and uv photon excitation functions at energies of 10.61 and 10.67 eV, respectively, and were classified by Brunt *et al.* (1976, 1977d) as members of the $4p^5\,(^2P^\circ_{1/2})\,5s5p\,(^3P^\circ)$ configuration, i.e., b resonances. A single feature was also observed at 10.66–10.69 eV in transmission by Sanche and Schulz.

Between the $5s$ and $5p$ neutral excited states a broad, relatively strong resonance has been observed, predominantly in the $4p^5\,(^2P^\circ_{1/2})5s$ excitation channels. The first observation of this feature was by Brunt *et al.* (1976) in the metastable atom excitation function at an energy of 11.06 eV. The classified it as a group of broad resonances belonging to the $4p^5\,(^2P^\circ_{3/2})5s5p\,(^1P^\circ)$ configuration, i.e., c resonances. These resonances, labeled c_1 by Brunt *et al.*, are observed in the inelastic electron excitation functions (Swanson *et al.*, 1973; Buckman *et al.*, 1981; Phillips, 1982; Bass *et al.*, 1987) dominating the $4p^5$ $(^2P^\circ_{3/2})5s$ $(J=2)$ and $(J=1)$ levels at low to intermediate scattering angles but not present at all in the $4p^5$ $(^2P^\circ_{1/2})5s$ excitation functions. The converse behavior is observed for a further broad feature located about 0.7 eV above the c_1 feature. This resonance, or group of resonances, is observed in all of the above spectra to decay strongly to the two $5s$ levels with core angular momentum $J=\frac{1}{2}$ but only weakly to those with $J=3/2$ (Fig. 39). Thus it would appear that this feature, labeled c_2 by Buckman *et al.* (1983b), is the higher-lying member of a c resonance pair, separated from c_1 by approximately the Kr^+ core splitting. If this analysis is correct, then these

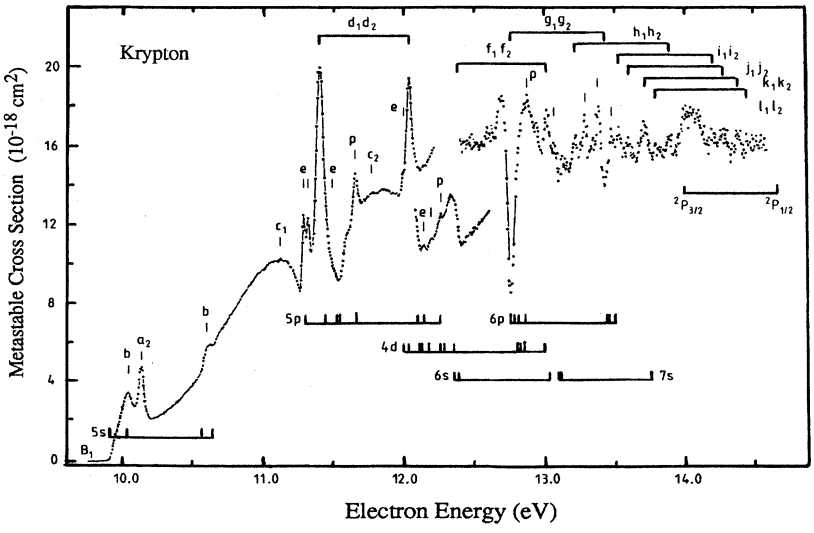

FIG. 38. Metastable atom excitation function for krypton. The two upper parts of the spectrum have had a background function subtracted, and the vertical scale has been expanded. The positions of observed resonances are indicated by the lines above the spectra, while those below indicate the energies of the excited states of neutral krypton (from Buckman *et al.*, 1983b).

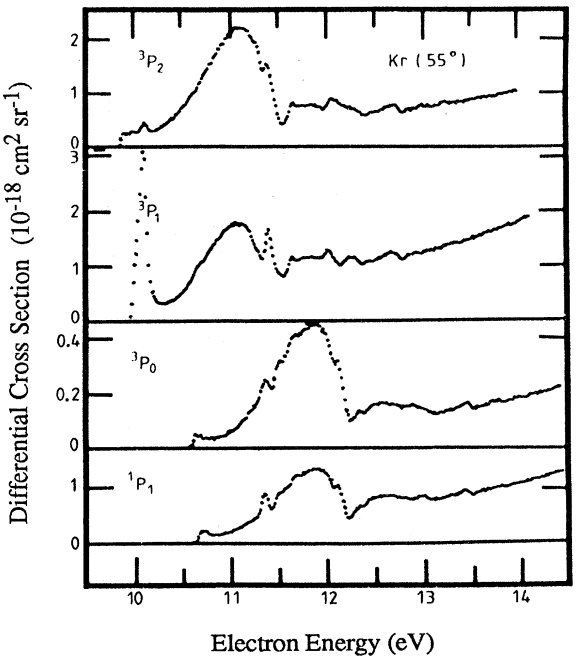

FIG. 39. Absolute differential excitation functions for the $4p^5 5s$ states of krypton at a scattering angle of 55° (from Phillips, 1982).

features also provide a further indication of the trend observed in argon whereby decay routes that preserve the nature of the ion core are favored over those involving a spin flip.

The c_1 resonance has an appearance remarkably similar to that of the c feature in Ar, as can be seen by overlaying Figs. 34 and 38. Given the different interpretations that have been proposed for the Ar c feature, it may be possible that the c features in Kr may also have some contribution from $5s4d$ and $5p^2$ externally coupled configurations. We shall return to this point in Secs. VI.C and VI.E.

In the same energy region as the c_1c_2 resonances are a number of sharp, strong features which are observed in most decay channels. The dominant features in this region are those labeled d_1 and d_2 by Brunt *et al.* (1976) at 11.388 and 12.022 eV (i.e., separated by 634 meV) and classified as $4p^5\ (^2P^\circ_{3/2,1/2})5p^2(^1S)$, respectively (Read *et al.*; Brunt *et al.*). As in argon, the classification of these states is supported by the elastic-scattering measurements of Hammond (1982), which show no intensity for the d_1d_2 resonances at a scattering angle of 90°, in accord with the predicted decay of these states into the elastic channel by p-wave emission.

When observed in the excitation functions for the $4p^5$ $5s$ levels, the most striking manifestation of the d_1d_2 pair is the strong final-state dependence that is exhibited. If we adopt jj coupling to describe the neutral excited states, the classification scheme of Read *et al.* (1976) indicates that, with two exceptions, both d_1 and d_2 can decay by s-wave emission to all of the $5s$ states. The two exceptions are the decay of d_1 to the $5s$ ($J=0$) level and d_2 to the $5s$ ($J=2$) level, both of which require the emission of a d-wave electron to satisfy angular momentum and parity considerations. The $5s$ excitation functions of Phillips (1982), Buckman *et al.* (1981), and Bass *et al.* (1987) all indicate a diminished contribution of d_1 and d_2 to these particular decay channels, although the intensity does not vanish completely at 54°, as would be expected for an outgoing d-wave electron. In general, the decay of the d_1d_2 resonance pair to the $5s$ states once again shows the preference for decay routes that do not involve a change of the core angular momentum.

Swanson *et al.* (1973) also measured excitation functions for the $4p^5(^2P^\circ_{3/2})5p$ excited states of Kr with an energy resolution of approximately 30 meV. With regard to the d_1d_2 resonances, two of these spectra are of particular interest, namely, the excitation functions for the $4p^5(^2P^\circ_{3/2})5p$ ($J=1$) and ($J=2$ and $J=3$) levels at 11.303 and 11.444 eV, respectively. The excitation function for the $J=1$ level, the lowest energetically of the $5p$ configuration, is strongly enhanced at threshold by the d_1 resonance. However, it is the excitation function for the $5p$ ($J=2$) and ($J=3$) levels that provides a most surprising result. In this spectrum (Fig. 40) the d_2 resonance $[4p^5\ (^2P^\circ_{1/2})5s^2(^1S)]$ is strongly present, rising about a factor of 2 above the nonresonant excitation cross section. From angular momentum and parity considerations, this decay route involves the emission of p- or f-wave electrons and a flip of the core angular momentum. Given the trends observed previously in other decay channels, this behavior is most unusual if the proposed classification is correct.

As in the case of Ne and Ar, several other sharp but generally weaker resonances are located in the vicinity of the d_1d_2 resonances in Kr. Evidence of these states was found by Sanche and Schulz, Swanson *et al.*, and Phillips. Further structure was revealed in the higher-resolution measurements of Brunt *et al.* (1976) and Buckman *et al.* (1981, 1983b). Buckman *et al.* (1983b; see also Fig. 38) identify five such structures in the d_1d_2 region, three near the d_1 resonance and two near the d_2. The width, intensity, and number of these features led to their classification as e resonances with the configuration $4p^5\ (^2P^\circ_{3/2,1/2})5p^2\ ^1D$. In the jLS-coupling scheme, the external configuration $5p^2\ ^1D$, when coupled to the $^2P^\circ_{3/2,1/2}$ core states, gives rise to three resonances associated with the $J=\frac{3}{2}$ core and to two with the $J=\frac{1}{2}$ core, in line with observation.

The scattered-electron excitation functions of Hammond (1982), Buckman *et al.* (1981), and Bass *et al.* (1987), with an energy resolution ≤ 20 meV, do enable some further observations to be made concerning the e resonances. Hammond's elastic-scattering measurements indicate no intensity of the e_1 and e_2 resonances at a scattering angle of 90°, in accord with the expectation based on the jLS-coupling scheme that they should decay

into the elastic channel by the emission of a p-wave electron. Further information which is consistent with the $5p^2\,{}^1D$ classification for the e resonances is available from the inelastic electron excitation functions of Buckman *et al.* (1981) and Bass *et al.* (1987). These measurements, particularly those at forward-scattering angles, show a very strong final-state dependence for the decay of e_1 and e_2. In the *jLS* external coupling scheme, there are five possible resonances with the configuration $4p^5(^2P^\circ_{3/2,1/2})5p^2(^1D.)$ Three of these, formed from the ground state by incident p-wave electrons, might be expected to have the largest cross sections. Of these, two would be associated with the $^2P^\circ_{3/2}$ core (with total angular momentum $J=\frac{1}{2},\frac{3}{2}$) and one with the $^2P^\circ_{1/2}$ core ($J=\frac{3}{2}$). As a result of their proximity to the d_1 $^2P^\circ_{3/2}$ resonance, e_1 and e_2 were considered by Brunt *et al.* (1976) to be coupled to the $^2P^\circ_{3/2}$ core. The e_1 feature is seen to dominate the inelastic electron excitation function for the $5s$ ($J=0$) state at 10° (Buckman *et al.*, 1981; Bass *et al.*, 1987) and to be present in the excitation functions for the $5s$ ($J=2$) level. This behavior is consistent with this resonance having a total $J=\frac{1}{2}$ and decaying to the $J=0,1$ levels by s-wave emission, but only by d-wave emission to the $J=2$ level. By default, the resonance e_2 was classified as having total $J=\frac{3}{2}$, which is, in turn, consistent with the observed behavior in the available excitation functions.

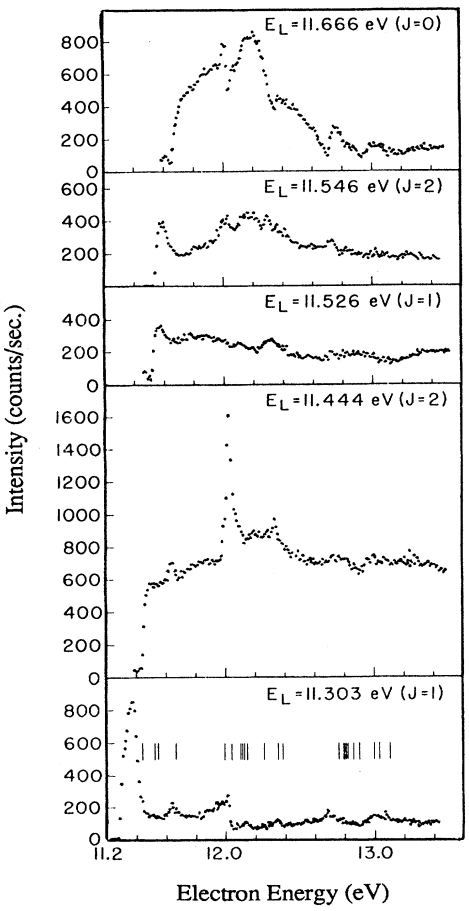

FIG. 40. Excitation functions for the $4p^55p$ states of krypton (from Swanson *et al.*, 1973).

A possible candidate for the third, strong e resonance is the sharp feature observed on the low-energy side of d_2 (Fig. 38). This classification [$5p^2\,{}^1D(J=\frac{3}{2})$] is also consistent with its observed decay to the $5s$ levels but not to the $5s$ ($J=0$) level.

Also observed in this energy region are a number of structures that are in close proximity to the energies of neutral excited states. These features, and in particular the strong resonance at 11.644 eV, are believed to be polarization or nonvalence resonances associated with neutral excited states.

At energies above the d_1d_2 resonance pair, many other such pairs have been observed in krypton (see, for example, Sanche and Schulz, 1972a; Buckman *et al.*, 1983b). Tentative classifications for these features are offered by Buckman *et al.*, who observed seven additional pairs of resonances with energy separations similar to that of the Kr^+ core.

As in Ar, a broad resonance is a dominant feature in the total cross section for electron scattering by Kr (e.g., Dababneh *et al.*, 1980). It is attributed to a $4p^6\varepsilon d$ shape resonance (see Sec. VI.D and Fig. 32).

The recommended values for the energies, widths, and classifications (in some cases tentative) for these states and the others discussed earlier are summarized in Table XI.

5. Xenon

The large spin-orbit splitting in the Xe^+ core (1.307 eV) indicates that it, like Kr, should be well described by a *jj*-coupling scheme and thus be more suitable as a test case for the *jLS* external coupling scheme for doubly excited Xe^- states than the higher noble gases, where intermediate coupling is more appropriate. Although the Xe^- resonance spectrum has been classified in a number of different experiments, the amount of experimental data available is considerably less than that in Kr. We are aware of only one calculation of Xe^- resonances.

Many resonance features were observed in the transmission spectrum of Sanche and Schulz (1972a) and in the elastic-scattering and metastable atom spectra of Kuyatt *et al.* (1965) and Pichanick and Simpson (1968), respectively. However, at the time of the Schulz (1973a, 1973b) review, only the a resonances [$5p^5\,(^2P^\circ_{3/2,1/2})6s^2\,{}^1S$] had been classified. Since then, Xe^- states have been studied in excitation functions for inelastic (Swanson *et al.*, 1976; Buckman *et al.*, 1981) and elastic (Heindorff *et al.*, 1976; Hammond, 1982) electrons, metastable atoms (Brunt *et al.*, 1976; Buckman *et al.*, 1983b), and vuv photons (Brunt *et al.*, 1977d).

As in Kr, the spin-orbit splitting in Xe^+ results in the a resonance pair straddling the lowest neutral excited

states. The a_1 resonance [$5p^5(^2P^\circ_{3/2})6s^2(^1S)$] is located at 7.90 eV (Sanche and Schulz, 1972a). The accurate determination of the $a_2(^2P^\circ_{1/2})$ resonance energy is somewhat more difficult, as it is a weaker, broader feature (a consequence of its location above the first inelastic thresholds) that overlaps with the broad c resonances in the energy region just above 9 eV. Sanche and Schulz estimated its energy as 9.18 eV, i.e., 1.28 eV above the $^2P^\circ_{3/2}$ resonance. Heindorff *et al.* (1976) made no absolute determination of the energy of the a_1a_2 resonances but did measure their energy separation as 1.28±0.04 eV. The energy resolution of their measurements was about 55 meV. The noble-gas elastic-scattering measurements of Brunt *et al.* (1977c) do not include any data on Xe; but, as was the case in Kr, their metastable excitation work (Brunt *et al.*, 1976) in Xe was performed simultaneously with an elastic-scattering measurement, and they quote energies of 7.900 and 9.176 eV, respectively, for the a_1a_2 resonances. Heindorff *et al.* also carried out a phase-shift analysis of the a_1 resonance profile in xenon, obtaining a value of 4.5±1.0 meV for its width. A MCHF calculation in LS coupling of the energy of the a_1 resonance was reported by Clark (1984), yielding an energy within 0.1 eV of the experimental value. These results are discussed in Sec. VI.A. We know of no other calculations of Xe^- resonances.

Several high-resolution electron excitation functions have been measured for the $5p^5$ $6s$ states of Xe. The metastable atom excitation functions [$5p^5$ ($^2P^\circ_{3/2}$) ($J=2$) and $5p^5$ ($^2P^\circ_{1/2}$) ($J=0$)] of Brunt *et al.* (1976) and Buckman *et al.* (1983b) reveal a wealth of structure (Fig. 41), even though the sensitivity of this channel is greatly reduced in comparison with the lighter rare gases due to the lower detection efficiency for the Xe metastables. As

TABLE XI. Recommended energies, widths, and classifications of resonances in Kr^- below the first ionization potential. The energies are expressed relative to the $4p^6\ ^1S$ ground state of atomic Kr. Unless otherwise specified, the values are from Brunt *et al.* (1976, 1977c) and Buckman *et al.* (1983b). Figures in parentheses represent the uncertainty in the least significant digit.

Classification	Energy (eV)	Width (meV)	Comments
$4p^5(^2P^\circ_{3/2})5s^2(^1S)$	9.484	8	*a*, width: Weingartshofer *et al.*
$4p^5(^2P^\circ_{3/2})5s5p(^3P^\circ)$	10.039(10)	130	*b*
$4p^5(^2P^\circ_{1/2})5s^2(^1S)$	10.119(5)	39	*a*, Jureta *et al.*, threshold spectroscopy
$4p^5(^2P^\circ_{1/2})5s5p(^3P^\circ)$	10.60(3)		*b*
$4p^5(^2P^\circ_{3/2})5s5p(^1P^\circ)$	11.12(3)		*c*
$4p^5(^2P^\circ_{3/2})5p^2(^1D)$	11.286(15)	30	
$4p^5(^2P^\circ_{3/2})5p^2(^1D)$	11.318(15)	30	
$4p^5(^2P^\circ_{3/2})5p^2(^1S)$	11.400(15)	63	
$4p^5(^2P^\circ_{3/2})5p^2(^1D)$	11.49(30)		
$4p^5(^2P^\circ_{3/2})5p]_0+\varepsilon s$	11.653(15)	32	
$4p^5(^2P^\circ_{1/2})5s5p(^1P^\circ)$	11.77(5)		*c*
$4p^5(^2P^\circ_{3/2})5p^2(^1D)$	11.996(30)		
$4p^5(^2P^\circ_{1/2})5p^2(^1S)$	12.036(15)	40	
$4p^5(^2P^\circ_{1/2})5p^2(^1D)$	12.138(30)		
	12.191		
$[4p^5(^2P^\circ_{1/2})5p]_0+\varepsilon s$	12.262(20)		
$4p^5(^2P^\circ_{3/2})6s^2(^1S)$	12.378(20)		
$4p^5(^2P^\circ_{3/2})5p^2(^1S)$	12.760(15)	47	
	12.875(30)		
$4p^5(^2P^\circ_{1/2})6s^2(^1S)$	13.016(20)		
	13.067		
$4p^5(^2P^\circ_{3/2})7l^2(^1S)$	13.221		
	13.291		
	13.379		
$4p^5(^2P^\circ_{1/2})5p^2(^1S)$	13.430		
	13.477		
$4p^5(^2P^\circ_{3/2})8l^2(^1S)$	13.528		
$4p^5(^2P^\circ_{3/2})9l^2(^1S)$	13.598		
$4p^5(^2P^\circ_{3/2})10l^2(^1S)$	13.714		
$4p^5(^2P^\circ_{3/2})11l^2(^1S)$	13.789		
$4p^5(^2P^\circ_{1/2})7l^2(^1S)$	13.891		
$4p^5(^2P^\circ_{1/2})8l^2(^1S)$	14.199		
$4p^5(^2P^\circ_{1/2})9l^2(^1S)$	14.273		
$4p^5(^2P^\circ_{1/2})10l^2(^1S)$	14.375		
$4p^5(^2P^\circ_{1/2})11l^2(^1S)$	14.441		

in the lighter gases, a number of broad resonances are seen near the lowest metastable-state threshold (8.315 eV) at energies of 8.338 and 8.430 eV (Buckman *et al.*, 1983b) and were classified by Brunt *et al.* as *b* resonances, i.e., $5p^5\ (^2P_{3/2})6s6p\,(^3P^\circ)$. Swanson *et al.* (1976) also observed these resonances in electron excitation functions for the $5p^5\ (^2P_{3/2})6s\ (J=2,1)$ levels of Xe at a scattering angle of 45° and an energy resolution of 30 meV (Fig. 42). Both excitation functions exhibit a strong threshold peak, some of which is due to instrumental effects; and the $J=2$ spectrum shows a strong resonance at 8.42 eV, in good agreement with the metastable spectra.

At higher energies two broad resonances, one of which, at an energy of 9.08 eV, is relatively strong, are observed in the metastable excitation functions. Both of these features appear to have an associated pair state resonance at higher energies (9.08–10.48 eV; 9.36–10.71), and several possible classifications have been advanced for them. In the lighter gases the broad *c* features have been classified as $nsnp\,(^1P^\circ)$ resonances and, in the case of neon, this classification was confirmed by Clark and Taylor (1982). However, as discussed earlier, the calculation by Ojha *et al.* (1982) determined that the analogous feature in argon was due to a mix of the configurations $np^2(^1D)$ and $(n+1)snd\,(^1D)$. Also expected in this region are a group of resonances resulting from the configuration $(n+1)p^2(^3P)$, which in the lighter gases were expected to form a broad, weak structure underlying the *c*, *d*, and *e* resonances. In xenon the situation is further clouded by the a_2 resonance, which is a relatively broad structure at an energy of 9.18 eV. In classifying these features in the metastable spectrum, Buckman *et al.* (1983b) considered all of these possibilities along with the differences introduced in the heavier noble gases due to the presence of the *nd* orbital, which does not exist in neon. They tentatively assigned these two pairs of broad resonances (c_1c_2 and $c_1'c_2'$) the configurations $6s5d\ (^1D)$ and $6p^2\ (^3P)$, respectively. These resonances, especially c_1, also dominate the $6s\,(^2P^\circ_{3/2})\ (J=2,1)$ excitation functions of Swanson *et al.* (1976). In both these spectra, this peak occurs at 9.09 eV, and it was classified as the a_2 resonance $5p^5\ (^2P^\circ_{1/2})6s^2(^1S)$.

This apparent discrepancy can be explained by a comparison with the similar excitation functions in Kr (Swanson *et al.*, 1973; Phillips, 1982), where the a_2 resonance occurs at a much lower energy than the c_1 resonance. In the Kr 5*s* ($J=2$) excitation function, the c_1 resonance dominates the spectrum with only a small con-

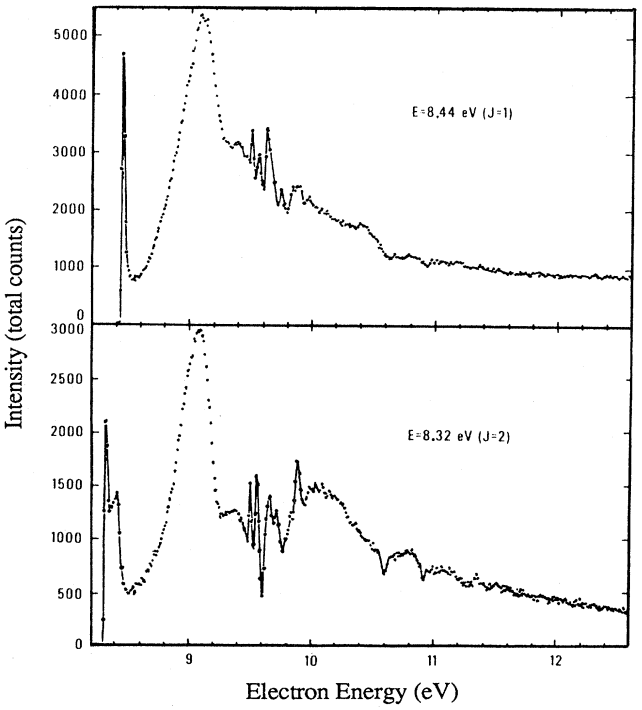

FIG. 42. Excitation functions for the $5p^5_{3/2}6s$ states of xenon at a scattering angle of 45°. Some parts of the sharp peaks observed at threshold are thought to be due to instrumental effects (from Swanson *et al.*,1976).

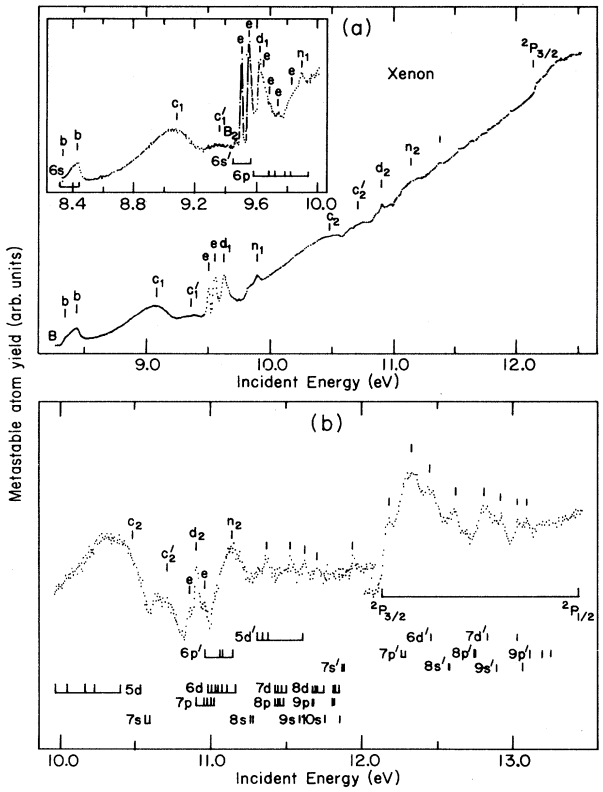

FIG. 41. Metastable atom excitation function for xenon. (a) Electron energies from threshold to 12.5 eV. The inset highlights the energy region between threshold and 10.0 eV. (b) The upper reaches of the spectrum from 10.0 eV to the $^2P_{1/2}$ ionization threshold following the subtraction of a quadratically varying background function. Assignment bars above the spectra indicate the positions of observed resonances, while those below indicate the energies of excited states of neutral xenon (from Buckman *et al.*, 1983b).

tribution from a_2, while in the $J=1$ excitation function the spectrum is dominated by a_2 and c_1 is considerably weaker. We would suggest that the same situation occurs in xenon but is complicated by the fact that the a_2 and c_1 resonances are close together in energy and have similar, broad widths. Thus the strong peak in the $6s$ ($J=1$) excitation function is due to the $(^2P^\circ_{1/2})6s^2\ (^1S)$ resonance, while in the $J=2$ excitation function it is due to the $6s5d\ (^1D)$ resonances. A similar conclusion can be reached by a comparison of the metastable and vuv excitation functions for Kr and Xe. In Kr the metastable excitation function, which below 10.562 eV represents the total excitation cross section for the $J=2$ state, shows a relatively small presence of a_2 but a large broad contribution from c_1. On the other hand, the vuv excitation function, representing the total cross section for the $^2P^\circ_{3/2}J=1$ state below 10.644 eV, is dominated by the a_2 resonance but shows no evidence of c_1. In Xe, the metastable and vuv spectra both show structure in the region of 9.1 eV; but it is significant that the feature in the vuv spectrum occurs at 9.14 eV, while in the metastable spectrum it is at 9.06–9.08 eV. It would appear therefore that the broad resonance labeled c_1 in the vuv excitation function of Brunt *et al.* (1977d) may, in fact, be the a_2 resonance.

In the energy region of the cc' resonances, many other strong, and in some cases spectacularly sharp, resonances are observed in various excitation functions, as well as the transmission spectra of Sanche and Schulz. The first attempt to classify these states was made by Brunt *et al.* (1976), who identified several d and e resonances near 9.6 and 11.0 eV. The lowest d resonance at 9.619 eV has what appears to be an associated pair resonance at 10.904 eV in the metastable channel. This pair was also observed in the transmission spectrum of Sanche and Schulz at 9.65 and 10.92 eV, by Swanson *et al.* (1976) and Buckman *et al.* (1981) in the electron excitation functions for the $6s$ states, and in the elastic channel by Hammond (1982), although in the latter the d_2 resonance is not clearly present at any of the scattering angles stud-

TABLE XII. Recommended energies, widths, and classifications of resonances in Xe^- below the first ionization potential. The energies are expressed relative to the $3p^6\,^1S$ ground state of atomic Xe. Unless otherwise specified, the values are from Brunt *et al.* (1976, 1977c) and Buckman *et al.* (1983b). Figures in parentheses represent the uncertainty in the least significant digit.

Classification	Energy (eV)	Width (meV)	Comments
$5p^5(^2P^\circ_{3/2})6s^2(^1S)$	7.90(2)	4.5(1)	*a*, width: Heindorff *et al.*
$5p^5(^2P^\circ_{3/2})6s6p(^3P^\circ)$	8.338(15)		*b*
$5p^5(^2P^\circ_{3/2})6s6p(^3P^\circ)$	8.430(15)		*b*
$5p^5(^2P^\circ_{3/2})6s6p(^1P^\circ)$	9.08(3)		*c*
$5p^5(^2P^\circ_{1/2})6s^2(^1S)$	9.18(2)		*a*
$5p^5(^2P^\circ_{3/2})6s6p(^1P^\circ)$	9.36(3)		*c*
$5p^5(^2P^\circ_{3/2})6p^2(^1D)$	9.505(15)	25	
$5p^5(^2P^\circ_{3/2})6p^2(^1D)$	9.551(15)	31	
$5p^5(^2P^\circ_{3/2})6p^2(^1S)$	9.623(15)		
	9.644		
	9.686		
	9.743		
	9.831		
	9.896		
$5p^5(^2P^\circ_{1/2})6s6p(^1P^\circ)$	10.48		*c*
$5p^5(^3P^\circ_{3/2})6s6p(^1P^\circ)$	10.71		*c*
	10.858		
$5p^5(^2P^\circ_{1/2})6p^2(^1S)$	10.901		
	10.957		
	11.14		
	11.37		
	11.525		
	11.62		
	11.70		
	11.94		
	12.18		
	12.33		
	12.45		
	12.62		
	12.81		
	12.92		
	13.03		
	13.09		

ied. As in the lighter noble gases, the d resonances are expected to decay into the elastic channel by p-wave autodetachment, and this is confirmed for d_1 by Hammond's measurements in the elastic channel. The inelastic electron measurements do not cover a large enough range of angles for any further conclusions to be drawn.

Below the d_1 resonance, two strong, sharp resonances are observed in all of the experiments outlined above. In the metastable atom spectrum of Brunt *et al.*, these features, at energies of 9.495 and 9.549 eV, were classified as e resonances associated with the $^2P^\circ_{3/2}$ core. These energies were also in good agreement with the observations of Sanche and Schulz and Swanson *et al.* In the metastable excitation function of Buckman *et al.* (1983b), several other sharp features were observed in the region of the $d_1 d_2$ resonance pair and were also generally classified as e resonances, although these authors point out that there are actually too many of these features in the vicinity of d_2 for them all to belong to the configuration $6p^2$ (^1D). The additional features appear on the high-energy side of d_1 and probably indicate that the original estimate of the width of this state (90 meV) by Brunt *et al.* is too large.

While the features on the high-energy side of d_1 are relatively weak in the metastable atom spectrum, some of them decay strongly to individual members of the $6s$ manifold as observed in the inelastic electron excitation functions of Swanson *et al.* (1976) and Buckman *et al.* (1981). In particular, in the excitation functions for the $(^2P^\circ_{3/2})6s$ ($J=2,1$) states at 10° (Buckman *et al.*) and 45° (Swanson *et al.*), strong features occur in the region of 9.70 eV. The expectations of the *jLS*-coupling scheme are that there will be only two strong e resonances in the vicinity of d_1; so it is possible that these structures are either due to members of the $6p^2$ (^3P) configuration or that they are the $^2P^\circ_{1/2}$ component of the $6s6p(^3P^\circ)$ configuration—i.e., b resonances. The experimental evidence is clearly not yet complete, and it would be premature to speculate any further on the classification of these states.

At higher energies many further resonances have been observed, but only one pair, $n_1 n_2$ at energies of 9.896 and 11.14 eV, respectively, has been tentatively classified by Buckman *et al.* (1983b) as $5d^2$ (^1S) resonances. These authors also observe a sharp onset in their metastable spectrum near the energy of the $^2P^\circ_{3/2}$ ionization threshold and many resonances in the energy region between the $^2P^\circ_{3/2}$ and $^2P^\circ_{1/2}$ limits. This section of the metastable spectrum shows a remarkable similarity to the excitation function for high-n xenon states measured by Hammond *et al.* (1984) and is attributed by Buckman *et al.* to be dominated by contributions from high-n Rydberg states whose lifetimes are longer than the target-detector transit time in their experiment. The similarity in the observed structure also indicates that many of the resonances in this region must decay principally via high-Rydberg levels.

The total cross section for electron scattering by Xe shows two broad features, centered near 8 eV and 20 eV, respectively (see Fig. 32). The 8-eV feature is a d-wave shape resonance, similar to those encountered in Ar and Kr. The 20-eV feature is attributed to an f-wave shape resonance. It is not present in Ar or Kr, as the f-wave effective potential only acquires a double-well structure in heavy atoms, as discussed in Sec. VI.D.

Recommended values for the energies, widths, and classifications of the Xe^- resonances are given in Table XII.

6. Resonances above the ionization limit

As was the case for helium, the identification and classification of resonances that lie above the first ionization limit in the rare gases are complicated by the occurrence of structure due to the excitation of neutral autoionizing states. To some extent these features can be separated by using information from photo- or ion-excitation experiments where only the doubly excited neutrals are formed; but in the case of electron-scattering experiments, both types of excited state are formed and, in general, they overlap substantially. Indeed, several authors (Heideman *et al.*, 1974; Wilden *et al.*, 1977) have pointed out that the assignment of features, observed in earlier experiments, as doubly excited autoionizing states may be incorrect.

Before discussing the details of the negative-ion resonance spectra of the rare gases in this autoionizing region, it is perhaps beneficial to outline some of the techniques that have been used to enable features due to negative ions and doubly excited neutrals to be separated experimentally, particularly those techniques that take advantage of the different decay dynamics of these two classes of excited state.

Following the first observation of the so-called post-collision interaction (PCI) by Hicks *et al.* (1973, 1974), it was proposed (Heideman *et al.*, 1974; Read, 1974) that PCI effects might provide a mechanism for the selective excitation of high-n singly excited atomic states. If, in the electron-impact excitation of an autoionizing state, the incident electron energy is sufficiently close to threshold, the energy transfer, $E_{\rm PCI}$, which occurs between the inelastically scattered and ejected electrons after the collision and subsequent autoionization, may be larger than the original excess energy of the scattered electron, $E_{\rm SC}$. As a result the scattered electron will remain bound in an excited state of the atom with a binding energy $E_b = -(E_{\rm SC} - E_{\rm PCI})$. Typical energy exchanges observed in PCI can range up to 1 eV (Hicks *et al.*, 1974), implying that for any particular interaction, E_b will have some upper limit and, consequently, that structure due to autoionization +PCI should not be evident in the excitation functions of singly excited states having excitation energies below some limiting value.

This was verified experimentally by both Heideman *et al.* (1974) and Smith *et al.* (1974). They observed that PCI structure associated with autoionizing levels oc-

curred only in the excitation functions for singly excited states with principle quantum number greater than some minimum value, for example, $n=4$. Conversely, it has also been demonstrated (Roy *et al.*, 1975a, 1975b) that the negative-ion states in this energy region decay preferentially to low-n singly excited states. Thus by a careful choice of observation channel it should be possible to optimize the detection of either the doubly excited neutral states or the triply excited negative-ion resonance states.

Another factor that complicates the classification of resonance features in the autoionizing region of the heavier rare gases is that the core of the associated parent states can either be singly or doubly ionized, corresponding to inner-shell or double excitation, and, in principle, resonances can be associated with any of these states. These ion cores will have the form $nsnp^6$ (^2S) and $ns^2\,np^4$ ($^1S, ^1D, ^3P$). In the first case there is no fine-structure splitting, while for the doubly ionized cores the ^3P-^1D and ^1D-^1S term splittings are 3.2 and 3.7 eV for Ne ($n=2$), 1.7 and 2.4 eV for argon ($n=3$), 1.8 and 2.3 eV for krypton ($n=4$), and 2.1 and 2.5 eV for xenon ($n=5$). The fine-structure splittings in the ^3P term are of the order of 0.1, 0.14, 0.5, and 1.2 eV, respectively.

a. Neon

There has been an extensive amount of experimental work on the negative-ion states in the autoionizing region of neon. The earlier work, prior to the Schulz review, has been summarized both in his review and in Sanche and Schulz (1972a, 1972b, 1972c), and some tentative assignments of resonance features were made by these authors. Subsequent studies have been carried out using several different techniques involving detection in various decay channels. The yield of Ne^+ ions resulting from electron impact in the energy region from 42 to 51 eV has been measured by Bolduc *et al.* (1972); inelastic electron excitation functions for selected $n=3,4$ levels of neutral neon have been measured by Roy and Carette (1974) and Roy *et al.* (1975a); Wilden *et al.* (1977) measured the spectrum of electrons ejected from neon following electron impact in the energy range 41–46 eV; Veillette and Marchand (1976) detected broadband photons resulting from electron impact in the energy range 42–54 eV; Spence (1980) measured the trapped-electron spectrum for neon in the energy region from 40 to 52 eV using a modified technique; and the metastable atom excitation function has been measured by Huard *et al.* (1978) and Dassen *et al.* (1983). There have, to our knowledge, been no calculations of the energies or widths of the negative-ion resonances in this region.

The situation regarding these Ne^- resonances has been extremely well summarized by Spence (1980), and almost all of his conclusions have been independently confirmed by Dassen *et al.* (1983). We shall therefore give only a relatively brief description of these resonances, highlighting the few areas where there are some discrepancies as well as the problems that must be addressed when attempting to detect and classify these states. The classification has generally been carried out by reference to the known positions of nearby inner-shell and doubly excited parent states. Some of the earlier attempts at classification of the resonance features were considered by both Wilden *et al.* and Spence to be in doubt, as the spectra they relied upon for the parent-state energies may have been affected by energy shifts due to PCI, or were contaminated by the presence of negative-ion features. The more recent attempts (e.g., Wilden *et al.*, Spence, Dassen *et al.*) have been mindful of the PCI effects and have also relied on analogies with alkali and alkaline-earth spectra, Rydberg-like formulas, and/or graphical analysis to assist in the classification process.

The lowest-lying resonance in this region occurs at 42.09 eV (our quoted energies represent an average of all recent measurements where resonances have been identified). It was first classified by Sanche and Schulz (1972a) as being associated with the doubly excited state $2s^2\,2p^4\,(^3P)3s^2\,(^3P)$, which earlier measurements (Grissom *et al.*, 1969; Bolduc and Marmet, 1973) had placed slightly above 42 eV. Roy *et al.* (1975a) first classified this resonance as $2s^2\,2p^4\,(^3P)3s^2\,3p$. The first positive identification of the neutral parent state was made by Wilden *et al.* (1977) in ejected-electron spectra at an energy of 41.87 eV; they observed a structure at 42.1 eV in the excitation function for this state and concurred with the previous classification. It is also confirmed by both Spence and Dassen *et al.* This and many other features at higher energies were also observed by Veillette and Marchand (1976) in broadband photon measurements; but in many of these, cases were incorrectly attributed to neutral excited states.

At about 43.09 eV a reasonably strong feature is observed in most of the decay channels studied, the exception being the ejected-electron spectrum of Wilden *et al.* This feature is particularly strong in the excitation function for the $2^5\,3s\,^1P^\circ$ level of neon (Roy *et al.*) and was classified by them as $2s\,2p^6\,(^2S)3s^2\,(^2S)$ based on observations by Sanche and Schulz and Bolduc *et al.* Wilden *et al.* note that this classification is entirely consistent with the lack of structure in their measured excitation function for the $2s^2\,2p^4\,3s^2\,^3P$ state, as autodetachment of the resonance to this state would be forbidden on the grounds of both parity and angular momentum. They also make an analogy with the measured electron affinity of Na (0.54 eV), which is consistent with the observed separation of the resonance in question from its proposed parent state, $2s2p^6\,3s\,^1S$ at 43.67 eV, of 0.58 eV.

At an energy of about 43.68 eV, a feature is observed in the trapped-electron (Spence), inelastic electron (Roy *et al.*), metastable atom (Dassen *et al.*), and transmission (Sanche and Schulz) experiments, but only weakly, if at all, in the ejected-electron spectra (Wilden *et al.*). It was classified by Roy *et al.* as a shape resonance with the configuration $2s2p^6\,(^2S)3s3p$ attached to the $2s2p^63s\,^3S$ neutral autoionizing state. This classification was confirmed by Spence, although his thorough examination

of the energies of possible parent states indicates that this resonance is most probably attached to the ^1S term of the $2s2p^6$ $3s$ state, which lies just below it at 43.66 eV. Dassen *et al.* are also in accord with this classification.

Two resonances that are observed at energies of 44.06 and 44.37 eV have been classified as $2s^22p^4$ (^3P) $3s3p^2$ by Roy *et al.*, with the parent state being the $2s^22p^4$ (^3P) $3s3p$ level at about 44.5 eV. Both Spence and Dassen *et al.* concur with this assignment, while Wilden *et al.* attributed these features to terms of the $2s2p^6$ $3s3p$ neutral excited states. Subsequent work (Spence, 1981) has shown this not to be the case. Spence (1980) also makes the observation that the lowest of these two resonances has an affinity of about 0.44 eV, which is unusual both for a resonance of this configuration and for these resonances in general, which, with a few exceptions, are all located close in energy to their parent state.

The only significant differences between the classifications of both Wilden *et al.* and Spence and that of Roy *et al.* occur for the resonances located at 45.19 and 45.43 eV. Wilden *et al.* classify these states as $2s^22p^4$ (^1D) $3s^2$ $3p$ and $2s2p^6$ (^2S)$3p^2$, respectively, with the first assignment being based on the splitting of the ^3P and ^1D terms of the $2s^22p^43s^2$ neutral autoionizing states, and the second on the predicted energy obtained from the modified Rydberg formula. Roy *et al.* also gave these assignments, but in the opposite energy order, based on an incomplete knowledge of the parent-state energies. The assignments of Wilden *et al.* and Spence have also been confirmed by Dassen *et al.* At a higher energy (46.39 eV) Roy *et al.* observed a weak structure in the excitation function for the $2p^53s$(^1P) level of neon, which they classified as $2s2p^6$ (^2S)$4s^2$, mainly on the basis of its position just below the core-excited $4s$ (^3S) state. Later work (Wilden *et al.*, Spence, Dassen *et al.*) all found this resonance at a significantly higher energy (46.52 eV) but still below the parent-state energy.

Several other features at energies near 46.9, 47.4, 47.6, and 49.0 eV have been identified by one or more of Roy *et al.* (1975a), Wilden *et al.* (1977), Spence or Dassen *et al.* (1983). The only discrepancy over classification occurs for the state at 47.64 eV, which Spence had designated as $2s^22p^4$ $5s5p$. Dassen *et al.* suggest that this is, in fact, another $3s3p^2$ resonance based on the $2s^22p^4$ (^1D) $3s3p$ parent state, as its position is consistent with the ^3P-^1D splitting in the core. Suggested configurations for the other resonances in this area are found in Table XIII, as are details for all of the resonances discussed in this section.

TABLE XIII. Recommended energies, widths, and classifications of resonances in Ne^- above the first ionization potential. The energies are expressed relative to the $2p^6$ ^1S ground state of atomic Ne. They represent average values of all of the measurements that specify a structure as a negative-ion state. Figures in parentheses represent the uncertainty in the least significant digit.

Classification	Energy (eV)	Width (meV)	Comments
$2s^22p^4(^3P)3s^23p$	42.09		
$2s2p^6(^2S)3s^2(^2S)$	43.06	70(20)	
$2s2p^6(^2S)3s3p$	43.68		
$2s^22p^4(^3P)3s3p^2$	44.06		
$2s^22p^4(^3P)3s3p^2$	44.36	50(20)	
$2s^22p^4(^1D)3s^23p$	45.19		
$2s2p^6(^2S)3p^2$	45.43		
$2s2p^6(^2S)4s^2$	46.52	35(10)	
$2s2p^6(^2S)4s4p$	46.91		
$2s^22p^4(^1D)3s3p^2$	47.38		
$2s^22p^4(^1D)3s3p^2$	47.61		
	48.0		
	49.04		

b. Argon

The negative-ion resonance spectrum of the autoionizing region of argon has been studied using many of the techniques applied to neon, although not quite as extensively. Features attributed to resonances have been observed in ionization efficiency curves (Bolduc *et al.*, 1971; Lefaivre and Marmet, 1975); broadband photon emission (Veillette and Marchand, 1974, 1975); electron excitation functions for the $3p^54s^1P$ excited state (Roy and Carette, 1975); metastable atom excitation functions (Marchand and Cardinal, 1979; Dassen *et al.*, 1983); and in the transmission experiments of Sanche and Schulz (1972a). Some earlier work has been summarized by Sanche and Schulz and in the Schulz (1973a) review. As there are many parallels between the spectra of neon and argon, only the essential features will be discussed here. Quoted energies represent the average values of those measurements where the resonances are clearly defined as such.

The most extensive effort to classify these states has been that of Dassen *et al.*, who used semiempirical techniques, such as the modified Rydberg formula and graphical analysis (see Sec. II), to make tentative assignments for most of the strong features observed in the metastable atom excitation function. These assignments were very strongly predicated on the known neon configurations, particularly those of Spence (1980), which were used as the starting point for the graphical analysis. Dassen *et al.* constructed two sets of straight-line plots, one set each for states based on the singly and doubly ionized cores, connecting resonances of similar configuration in Ne, Ar, and Kr. They were also guided by similarities in shape and relative intensity of the features in these atoms, by the known splittings for the different terms of the doubly ionized core, and by the ordering implied by the MRF, which was applied to resonances based on both singly and doubly ionized cores.

The lowest-lying resonance, the $3s3p^6$ (^2S)$4s^2$ ^2S at 24.51 eV, was first observed and assigned by Bolduc *et al.* (1971) as a weak structure in the ionization efficiency curve for argon. It has been observed in all experimental investigations and has an estimated width of 90 meV (Dassen *et al.*). At higher energies there have

been, with the exception of the work of Dassen *et al.*, only a few attempts at classification of the observed structure in terms of negative-ion resonances (Sanche and Schulz, 1972a; Roy and Carette, 1975). The other experimental investigations have attributed the bulk of the observed structure to singly and doubly excited autoionizing states of neutral argon, although there is, in general, good agreement in the energies of the observed features in these experiments and in those that attribute the structure to Ar^- states.

Dassen *et al.* offer tentative classifications for some 16 other features between 24.5 and 32.5 eV. The first two of these at 25.03 and 26.50 eV were also classified by Roy and Carette as $3s3p^6\ (^2S)4s4p$ and $3s3p^6\ (^2S)4p^2\ ^2D$, respectively, the first being a shape resonance associated with the $3s3p^6\ (^2S)4s\ ^3S$ autoionizing state at 25.03 eV (Mitchell *et al.*, 1980). The only other feature for which Roy and Carette offer an assignment is at about 27.05 eV and is classified by them as $3s3p^6\ (^2S)5s^2$ or $3d^2$. However, based on their graphical analysis, Dassen *et al.* believe this feature to be the $4s^2\ 4p$ configuration associated with the triplet term of the doubly ionized core. Indeed, their analysis reveals that the $5s^2$ resonance is probably 0.6 eV higher in energy, if the assignments in neon are correct. Furthermore, application of the MRF to the $3s^23p^4\ (^3P)4s^2\ 4p$ configuration reveals a predicted energy in the vicinity of 27 eV.

Similar techniques are applied throughout the higher reaches of the argon spectrum by Dassen *et al.* in an attempt to provide tentative classifications for the remaining structures. They do not consider intershell resonances or states involving *d* electrons and stress the tentative nature of the assignments that have been made. Tabulated values for these resonances and those discussed above are found in Table XIV.

TABLE XIV. Recommended energies, widths, and classifications of resonances in Ar^- above the first ionization potential. The energies are expressed relative to the $3p^6\ ^1S$ ground state of atomic Ar. They represent average values of all of the measurements that specify a structure as a negative-ion state. Figures in parentheses represent the uncertainty in the least significant digit.

Classification	Energy (eV)	Width (meV)	Comments
$3s3p^64s^2\ ^2S$	24.52	90(15)	
$3s3p^64s4p\ ^2P^\circ$	25.02		
$3s3p^64p^2\ ^2D$	26.50		
$3s3p^63d^2$(?)	26.91		
$3s^23p^4(^3P)4s^24p$	27.10		
$3s3p^65s^2\ ^2S$	27.53	70(10)	
$3s3p^65s5p\ ^2P^\circ$	27.92	75(10)	
$3s^23p^4(^3P)4s4p^2$	28.30		
$3s^23p^4(^3P)4s4p^2$	28.50		
$3s^23p^4(^1D)4s^24p$	28.96	120(20)	
$3s^23p^44s4p^2$(?)	29.46		
$3s^23p^4(^1D)4s4p^2$	29.84		
$3s^23p^4(^1D)4s4p^2$	30.30		
$3s^23p^4(^1S)4s^24p$	30.86		
$3s^23p^4(^1S)4s^24p$	31.31		
$3s^23p^4(^1S)4s4p^2$(?)	31.73		
$3s^23p^4(^1S)4s4p^2$	32.12		
$3s^23p^4(^1S)4s4p^2$	32.40		

c. Krypton

The experimental information available for the autodetaching resonances in the autoionizing region of krypton is similar to that for argon. Studies have been carried out in transmission experiments (Sanche and Schulz, 1972a); in elastic electron-scattering measurements (Roy *et al.*, 1976); and in the yield of positive ions (Valin and Marmet, 1975), broadband photons (Boulay and Marchand, 1982), and metastable atoms (Dassen *et al.*, 1983). In general, there is good agreement between the energies at which features are observed in these various spectra, although this is not always the case for the corresponding classifications, despite considerable effort being invested in the identification of possible neutral parent states (Roy *et al.*) and in the application of graphical and MRF techniques (Dassen *et al*). Additional problems with the heavier rare gases are encountered, due to the substantial overlap that occurs between resonances based on the singly and doubly ionized cores, and most attempts at classification in this region are couched in some uncertainty.

The lowest-lying feature attributed to a negative-ion state was observed by Valin and Marmet (1975) in the ionization efficiency curve at an energy of 22.68 eV and was assigned by them the configuration $4s^24p^4\ (^3P_2)\ 5s^2\ 5p$—that is the first occurrence of an observed resonance associated with the doubly ionized core lying below the singly ionized $(n+1)s^2$ resonance. This state has not been observed in any other spectrum, although its position is consistent with the observation and classification of a similar resonance associated with the $^3P_{0,1}$ terms at an energy of about 23.40 eV (Roy *et al.*, 1976), the separation of these features being close to the known term splitting of about 0.6 eV. The $(n+1)s^2$ resonance, in this case $5s^2$, was first located at about 22.85 eV (Sanche and Schulz) with a width of 65±10 meV (Dassen *et al.*), and there is good agreement among all experiments, with the exception of the I.E. measurement where this state is not observed, as to its position and assignment. There is also general agreement on the assignment of the next feature in the spectra, at about 23.26 eV, as the $4s4p^6\ 5s5p$ resonance. At about 23.40 eV, both Sanche and Schulz and Roy *et al.* observe a feature which the latter have classified as $4s^24p^4\ (^3P_{0,1})5s^2\ 5p$, a state to which we alluded earlier. At about 24.1 eV a resonance is observed in most decay channels, with the exception of the inelastic electron measurements of Roy *et al.* It was classified by Valin and Marmet at $4s^24p^4\ (^3P_{0,1})5s5p^2$, and Dassen *et al.* are in agreement with this configuration. However, it is here that the degree of consensus on the classification of these states changes abruptly, with the

two major attempts (Roy *et al.* and Dassen *et al.*) disagreeing on almost all subsequent assignments at higher energies, even though they are in good agreement in most cases for the energies.

The level of complexity of the spectrum makes it difficult to offer too much guidance in this situation. The assignments given in both cases are largely speculative and several of the differences may arise as a direct result of Dassen *et al.* not considering intershell states or states involving *d* orbitals. As a result, we refrain from suggesting definite assignments for many of these states but rather present the various alternatives, along with energies and suggested widths, in Table XV.

d. Xenon

There have been only two direct experimental investigations of the negative-ion resonance states of xenon in the autoionizing region: the transmission study of Sanche and Schulz (1972a) and the inelastic electron excitation functions of Delâge *et al.* (1977). Although they carried out no direct measurements on xenon, Dassen *et al.* (1983) extrapolated their graphical analysis to enable some predictions on the positions of the lower-lying Xe^- resonances, associated with the singly ionized core, to be made. They also made the observation, based on the low-*n* inelastic electron excitation functions of Roy and Carette (1975), Roy *et al.* (1976), and Delâge *et al.* (1977) for the rare gases, that the spectra observed appear to become increasingly complex as the atomic weight increases, due mainly to the increasing presence of neutral excited states.

Delâge *et al.* made a thorough investigation of the resonances in this region by measuring excitation functions at 0° scattering angle for five of the 6*s*, 6*p*, and 5*d* bound states of Xe, in the energy region between 18 and 24 eV, and by measuring an energy-loss spectrum, in the autoionizing region, for an incident electron energy of 50 eV. Much of the structure they observed in the excitation functions has been attributed to either doubly excited states of the neutral atom or multiple excitation (double scattering) of singly excited levels. Nonetheless, they have offered classifications, in terms of negative-ion states, for several of the observed features. These are largely based on an analysis of their own energy-loss spectrum from which they have attempted to identify the positions of the doubly excited parent states of the Xe^- resonances. Their energies can be compared with the energies recorded by Sanche and Schulz and with the predictions of the graphical analysis (Dassen *et al.*).

At an energy of 18.92 eV, Delâge *et al.* observed a structure which they classified as $5s5p^6 6s^2\ (^2S)$. This is in excellent agreement with the predicted energy for this state (18.84 eV) based on a graphical extrapolation of similar configurations in the lighter gases, and with the measured energy and classification of Sanche and Schulz. Similar correspondences are observed between the two experimental measurements for resonances at 19.11,

TABLE XV. Recommended energies, widths, and classifications of resonances in Kr^- above the first ionization potential. The energies are expressed relative to the $4p^6\,{}^1S$ ground state of atomic Kr. They represent average values of all of the measurements that specify a structure as a negative-ion state. Figures in parentheses represent the uncertainty in the least significant digit.

Classification	Energy (eV)	Width (meV)	Comments
$4s^2 4p^4(^3P_2)5s^2 5p$	22.68		
$4s4p^6 5s^2\,{}^2S$	22.85	65(10)	
$4s4p^6 5s5p\,{}^2P^\circ$	23.24		
$4s^2 4p^4(^3P_{0,1})5s^2 5p$	23.40		
$4s^2 4p^4(^3P_{0,1})5s5p^2$	24.08		
$4s^2 4p^4(^3P_{0,1})5s5p^2$ or $4s4p^6 5p^2\,{}^2D$	24.51		
$4s4p^6 5p^2\,{}^2D$	24.85		
$4s^2 4p^4(^1D)5s^2 5p$ or $4s4p^6 5d^2$	25.11		
$4s^2 4p^4(^1D)5s5p^2$	25.66		
$4s4p^6 6s^2\,{}^2S$ or $4s^2 4p^4(^1D)5s5p^2$ or $4s^2 4p^4(^1D)5s4d^2$	25.95		
$4s4p^6 5s5p\,(^2P)$ or $4s^2 4p^4(^1D)5s5p^2$ or $4s^2 4p^4(^1D)5s4d^2$	26.15		
$4s^2 4p^4(^1D)5s5p^2$	26.59		
?	26.90		
$4s^2 4p^4(^1S)5s^2 5p$	27.19		
$4s^2 4p^4(^1D)5s5p^2$	28.80		

TABLE XVI. Recommended energies, widths, and classifications of resonances in Xe^- above the first ionization potential. The energies are expressed relative to the $5p^6\,{}^1S$ ground state of atomic Xe. They represent average values of all of the measurements that specify a structure as a negative-ion state. Figures in parentheses represent the uncertainty in the least significant digit.

Classification	Energy (eV)	Width (meV)	Comments
$5s5p^6 6s^2$	18.92		
$5s^2 5p^4(^3P_2)6s^2 6p$ or $5s5p^6 6s6p\,(^2P)$	19.11		
$5s5p^6 6s6p(^2P)$	19.43		
$5s^2 5p^4(^3P_{0,1})6s^2 6p$	19.82		
$5s^2 5p^4(^1D)6s^2 6p$	20.13		
$5s5p^6 6p^2$ or $5s^2 5p^4(^1D)6s^2 6p$	20.55		
$5s^2 5p^4(^1S)6s^2 6p(?)$	22.79		

19.43, 19.82, and 20.13 eV. The feature at 19.43 eV is classified by Delâge *et al.* as $5s5p^6 6s6p$, in good agreement with the prediction of Dassen *et al.*, while the other three features are tentatively classified by Delâge *et al.* as $5s^2 5p^4 6s^2 6p$. The only other features that are tentatively classified as resonances by Delâge *et al.* are at 20.55 ($5s5p^6 6p^2$ or $5s^2 5p^4 6s^2 6p$) and 22.79 eV ($5s^2 5p^4 6s^2 6p$). Dassen *et al.* predict the positions of the $5s5p^6 6p^2$, $5s5p^6 7s^2$, and $5s5p^6 7s7p$ resonances at 20.81, 21.73, and 22.02 eV, respectively, all of which are in good agreement with features that Delâge *et al.* ascribe to neutral autoionizing states. Their true nature thus remains uncertain, as does that of many of the other so-called resonances in this region. As a result, we once again refrain from suggesting definite assignments for many of these states but rather present the various alternatives, along with energies and suggested widths, in Table XVI.

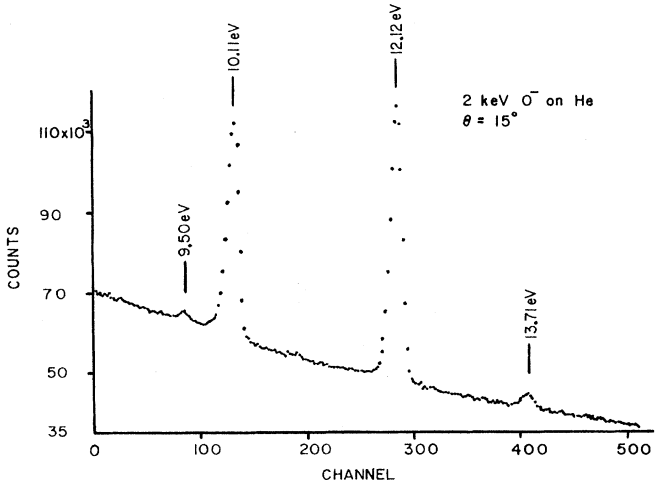

FIG. 43. Spectrum of ejected electrons resulting from collisions of O^- with helium (from Edwards and Cunningham, 1973).

E. Oxygen

The autodetaching states of O^- have been investigated experimentally by both O^--atom and e^--O scattering techniques and theoretically by many-body perturbation-theory, close-coupling, and configuration-interaction calculations. They are thus among the best-documented resonances in the periodic table. However, the known resonances are contained within a fairly narrow range of energy, as they consist primarily of low-lying doubly excited states associated with the various terms of the grandparent $O^+ 2p^3$ ion core. The apparent weak dependence of these doubly excited states upon the grandparent term is quite similar to the case of the noble gases, where one often finds resonances in pairs that replicate the doublet fine structure of the grandparent ion. We shall make use of this fact in the discussion of systematics in Sec. VI. It suggests that there should exist many resonances at higher energies, which have not yet been observed or calculated.

The first experimental evidence for autodetaching states of O^- was obtained by Edwards *et al.* (1971) in keV collisions of O^- with He, H_2, Ne, N_2, and Ar. The apparatus used was of the type described in Sec. III.C, with the ejected electrons observed at angles around 10° with respect to the ion beam. In collisions of O^- with H_2, the only autodetachment features observed were associated with resonances of H^-; in O^--Ar collisions, the only such features were derived from the *a* resonances of Ar. In O^--He collisions, electron peaks were seen at energies of 10.112 eV and 12.115 eV (in the rest frame). These were attributed to autodetaching states of O^-, for which some candidate configurations were proposed.

Subsequent work by the same group (Edwards and Cunningham, 1973) completed the experimental contribution, to date, of O^--atom scattering to the understanding of autodetaching states. The electron spectrum obtained by Edwards and Cunningham from O^--He collisions is shown in Fig. 43. The peaks at 9.50, 10.11, 10.87, 12.12, and 13.71 eV were attributed to autodetachment of the negative-ion resonances b_1, x, e_2, a_2, and a_3 (our notation; see Table XVII), which will be discussed specifically below. These peaks were demonstrated to be due to autodetaching states of O^-, rather than autoionizing states of neutral O, by comparison with an O-He collision spectrum obtained by passing the incident beam through a stripping cell.

Electron transmission spectroscopy was used by Spence and Chupka (1974; see also Spence, 1975b) to observe resonances in electron scattering by atomic oxygen. These experiments are among the few successful attempts at studying electron scattering by highly reactive atomic and molecular species. They were carried out by placing the interaction region of a transmission electron spectrometer in the flowing afterglow of an O_2 discharge. Discrimination of features associated with *e*-O from *e*-O_2 scattering was accomplished by comparing spectra obtained with the microwave discharge on and off. The experimental results of Spence (1975b) are shown in Figs. 44(a) and 44(b). In the two experiments reported by this group, all but one of the resonances seen by Edwards *et al.* were observed, and six others were discovered. Together these constitute the totality of published experimental data on autodetaching states of O^-. It is summarized in Table XVII.

On the theoretical side, studies of resonances in electron scattering by oxygen were initiated by Rountree and Henry (1972). They calculated the cross section for $2p^4\ ^3P$-$2p^3 3s\ ^3S°$ excitation by various approximations, and in a two-state (^3P and $^3S°$) close-coupling calculation they found resonances in the ^2P and ^4P channels at collision energies of 9.67 eV and 9.94 eV, respectively. These appeared in the total excitation cross section as a single (i.e., blended) shape resonance feature just above the threshold. The widths of the resonances are not stated explicitly by Rountree and Henry, but they appear to be

TABLE XVII. Recommended energies and classifications for negative-ion resonances in oxygen. Subscript labels are for reference to discussion in text. The energies are expressed relative to the $2p^4\,^3P_2$ state of O. Experimental values are from Edwards and Cunningham (1973) and Spence (1975b). Figures in parentheses represent the uncertainty in the least significant digit.

Classification	Energy (eV)	Width (meV)	Comments
$2p^3(^4S^\circ)3s^2$	8.78(5)		a_1
$2p^3(^4S^\circ)3s3p(^3P^\circ)$	9.50(2)		b_1
$2p^3(^4S^\circ)3p\,^4P^\circ$	10.73(5)		
$2p^3(^4S^\circ)3p^2\,^2P^\circ$	10.87(2)		
$2s2p^6\,^2S$?	12.07(2)		Uncertain—see text
$2p^3(^2D^\circ)3s^2$	12.12(2)		a_2: presumably doublet with unresolved (3 meV) splitting
$2p^3(^2D^\circ)3s3p(^3P^\circ)$	12.55(5)		b_2
$2p^3(^2P^\circ)3s^2$	13.71(2)		a_3: presumably doublet with unresolved (<1 meV) splitting
$2p^3(^2D^\circ)3p^2$	14.05(5)		
$2p^3(^2P^\circ)3s3p(^3P^\circ)$	14.40(5)		
$2p^3(^2D^\circ)3p^2$	15.65(5)		

about 1 eV. As we shall discuss below, these resonances almost certainly correspond to the b_1 feature observed experimentally.

A calculation of the photodetachment cross section of $O^-\ 2p^5\ ^2P^\circ$ was performed by Chase and Kelly (1972) using many-body perturbation theory. They found a strong resonance in the cross section at a photon energy of 14.089 eV, which corresponds to the process

$$2s^22p^5\ ^2P^\circ + h\nu \rightarrow O^{-*}\ 2s2p^6\ ^2S\ ,$$
$$O^{-*} \rightarrow O\ 2s^22p^4\ (^1D \text{ or } ^1S) + e\ (\varepsilon d \text{ or } \varepsilon s)\ . \tag{36}$$

Decay of this resonance to the ^3P ground state of O is forbidden in LS coupling. The calculated width of the resonance is 2.45 eV. Edwards and Cunningham (1973) attributed their 10.11 eV autodetachment feature to the decay of the $O^{-*}\ 2s2p^6\ ^2S$ state in the ^1D channel; we consider this point below. A second resonance associated with $1s \rightarrow 2p$ excitation is calculated to occur at a photon energy of 546 eV, with a width of 38 meV.

Matese *et al.* (1973) performed configuration-interaction calculations to find Feshbach resonances in oxygen. They represented the wave functions of states of O^+ and O by single configurations, and the wave functions of states of O^- by a multiconfiguration expansion upon a fixed O^+ core state: for example, $2p^3\ ^4S$ $(c_1 3s3p + c_2 3s4p + c_3 3p4s + \cdots)$. The orbitals used in the expansion were essentially the Hartree-Fock orbitals for excited states of O. Only spin doublet states were considered, as these are the only states likely to be excited under the experimental conditions of Edwards *et al.* A Feshbach resonance was deemed to occur if the total energy calculated for a state was less than that of an appropriate "parent" excited state of O. Four such resonances were found, corresponding to the b_1, a_2, a_3, and e_1 features. A subsequent set of similar calculations by Matese (1974), in work stimulated by the advent of electron-scattering experiments, used the same method to investigate quartet and sextet states. Eight additional Feshbach resonances were found. Of the 12 resonances predicted by this method, about seven have been observed in either e-O or O^--He scattering (or both). As we shall discuss below, in some cases there is good reason to think that shape resonances should be present at about the same energies as the computed Feshbach resonances. The method used by Matese *et al.* is not capable, in principle, of generating shape resonances, but the distinction between the two types may be blurred in these cases.

Close-coupling calculations of electron scattering by oxygen were performed by Ormonde *et al.* (1973). In particular, they reported a calculation in overall $^2P^\circ$ symmetry that included the five O target states $2p^4$ $(^3P, ^1D, ^1S)$, $2p^3(^4S^\circ)3p\ ^3P$, and $2p^3(^2D^\circ)3s\ ^3D^\circ$. This yielded two resonances. The first, at a collision energy of 10.38 eV with a width $\Gamma = 20$ meV, is probably the e_1 feature, though its energy does not agree well with experimental or other calculated values. The second resonance occurs at an energy of about 11.36 eV and has a width of approximately 1 eV (as estimated from Fig. 6 of Ormonde *et al.*); it appears as a shape resonance just above the $2p^3(^4S^\circ)3p\ ^3P$ threshold. This resonance does not fit well into conventional classification schemes and does not correspond in an obvious way to experimental observations. We believe it may be an artifact of the calculation.

We have performed some MCHF calculations for the a resonances of O^- (Clark, 1986, and present work) that give energies similar to those of Matese, Rountree, and Henry (1973). These results are described in Sec. VI.A.

We now briefly discuss some of the states presented in Table XVII.

The a_1 feature is well established. It is not seen in O^--He scattering because of spin conservation, but it is a very strong feature in electron scattering. Its binding energy with respect to $O^+\ 2p^3(^4S^\circ)$ fits the pattern of a resonances, and calculations by Matese (1974) and the

present work are in good agreement with the experimental energy.

The b_1 feature: Matese (1974) finds a Feshbach resonance here, of dominant configuration $2p^3(^4S^\circ)3s\,3p\ ^2P$. However, its calculated binding energy of 18 meV with respect to the O $2p^3(^4S^\circ)3s\ ^3S^\circ$ parent state is less than the uncertainty in the calculation, which would be of the order of 100 meV. Note that Rountree and Henry (1972) find shape resonances here in both the ^2P and ^4P channels. We therefore believe that this resonance has the typical b character; i.e., it is described by the two outer electrons being coupled to form a $^3P^\circ$ pair, which is then coupled to the $^4S^\circ$ core to yield states of ^2P, ^4P, and ^6P symmetry. This is analogous to the case of the b resonance in Ne, where the observed single feature is a blend of ^2S and ^2D negative-ion states (Clark and Taylor, 1982). Matese (1974) finds the ^6P state at a somewhat lower energy of 9.14 eV; it would not be strongly excited in electron scattering or in O^--He collisions because of spin conservation. By the same argument, the ^2P component must be the one observed by Edwards and Cunningham (1973); we suppose that the ^4P channel also supports a resonance, but there is as yet no positive experimental evidence for this. A remaining puzzle is the absence of the b_1 feature in the electron transmission spectra of Spence and Chupka (1974) and Spence (1975b). In the transmission experiment of Sanche and Schulz (1972a, 1972b, 1972c) on Ne, the b feature appears with about $\frac{1}{30}$ the intensity of the a. As the excitation mechanisms in Ne and in O are presumably similar, one might suppose that an intensity ratio of the same order of magnitude would exist for O. This would give a feature on the upper trace of Fig. 44(a) of about $\frac{1}{30}$ the size of the structure of 8.78 eV, but none can be seen clearly.

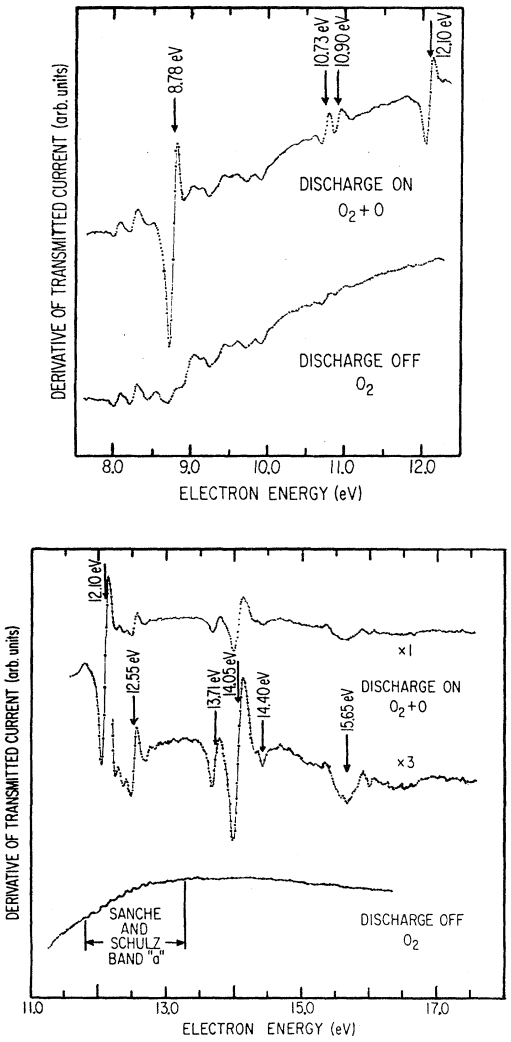

FIG. 44. Derivative of the transmitted electron current through a beam of partially dissociated oxygen: (a) 7.5 to 12.5 eV; (b) 11.5 to 18.0 eV. Vertical arrows indicate the location of atomic oxygen resonances (from Spence, 1975b).

The 10.73 eV feature: Spence (1975b) identifies this as a sextet state, apparently based on the calculation of Matese (1974). However, the formation of a sextet state in an electron collision with the triplet ground state would require change in the total spin of the complex, which is rather improbable in an atom as light as oxygen. In neon, where spin-orbit effects are somewhat larger, there is no evidence for quartet resonances, which would be produced by analogous spin-flip processes. The only reason for making a sextet assignment would appear to be that Matese had found a Feshbach resonance of this symmetry; but, as we have noted above, there is significant uncertainty in these calculations, and it is quite likely that if a $2p^3 3p^2\ ^6P^\circ$ resonance exists, then so does a $^4P^\circ$ term of the same configuration. Approximate spin conservation allows the formation of this resonance in electron collisions with the ground state, so we make this assignment. The other possible term of this configuration, $^2P^\circ$, ought to lie higher, and we have assigned it to the feature at 10.87 eV.

The x feature: This state poses some problems in interpretation. Both Edwards and Cunningham (1973) and Spence (1975b) observed features that were attributed to this resonance. Edwards and Cunningham observed an autodetachment transition at 10.11 eV, which could not be assigned to any of the Feshbach resonances computed by Matese, Rountree, and Henry. The transition energy corresponds to that of a state 12.07 eV above the $2p^4\ ^3P$ ground state of O decaying to the excited state $2p^4\ ^1D$. There is no feature observed that would correspond to the autodetaching transition to the ground state, which would, of course, be consistent with the resonance's being a singlet. However, one would expect a possible transition to the other excited term of the ground configuration, $2p^4\ ^1S$. Edwards and Cunningham looked in the appropriate energy region, but observed no such transition and concluded that under the conditions of measurement the branching ratio for ^1S to ^1D decay was less than 1:100. Their classification of the resonance as a

$2s2p^6$ state was based upon the photodetachment calculation of Chase and Kelly (1972), which put this resonance 12.63 eV above the ground state of O (this number is obtained by subtracting the experimental value of the O electron affinity from the excitation energy reported by Chase and Kelly). The discrepancy of 0.5 eV is not too worrisome, given the nature of the approximation used by Chase and Kelly. Spence and Chupka (1974) observed the resonance as a rather weak feature at 10.10 eV in transmission spectroscopy, but Spence (1975b) subsequently found that the feature vanished when the collision interaction region was moved farther from the discharge source. This was interpreted as resulting from the quenching of metastable O $2p^4\,{}^1D$ that is produced in the discharge source, and which, according to the classification given above, must be present if the resonance is to be observed in electron scattering. In this sense, the two independent experimental approaches may be said to point consistently to the assignment given by Edwards and Cunningham.

The main difficulty with this interpretation lies in the apparent mode of decay of the resonance. The width of the feature observed by Edwards and Cunningham is instrumentally limited, but therefore cannot be much greater than 200 meV; the structure observed by Spence and Chupka is also very narrow. The calculations of Chase and Kelly, however, yield a resonance width of 2.45 eV. This is due to the very large matrix element for the interaction of $2s2p^6$ with the $2s^22p^4\,\varepsilon d$ continuum, i.e., a $2p^2\rightarrow 2s\varepsilon d$ dipole interaction. This interaction is known to be very large in the case of the heavier neutral halogens, where it is manifest as a pronounced mutual perturbation of the $ns^2np^4({}^1D)md_{1/2}$ Rydberg series by the $nsnp^6$ state (Reader, 1974; Hansen, 1977). The $2s2p^6$ state has, to date, not been observed in fluorine, which is isoelectronic to O^-; the $2p^4md$ Rydberg series do not exhibit perturbations, but this may be because the $2s2p^6$ state lies well above the $F^+\ 2s^22p^4\ {}^1D$ limit. A photoionization calculation by Nicolaides *et al.* (1981) finds F $2s2p^6$ at an energy of about 0.5 a.u. above $F^+\ 2s^22p^4\ {}^1S$, which would be about 17 eV above the ${}^1D$ limit. Their computed width of the resonance was 3.1 eV, the bulk of which comes from interaction with the εd continuum. We have performed a calculation of the width of $2s2p^6$ by a simple Fano-type treatment of a discrete state (represented by a Hartree-Fock wave function) with a continuum (represented by a frozen-core Hartree-Fock continuum wave function); this gives a width of 2.4 eV, in agreement with the result of Chase and Kelly. It is conceivable that configuration-interaction effects could reduce the width of this state somewhat, but it is difficult to see how it could be decreased by an order of magnitude. The absence of the $2s2p^6\ {}^2S\rightarrow \mathrm{O}\ 2s^22p^4\ ({}^1S)+\varepsilon s$ autodetachment transition is also somewhat puzzling, since there is no symmetry restriction against it. This decay branch would be expected to be weaker than the εd branch, but should take place at a rate typical of that of other sharp features.

F. The halogens

Resonances have been observed in all of the halogen atoms lighter than astatine. Because of their large binding energies and ease of production, the stable negative halogen ions are often employed in negative-ion–atom collision experiments, which have provided most of the information on resonance structure. Some possible evidence for resonances in iodine comes from observations of photoattachment continuum radiation. The only theoretical studies of halogen negative-ion resonances that have been reported to date have utilized bound-state methods. Significant work has been done on the calculation of photodetachment of the ground states of halogen negative ions (Ishihara and Foster, 1974; Rescigno, Bender, and McKoy, 1978; Radojevic *et al.*, 1987); they are $np^6\ {}^1S$ closed-shell systems isoelectronic to the noble gases, the standard proving ground for theories of atomic photoabsorption. However, such calculations have not yet incorporated the excited np^4nl target channels that are required to support doubly excited $np^4nln'l'$ negative-ion resonances, and thus far no photodetachment calculations have given resonance structure.

1. Fluorine

Edwards and Cunningham (1974a) observed ejected electron spectra in collisions of F^- with He. A dozen clearly resolved peaks were observed, all but one of which could be attributed (by means discussed above) to autoionizing states of F* of the configurations $2p^4({}^1D$ or ${}^1S)ns$ or nd (Palenius, 1968; Palenius *et al.*, 1978). However, an ejected electron peak at 14.85 ± 0.04 eV is clearly associated with an autodetaching state of F^-. This feature was classified as the $F^-\ 2p^4({}^1D)3s^2$, based on the agreement in energy with a calculation of Matese, Rountree, and Henry. The autodetaching transitions are thus $2p^4({}^1D)3s^2\rightarrow 2p^5\,{}^2P^{\circ}_{1/2,3/2}\varepsilon l$, and the electron spectrum shows the doublet structure associated with the ground term of F (Fig. 45). The observed width of the resonance is instrumentally limited, and the natural width is thus less than 50 meV. Grouard *et al.* (1986) investigated collisions of F^- with all noble gases, measuring both ejected electron spectra and the yield of neutral F atoms by a time-of-flight technique. The 14.85-eV autodetaching feature and autoionizing states of F* were observed in collisions with He and Ne, but not in collisions with Ar, Kr, and Xe. Correspondingly, electron spectra associated with autoionizing or autodetaching states of the target noble gas were not observed for He or Ne, but the a resonances and some autoionizing states were excited in Ar, Kr, and Xe. No signal clearly attributable to any other autodetaching state of F^- was observed.

The $F^-\ 2p^4({}^1D)3s^2$ state is evidently an a resonance, and the other terms of the F^+ core may also be expected to support a resonances, as is the case in the noble gases. Of these, the $F^-\ 2p^4({}^3P)3s^2$ resonances would not be ex-

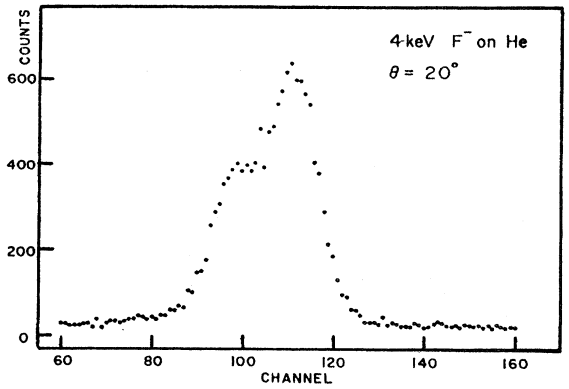

FIG. 45. Spectrum of ejected electrons resulting from collisions of F^- with helium (from Edwards and Cunningham, 1974a).

pected to be excited in collisions with He or Ne, due to spin conservation (since the target is not excited). The reason for the absence of F^- $2p^4(^1S)3s^2$ is not obvious, but this state would correlate to a completely different potential curve of the F^- + noble gas quasimolecule, and its excitation probability need not be related in any simple way to that of the ^1D state. Three low-energy electron peaks (E =93, 224, and 256 meV) observed by Grouard *et al.* do not appear to correspond to autoionizing transitions of F*, and it is possible that they derive from other autodetaching states of F^-. For example, a *b* resonance of the type $2p^4$ $3s$ εp could autodetach into the $2p^4$ $3s$ parent configuration, which would yield electrons with energies of the order of 100 meV. However, such a resonance should also produce a higher-energy peak associated with autodetachment to the F ground state; no such peak is noted by Grouard *et al.* On the other hand, the F^- $2p^4(^1D)3s^2$ state can autodetach into excited states F*, yielding low-energy electrons. Given the energy of F^- $2p^4(^1D)3s^2$ to be 14.85 eV, tabulations of F energy levels (Moore, 1971) show that the only possible states are all those of the $2p^4(^3P)3s$ and $2p^4(^3P)3p$ configurations. Of these, the quartets can be excluded by spin conservation, and F* $2p^4(^3P)3p$ $^2S^\circ$ is forbidden by angular momentum/parity considerations. Such considerations also require that detachment to F* $2p^4(^3P)3s$ ^2P proceed by ejection of an εd electron with an energy of 1.8 eV, which should be suppressed by the centrifugal barrier. This leaves the four states F* $2p^4(^3P)3p$ $^2D^\circ_{5/2,3/2}$, $^2P^\circ_{5/2,3/2}$, which are accessible through the emission of a p electron at energies of 267, 235, 104, and 69 meV, respectively. The first three of these energies appear to be consistent with those reported by Grouard *et al.*, within the limits of their resolution. The experimental peak at 93 meV is much smaller than those at 224 and 256 meV, as would be expected in p-wave emission. The electron detachment continuum rises rapidly at low energies and could very well mask a weak feature.

The photoattachment continuum at wavelengths greater than 270 nm was observed by Popp (1974) in a low-current arc discharge. No evidence of resonance structure was found.

The only reported calculations of doubly excited F^- resonances appear to be the unpublished results of Matese *et al.* cited by Edwards and Cunningham (1974a) and a MCHF calculation of the $2p^4(^3P)3s^2$ resonance by Clark (1986). We have performed similar calculations for the ^1D and ^1S counterparts of this resonance in the present work. The energy of the ^1D resonance agrees with the experimental value, and analysis of the wave functions shows that the outer electron pair is relatively insensitive to the term of the grandparent positive-ion core. The ^1D resonance thus fits into the *a* category very well. Exclusion of the autodetachment continuum from these calculations introduces a false element of stability into the description, and it is conceivable that the ^3P and ^1S resonances could decay much more rapidly than the ^1D. In O and Ne, however, the widths of *a* resonances built on different core states are roughly comparable; this is also the case for the heavier halogen atoms. The $2p^4(^1S)3s^2$ state is actually calculated to lie about 0.27 eV above the F^+ $2p^4(^3P_2)$ limit [based on the energy of F $2p^4(^1S)3s$ given by Palenius, 1968], and could therefore decay by two-electron autodetachment, though the rate of this process would presumably be rather low. It thus seems that further experimental investigation of these states would be worthwhile, perhaps in the context of negative-ion–molecule collisions where spin exchange could occur.

Ormonde (1977) performed a close-coupling calculation of electron scattering by F and obtained shape resonances in the $2p^5\varepsilon d$ $^1P^\circ$ and $^1D^\circ$ channels very close to threshold. These results were disputed by Rescigno, Bender, and McKoy (1978) and by Robb and Henry (1977), who performed similar calculations within a variety of models. It seems probable that Ormonde's results are an artifact due to inaccurate solution of the Schrödinger equation in the asymptotic region. As discussed in Sec. VI.D, Ne exhibits no *d*-wave shape resonance, and it is thus unlikely that F would. However, the heavier halogens probably do support broad *d*-wave shape resonances, similar to those encountered in their noble-gas neighbors.

TABLE XVIII. Recommended energies, widths, and classifications for negative-ion resonances in fluorine. No specific measurements of widths have been reported. The energies are expressed relative to the $2p^5\,^2P^\circ_{3/2}$ ground state of F. Experimental value is from Edwards and Cunningham (1974a). Figures in parentheses represent the uncertainty in the least significant digit.

Classification	Energy (eV)	Width (meV)	Comments
$2p^4(^3P)3s^2$	12.29		Calculated value by Clark (1986)
$2p^4(^1D)3s^2$	14.85(4)		
$2p^4(^1S)3s^2$	17.69		Calculated value, present work

The experimental values of resonance energies are summarized in Table XVIII.

2. Chlorine

A very rich spectrum of ejected electrons has been produced in the experiments of Cunningham and Edwards (1973) on collisions of Cl^- with He and H_2. The outstanding characteristic feature of these spectra is the occurrence of pairs of peaks separated by an interval of 109 meV, the fine-structure interval of Cl $3p^5\,{}^2P^\circ_{3/2,1/2}$, which establishes them as autodetaching states of Cl^-. Collisions with He and H_2 show some of the same peaks. However, autodetaching states of H^- are observed in the Cl^--H_2 spectrum, some of which are shifted in energy to overlap Cl^- autodetachment electrons. In addition, a resonance attributed to Cl^- $3p^4(^3P)4s^2$ is seen in Cl^--H_2 collisions but not in Cl^--He; this is believed to be due to the greater probability of excitation of triplet states in H_2 than in He, which allows the $3p^4(^3P)4s^2$ resonance to be formed by spin exchange. Cunningham and Edwards also note that in Cl^--Ar collisions there is a strong signal from the autodetaching Ar^- *a* resonances; this signal provided the energy calibration for their electron spectra.

Identifications of the states were proposed on the basis of calculations of Matese *et al.* (1973). All the *a* resonances that are to be expected from the alternative terms of the grandparent core are present, and the fine structure associated with ^3P is also evident, though it could not be fully resolved (Fig. 46). The agreement of the calculations with the experimental values is remarkably good in the case of the *a* resonances observed. The computational approach of Matese *et al.* was used only to identify Feshbach resonances and would therefore not yield *b* resonances that lie above the appropriate parent state.

Fayeton *et al.* (1978) studied Cl^-–rare-gas collisions by the time-of-flight method, in which neutral Cl atoms are detected. The recoil effect of ejection of electrons at arbitrary angles induces a spread in the velocity distribution of neutral Cl atoms. This spread is sufficiently large that autodetaching states cannot be easily individuated. The main results of interest for the purpose of the present paper are the absence of the Cl^- $3p^4(^3P)4s^2$ resonance in collisions with Ne and Ar, consistent with spin-conservation arguments; and the apparent absence of Cl^- autodetaching features in collisions with Kr and Xe, but the presence of Kr^- and Xe^- resonances. Fayeton *et al.* conclude that in asymmetric collisions only the heavier partner is excited. These results were subsequently corroborated by De Vreugd *et al.* (1982a, 1982b), who looked at electron detachment spectra in all halogen anion–noble-gas collision systems.

Bydin (1967), who performed the first experiments on the detachment of negative ions in atomic collisions, saw no resonance features in Cl^--He collisions.

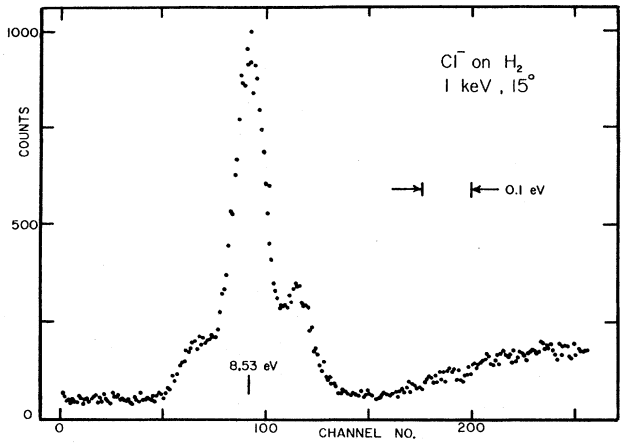

FIG. 46. Spectrum of ejected electrons resulting from collisions of Cl^- with H_2 (from Cunningham and Edwards, 1973).

TABLE XIX. Recommended energies, widths, and classifications for negative-ion resonances in chlorine. No specific measurements of widths have been reported, but the experimental data suggest that none are much larger than 200 meV. The energies are expressed relative to the $3p^5\,{}^2P^\circ_{3/2}$ ground state of Cl. All values are from Cunningham and Edwards (1973). Figures in parentheses represent the uncertainty in the least significant digit.

Classification	Energy (eV)	Width (meV)	Comments
$3p^4(^3P_{2,1,0})4s^2$	8.53(5)		*a*: fine structure apparent, but not clearly resolved
$3p^4(^3P)4s4p\,(^3P^\circ)$	9.15(5)		*b*
$3p^4(^1D)4s^2$	9.97(4)		*a*
$3p^4(^3P)4p^2$?	10.47(5)		
$3p^4(^3P)4p^2$?	10.61(5)		
?	11.23(8)		Possibly $3p^4(^3P)3d$ parent state
?	11.96(8)		Possibly $3p^4(^3P)3d$ parent state
$3p^4(^1S)4s^2$	12.09(6)		*a*
?	12.44(6)		

The experimental values of resonance energies are summarized in Table XIX. Our assigned classification of the *b* resonance differs somewhat from that of Matese *et al.* (1973), since we believe that the essential feature of this state is the triplet external coupling between the 4*s* and 4*p* electrons. Matese *et al.* found only one term of this configuration, $3p^4(^3P)4s4p(^3P^\circ)\ ^1P^\circ$, to occur as a Feshbach resonance. However, the other terms of $3p^4(^3P)4s4p(^3P^\circ)$ are likely to be low-lying shape resonances, as is the case in the noble gases. Six resonances observed by Cunningham and Edwards were not assigned classifications by them; and although Matese *et al.* find additional Feshbach resonances in the same region, all but one are triplet states. All *b*-type resonances that could be built upon the ^1D and ^1S states of the Cl^+ core would also necessarily be triplets. Since triplet excitation is thought to be highly unlikely in Cl^--He collisions, neither the computed Feshbach resonances nor the obvious *b* features are good candidates for classification. We have assigned several resonances to the $3p^44p^2$ configuration, based on their proximity to $3p^44p$ states of Cl (Radziemski and Kaufman, 1969) and the existence of analogous $3p^54p^2$ resonances in Ar. These assignments should be regarded as tentative.

Chlorine exhibits broad *d*-wave shape resonances in all $3p^5\varepsilon d$ channels, similar to the $3p^6\varepsilon d$ shape resonance in Ar, when treated in the frozen-core, continuum Hartree-Fock approximation (see Fig. 62). We known of no experiments on electron scattering by Cl, or on photodetachment of Cl^- in the appropriate range of wavelengths, that would exhibit such resonance structure. The large shift of the $3p^6\varepsilon d\ ^1P^\circ$ resonance away from all other terms is due to the repulsive $3p$-εd dipole exchange interaction in that channel. This resonance is apparent in calculations of photodetachment of Cl^- done in the relativistic random-phase approximation (Radojevic *et al.*, 1987). The same mechanism is responsible for the displaced maximum in the 3*p* photoionization cross section of Ar (Hansen, 1980). We discuss this correspondence in Sec. VI.D.

3. Bromine

Edwards and Cunningham (1974) observed three autodetaching states of Br^- in collisions of Br^- with He and Ar. These states are *a* resonances built on the two lowest terms of the $Br^+\ 4p^4$ ion core. As was the case in Cl^-, the autodetaching transitions to the two states Br $4p^5\ ^2P^\circ_{3/2,1/2}$ could be resolved, so that the presence of the Br^+ fine-structure interval in the detachment spectrum enables one to attribute a pair of autodetachment features to a single state. In particular, one pair of transitions can be associated with $Br^-\ 4p^4\ (^3P_2)5s^2 \rightarrow Br\ 4p^5\ ^2P^\circ_{3/2,1/2}+e$, another to $Br^-\ 4p^4\ (^1D_2)5s^2 \rightarrow Br\ 4p^5\ ^2P^\circ_{3/2,1/2}+e$. A fifth autodetachment feature corresponds to $Br^-\ 4p^4\ (^3P_{1\text{ or }0})5s^2 \rightarrow Br\ 4p^5\ ^2P^\circ_{3/2}+e$; the expected accompanying transition to the $J=\frac{1}{2}$ final state would lie within 10 meV of the energy of the $^3P_2 \rightarrow {}^2P^\circ_{3/2}$ transition, and could not be resolved. The general picture of the *a* resonances would lead one to expect resonances associated with both the $J=0$ and $J=1$ states of $Br^+\ 4p^4\ ^3P$. However, the Br^+ states are separated by only 87 meV, so that these resonances cannot be resolved in the experiment. The resonance energies and classifications are given in Table XX. The binding energies of these resonances with respect to their appropriate grandparent states are the same (4.4 eV) to within 0.1 eV. One would expect there to be an *a* resonance associated with the $4p^4\ (^1S_0)$ grandparent state; if this were attached to the $4p^4\ 5s\ (^2S_{1/2})$ parent state by the usual electron affinity of 0.5 eV, it would be found at 10.9 eV above the ground state of Br (Tech, 1963). No autodetaching transition near this energy was reported by Edwards and Cunningham.

TABLE XX. Recommended energies and classifications for negative-ion resonances in bromine. No specific measurements of widths have been reported, but the experimental data suggest that all widths are less than ~100 meV. The energies are expressed relative to the $4p^5\ ^2P^\circ_{3/2}$ ground state of Br. All values are from Edwards and Cunningham (1974b). Figures in parentheses represent the uncertainty in the least significant digit.

Classification	Energy (eV)	Width (eV)	Comments
$4p^4(^3P_2)5s^2$	7.39(6)		*a*
$4p^4(^3P_{1,0})5s^2$	7.84(6)		*a*: fine-structure of ~90 meV not resolved in experiment
$4p^4(^1D_2)5s^2$	8.85(6)		*a*

It is worth noting that both triplet and singlet resonances are produced in Br^- collisions with He. This contrasts with the results of experiments on lighter negative ions, in which the spin of the resonance is usually equal to that of the ground state.

We know of no theoretical calculations of resonances in Br^-, nor of other experimental measurements. Bydin (1967) specifically remarks upon the absence of resonance structure in collisions of Br^- with He, Ne, and Ar. It is likely that $4p^5(^2P^\circ)\varepsilon d$ shape resonances, similar to those in Cl, would occur in some channels.

4. Iodine

The first reported observations of autodetachment resonances in negative-ion–atom collisions are apparently those of Bydin (1967), who measured detachment spectra of Cl^-, Br^-, and I^- collisions with various noble gases. He observed a pronounced resonancelike electron detachment feature in the case of I^- only, with ejected-electron energies in the range 6–7 eV. The energy resolution of his apparatus was not sufficient to distinguish

any fine structure in this feature. The presence of this structure in collisions of I^- with He, Ar, and Kr and the independence of its energy from the collision energy (above a certain threshold) establish it as an intrinsic I^- resonance. No more specific identification was proposed by Bydin.

Cunningham and Edwards (1974) conducted experiments on I^--He collisions and observed a number of detachment features that could be associated with four different autodetaching states. The energies of the autodetachment electrons ranged between 5.5 and 8 eV, but the spectrum was dominated by a transition at 6.41 eV [assigned to $I^-\ 5p^4\ (^3P_2)6s^2 \rightarrow I^-5p^5\ ^2P^\circ_{3/2}+e$] that was an order of magnitude stronger than any other transition, and which presumably corresponds to the feature observed by Bydin. As in their previous work, Cunningham and Edwards were able to identify autodetachment transitions from a common upper state to the two different states of the I ground configuration. As in Br, but in contrast to Cl and F, triplet resonances were excited in collisions of the halogen anion with He. The energies and assignments reported by Cunningham and Edwards are listed in Table XXI.

Several groups have reported results of radiation measurements in iodine plasmas that have been interpreted as showing the existence of I^- resonances at significantly lower energies. Mandl and Hyman (1973) measured the photodetachment cross section of I^- in a shock-heated CsI vapor, over the photon energy range 3–6.5 eV. They observed a pronounced local maximum in the cross section at a wavelength of 225 nm, which they attributed to an autodetaching resonance of I^-. The half-width of this feature was approximately 0.25 eV. Mandl and Hyman proposed a tentative classification of this resonance as a $5p^4\ 6s6p$ state, with a *b*-type coupling scheme. The electron affinity of I $5p^5\ ^2P^\circ_{3/2}$ is 3.06 eV (Hotop and Lineberger, 1985), so absorption of a photon of wavelength 225 nm (5.51 eV) yields a state 2.45 eV above I $5p^5\ ^2P^\circ_{3/2}$. Such a state would be bound with respect to the lowest excited state of I ($5p^46s\ ^4P_{5/2}$) by 4.32 eV. A binding energy of this magnitude would be inconsistent with all known data on doubly excited negative-ion resonances, which are typically bound by less than 0.5 eV to a parent state; the *b* resonances are usually within 0.1 eV of the parent. This is true of the *b* state identified by Cunningham and Edwards (1974), the energy of which cannot be distinguished from that of the I $5p^46s\ ^4P_{5/2}$ state within the experimental uncertainties. We therefore consider the assignment of Mandl and Hyman to be incorrect.

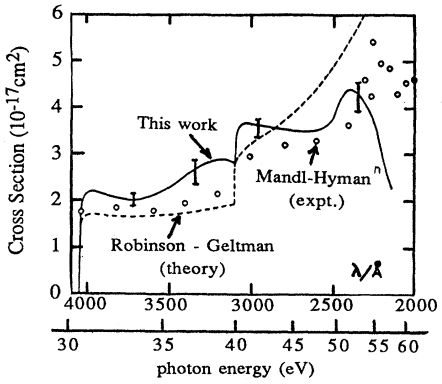

FIG. 47. Comparison of experimental results for photoattachment continuum radiation from an iodine plasma (Neiger, 1973, 1975) and the photodetachment cross section of I^- (Mandl and Hyman, 1973).

Subsequent observations by Neiger (1973, 1975) of the photoattachment continuum radiation in iodine plasmas also showed a broad feature centered at photon energy of about 5.3 eV. This was interpreted as being the same feature seen by Mandl and Hyman, though the two experiments yield rather different results in that energy range (see Fig. 47). A review of this work by Popp (1974) also presents arguments for the existence of a broad excited state of I^-, presumed to be $5p^56s\ ^3P_1$, at an energy of 2.1 eV above the ground state of I^-.

Since it is not easy to attribute the resonance proposed by Mandl and Hyman and by Neiger to a doubly excited state, we consider whether it is likely for a single electron to be attached to the I ground state, e.g., as a shape resonance. Iodine does appear to support shape resonances

TABLE XXI. Recommended energies and classifications for negative-ion resonances in iodine. No specific measurements of widths have been reported, but the experimental data suggest that all widths are less than ~200 meV. The energies are expressed relative to the $5p^5\ ^2P^\circ_{3/2}$ ground state of I. All values are from Cunningham and Edwards (1974b). Figures in parentheses represent the uncertainty in the least significant digit.

Classification	Energy (eV)	Width (meV)	Comments
$5p^4(^3P_2)6s^2$	6.41(6)		*a*
$5p^4(^3P_2)6s6p(^3P^\circ)$	6.75(6)		*b*
$5p^4(^3P_{1,0})6s^2$	7.15(6)		*a*: presumably two fine-structure states separated by ~80 meV. Not clearly resolved in the experiment
$5p^4(^1D_2)6s^2$	8.06(6)		*a*

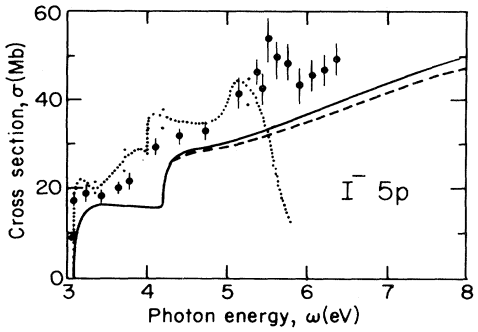

FIG. 48. Photodetachment spectrum of I^- as computed by Radojevic *et al.* (1987).

in the *d* and *f* waves, quite similar to those known in Xe; but these would occur at higher energies (10–20 eV; see Sec. VI.E), and their widths are also too large to explain the observations. Singly excited resonances of this type would presumably show up in the relativistic random-phase-approximation calculations of I^- photodetachment by Radojevic *et al.* (1987), but these calculations do not display any structure in this energy range other than that attributable to thresholds (Fig. 48). The binding energy required for a singly excited state of I^-, bound with respect to core-excited I $5s5p^6$, is also unrealistically large. We thus believe that the observed photodetachment features are not caused by excited states of I^-.

G. The Alkaline Earths

1. Beryllium

The presence of a long-lived state of Be^- in Penning ion sources gave rise to conjectures that a true bound state of the negative ion might exist (Moiseiwitsch, 1965 and Bethge *et al.*, 1966; see also Massey, 1976). However, extensive theoretical calculations have indicated that the electron affinity of Be $1s^22s^2$ is negative (Weiss, 1968; Bunge *et al.*, 1982), but that several excited states of Be can support negative-ion states with relatively long lifetimes (Nicolaides *et al.*, 1981; Bunge *et al.*, 1982; Aspromallis *et al.*, 1985, 1986). These states, for example, $Be^-\,1s^22s2p^2\,{}^4P$, can undergo direct autoionization only via intermediate coupling (in this particular example, to ^2S and ^2D terms, depending upon the value of *J*). This effect is sufficiently weak in a light atom such as Be to give rise to lifetimes of 10^{-6} sec or longer, and in some cases the lifetimes are determined by radiative processes (Aspromallis *et al.*, 1985). These metastable states are beyond the scope of the present article, but for reference purposes we list some of them in Table XXII. Further information can be found in Bunge *et al.* (1982) and Aspromallis *et al.* (1985, 1986).

There are no high-resolution experimental data available on electron-scattering resonances of Be^-. Some low-resolution ($\Delta E \approx 1.0$ eV) optical excitation functions have been measured by Aleksakhin and Zayats (1974), and in some cases, particularly the $3^3S \rightarrow 2^3P$ transition at 332.1 nm, they found strong near-threshold structure which may have been due in part to resonances.

TABLE XXII. Recommended energies, widths, and classifications for negative-ion resonances in beryllium. The energies of the metastable states are average-of-configuration values and are referenced with respect to the energies of the appropriate parent states, respectively, $2s2p\,{}^3P^\circ$ and $2p^2\,{}^3P$. All values are theoretical.

Classification	Energy (eV)	Width (meV)	Comments
$2s^2\varepsilon p\,{}^2P^\circ$	0.323	296	*b*: McNutt and McCurdy (1983)
$2s2p^2\,{}^4P$	−0.285		Bunge *et al.* (1982) Fine structure <0.1 meV Aspromallis *et al.* (1985)
$2p^3\,{}^4S^\circ$	−0.262		Bunge *et al.* (1982)

A low-energy *b*-type shape resonance has been investigated quite extensively by various theoretical approaches. This resonance, which takes the configuration Be^- $1s^22s^2\varepsilon p\,{}^2P^\circ$, has been of particular interest in the development of complex-coordinate rotation methods. Two semiempirical methods have been used to compute the resonance parameters. Hunt and Moiseiwitsch (1970) performed model potential calculations for a number of *p*-wave shape resonances in electron scattering by neutral atoms. Their model potential is identical to the one used by Allis and Morse (1931) for the description of elastic electron scattering:

$$V(r) = -Z/r + (Z-z)/r_0, \quad r < r_0 ,$$
$$= -z/r, \quad r > r_0 , \tag{37}$$

in atomic units, where *Z* is the atomic number, *z* is the effective asymptotic charge or ionization stage ($z=0$ for a neutral target), and r_0 is a parameter that depends quadratically upon *Z* and which is adjusted to give the best fit to the ionization limit along an isoelectronic series. For electron scattering by Be, this fit yielded $r_0 = 2.53a_0$. The model potential [Eq. (37)] has the proper coefficient of r^{-1} in the limits $r \rightarrow 0$ and $r \rightarrow \infty$, and the resulting Schrödinger equation can be solved in closed form in terms of Whittaker and Bessel functions. Much physics is left out of this model, most notably the long-range polarization potential, and it is not an approach that can be improved systematically. Nevertheless, its results are often found to be qualitatively correct. Ground-state electron affinities computed in this model are usually accurate to within 0.2 eV. It yields a shape resonance in *p*-wave scattering by Be, with an energy of 0.60 eV and a width of 0.22 eV.

A more detailed, and presumably more realistic, model potential has been utilized by Kurtz and co-workers (Kurtz and Öhrn, 1979; Kurtz and Jordan, 1981). They perform two types of calculation: (i) the static-exchange

(SE) approximation, i.e., solution of the Hartree-Fock equations for a p electron in the field of a frozen Hartree-Fock Be $1s^2 2s^2$ target; (ii) a static-exchange-with-polarization (SEP) approximation, in which the SE equations are supplemented by a polarization potential of the form

$$V_l(r) = -(\alpha/2r_0^5)r, \quad r < r_0 ,$$
$$= -(\alpha/2)r^{-4}, \quad r > r_0 , \tag{38}$$

in atomic units, where α is the static electric polarizability of the target, and r_0 is chosen to be the distance at which the centrifugal and polarization potentials cancel, $r_0 = [\alpha/l(l+1)]^{-1/2}$. This potential has the correct behavior to order r^{-4} at large r, but the means by which it is cut off at small r is arbitrary. As will be discussed below, the SEP model gives reasonable agreement with experiment for electron scattering by Mg; and the general picture of low-energy shape resonances deriving from the potential barrier structure due to polarization and centrifugal potentials has been quite successful (Johnston, 1983). The resonance parameters E, Γ were determined by Kurtz *et al.* from the maximum value and width of the computed cross section and from the maximum value of $d\delta/dE$. These two methods give different results, and neither need necessarily coincide with values obtained from the Blatt-Jackson formula. We cite here only the values from the phase-shift analysis, since the SE results are closest to those of Rescigno, McCurdy, and Orel (1978) discussed below, which were obtained by a mathematically equivalent method. In the SE approximation, $E = 0.75$ eV, $\Gamma = 1.64$ eV; in the SEP approximation, $E = 0.14$ eV, $\Gamma = 0.13$ eV. It is clear that polarizability significantly affects the position and width of this resonance. The simple barrier-height model of Kurtz and Jordan (see Sec. IV.C.1) gives an energy of 0.360 eV for the top of the potential barrier formed by a combination of centrifugal and polarization effects. Later work by Yuan and Zhang (1989), using static exchange supplemented by a correlation-polarization potential derived from density-functional theory, obtained similar results.

The first approach to computation of the b resonance in Be^- by purely *ab initio* means was a complex-coordinate rotation calculation by Rescigno, McCurdy, and Orel (1978). This calculation was also apparently among the first attempts to apply complex-coordinate techniques to a system with more than two electrons. However, since it was limited to a solution of the frozen-core Hartree-Fock equations of motion for a p wave in the field of Be $1s^2 2s^2$, it was, in effect, a description of a resonance in the motion of a single electron in a (nonlocal) potential. In this calculation the $1s$ and $2s$ orbitals were the Hartree-Fock orbitals of Be $1s^2 2s^2$, as constructed from a basis of five Slater-type orbitals (STOs), and the p wave was represented by a set of 14 STOs that were evidently chosen by standard criteria, i.e., partial arithmetical and geometrical progression of the exponents. No optimization of the orbital basis was reported, but the results were found to be relatively insensitive to variations of the exponents. The coordinates of the p orbital alone were subject to complex rotation. As has usually been the case in practical calculations, the complex energy of the resonance was found to be dependent upon the rotation angle, but it "stabilized" within a certain range of angles. The resulting parameters associated with the solution in the stable range were $E = 0.76$ eV, $\Gamma = 1.11$ eV. Rescigno *et al.* also performed a standard frozen-core continuum Hartree-Fock calculation of $e + \mathrm{Be}$ scattering and found a phase-shift curve typical of a low-energy shape resonance. A fit of the computed phase shift to the Blatt-Jackson effective-range formula gave values of E and Γ that agreed with the rotated-coordinate calculation, as expected from the mathematical identity of the two approaches. These calculations are equivalent to the later SE calculations of Kurtz *et al.*

Donnelly and Simons (1980) utilized a variant of the complex-coordinate technique, in which the electron propagator is analytically continued into the complex energy plane, its poles corresponding to resonances. In their specific approach, the propagator accounts for the effects of electron-electron interaction to second order of perturbation theory (zeroth order constituting the Hartree-Fock approximation). A Gaussian orbital basis of $5s$ and $7p$ functions was used to construct the propagator. The coordinate transformation used by Donnelly and Simons took the form $r \rightarrow (\alpha e^{i\theta})r$. Variation of both a and θ gives both complex-coordinate rotation and dilation, which effectively provides a uniform scaling of the exponents of the basis functions. The resonance parameters were found to be $E = 0.57$ eV, $\Gamma = 0.99$ eV. The lowering of E from the frozen-core Hartree-Fock value of Rescigno, McCurdy, and Orel (1978) is to be expected from the inclusion of some effects of electron correlation and core relaxation. A subsequent Gaussian basis set calculation was undertaken by McCurdy *et al.* (1980), who derived complex self-consistent-field equations for *all* orbitals subject to complex-coordinate rotation. This generalization of the frozen-core approximation takes account of core relaxation (but not electron correlation) and yields an energy of 0.70 eV and a width of 0.51 eV. Subsequent work by the same group (McNutt and McCurdy, 1983) provides the most comprehensive structural account of the Be^- shape resonance to date. This approach generated the complex self-consistent-field solution of Be^- $1s^2 2s^2 \varepsilon p$ in terms of STO's and then allowed it to interact with all configurations that could be reached by single, double, and triple excitations out of the valence shell $2s^2 \varepsilon p$ in an orbital space of five additional s, four p, and four d STOs. A 229-configuration calculation incorporating all single and double valence excitations gave $E = 0.58$ eV, $\Gamma = 0.377$ eV; a 745-configuration calculation including up to triple excitations yielded $E = 0.323$ eV, $\Gamma = 0.296$ eV. We regard these latter values as the most reliable resonance parameters and use them for the sole resonance entry for Be in Table XXII. They could presumably be improved by

refinement of the approximation, e.g., to include polarization of the K shell. This has been done in a modelistic way by Kim and Greene (1989), whose results are discussed below. Results of comparable accuracy could presumably be obtained with a much smaller set of configurations if the orbitals were generated by a complex multiconfiguration self-consistent-field procedure, as is routinely done for bound states of atoms and small molecules. However, such an approach to rotated-coordinate calculations apparently has not yet been implemented.

Another version of the electron propagator technique, similar to that of Donnelly and Simons, is described by Mishra, Goscinski, and Öhrn (1983), who obtain $E=0.62$ eV, $\Gamma=0.60$ eV. Krylstedt *et al.* (1987, 1988) have used a rotated-coordinate approach, with either an $X\alpha$ approximation for the exchange potential or an exact treatment of exchange, and with a long-range polarization potential with an adjustable cutoff parameter r_0; they find a significant dependence of the resonance parameters upon r_0 and obtain values that are comparable to those of Kurtz and Jordan (1981). Krylstedt *et al.* (1987) contains a useful table that compares the theoretical results known at the time. A related review of complex-coordinate multiconfiguration self-consistent-field methods with application to some of the alkaline-earth resonances is given by Elander *et al.* (1989).

The most recent rotated-coordinate treatments of the Be^- shape resonance, as of the time of this writing, are the rotated-coordinate calculations of Frye and Armstrong (1986) and Bentley (1990). These authors derive the complex Hartree-Fock equations for the $1s$, $2s$, and εp orbitals in a manner equivalent to that of McCurdy *et al.* (1980). However, they solve them by using a modification of the Hartree-Fock code of Froese Fischer (1978), in which the orbitals are represented by numerical functions defined on a radial mesh, rather than by a superposition of STO or Gaussian basis functions. This approach should eliminate any artifacts due to basis set dependence that may have been present in previous calculations. In this approach the complex energy of the resonance is found to be independent (to within 10^{-5} a.u.) of the rotation angle θ, a situation that is unique among the rotated-coordinate treatments of this case. Frye and Armstrong conjectured that this independence of θ derives from the use of numerical vs expansion methods for the solution of the Hartree-Fock equations. This is substantiated by Bentley, who finds a similar θ independence for all other systems treated by this method. Their computed parameters $E=0.69$ eV, $\Gamma=0.51$ eV are essentially the same as those of McCurdy *et al.* (1980), which is to be expected since the two approximations differ only in computational implementation.

Kim and Greene (1989) employ an approach in which correlations of the outer three electrons of the Be^- complex are treated extensively, and the electron-core interaction is represented by a model potential that gives accurate energy levels of Be^+. They use an R-matrix approximation in which the three outer electrons are represented explicitly in a spherical box of radius $r_0=18a_0$; diagonalization of the Hamiltonian within the box then provides a logarithmic-derivative boundary condition for the wave function of the continuum electron at $r=r_0$, from which the scattering phase shift can be inferred. The three-electron wave function inside the box was represented by a superposition of 242 configurations. The resulting resonance parameters $E=0.254$ eV, $\Gamma=0.206$ eV are comparable to those obtained in the SEP and the multiconfiguration self-consistent-field approaches. Kim and Greene present an interesting analysis of the behavior of the b resonance along the alkaline-earth sequence, which we discuss in Sec. VI.B.

It is probable that excited states of Be support resonances, and the low-resolution optical excitation functions of Aleksakhin and Zayats (1974), which were mentioned above, may be an indicator of such states; but we are otherwise unaware of any calculations that exhibit them. The most obvious candidates for investigation are other terms of the configuration of the metastable states of Be^-, e.g., $2s2p^2\ ^2P,^2S$, and ^2D, and $2p^3\ ^2P^\circ$ and $^2D^\circ$.

2. Magnesium

Magnesium is the first member of the alkaline-earth series for which some high-resolution electron-scattering data are available, although, consistent with the other members of the group, this is generally limited to the low-lying resonances and is not particularly extensive.

Similar to beryllium, the electron affinity for the Mg^- ground state is negative. This was first demonstrated experimentally in electron transmission experiments (Burrow and Comer, 1975; Burrow *et al.*, 1976) where magnesium was shown to support a low-energy b-type shape resonance $3s^2\varepsilon p\ ^2P^\circ$ at $E=0.15$ eV (Fig. 49). These experiments, which to our knowledge represent the only

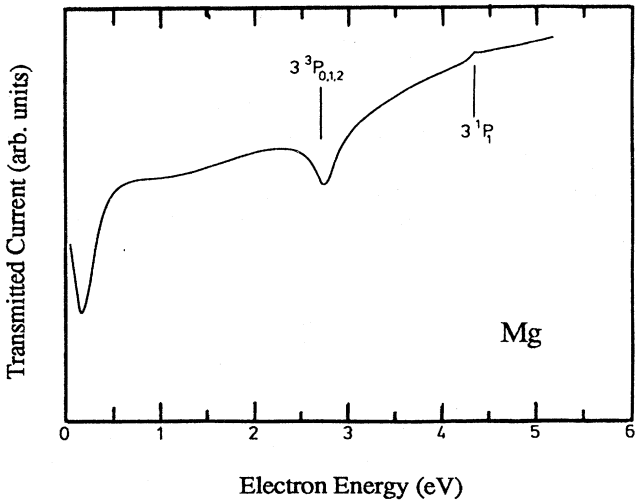

FIG. 49. Transmitted electron spectrum for Mg (from Burrow *et al.*, 1976).

direct experimental investigation of resonances in Mg, also indicated further structure due to short-lived states of Mg^- near the thresholds of the $3s3p\ ^3P^\circ$ states at 2.71 eV and the $3s3p\ ^1P^\circ$ state at 4.36 eV. No comment is given on the possible origins of these structures. They do comment on a broad, weak feature centered at about 1.2 eV which they postulate is due to a *d*-wave shape resonance, i.e., $3s^2\varepsilon d\ ^2D$. Long-lived excited states of Mg^- have been observed in Penning ion sources (Bethge *et al.*, 1966); their energies have been calculated by Weiss (1968). They have the term designation $3s3p^2\ ^4P$ and cannot autodetach in *LS* coupling. This work has been summarized by Hotop and Lineberger (1975).

There have been quite a number of calculations on the Mg^- *b* resonance, many of which were performed by the methods applied to Be^- and which are described in the previous section. The model potential calculation of Hunt and Moiseiwitsch (1970) gives an energy of 0.37 eV for this state, while the other empirical technique, horizontal analysis, places this resonance at 0.52 eV (Zollwegg, 1969). Two early close-coupling calculations by Van Blerkom (1970) and Fabrikant (1974) yielded significantly different values for the low-energy elastic-scattering cross section for Mg. Van Blerkom's cross section indicates a *p*-wave resonance at about 0.95 eV, while no low-energy resonance was found by Fabrikant, although he proposes several reasons for the enormous differences in the two cross sections as $E \rightarrow 0$. Both calculations indicate further resonance activity at higher energies. Fabrikant finds a resonance in the *d* wave at an energy of about 2.6 eV, van Blerkom resonances in both the *p* and *d* wave around 3.25 eV above the threshold of the $3\ ^3P$ states, and *s*- and *d*-wave resonances at about 5.8 eV. Hazi (1978) used a projection method to compute the width of the *b* resonance, obtaining a value of 200 meV.

Kurtz and co-workers (Kurtz and Öhrn, 1979; Kurtz and Jordan, 1981) have calculated resonance parameters for magnesium in the SE and SEP approximations. The $3s^2\varepsilon p\ ^2P^\circ$ resonance parameters in the SEP approximation are $E=0.14$ eV, $\Gamma=0.24$ eV, which are in good agreement with the experimental values. As in Be, the inclusion of polarization greatly affects these values; in the SE approximation, they are $E=0.46$ eV, $\Gamma=1.53$ eV. Kurtz and Jordan also use their calculated elastic-scattering cross section for Mg to derive an attenuation curve which can be compared, quite favorably, with the experimental result of Burrow *et al.* They also calculate the energy of the $3s^2\ \varepsilon d\ ^2D$ resonance to be about 2 eV. In making comparisons between experiment and theory for the low-energy shape resonances in this and other atomic systems, Kurtz and Jordan also comment on the uncertainties that can arise from determining the position of a weak resonance when its width is comparable to its absolute energy. Their barrier-height model predicts energies of about 0.19 and 1.7 eV for the $^2P^\circ$ and ^2D resonances, respectively. Subsequent calculations using a similar approximation (Yuan and Zhang, 1989) gave very similar results.

As for Be, a considerable number of calculations using variants of the rotated-coordinate method have been applied to the Mg^- shape resonance. McCurdy *et al.* (1981) used the complex self-consistent-field method in a single-configuration calculation with self-consistent solution of all orbitals; they obtained $E=0.505$ eV, $\Gamma=0.542$ eV. As for Be, the effects of core relaxation can be determined by comparison between self-consistent-field and SE results; in this case, *E* is slightly *increased* by core relaxation, and the width is reduced by a factor of 3. Mishra, Kurtz, *et al.* (1983) used the second-order propagator method and obtained results that are roughly consistent with those of the SEP method, but which exhibit strong basis set dependence. Krylstedt *et al.* (1987, 1988) used several SEP-type methods to obtain results comparable to those of Kurtz and Jordan (1981); Krylstedt *et al.* (1987) contains a useful table of comparisons with previous work. Bentley (1990) used a fully numerical self-consistent-field technique and obtained results very close to those of McCurdy *et al.* (1981), as is to be expected: $E=0.5055$ eV, $\Gamma=0.5520$ eV. Kim and Greene (1989) used the *R*-matrix approach they applied to Be to get $E=0.161$ eV, $\Gamma=0.16$ eV, in good agreement with the experimental values.

At higher energies, structure that may be due to resonances has been observed in optical excitation functions for the $3s3p\ ^1P^\circ$ state (Karstensen and Köster, 1971; Aleksakhin *et al.*, 1973; Leep and Gallagher, 1976). In most cases in this work, structure in the excitation function is attributed to cascade contributions from higher excited states. It would appear, however, that a sharp, quite strong feature observed by Leep and Gallagher in the linear polarization fraction of the 285.2-nm line at about 5.0 eV may be due to a resonance of unknown symmetry. It is well below the next excited state that can cascade via the $3s3p\ ^1P^\circ$, the $3s4s\ ^1S$ state at 5.39 eV and is presumably too far above the $3s3p\ ^1P^\circ$ to be a shape resonance associated with that state. One possible configuration is $3s3p^2$, although this is highly speculative. No similar structure is observed in the transmission experiments of Burrow *et al.* near this energy.

Recommended values for the energies, widths, and classifications of Mg^- resonances are given in Table XXIII.

TABLE XXIII. Recommended energies, widths, and classifications of negative-ion resonances in magnesium. Values are from the experiments of Burrow *et al.* (Burrow and Comer, 1975; Burrow *et al.*, 1976).

Classification	Energy (eV)	Width (meV)	Comments
$3s^2\varepsilon p\ ^2P^\circ$	0.15	≈ 160	*b*
$3s^2\varepsilon d\ ^2D$	≈ 1.5	≈ 1.0	
	2.5–3.0		

3. Calcium

At least one long-lived state of Ca^- is produced copiously in Penning ion sources (Heinicke and Baumann, 1969), and for many years it was thought to be a metastable state, such as those of Be^- and Mg^-, for which autoionization is forbidden in *LS* coupling. The $4s4p^2\ ^4P$ state of Ca^- has indeed been calculated to lie below Ca $4s4p\ ^3P^\circ$ (Bunge *et al.*, 1982). However, estimates of relativistic effects by Beck (1987) indicated that the lifetime of this state should be substantially shorter than that inferred from experiment. We discuss this further in the final paragraph of this section.

Correspondingly, it was also widely believed that the $4s^24p\ ^2P^\circ$ state of Ca^- would be unbound, i.e., that Ca would support a *p*-wave shape resonance at low energy. Amusia and Cherepkov (1975) calculated phase shifts for *p*- and *d*-wave scattering by Ca in both Hartree-Fock and random-phase with exchange approximations and found low-energy shape resonances in both approximations. The calculations of Kurtz and Jordan (1981) gave shape resonances in both the static-exchange (SE) and the static-exchange-plus-polarization (SEP) approximations: the SE results gave $E=0.24$ eV, $\Gamma=0.54$ eV; the SEP approximation yielded $E=0.06$ eV, $\Gamma=0.1$ eV. Complex-coordinate self-consistent-field calculations by McCurdy *et al.* (1981) gave $E=0.225$ eV, $\Gamma=0.162$ eV; these calculations represented the Ca^- wave function by a single Slater determinant and so should give results that differ from the SE approximation due only to effects of core relaxation. On the other hand, a more recent calculation (Yuan and Zhang, 1989), in which the SE potential was supplemented by a correlation-polarization potential derived from density-functional theory, found no *p*-wave shape resonance. In a transmission experiment by Johnston and Burrow (1979) no low-energy resonance was observed. Total-cross-section measurements made by Romanyuk *et al.* (1980) using a trapped-electron method found the cross section to increase monotonically as the electron energy went to zero, and did not reveal any structure at collision energies less than 1 eV (both experiments did find higher-energy resonances, which we discuss below).

However, recent evidence, both experimental (Pegg *et al.*, 1987; Garwan *et al.*, 1990; Walter and Peterson, 1991) and theoretical (Froese Fischer *et al.*, 1987, and references in Walter and Peterson, 1991), indicates that the $4s^24p\ ^2P^\circ$ ground state of Ca^- is indeed bound, with a binding energy of less than 0.05 eV. At the time of this writing, there is a discrepancy between the two experimental values of the binding energy, which have been determined independently by photoelectron spectroscopy (Pegg *et al.*, 1987: 43 ± 7 meV) and a fit of the threshold behavior of the photodetachment cross section (Walter and Peterson, 1991: 18.4 ± 2.5 meV). In the light of this new information, it is interesting to reexamine older experiments on Ca^- from discharge sources to see whether previously unidentified features can now be understood. Photodetachment of Ca^- from a discharge source was measured by Heinicke *et al.* (1974) over the photon energy range 0.45–3.2 eV. The total photodetachment cross section was found to decrease monotonically from 0.45 eV to a minimum at 1.2 eV, and then to rise steadily, exhibiting a shoulder at 2.2 eV and, finally, a pronounced resonance-type structure at 3 eV with a width of ~0.5 eV. In the electron transmission measurements referred to earlier, Johnston and Burrow did identify two resonance features, a broad structure at an energy of 1.1 eV and a significantly sharper feature at about 2.8 eV. The lower-energy resonance was classified as a $4s^23d$ shape resonance. The calculated barrier height (Kurtz and Jordan, 1981) for such a resonance is 0.725 eV, while the SEP approximation of the same authors gives an energy of about 0.8 eV for this state. Based on correspondences with the behavior exhibited in the group-IIB metals Zn, Cd, and Hg, the higher-energy resonance has been classified (Johnston *et al.*, 1989) as the $4s4p^2\ ^2D$ state of Ca^-. They note that the correspondence with the heavier targets indicates that this state should lie close in energy to the $4s4p\ ^3P^\circ$ excited states of calcium at about 1.89 eV. That it lies significantly above this energy is interpreted by Johnston *et al.* as resulting from significant configuration interaction with the lower resonance. They substantiate this view by performing configuration-interaction calculations for the $4s^2\ 3d$ and $4s4p^2$ resonances and finding that the actual eigenstates involve nearly complete mixing of these two configurations.

They further note that since both of these resonances are accessible from the Ca^- ground state by photon excitation, they may also be present in the photodetachment cross section. Indeed, they postulate that the structure observed at around 3 eV by Heinicke *et al.* may be due to this resonance.

Walter and Peterson (1991) have very recently carried out a series of photodetachment measurements on Ca^- that confirm the existence of the bound ^2P ground state, but their measurements indicate an electron affinity of 18 ± 2 meV. These measurements also clearly show a large shape resonance at around 3 eV, which they confirm as the $4s4p^2\ ^2D$ resonance observed in the electron-scattering measurements.

A feature at about 1.7 eV was seen in the total-cross-section measurements of Romanyuk *et al.* (1980) and was attributed by them to the *d*-wave shape resonance. No other resonances were found by them in the 0–10-eV energy range. Kazakov and Khristoforov (1985) measured differential elastic cross sections and $4s4p\ ^3P^\circ$ and $4s3d\ ^3D$ excitation functions at 90°, for electron scattering by Ca vapor, in the energy range 0–7 eV. They observed a broad resonance in elastic scattering at around 1.25 eV, which is attributable to the ^2D shape resonance. They also note a relatively sharp feature at the $4s4p\ ^3P^\circ$ threshold, which is visible both in the elastic cross section and the $4s4p\ ^3P^\circ$ excitation function, and speculate that it may be due to a resonance. Their data exhibit a broad feature around 3 eV that might be associated with the

TABLE XXIV. Recommended energies, widths, and classifications for negative-ion resonances in calcium. Figures in parentheses represent the uncertainty in the least significant digit.

Classification	Energy (eV)	Width (meV)	Comments
$4s^2 4p\ ^2P^\circ$	−0.0184(25)	Stable	Walter & Peterson (1991)
$4s^2 3d$	1.1		Johnston & Burrow
$4s4p^2\ ^2D$	2.95		Photodetachment: Walter & Peterson (1991)

$4s4p^2\ ^2D$ resonance. They comment upon the existence of other structure in the cross section near the $4s5s\ ^{3,1}S$ and $4s5p\ ^3P^\circ$ thresholds, but the data shown in their paper does not lend itself to extensive interpretation.

At higher energies there is once again a series of optical excitation function measurements for excited states of calcium following electron impact. Ehlers and Gallagher (1973) measured the absolute excitation cross section for the $4p\ ^1P^\circ$ emission at 422.7 nm with an energy resolution of about 0.3 eV. The structure that they observed in both the excitation cross section and the linear polarization fraction adjacent to the threshold region for higher excited states was attributed to cascading from some of these states. The possibility that some of this structure is due to resonances cannot be discounted.

Garga *et al.* (1974) measured optical excitation functions for more than 25 excited states of calcium with an energy resolution of 1.0–1.2 eV. They observed a large amount of structure and noted the possibility that some of it may be due to the decay of temporary negative ions. Given the resolution of these experiments and the lack of detailed information concerning the observed structures, it is not wise for us to comment further upon them.

After the discovery of stable Ca^-, a metastable state of Ca^- was discovered by Hanstorp *et al.* (1989) and identified as $4s4p^2\ ^4P^\circ_{5/2}$. Both the lifetime ($290\pm100\ \mu s$) and binding energy (562 ± 5 meV with respect to $4s4p\ ^3P^\circ$) were determined.

Recommended values for the energies, widths, and classifications of Ca^- resonances are given in Table XXIV.

4. Strontium

There is little information on the spectrum of the negative strontium ion. Kaiser *et al.* (1971) found evidence for a long-lived state of Sr^- in Penning discharges. This was, at one time, thought to be a metastable state (Hotop and Lineberger, 1975) analogous to those known in Be and Mg, e.g., a $5s5p^2\ ^4P$ state. However, since the lifetimes of such metastable states are limited by relativistic autoionization, which should become more probable with increasing nuclear charge, the results of Beck (1987) for Ca would suggest that such a state would be too short-lived to be detected by these means. Several theoretical calculations, reviewed in Sec. VI.B, suggest that Sr^- has a stable bound state analogous to that of Ca^-, i.e., a $5s^2 5p\ b$ state. A long-lived state of Sr^- has recently been observed by Garwan *et al.* (1990).

Optical excitation functions have been measured with low-energy resolution by Starodub *et al.* (1973) and Aleksakhin *et al.* (1974) and with somewhat better resolution by Chen and Gallagher (1976). The former have measured excitation functions for a large number of excited states of strontium, many of which exhibit strong threshold peaks or near-threshold structure which may be due to resonances. Chen *et al.* measured the absolute excitation cross section for the $5p\ ^1P^\circ$ state of strontium with an energy resolution of 0.22 eV. They observed several features in the excitation function that are attributed to cascade contributions from higher-lying states. It is possible that a strong, sharp feature observed in both the total photon yield and in the derived linear polarization fraction at an energy of about 4.0 eV is due to resonance effects near the threshold of the $6s\ ^1S$ state at 3.793 eV, but it is not profitable to speculate any further on this.

Romanyuk *et al.* (1980) measured total cross sections for electron scattering by Sr in the energy range 0–10 eV. They saw one feature which they attributed to a resonance, at 1.2 eV. It is likely that Sr supports a *d*-wave shape resonance analogous to that of Ca, and this is the identification made by Romanyuk *et al.* No other structure is discernible in their published data.

5. Barium

The situation in barium is very similar to that outlined above, although there is even less evidence for the presence of Ba^- resonances than in the case of strontium. Once again, long-lived negative ions have been observed by Kaiser *et al.* (1971) and by Garwan *et al.* (1990), which are presumed to account for the *b* state (see Sec. VI.B). There is essentially no evidence for structures that may be interpreted as resonances either in the electron-impact-induced optical excitation functions of Aleksakhin *et al.* (1973) or in the work of Chen and Gallagher (1976). Total-cross-section measurements by Romanyuk *et al.* (1980) revealed no structures in electron scattering by Ba in the 0–10-eV energy range, in contrast to similar experiments on Ca and Sr, where low-energy *d*-wave shape resonances were observed. However, it should be noted that the strength of the Ca and Sr resonances was quite weak in these experiments, so the absence of any features in Ba is not conclusive.

H. Group-IIB elements

The group-IIB elements, Zn, Cd, and Hg, have ground configurations $(n-1)d^{10}ns^2$, and they exhibit low-energy *b* shape resonances similar to those in alkaline earth (np^6ns^2) and alkali (np^6ns) atoms. Mercury, in particu-

lar, also displays exceedingly rich resonance structure at higher energies that has been studied by a wide variety of electron collision techniques.

1. Zinc

The ground state of the zinc negative ion is formed by the addition of an electron to the $3d^{10}4s^2$ neutral ground state. This state ($3d^{10}4s^24p\ ^2P^\circ$) is not bound and has been observed in transmission measurements of the total cross section (Burrow *et al.*, 1976) at an energy of 0.49 eV. To our knowledge this is the only experimental observation of this resonance. Its position has been calculated in a semiempirical fashion by Zollweg (1969), using horizontal analysis techniques, and by Sinfailam (1981), who used a semirelativistic Dirac-Fock approach to calculate shape resonances in elastic electron scattering in a number of group-II elements. These calculations find this state at 0.67 and 0.23 eV, respectively. In the latter case the resonance position is likely to depend critically on the polarization potential, and the approximation used in this case (Pople and Schofield, 1957) may result in this potential's being overestimated (Sinfailam, 1981).

The simple barrier-height model (Kurtz and Jordan, 1981—see Sec. IV.C.1) can also be applied to estimate the energy of this p-wave shape resonance. Using the tabulated polarizability for zinc of Miller and Bederson (1977) of 47.78 a.u., we obtain an energy of 0.29 eV for the barrier height for such a configuration.

At higher energies, there have been only two observations of structure in electron-scattering cross sections that are attributed to resonances (Shpenik *et al.*, 1973; Burrow *et al.*, 1976). Shpenik *et al.* measured optical excitation functions for six levels of neutral zinc excited by electron impact. They observed, with an energy resolution of about 80 meV, 11 structures in these excitation functions, and, although they believed that one of these structures may have been due to a cascade contribution from a higher-lying state, it is most likely that many are due to resonances. Three of these features also lie above the $^2S_{1/2}$ ionization limit at 9.391 eV. Burrow *et al.*, whose transmission results extend to about 6.5 eV, observe a strong, broad structure just above the $4s4p\ ^3P^\circ$ thresholds and a cusp at the $4s4p\ ^1P^\circ$ threshold, but they make no comment on the likely classifications of these states. In addition, they observe, in each of the group-II metals that they studied, a very weak, broad structure that lies between the low-energy shape resonance and the first excited levels of the neutral atom. In zinc this feature seems to occur between 2 and 3 eV. From a survey of the levels of isoelectronic atoms, they speculate that this may be a shape resonance in the d wave ($4s^24d\ ^2D$). The height of the potential barrier associated with such a d-wave resonance (in the barrier-height model) is about 2.56 eV).

Apart from their tabulated positions, there is little information available concerning the resonances observed by Shpenik *et al.* One could to some extent be guided by isoelectronic sequences and by the extensively studied levels of Hg^- (see Sec. IV.H.3), although, in the latter case, there is a large number of resonances observed and the individual terms are well defined due to the larger spin-orbit splitting.

TABLE XXV. Recommended energies, widths, and classifications of negative-ion resonances in Zn. The figures in parentheses represent the uncertainties in the least significant digit. Except where indicated otherwise, all energies are from Shpenik *et al.* (1973).

Classification	Energy (eV)	Width (meV)	Comments
$3d^{10}4s^24p\ ^2P^\circ$	0.49		Burrow *et al.* (1976)
$3d^{10}4s^24d\ ^2D$	≈2.5		Burrow *et al.* (1976)
$3d^{10}4s4p^2$	4.36		Present classification
$3d^{10}4s5s^2$	6.0–6.4		Present classification
	7.18		
$3d^{10}4s5p^2$	7.56		Present classification
	7.80		
	8.22		
	8.33		
	8.60		
	8.80		
	10.87		
	11.27		
	11.80		

Based on the above and on the predictions of the modified Rydberg formula, we have applied tentative classifications to some of those resonances below the $^2S_{1/2}$ ionization potential. The broad feature observed at 4.36 eV in the excitation function for the $4s4p\ ^3P_1^\circ$ state is presumably due to one or more terms of the configuration $3d^{10}4s4p^2$. Although it is not tabulated by Shpenik *et al.*, there appears to be a broad, weak structure at about 6.0–6.4 eV in this same excitation function. This could be the $3d^{10}4s5s^2$ configuration which the modified Rydberg formula places at about 6.4 eV, about 0.3 eV below the center of gravity for the $4s5s$ neutral excited states. Some of the group of structures between 7.18 and 8.0 eV in the excitation function for the $4s5s\ ^3S_1$ state probably belong to the configuration $3d^{10}4s5p^2$. Such states would have even parity and could decay to the $5s\ ^3S_1$ level by emission of an s- or d-wave electron. There is not enough information to make even speculative classifications for the higher-lying structures.

Our assessments of the energies and widths of the Zn^- resonances together with their proposed classifications, where appropriate, are shown in Table XXV.

2. Cadmium

The situation in cadmium is very similar to that outlined for zinc. Once again there have been very few experimental or theoretical studies of Cd^-, and only the lowest-lying levels have been classified. The protagonists in these studies are also those who carried out the investigations in zinc.

Once again, cadmium also exhibits a low-lying shape resonance with the configuration $4d^{10}5s^25p\ ^2P^\circ$. In their transmission experiment, Burrow *et al.* find this state at 0.33 eV, in good agreement with the calculated value of 0.28 eV (Sinfailam—see above) but not with the extrapolated value of 0.78 eV (Zollweg, 1969). The barrier-height model predicts a value of 0.34 eV for the height of the p-wave potential barrier. The broad structure that Burrow *et al.* associate with a possible d-wave shape resonance occurs at about 2 eV in cadmium, which can be compared to the calculated barrier height of just over 3 eV.

The situation at higher energies in cadmium is essentially identical to that in zinc. Burrow *et al.* observe a single broad structure in the vicinity of the $5s5p\ ^3P^\circ_{0,1,2}$ thresholds, just below 4 eV. This structure also dominates the excitation function for the $5p\ ^3P^\circ_1$ state (Shpenik *et al.*, 1973; Zapesochnyĭ *et al.*, 1974), where it appears at an energy of 4.16 eV. It is most likely due to one or more resonances with the configuration $4d^{10}5s5p^2$. In addition to this feature, Burrow *et al.* also detect a cusp at the threshold of the $5p\ ^1P^\circ_1$ state at 5.417 eV, similar to the case in zinc. However, unlike the corresponding situation in zinc, Shpenik *et al.* have measured the excitation function for this state and, while it is not specified in their list of tabulated resonance values, there is clear evidence of a sharp structure at the threshold for this state which may, in fact, be a resonance. If this is so, and we stress that the uncertainty involved in assessing such spectra is considerable, it is most likely another member of the $4d^{10}5s5p^2$ configuration.

The next feature tabulated by Shpenik *et al.* is at an energy of 6.82 eV. However, once again it appears that there may be other weak structures present in the excitation function for the $5p\ ^1P^\circ_1$ state at energies of about 5.9 eV and 6.4 eV. The higher of these is a small discontinuity that is apparently coincident with the opening of the $5s6s\ ^3S_1$ channel. The lower-energy feature is a weak, broad dip in the excitation cross section that is consistent with a similar structure observed in zinc and with the predicted (modified Rydberg formula) position of the $4d^{10}5s6s^2$ resonance at 6.1 eV.

The resonances in the region of 7 eV, at 6.82, 7.24, and 7.38 eV, are observed in three of the excitation functions measured by Shpenik *et al.*, namely, those for the $5p\ ^3P^\circ_1$, $5p\ ^1P^\circ_1$, and $6s\ ^3S_1$ states. Their dominant contribution is undoubtedly to the latter state, which is consistent with a speculative classification as $4d^{10}5s6p^2$. Such a configuration is predicted by the modified Rydberg formula to occur at about 7.3 eV and could decay to the $6s\ ^3S_1$ by emission of an s- or d-wave electron, while a p- or f-wave outgoing electron is required for decay to the $5p\ ^{1,3}P^\circ_1$ states to conserve parity.

Tabulated values of the energies and widths of the Cd^- resonances together with their proposed classifications, where appropriate, are shown in Table XXVI.

TABLE XXVI. Recommended energies, widths, and classifications of negative-ion resonances in Cd. The figures in parentheses represent the uncertainties in the least significant digit. Except where indicated otherwise, all energies are from Shpenik *et al.* (1973).

Classification	Energy (eV)	Width (meV)	Comments
$4d^{10}5s^25p\ ^2P^\circ$	0.33		Burrow *et al.* (1976)
$4d^{10}5s^25d\ ^2D$	≈2.0		Burrow *et al.* (1976)
$4d^{10}5s5p^2$	4.16		Present classification
$4d^{10}5s5p^2$	5.42		"
$4d^{10}5s6s^2$	≈5.9		"
$4d^{10}5s6p^2$	6.82		"
$4d^{10}5s6p^2$	7.24		"
$4d^{10}5s6p^2$	7.38		
	7.96		
	8.19		
	8.37		
	9.38		
	11.83		
	11.99		
	12.18		

3. Mercury

A large amount of experimental and theoretical work has been devoted to the study of the negative-ion resonance spectrum of Hg. In particular, low-energy electron scattering from mercury provides an ideal situation for testing theoretical approximations in which the inclusion of relativistic effects are crucial. Resonance structure has been observed in both electron-scattering and electron swarm experiments at energies ranging from a few hundred millivolts to the $^2D_{3/2}$ ionization potential at 16.7 eV. In addition to the more conventional differential, total- (σ_T), and momentum-transfer (σ_M) cross-section measurements, a number of measurements of the polarization of the radiation emitted by various excited states have also been made. Theoretical calculations on this target include fully relativistic solutions of the Dirac equation, the inclusion of relativistic effects in various approximate means in the nonrelativistic Schrödinger equation, and the relativistic R-matrix method.

The outer electron configuration of the ground state of mercury is $5d^{10}6s^2\ ^1S_0$. The lowest-lying negative-ion state involves the attachment of an extra electron in the next available, unfilled $6p$ orbital: a standard b shape resonance. It was first predicted by Rockwood (1973), who analyzed the electron swarm data of McCutchen (1958) and derived a σ_M which exhibited a broad resonance at an energy of about 0.65 eV. The first direct experimental observation of this resonance was made by Burrow and Michejda (1974; see also Burrow *et al.*, 1976) in high-resolution electron transmission measurements. They found that this state, which they classified as $6s^26p\ ^2P^\circ_{1/2,3/2}$, occurred at an energy of 0.63 ± 0.03 eV in their spectrum, which is proportional to a measurement of the

total cross section. This resonance was observed subsequently in several cross sections derived from swarm measurements (Nakamura and Lucas, 1978a, 1978b; Elford, 1980; England and Elford, 1991) and in a total-cross-section measurement by Jost and Ohnemus (1979). However, the level of agreement between these experiments is not good. In the case of the σ_M measurements, Nakamura and Lucas place the resonance peak at 0.6 eV, while Elford and England and Elford place it at 0.5 eV and 0.44 eV, respectively. Of the latter two swarm-based measurements, the last figure is favored, as it has been derived from experiments using gas mixtures (Hg with He), which increases the accuracy of the cross-section determination at low energies. Jost and Ohnemus place this resonance at 0.4 eV in their σ_T measurement, considerably lower than the value given by Burrow and Michedja. This observation prompted Burrow and coworkers to remeasure this resonance energy, and they found a value of 0.42 ± 0.03 eV (Johnston and Burrow, 1982), in good agreement with Jost and Ohnemus. This latter value is the preferred value from Burrow's transmission measurements, although the reason for the difference is apparently not understood (Burrow, 1992).

On the theoretical side, the first calculations on this state were performed by Walker (1975), who solved the Dirac equation, including both exchange and polarization effects but with no coupling to inelastic channels. He found resonances in both the $p_{1/2}$ and $p_{3/2}$ partial waves, the former being quite sharp and located at an energy of 0.20 eV, while the latter was at a higher energy and considerably broader. The position, and, indeed, existence, of these resonances was found to be critically dependent on the approximation used, particularly for the exchange interaction. Hutt and Bransden (1974; see also Hutt, 1975) carried out a phase-shift analysis of all available low-energy scattering data, deriving phase shifts that were in reasonable agreement with Walker and that confirmed the earlier suggestion of a broad resonance in the p wave at about 0.7 eV. Prompted by the σ_M measurements of Elford, Walker performed another calculation (Sinfailam, 1980) in which he used a pseudopolarization potential with a cutoff chosen to give the best fit to the experimental cross section. The corresponding σ_T calculated from this work is not, however, in agreement with the experiment of Jost and Ohnemus. In a more recent calculation, Sinfailam (1980) found similar behavior in the low-energy elastic-scattering phase shifts to that observed by Walker. This calculation involved the use of a perturbation method applied to the solution of the nonrelativistic Schrödinger equation, with relativistic effects included in two separate models, one using the Pauli approximation and the other a second-order Dirac potential. The σ_T and σ_M calculated from these approximations give quite different results. For the total cross section, the Pauli approach results in a single, broad structure in reasonable agreement with experiment (Jost and Ohnemus, 1979), while the Dirac solution gives two resonance structures at about 0.20 and 0.45 eV. For the momentum-transfer cross section, similar differences between the calculations are also noted, and neither gives good agreement with the cross section of England and Elford. Wijesundera *et al.* (1992a), using a relativistic R-matrix treatment, found resonances in both the odd-parity $j=\frac{1}{2}$ and $j=\frac{3}{2}$ channels, at energies of 0.72 and 0.96 eV, respectively. They also performed a superposition-of-configurations calculation of nominal $6s^2 6p$ states of Hg^-, using spectroscopic orbitals from a Dirac-Fock–type calculation of excited states of Hg. The resonance energies that they quote from this calculation are 0.19 and 0.21 eV, respectively. We are uncertain how to interpret these latter energies, in that they originate from a square-integrable representation of a resonance that is unbound with respect to its parent state, and which therefore presumably depends strongly on the orbital basis employed.

In a summary of the situation with respect to the position and magnitude of this resonance, England and Elford note that a recent calculation by Walker, with an adjustable polarization potential, gives best agreement with the total cross section when the range is fixed at $4.2a_0$, and with the momentum-transfer cross section when the range is set to $4.8a_0$. In the latter case the use of the shorter range results in differences of more than 20% between the calculated and swarm cross section below 0.5 eV.

The next possible configuration for the addition of an extra electron to the neutral mercury atom is $5d^{10}\,6s6p^2$. These states may *a priori* be expected to lie in the energy region near the $5d^{10}6s6p$ neutral excited states, which extend from 4.7 to 6.7 eV. Indeed, structure observed in this region in electron-scattering cross sections was among the first experimental evidence for the existence of negative-ion resonances in atomic systems (e.g., Jongerius, 1961). Since then, the higher-lying mercury resonances have been widely studied in a comprehensive range of experiments including elastic and inelastic electron scattering with both unpolarized and polarized incident beams, inelastic excitation functions in which decay photons (and their polarizations) and metastable atoms have been detected, stepwise electron+laser photon excitation, superelastic-scattering experiments, and experiments where excitation transfer in gas mixtures is measured. This diversity of experimental approaches has, in conjunction with several comprehensive theoretical calculations, provided a unique level of agreement to be reached for the position and classification of resonances for such a complicated atomic system.

Most of the earlier work on the higher-lying Hg^- resonances, in particular the transmission experiments of Kuyatt *et al.* (1965) and the optical excitation measurements of Smit and Fijnaut (1965) and Zapesochnyĭ and Shpenik (1966), have been reviewed and summarized by Schulz (1973a). In addition to this experimental work, resonances were also observed in the optical excitation function measurements of Fedorov and Mezentsev (1965), in the metastable excitation cross sections of

Borst (1969), in the superelastic electron-scattering experiments on the $6p\,^3P^\circ_{0,1}$ states by Burrow (1967) and Korotkov (1970), and in the cross sections derived from excitation experiments on Na-Hg gas mixtures (Bogdanova and Marusin, 1971).

The first attempt at classification of the observed Hg^- states was made by Fano and Cooper (1965) in an analysis of the transmission spectra of Kuyatt *et al.* They proposed that the lowest-lying states in the vicinity of the first neutral excited levels had the configuration $5d^{10}6s6p^2$, for which there were eight possible levels: $^4P_{1/2,3/2,5/2}$, $^2D_{3/2,5/2}$, $^2P_{1/2,3/2}$, and $^2S_{1/2}$. From a comparison with the ordering of the spectrum of the isoelectronic atom Tl, they classified the lowest three states observed by Kuyatt *et al.* as the ^4P levels. The lowest of these lies below the threshold of the $6p\,^3P^\circ_0$ state (4.667 eV) and so is only observable in the elastic channel, to which it can decay, if parity and angular momentum are conserved, by the emission of an $s_{1/2}$ electron. It has been observed in several experiments, in both the total (Kuyatt *et al.*, 1965; Burrow *et al.*, 1976; Jost and Ohnemus, 1979) and differential (Düweke *et al.*, 1973, 1976; Albert *et al.*, 1977; Koch *et al.*, 1984) cross sections and with the exception of the measurements of Kuyatt *et al.* and Duweke *et al.* (1973), which appear to have incorrect energy scales, that there is uniform agreement that this resonance lies at 4.55 eV and its angular behavior in the differential cross section (Fig. 50) supports the earlier classification of $5d^{10}6s6p^2\,(^4P_{1/2})$.

The next observed resonance lies above the threshold of the $6p\,^3P^\circ_0$ state and has been observed in both elastic and inelastic electron excitation functions (Kuyatt *et al.*, 1965; Düweke *et al.*, 1973, 1976; Shpenik *et al.*, 1975; Burrow *et al.*, 1976; Albert *et al.*, 1977; Koch *et al.*, 1984) and metastable atom excitation functions (Koch *et al.*, 1984; Newman *et al.*, 1985). In particular, the latter measurement of this and many other higher-lying resonances with high resolution ($\Delta E \approx 20$ meV) in the sensitive metastable atom channel has enabled an accurate determination of the resonance energies to be made. Newman *et al.* place this resonance, which appears as a sharp peak in the $6p\,^3P^\circ_0$ excitation function (Fig. 51), at 4.702 eV, in good agreement with other recent measurements. They estimate its width to be about 18 meV. Based on earlier integral measurements and the energies of the terms of the $6s6p^2$ configuration in isoelectronic BiIII, PbII, and TlI, Heddle (1975) suggested classifications for several resonance states in Hg, and for this state, in particular, of $5d^{10}6s6p^2\,(^4P_{3/2})$. This was supported by Albert *et al.*, who calculated the energy dependence of the elastic differential cross sections in this energy region and found agreement with their own experimental data at this energy only when a resonance in the d wave was assumed. An outgoing $d_{3/2}$ wave is consistent with conservation of total angular momentum and parity for such a configuration decaying into the ground state.

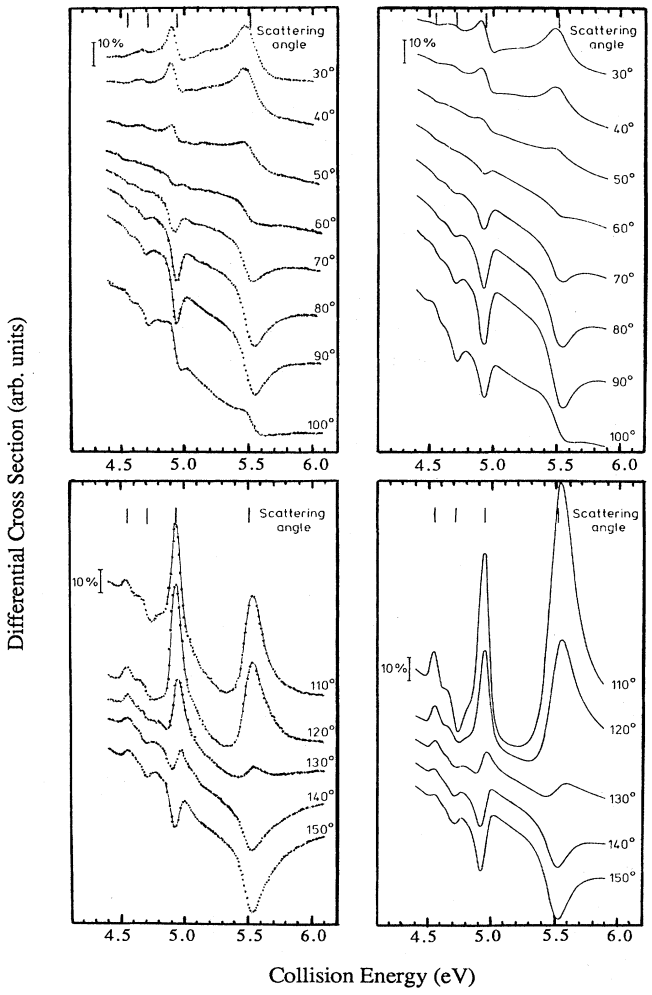

FIG. 50. Energy dependence of the differential elastic-scattering cross section for Hg at various scattering angles (from Albert *et al.*, 1977).

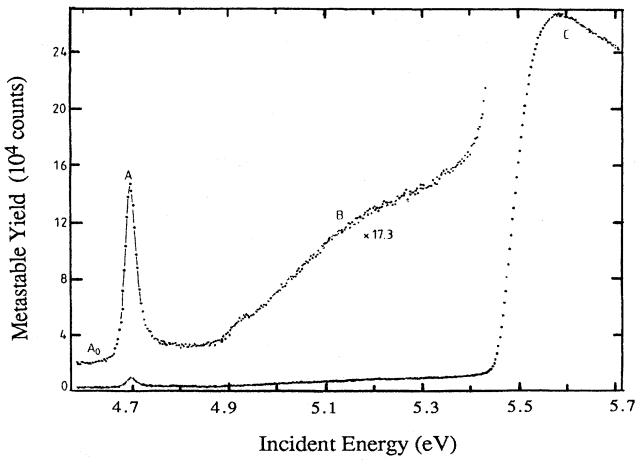

FIG. 51. Metastable atom excitation function for Hg in the energy range 4.5–5.7 eV (from Newman *et al.*, 1985).

For many years there was considerable confusion concerning the existence, energies, and classification of the remaining members of the Hg^- $6s6p^2$ configuration, in particular the structures observed in many experiments between 4.9 and 5.6 eV. The first such feature occurs in the vicinity of the threshold (4.886 eV) of the $6p\ ^3P_1^\circ$ state. That it lies above this threshold is confirmed by its observation in optical excitation functions ($\lambda = 253.7$ nm) for this state (Zapesochnyĭ and Shpenik, 1966; Ottley and Kleinpoppen, 1975; Shpenik *et al.*, 1975; Düweke *et al.*, 1976; Wolcke *et al.*, 1983). These measurements place this resonance at energies that vary between 4.90 and 4.94 eV. We favor the latter value, which is obtained, among others, from the experiment of Düweke *et al.* which involved a simultaneous measurement of the elastic differential cross section at a scattering angle of 117° (where this resonance manifests itself as a symmetric peak) and of the yield of 253.7 nm photons, with an energy resolution of about 120 meV. This is supported by the observation of a weak feature at 4.93 eV in the metastable excitation function of Newman *et al.*

Heddle (1975) classified this state as $5d^{10}6s6p^2\ (^2D_{3/2})$, but pointed out in a subsequent paper (Heddle, 1978) that this was inconsistent with the elastic-scattering measurements of Albert *et al.* These authors found that their analysis of the experimental differential cross section was consistent with a resonance in the d wave with total angular momentum $J = \frac{5}{2}$. Their classification was also consistent with the appearance of this resonance in the $6p\ ^3P_1^\circ$ state but not the $6p\ ^3P_0^\circ$ metastable level, as decay into the latter can only occur via emission of an $f_{5/2}$-wave electron, which would not be favored because of the strong centrifugal barrier. The weak manifestation of this state in the $6p\,^3P_0^\circ$ excitation function of Newman *et al.* is believed to be due to the detection, with very low efficiency, of 253.7 nm photons in their metastable atom detector. Heddle (1978) classified this state as $5d^{10}6s6p^2\ (^4P_{5/2})$.

There is further, rather unique experimental evidence to support this classification. The experiments of Albert *et al.* also involved the determination of the spin polarization of the scattered electrons as a function of energy in the resonance region. The analysis of these measurements for electron-scattering angles of 50°, 117°, and 135° (Fig. 50) is consistent with the data only if the total angular momentum of the resonance state is taken to be $\frac{5}{2}$. Wolcke *et al.* (1983) measured the Stokes parameters for the light emitted in the decay of the $6p\,^3P_1^\circ$ state following excitation by polarized electrons. Their theoretical analysis, which was a generalization of the theory of Baranger and Gerjuoy (1958) for the effects of near-threshold resonances on the polarization of emitted radiation, also revealed that the only resonance term compatible with the experimental results was $^4P_{5/2}$. It has also been demonstrated (Albert *et al.*) that the near-threshold linear polarization measurements of Ottley and Kleinpoppen are consistent with such a resonance configuration.

The next strong resonance feature which is believed to belong to this configuration occurs at an energy of 5.54 eV (Düweke *et al.*, 1976), just above the threshold for the $6p\ ^3P_2^\circ$ state at 5.461 eV. It has been observed in a host of experiments in which a variety of techniques have been used. In the high-resolution experiment of Newman *et al.* it occurs as a broad asymmetric feature, and the energy assigned in this channel is somewhat higher (5.59 eV) than that derived from the scattered-electron and decay photon experiments where it has a symmetric profile. The analysis of the elastic differential cross sections of Albert *et al.*, including the spin polarization of the scattered electrons, suggests that this resonance decays into the elastic channel by autodetachment of a $d_{5/2}$ electron. Based on this and other observations, Heddle (1978) has classified this state as $5d^{10}6s6p^2\ (^2D_{5/2})$. This would appear to be consistent with its observed strong decay into both the $6p\ ^3P_1^\circ$ and $6p\ ^3P_2^\circ$ excited states, in contrast with its weaker presence in the $6p\ ^3P_0^\circ$ state (see, for example, Shpenik *et al.*, 1975; Krause *et al.*, 1977; and Kazakov *et al.*, 1980). The former can occur by emission of $p_{3/2}$ and $p_{1/2}$ electrons, respectively, while the latter requires an $f_{5/2}$ wave for conservation of angular momentum and parity.

The main uncertainty in this energy region for some time was the existence of the remaining $^2D_{3/2}$ term. A weak, relatively sharp structure was observed at about 5.2 eV in several of the earlier experiments on the optical excitation function for the $6p\,^3P_1^\circ$ state (Zapesochnyĭ and Shpenik, 1966; Ottley and Kleinpoppen, 1975). In addition, measurements of superelastic scattering from $6p\ ^3P_1^\circ$ (Burrow, 1967) and $6p\ ^3P_0^\circ$ (Korotkov, 1970) showed evidence of a weak feature in this energy region. Krause *et al.* (1977) measured the separate electron-impact excitation functions for $6p\ ^3P_{0,2}^\circ$ by observing the forbidden radiation at 265.56 and 226.98 nm, respectively, which results from the decay of these states to the $6s^2\ ^1S_0$ ground state. These measurements were carried out with an energy resolution of about 0.25 eV and clearly showed a resonancelike maximum in the $6p\ ^3P_0^\circ$ excitation function at 5.2 eV. On analyzing these results, Heddle (1978) suggested that this feature was due to the "missing" configuration $5d^{10}6s6p\ (^2D_{3/2})$.

Subsequent experiments have only served to confirm this classification, although it would appear that this resonance has a much shorter lifetime than originally believed. It has been observed in elastic scattering (Kazakov *et al.*, 1980); in metastable atom ($6p\ ^3P_0^\circ$) excitation functions (Koch *et al.*, 1984; Newman *et al.*, 1985), where it is clearly present as a broad structure; and in an ingenious experiment by Hanne *et al.* (1985), who use a stepwise electron + laser photon technique to measure the separate $^3P_{0,2}^\circ$ excitation functions near threshold.

These experimental investigations and classifications have not, of course, continued in isolation from any theoretical input. Indeed, the extended speculation as to the nature of the resonances in the energy region below 6

eV has led to a number of calculations using the relativistic R-matrix method (Scott *et al.*, 1983; Bartschat *et al.*, 1984; Bartschat and Burke, 1986; Wijesundera *et al.*, 1992a). The first of these was specifically undertaken in an attempt to calculate elastic- and inelastic-scattering cross sections in which relativistic, exchange, and channel-coupling effects had been taken into account. The resonances revealed in the total cross sections for elastic scattering and excitation of the $6p\ ^3P^o_{0,1,2}$ states were found to be in reasonable accord with experiment with regard to both position and assignment, although there were some notable differences. Firstly, they found the lowest $^4P_{1/2}$ resonance about 0.15 eV higher than experiment, i.e., in the vicinity of the $^3P^o_0$ threshold; secondly, they found that the $^2D_{3/2}$ and ^2D resonances were essentially degenerate at 5.5 eV, from which they concluded that the weak resonance at 5.2 eV was probably an experimental artifact.

Bartschat and Burke extended these calculations by including the mass correction and Darwin terms in the relativistic Hamiltonian and the $6s^26d$ and $6p^26d$ configurations in the total wave function. The additional terms caused a slight shift in the calculated resonance positions to lower energies, but had little effect on the splittings or the overall structure of the calculated cross sections. As such, they did not change the situation regarding the bona fides of the "5.2-eV resonance." On the other hand, the inclusion of additional correlation effects had a significant effect on the resonance energies relative to the neutral target-state energies, and it changed the splitting between the various terms. In particular, the $^2D_{3/2,5/2}$ terms were no longer degenerate but appeared to be split by about 0.4 eV, in much better agreement with the experimentally determined splitting of 0.35 eV.

The approach of Bartschat and Burke (1986) utilizes a model potential to describe the interaction of valence and core electrons and treats relativistic effects on the valence electrons by perturbation theory: the many-electron wave function is an approximate solution of a Schrödinger equation with relativistic correction terms. Wijesundera *et al.* (1992a) use a relativistic R-matrix formulation based on the Dirac equation and represent the core electrons explicitly. They find resonances in all channels that would be associated with levels of the $6s6p^2$ configuration, and their results are generally in good agreement with those of Bartschat and Burke.

There have been few observations of the remaining three terms of the $6s6p^2$ configuration of Hg^-. The only assignments of these resonances have been made by Newman *et al.* (1985), who observed several weak structures between 6.3 and 8.1 eV in their metastable atom excitation function (Fig. 52). On the basis of the relative widths of these structures, the ordering of the isoelectronic series, and the predictions of the modified Rydberg formula, they assigned a sharp feature at 6.702 eV (within 2 meV of the $6p\ ^1P^o_1$ threshold) as $5d^{10}6s6p^2$ ($^2S_{1/2}$) and two broad bumps at 6.3–6.8 eV and 7.6–8.1 eV as $5d^{10}6s6p^2$ ($^2P_{1/2,3/2}$). The only other observation

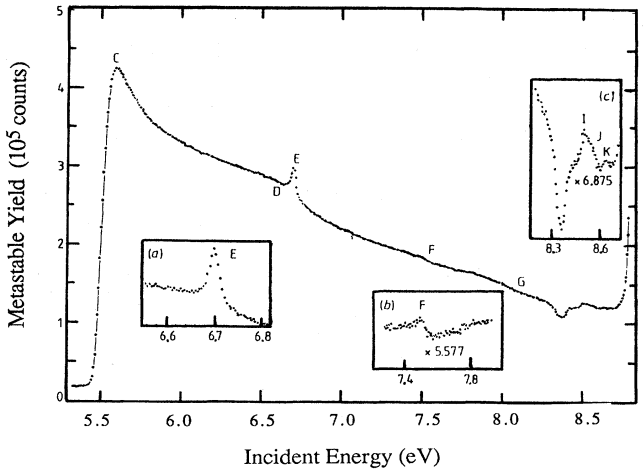

FIG. 52. Metastable atom excitation function for Hg in the energy range 5.4–8.7 eV (from Newman *et al.*, 1985).

of these states, the $^2S_{1/2}$, is in the metastable excitation function of Koch *et al.* The only theoretical evidence for these states comes from the calculation of Scott *et al.* (1983), who found a broad resonance with $J=\frac{1}{2}$ at 5.8 eV and two weak resonances at 6.7 eV with $J=\frac{1}{2}$ and $\frac{3}{2}$. Given the problems outlined above with this calculation for the lower-energy resonances, these are presumably the $^2P_{1/2}$, $^2S_{1/2}$, and $^2P_{3/2}$ resonances.

The classification of higher-lying resonances in mercury has stemmed almost exclusively from the metastable excitation functions of Newman *et al.* (1985) and Zubek and King (1987, 1990). They have observed in excess of 40 resonances in the energy region between 8.0 and 18.0 eV and have offered tentative classifications for all but a few of them, based mainly on the predictions of the modified Rydberg formula and the sequence of isoelectronic excited states. Some of these resonances have also

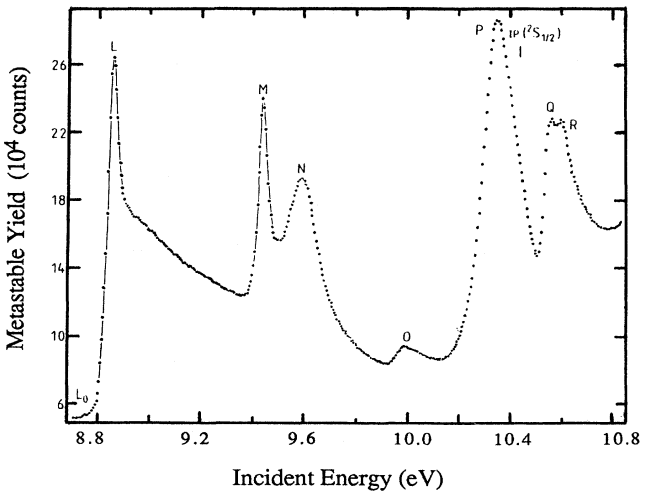

FIG. 53. Metastable atom excitation function for Hg in the energy range 8.8–10.8 eV (from Newman *et al.*, 1985).

been clearly observed by other groups (e.g., Smit and Fijnaut, 1965; Shpenik *et al.*, 1975; Jost and Ohnemus, 1979; Koch *et al.*, 1984), but there has been no other comprehensive effort towards their classification.

It is perhaps neither necessary nor appropriate for us to discuss here each of the resonances and their proposed classifications in detail. The measured energies and suggested classifications of Newman *et al.* and Zubek and King are reproduced in Table XXVII, and we shall restrict our discussion to only a few aspects of this work.

TABLE XXVII. Recommended energies, widths, and classifications of resonances in Hg^- above the first ionization potential. The energies are expressed relative to the $6s^2\,{}^1S_0$ ground state of atomic Hg. Unless otherwise specified, the energies are from Newman *et al.* (1985) and Zubek and King (1987, 1990). Figures in parentheses represent the uncertainty in the least significant digit.

Classification	Energy (eV)	Width (meV)	Comments
$5d^{10}6s^26p\ {}^2P^o_{1/2,3/2}$	0.4–0.5		Much uncertainty regarding the position of this state
$5d^{10}6s6p^2\,{}^4P_{1/2}$	4.55	≈ 1	Many observations
$5d^{10}6s6p^2\,{}^4P_{3/2}$	4.702	18	
$5d^{10}6s6p^2\,{}^4P_{5/2}$	4.94	≈ 50	Düweke *et al.*
$5d^{10}6s6p^2\,{}^2D_{3/2}$	5.20	≈ 500	Hanne *et al.* (1985; see text)
$5d^{10}6s6p^2\,{}^2D_{5/2}$	5.54	≈ 200	Düweke *et al.*
$5d^{10}6s6p^2\,{}^2P_{1/2}$	6.3–6.8		
$5d^{10}6s6p^2\,{}^2S_{1/2}$	6.702	20	
$5d^{10}6s7s^2\,{}^2S_{1/2}$	7.50		
$5d^{10}6s6p^2\,{}^2P_{3/2}$	7.6–8.1		
$5d^96s^2(^2D_{3/2})6p^2$	8.367		
	8.508		
$5d^{10}6s7p^2$	8.560		
	8.650		
$5d^96s^2(^2D_{5/2})6p^2$	8.854		
$5d^96s^2(^2D_{5/2})6p^2$	9.439		
$5d^96s^2(^2D_{5/2})6p^2$	9.593		
	9.988		
$5d^96s^2(^2D_{5/2})6p^2$	10.356		
$5d^96s^26p^2$	10.612		
$5d^96s^26p^2$	10.90		
$5d^96s^26p^2$	11.05		
$5d^96s^26p^2$	11.3–11.5		
$5d^96s^26p^2$	11.788		
$5d^96s^26p^2$	12.095		
$5d^96s^2(^2D_{5/2})7p^2$	12.852		
$5d^96s^2(^2D_{5/2})7p^2$	12.989		
$5d^96s^2(^2D_{5/2})7p^2$	13.041		
$5d^96s^2(^2D_{5/2})7p^2$	13.190		
$5d^96s^2(^2D_{5/2})7p^2$	13.325		
$5d^96s^2(^2D_{5/2})8s8p$	13.575		
$5d^96s^2(^2D_{5/2})8s8p$	13.625		
	13.718		
$5d^96s^2(^2D_{5/2})8p^2$	13.881		
$5d^96s^2(^2D_{5/2})8p^2$	13.944		
$5d^96s^2(^2D_{5/2})9s9p$	14.034		
$5d^96s^2(^2D_{5/2})9s9p$	14.135		
$5d^96s^2(^2D_{5/2})9p^2$	14.284		
$5d^96s^2(^2D_{5/2})10p^2$	14.450		
	14.7		
$5d^96s^2(^2D_{3/2})7p^2$	14.869		
$5d^96s^2(^2D_{3/2})7p^2$	15.014		
$5d^96s^2(^2D_{3/2})8s8p$	15.444		
	15.574		
	15.656		
$5d^96s^2(^2D_{3/2})8p^2$	15.80		
$5d^96s^2(^2D_{3/2})9p^2$	16.155		
$5d^96s^2(^2D_{3/2})10p^2$	16.29		
	16.57		
	17.16		

Between the threshold for the $5d^9 6s^2\ (^2D_{5/2})6p\ ^3D_3^\circ$ metastable state at 8.79 eV and the $^2S_{1/2}$ ionization potential at 10.438 eV, Newman *et al.* observe several strong resonances that dominate the metastable excitation function (Fig. 53). They interpret this strong presence as suggesting the resonances are decaying principally via the newly opened metastable channel rather than via the lower $6p\ ^3P_{0,2}^\circ$ states, and that they are thus most likely to be core-excited states having the dominant external configuration $5d^9 6s^2\ nln'l'$, with the most appropriate configuration for this energy region being $5d^9 6s^2 6p^2$. In classifying these levels, they use a *jj*-coupling scheme, which was successfully applied to the classification of the isoelectronic atom Tl (Connerade *et al.*, 1976). In particular, they select five configurations (from a possible 28) which, on the basis of the nature of their ion core and the way in which they can be formed from the ground state of neutral Hg, are likely to be the most probable sources of resonances in this region. One of these lies below the threshold for the $^3D_3$ state, and the other four are assigned to the four prominent structures at 8.854, 9.439, 9.593, and 10.356 eV. These states are summarized in Table XXVII.

There is some controversy concerning the classification of resonance structure observed in the metastable atom excitation functions above the $^2S_{1/2}$ ionization potential. Newman *et al.* postulated the existence of a further metastable level of Hg at an energy of about 10.54 eV. This was further investigated by Zubek and King, who used an energy-selective metastable atom detector to separate contributions from various metastable levels of Hg. They supported this observation and the classification of this state as $5d^9 6s^2\ (^2D_{3/2})6p_{1/2}\ (J=2)$, based on the theoretical calculations of Martin *et al.* (1972) and on the fact that it is the lowest energy state based on the $^2D_{3/2}$ ion core, and part of its metastability may arise from the need for the ion core to change during decay. Based on experimental parameters, they estimate a lower limit for its lifetime to be 200 μs. Cowan *et al.* (1988) have questioned the classification (but not the existence) of such a state in this region. While that in itself is of little consequence to this review, it may bear upon some of the classifications made by Zubek and King (1987) of resonances that lie above this state and appear to decay strongly into it. They tentatively assign five resonance structures between 10.5 and 12.2 eV to various terms of the configuration $5d^9 6s^2\ (^2D_{3/2})6p^2$ based, to a certain extent, on the notion that a favored resonance decay path is one that preserves the nature of the ion core. Based on *ab initio* calculations of the lifetime of this state against both radiative decay and autoionization, Cowan *et al.* argue that it cannot be the proposed metastable state. They propose an alternative configuration, $5d^9 6s^2(^2D_{5/2})6p_{3/2}\ (J=3)$, which, if correct, may have obvious ramifications on the proposed angular momenta of the resonance states by Zubek and King, although the external electron configurations are most likely correct.

This and other uncertainties in the spectrum of both Hg and its negative ion have been investigated further by Zubek and King (1990) in a comprehensive series of high-resolution electron-scattering measurements. They have carried out near-threshold studies of several high-lying excited states of Hg by detecting both scattered electrons and selected metastable atoms. The presence of several structures which had previously been classified by Newman *et al.* as $5d^9 6s^2 6p^2$, at energies of 8.854 and 9.953 eV, in the excitation functions for the $5d^9 6s^2 6p$ state at a scattering angle of 90°, contrary to the expectations of the decay of these states by emission of a *p*- or *f*-wave electron, led them to speculate that these resonances may have some 6*d* character. However, the strong resonance observed in metastable atom spectra at 10.356 eV, also classified by Newman *et al.* as $6s^2 6p^2$, is not present in the 90° electron-scattering spectra, thus supporting the earlier classification. They also observed a slightly different energy position and width for the resonance observed at 8.854 eV by Newman *et al.*, indicating that there may, in fact, be two sharp structures in this region.

In addition to these resonance studies, Zubek and King (1990) have also further investigated the high-lying metastable state they proposed in their earlier work. Their new experiments support the classification of Cowan *et al.* for this state.

An enormous amount of resonance structure is observed in the spectrum of Newman *et al.* above 12.5 eV, and these authors have made a valiant effort to classify these states. However, the situation is extremely complicated as this is also the autoionization region above the $^2S_{1/2}$, $^2D_{5/2}$, and $^2D_{3/2}$ ionization potentials at 10.437, 14.84, and 16.705 eV, respectively. Nonetheless, they have used the MRF, information on isoelectronic sequences, and the known ion core splittings to aid in presenting tentative assignments for most of the observed features.

Our assessments of the energies and widths of the Hg^- resonances together with their proposed classifications, where appropriate, are shown in Table XXVII.

I. Miscellaneous

There are several elements for which observations of resonances are quite limited, yet of sufficient interest to be noted.

1. Carbon

C^- is one of the few negative ions to possess a bound excited state. The ground state of C^- is $2p^3\ ^4S^\circ$, which is bound with respect to the $2p^2\ ^3P$ ground state of C by 1.27 eV; the C^- $2p^3\ ^2D^\circ$ term is also bound by 35 meV (Hotop and Lineberger, 1975). The third term of the $2p^3$ configuration, $^2P^\circ$, is not bound, but it is expected to occur as a resonance. Its energy may be estimated in several ways. First of all, in the simplest single-

configuration approximation, the ratio of term intervals is given by (Slater, 1960)

$$[2p^3\,{}^2P^\circ - 2p^3\,{}^2D^\circ]/[2p^3\,{}^2D^\circ - 2p^3\,{}^4S^\circ]$$
$$= (6/25)F^2(2p,2p)/(9/25)F^2(2p,2p)$$
$$= 2/3\ .$$

This would put the $2p^3\,{}^2P^\circ$ state at 0.79 eV above the $2p^2\,{}^3P$ ground state of C. The accuracy of this estimate is somewhat limited. In the case of the isoelectronic ground configuration of neutral nitrogen, the observed ratio of term intervals is 0.500 (Moore, 1975), vs the predicted 2/3. If the value 0.5 is thus adopted for this ratio, the $^2P^\circ$ resonance would occur at 0.62 eV above the ground state of C. These energies are in reasonable agreement with the results of accurate calculations (see below), which suggests that the $2p^3$ states of C^- are reasonably well described by a single configuration.

Alternatively, the $^2P^\circ$ state might be viewed as a $2p^2 2\bar{p}$ resonance, in which a $2\bar{p}$ electron is attached to a specific parent term of the C $2p^2$ configuration. This type of description is certainly appropriate to a variety of low-energy shape resonances, such as the *b* and *c* states discussed elsewhere in this paper. The $C^-\ {}^2D^\circ - {}^4S^\circ$ interval is comparable in energy to the C $^1D - {}^3P$ term separation of 1.26 eV (Moore, 1970). Thus the binding energy of C^- $^4S^\circ$ to its unique parent state C ^3P is comparable to the binding energy of $C^-\ {}^2D^\circ$ to the C ^1D parent state. Supposing that all terms of the ground configuration of C have approximately the same electron affinity of 1.27 eV, an assumption that is reasonable for the above-mentioned shape resonances, then the $C^-\ {}^2P^\circ$ resonance (built upon the C ^1S parent term) is placed at 1.41 eV above the C ^3P ground state. This is much higher than reliable calculated values, which suggests that the $2p^3$ description is indeed more appropriate.

At the present time there appear to be no experimental data on the $C^-\ {}^2P^\circ$ resonance. We are unaware of any electron-scattering experiments on atomic C; autodetachment spectra from C^--He collisions (Lee and Edwards, 1975) do not extend to sufficiently low electron energies, and analysis of measurements of vuv radiation from CO_2 plasmas (D'yachkov *et al.*, 1978) has not included the photoattachment continuum that would be associated with this resonance. *Ab initio* calculations have been performed in several approximations. The close-coupling method (Henry *et al.*, 1969; Thomas *et al.*, 1974), including only the states of the ground configuration of C, yields resonances in both $^2D^\circ$ and $^2P^\circ$ channels. The $^2D^\circ$ resonance becomes bound when interaction with other target configurations is included, as in the later matrix variational or Bethe-Goldstone (BG) calculations of Thomas and Nesbet (1975b; see also Nesbet, 1977) and in the polarized pseudostate (PS) approximation of Le Dourneuf (1976, 1978; Le Dourneuf, Vo Ky Lan, and Burke, 1977). The $^2P^\circ$ resonance is manifested as a rapid increase in the *p*-wave phase shift δ_p which, as for many low-energy resonances, does not develop fully through π radians. Thus the cited "energy" of the resonance refers to the energy *E* (above C ^3P) at which the total cross section attains its maximum, and the width Γ is determined by the maximum value of $d\delta_p/dE$. The energy $E = 0.57$ eV given by the PS method is presumably more reliable than the value of 0.46 eV obtained in the BG approach, since the PS approximation gives excellent agreement with the experimental values of electron affinities of $2p^n$ states of C, N, and O. The width of the resonance is computed to be 0.233 eV.

A resonance in the ^4P channel is found to occur at about 6 eV in both BG and PS calculations and is attributed to the $2s2p^4\,{}^4P$ state of C^-. This resonance lies about 1.2 eV above the $2s2p^3\,{}^5S^\circ$ state of C and can autodetach to either the $^5S^\circ$ state or the ^3P ground state. The PS calculations have been performed at higher energies and have found resonances associated with the other terms of the $2s2p^4$ configuration: ^2D at 9.5 eV, ^2S at 11.6 eV, and ^2P at 12.7 eV. The only autodetaching line observed in the C^--He collision spectra (Lee and Edwards, 1975) is at 7.44 ± 0.07 eV, which does not match any energy expected from these resonances to within 0.5 eV. The identification of this line is discussed below. D'yachkov *et al.* (1978) have observed an emission line at 235 nm (with a width of 4 nm) in a stabilized arc run in argon mixed with CO_2. They propose that this line could be due to a $2s2p^4 \rightarrow 2s^2 2p^3$ radiative transition in C^-, with an oscillator strength *f* in the range $0.7 < f < 2$. The magnitude of this oscillator strength would seem to preclude any intercombination transition between these configurations. For this line to be associated with the $^4P \rightarrow {}^4S^\circ$ transition, the ^4P state would have to be located at 4 eV above the ground state of C, which is 2 eV below the calculated position. A common error of this magnitude in the two independent calculations seems unlikely. Transitions originating from the higher resonances of the $2s2p^4$ configuration at the calculated energies are also too energetic to correspond to this emission line. Thus the identification proposed by D'yachkov *et al.* is not consistent with the results of electron-scattering calculations.

Recent calculations by Johnson *et al.* (1987) have used the target orbitals of Le Dourneuf and Vo Ky Lan (1977a) in a relativistic *R*-matrix treatment of low-energy $e + C$ collisions. Particular attention was paid to the cross sections for transitions between fine-structure levels of the ground state, which is of interest in some astrophysical applications. These fine-structure levels are explicitly represented in the calculation by the method of Scott and Taylor (1982). The $2s^2 2p^3\,{}^2P^\circ$ and $2s2p^4\ {}^4P$ resonances are found at energies of 0.57 and 6.1 eV, respectively. All expected fine-structure levels of the resonances are reported. The resonance energies are independent of *J* to the accuracy reported; however, the widths exhibit variation as large as 20% in the ^4P term. The results of this computation emphasize again the difficulty of obtaining accurate energies for $2p^q$ states: the binding energies computed for the bound $2p^3\ {}^4S^\circ$ and $^2D^\circ$ states

of C^- are too large by 0.29 and 0.08 eV, respectively.

No e^-+C scattering calculations have been reported that include target states of the type $2s^p2p^qnl$ with $n \geq 3$. Bound-state calculations have been performed for resonances associated with $2p3s$, $2p3p$, and $2p4s$ configurations by Matese (1974) and Clark (1986). The calculations of Matese utilized six nl orbitals ($3s, 4s, 5s, 3p, 4p, 3d$) that were optimized with respect to the energies of the C $2pnl$ parent states, and expanded the resonance wave function in states of the form $2pnln'l'$. A Feshbach resonance was recorded if the computed C^- energy was less than the calculated energy of an appropriate parent state. Four such resonances were found. The calculation of Clark treated only the lowest of these; it employed the MCHF procedure including $3s$, $4s$, $3p$, and $3d$ orbitals that were optimized self-consistently with respect to the resonance energy. The resonances are listed below in terms of the dominant configuration in the expansion, the appropriate parent state, and the corresponding electron affinity (E.A.) of the parent state:

Resonance	Parent state	E.A. (eV)	E (eV)	Reference
$2p3s^2\,^2P^\circ$	$2p3s\,^3P^\circ$	0.416	7.07	Matese (1974)
		0.432	7.05	Clark (1986)
$2p3s3p\,^4D$	$2p3s\,^3P^\circ$	0.023	7.45	Matese (1974)
$2p3p^2\,^4D^\circ$	$2p3p\,^3D$	0.045	8.59	Matese (1974)
$2p4s^2\,^2P^\circ$	$2p4s\,^3P^\circ$	0.201	9.48	Matese (1974)

The $2p3s^2$ resonance is a classical a feature, as shown in Clark (1986). No experimental observation of this state is known. Selection rules in LS coupling would prevent it from autodetaching to the ground state of C. Lee and Edwards (1975) observed a single autodetaching feature in $C^-(^4S^\circ)$-He collisions at an energy of 7.44 ± 0.07 eV. Spin conservation indicates that the resonance should be a quartet state. They identified the resonance with the ^4D state calculated by Matese, based on the agreement of experimental and computed energies. However, it should be noted that the magnitude of the computed electron affinity is probably smaller than the uncertainty in the calculation, which derives from neglect of core relaxation and polarization effects, and incomplete treatment of correlation among the outer two electrons. Note that the attachment energy of the $2p3s^2\,^2P^\circ$ state calculated by Clark is larger than that of Matese by 0.016 eV, and it reflects a more comprehensive account of the outer pair correlations. Thus, at the level of approximation used by Matese, one cannot be certain whether the $2p3s3p\,^4D$ state is actually bound with respect to $2p3s\,^3P^\circ$, or whether it is the only state of the $2p3s3p$ configuration that is bound. We believe that the calculations of Matese indicate that the $2p3s$ configuration of C is able to support b shape resonances of the type encountered in the noble gases and alkalis, i.e., states described by $2p(3s\varepsilon p\,^3P^\circ)$. As in neon, the differences in the energies of states associated with alternative couplings of the outer $^3P^\circ$ electron pair to the $^2P^\circ$ core are probably of the same order as the widths of the resonances. Thus it is conceivable that the feature observed by Lee and Edwards is a blend of the three quartet states associated with the b resonance configuration $2p(3s\varepsilon p\,^3P^\circ)$.

The energies and widths of the C^- resonances, together with their proposed classifications, where appropriate, are shown in Table XXVIII.

2. Nitrogen

Hund's rules predict the lowest state of N^- to be $2p^4\,^3P$. There exist a number of older estimates of the electron affinity of N $2p^3\,^4S^\circ$, based on semiempirical methods, which give values ranging between -0.56 and $+0.54$ eV (Glockler, 1934; Bates and Moiseiwitsch, 1955; Kaufman, 1963; Clementi and McClean, 1964; Crossley, 1964). Isoelectronic extrapolations of binding energies by Edlén (1960), which gave good estimates of the affinities of C, O, and F, predict an electron affinity of N $2p^3\,^4S^\circ$ of 0.05 eV. Such a small value is at the margins of accuracy of such extrapolations. Fairly extensive configuration-interaction calculations by Schaefer *et al.* (Schaefer and Harris, 1968; Schaefer *et al.*, 1969) predicted N^- $2p^4\,^3P$ to lie 0.213 eV above N $2p^3\,^4S^\circ$. As will be

TABLE XXVIII. Recommended energies, widths, and classifications for negative-ion resonances in carbon. Energies are expressed relative to the $2p^2\,^3P_0$ state of C. The sole experimental value (b) is from Lee and Edwards (1975). Figures in parentheses represent the uncertainty in the least significant digit.

Classification	Energy (eV)	Width (meV)	Comments
			Calculated values:
$2s^22p^3\,^2P^\circ$	0.57	440	Johnson *et al.* (1987)
	0.46	233	Thomas and Nesbet (1975b); see also Le Dourneuf (1976)
$2s2p^4\,^4P$	6.1	390 ($^4P_{1/2}$)	Johnson *et al.* (1987)
		310 ($^4P_{3/2}$)	
		370 ($^4P_{5/2}$)	
$2p(^2P^\circ)3s3p(^3P^\circ)$	7.44(7)		b: Quartet states, possibly unresolved L

discussed below, subsequent scattering calculations give results in roughly the same range. There is greater agreement among various theoretical estimates of the energies of the N^- $2p^4$ ^1D, ^1S terms. These are usually estimated to be bound, respectively, to the $^2D^\circ$ and $^2P^\circ$ states of N by at least 0.5 eV (Hotop and Lineberger, 1975). If this be so, these terms will be metastable against autodetachment: the $2p^3$ $^4S^\circ$ εl continuum can have only quintet or triplet spin, so in LS coupling neither the ^1D nor the ^1S state can autodetach in the N $2p^3$ $^4S^\circ$ channel; and $2p^3$ $^2D^\circ$ εl cannot couple to a state of overall ^1S symmetry.

No stable negative ion of nitrogen has been observed, although metastable states have been detected in mass spectrometry of electron-impact dissociation of N_2 (Hiraoka *et al.*, 1977) and in dissociative collisions of N_2, NO, and NO^- with Ar (Heber *et al.*, 1988). These metastable states have not been spectroscopically identified and are generally assumed to be the N^- $2p^4$ ^1D and ^1S states; their lifetimes are in excess of 1 μsec. Analysis of continuum radiation from nitrogen plasmas (D'yachkov *et al.*, 1973, 1978) does not seem to give specific information on states of N^-. Numerous scattering calculations have suggested that the $2p^4$ ^3P state is, in fact, a low-energy resonance (Burke *et al.*, 1974; Berrington, Burke, and Robb, 1975; Le Dourneuf, Vo Ky Lan, and Burke, 1977; Nesbet, 1977; Le Dourneuf, 1978) at an energy between 0 and 0.2 eV above N $^4S^\circ$. Some preliminary $e+N$ scattering measurements, which apparently have not been published in detail, showed an increase in the cross section at low energies that might be due to a resonance (Miller *et al.*, 1970). However, the most striking evidence for the ^3P resonance comes from electron-energy-loss spectroscopy of N_2 and NO (Mazeau *et al.*, 1978; Spence and Burrow, 1979; Allan, 1989). The experiment of Mazeau *et al.* utilized an electron-impact spectrometer with an electrostatic energy analyzer to measure the angular differential cross section for electron-energy-loss spectroscopy with fixed final-state electron energy E_f. A broad peak was observed (Fig. 54) near the dissociation energy of N_2, which is attributed to the process

$$e+N_2(^1\Sigma_g^+)\rightarrow N_2^-(^2\Pi_u)\rightarrow N(^4S^\circ)+N^-(^3P)$$

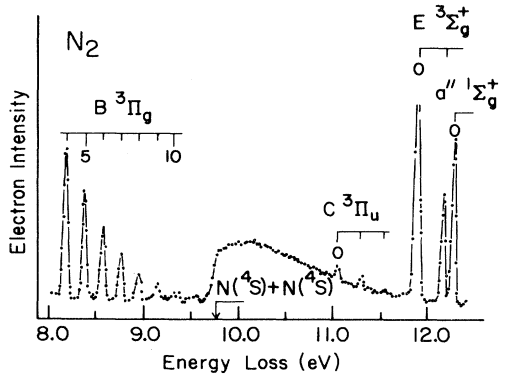

FIG. 54. Electron-energy-loss spectrum for N_2 (from Mazeau *et al.*, 1978).

followed by

$$N^-(^3P)\rightarrow N(^4S^\circ)+e\ .$$

It is important to note that this mechanism, in which the N^- resonance decays by autodetachment *after* the dissociation of the molecule, should give an electron-energy spectrum that is independent of the initial electron energy E_i (except for a factor determining the overall yield). This is consistent with the experimental observations. A low-energy continuum was also observed in electron scattering by NO near the dissociation limit, though it is more complicated due to the presence of inelastic molecular excitations. Spence and Burrow (1979) used the trapped-electron method (see Sec. III) to measure the total cross section for electron-energy-loss spectroscopy with fixed E_f in $e+N_2$ collisions. They found a similar low-energy continuum peak. Both groups determined the energy of the resonance from the variation of the signal as a function of E_f. Mazeau *et al.* give a value of $E(N^-\ ^3P)-E(N\ ^4S^\circ)=70\pm20$ meV. Spence and Burrow, whose apparatus had a somewhat lower energy resolution, cite an energy between 0.065 and 0.090 eV, in agreement with that of Mazeau *et al.* The width of the resonance was determined by Mazeau *et al.* to be 16 ± 5 meV by assuming a Gaussian response function for their electron-energy analyzer (with a width of 20 meV as determined from a sharp excitation function) and a Lorentzian distribution of autodetaching electrons. These results have been confirmed by measurements with somewhat higher resolution by Allan (1989).

The experimental values of the energy and width of the $N^-(^3P)$ resonance agree quite well with the values $E=62$ meV, $\Gamma=13$ meV calculated by Burke *et al.* (1974). These calculations, similar to those for carbon as described above, applied the R-matrix technique to systems including up to six target states. The most extensive of these calculations included all terms of the $1s^22s^22p^3$ ground configuration (with a limited treatment of configuration interaction); of the $1s^22s2p^4$ ^4P and ^2P pseudostates constructed to give a good value of the static polarizability of the ground state; and of the $1s^22p^5$ state. However, it is not clear that this calculation is fully converged with respect to the target representation. A subsequent similar calculation by Berrington, Burke, and Robb (1975) included eight target states in a single-configuration representation (the six noted above plus two additional $2s2p^4$ states) and found the N^- ^3P state to lie 0.07 eV below N $^4S^\circ$. However, the representation of the N^- state in terms of coupled-channel wave functions accounts for electron correlation that is not present in the single-configuration description of the N target states. Configuration interaction could easily lower the energy of N $^4S^\circ$ by 0.07 eV, thus making N^- ^3P unbound. An extensive study of $e+N$ scattering at various levels of approximation is reported in the thesis of Le Dourneuf (1976; see also Le Dourneuf and Vo Ky Lan, 1977b and Le Dourneuf, 1978). Although the better calculations reported there always find the N^- ^3P state to lie within 0.1

eV of N $^4S^\circ$, they are not conclusive as regards the relative position of the two states. It thus appears that computations give results for the resonance parameters that are consistent with the experimental values, but that they have not converged to the point where detailed comparison of theory and experiment is meaningful.

We are not aware of calculations that have treated the effects of fine structure in the N^- ^3P state. These may need to be considered in evaluating the experimental data. A simple calculation (present work) of the fine structure of N^- $2p^4$ ^3P, using the standard ζ parameter as computed from Hartree-Fock orbitals, gives relative energies of 0, 9.4, and 14 meV for the $J=2$, 1, and 0 states, respectively. It is difficult to estimate the error in this approach, but it agrees to within 1 meV with the experimental values for isoelectronic O $2p^4$ ^3P. The total-energy spread of fine-structure components is thus likely to be comparable to the measured width of the resonance, which leaves open the possibility that the true width is somewhat smaller than the apparent one.

Calculations of resonances associated with the N^- $2s2p^5$ configuration have been reported by Berrington, Burke, and Robb (1975) and Le Dourneuf (1976). In both cases the N^- $2s2p^5$ $^3P^\circ$ state is found to lie very close to N $2s2p^4$ ^4P (which is a bound state of N), and N^- $2s2p^5$ $^1P^\circ$ occurs near N $2s2p^4$ ^2D (an autoionizing state). Neither of these calculations includes target states of the type $2s^22p^2nl$ with $n>2$. Two of these states ($2s^22p^23s$ $^{2,4}P$) lie below N $2s2p^4$ ^4P, and an infinite number lie below N $2s2p^4$ ^2D. It is not known how their inclusion would affect the results. These channels may be only weakly coupled to those in which the resonances are found, since the autodetaching transition $2s2p^4 \rightarrow 2s^22p^2nl\varepsilon l'$ involves three electrons. We give in Table XXIX the values of the resonance parameters given by the most extensive calculations reported by Le Dourneuf. Berrington *et al.* do not state numerical values, but their figures show the resonances to be located at the same energy (within their width) as their respective parent states. Both groups also report a very broad resonance ($\Gamma\sim 6$ eV) associated with the N^- $1s^22p^6$ ^1S state, at an energy of about 30 eV.

The only report of an N^- resonance associated with a $2p^2nl$ parent state appears to be a MCHF calculation of N^- $2p^2(^3P)3s^2$ (Clark, 1986). This is found to be an *a* resonance similar to others that occur in the sequence $2p^q3s^2$. We have undertaken similar calculations in the present work for the two other *a* resonances expected to be associated with the ^1D and ^1S terms of the N^+ grandparent core. As in all MCHF calculations, continuum channels are excluded, with unknown consequences. However, similar calculations for oxygen (noted above) give reasonable agreement with the available experimental data.

Apart from the above-mentioned work of Miller *et al.* (1970), the only $e+N$ scattering experiment reported appears to be that of Neynaber *et al.* (1963). This experiment showed no resonance features in the total cross section for incident energies between 2 and 10 eV, but it probably did not have the sensitivity to detect resonances with widths of less than ~ 0.3 eV. The N^- system therefore remains relatively unexplored by experiment. The energies and widths of the N^- resonances, together with their proposed classifications, where appropriate, are shown in Table XXIX.

TABLE XXIX. Recommended energies, widths, and classifications for negative-ion resonances in nitrogen. Energies are expressed relative to the $2p^3$ $^4S^\circ$ state of N. Figures in parentheses represent the uncertainty in the least significant digit.

Classification	Energy (eV)	Width (meV)	Comments
$2p^4(^3P)$	0.070(20)	16(5)	Mazeau *et al.* (1978),
"	0.065–0.090		Spence and Burrow (1979). Fine structure estimated at ~ 10 meV

3. Lead

Atomic Pb has the ground configuration $5d^{10}6s^26p^2$, and so Pb^- may exhibit valence resonances similar to those of C^- and Hg^-. The ground state of Pb^- is known to be $6p^3$ $^4S^\circ$ (Feigerle *et al.*, 1981), which is bound by 365 meV with respect to Pb $6p^2$ $^3P_0$. It was thought at one time that the $6p^3$ $^2D^\circ_{3/2}$ state of Pb^- might also be bound (see discussion by Hotop and Lineberger, 1985), but the experiment of Feigerle *et al.* appears to rule this out. One may therefore expect resonances associated with the two higher terms of the ground configuration.

Bartschat (1985) has performed a calculation of $e+$Pb scattering using the *R*-matrix method with the inclusion of spin-orbit interaction. The calculation includes the five states of the Pb ground configuration, represented by single-configuration wave functions in intermediate coupling. Apparent resonance structures are found in the energy variation of the eigenphase sums for all channels that would be associated with the several terms of the Pb^- $6p^3$ configuration: one such structure for $J=1/2$, odd parity ($^2P^\circ$); three for $J=3/2$, odd ($^4S^\circ$, $^2D^\circ$, and $^2P^\circ$); and one for $J=5/2$, odd ($^2D^\circ$). However, the lowest of these, the $^4S^\circ$ resonance, occurs at about 0.7 eV above Pb $6p^2$ $^3P_0$, whereas experiment places it 0.365 eV below. An error of this magnitude could be due to neglect of $6s6p^3$ target states: for example, in the calculation of C^- $2p^3$ $^4S^\circ$, Le Dourneuf and Vo Ky Lan (1977a) found that the binding energy increased by 0.8 eV when the analogous $2s2p^3$ states were included. If these states are absent from the representation of the target wave function, the scattering electron will not experience the proper long-range polarization potential. As in the case of C^-, it might be that the intervals between the several Pb^- $6p^3$ resonances are, nevertheless, given fairly accurately by a calculation of this type. If this is so, the $^2D^\circ$ resonances would be expected at about 0.26 eV above

Pb $6p^2\,{}^3P_0$. The $^2P^\circ$ features are exceedingly weak in this calculation, giving mere inflections of the eigenphase sums rather than sharp increases (note also that according to the usual convention, the eigenphase sum for $J=1/2$, odd parity should tend to zero at low energy, rather than the value π indicated by Bartschat).

Wijesundera *et al.* (1992b) have performed relativistic R-matrix calculations, based on the Dirac equation, for $e+$Pb scattering. They find resonances associated with all levels of the $6p^3$ configuration, including a $^4S^0_{3/2}$ resonance at 0.22 eV above the ground state.

Electron-scattering experiments have yielded only limited information on resonances of Pb^-. Aleksakhin *et al.* (1979) have measured electron-impact excitation functions for optical emission from states of the $6p6d$, $6p7s$, and $6p7d$ configurations. The energy spread of the electron beam in this experiment was relatively large, ~ 1 eV, and the excitation functions were not corrected for cascade contributions. Resonance features at approximately 8 eV collision energy are evident in several emission lines originating from the $6p6d$ and $6p7s$ configurations. It is possible that these derive from b-type shape resonances built on those parent configurations, e.g., $6p7s\varepsilon p$, although the energy of the resonance with respect to the parent state would be a bit high (~ 2 eV). Another resonance is seen in several emission lines at around 10 eV. No classification of these features has been proposed by Aleksakhin *et al.* A study of spin-polarization effects in elastic electron scattering by Hg, Tl, Pb, and Bi atoms (the sequence $Z=80-83$) has been reported recently by Kaussen *et al.* (1987). Although the focus of this work was not on resonance spectroscopy, known resonance features of Hg were used to calibrate the collision energy, and a search was made for resonances in the other atoms in order to investigate specifically their effects on electron-spin polarization. This was done by detecting electrons scattered elastically through 100°. Kaussen *et al.* state that no resonance features were found in atoms other than Hg in the energy range 6–12 eV.

4. Thallium

The ground state of the negative thallium ion ($6p^2\,{}^3P$) is believed to be bound with an electron affinity of 0.3 ± 0.2 eV, as measured in laser photodetachment experiments (Feldman *et al.*, 1973; Hotop and Lineberger, 1975). There is little experimental evidence for higher-lying, unbound states of this ion, although several low-resolution electron-scattering experiments indicate structure that may be indicative of one or more temporary negative-ion resonances.

These experiments have consisted of the measurement of absolute optical excitation functions for the $7s\,{}^2S_{1/2}$ and $6d\,{}^2D_{3/2,5/2}$ levels of thallium following electron impact (Shimon *et al.*, 1972; Zapesochnyĭ *et al.*, 1973; Chen and Gallagher, 1977). While the energy resolution in these experiments was typically no better than 0.3 eV, there are definite indications of structure in the excitation functions, particularly near the peak in the cross section for the $6d\,{}^2D_{5/2}$ state (Chen and Gallagher) and in the $np\,{}^2P$ series ($n=8-13$, Shimon *et al.*). Chen and Gallagher discuss the possibility that some of the structures they observed may be due to resonances, but do not attempt any classification.

TABLE XXX. Recommended energies, widths, and classifications for negative-ion resonances in thallium. Energies are expressed relative to the $6p\,{}^2P^\circ_{1/2}$ ground state and are from the calculations of Bartschat and Scott (1984).

Classification	Energy (eV)	Width (meV)	Comments
$6p7p\,{}^3P$	0–0.3 eV		Relativistic calculation
$6p6d$	0.3–1.3		
$6p^2\,{}^1S$	≈ 1.1		
$6p7p\,{}^1S$	1.5		
$7s^2\,{}^1S$	2.861	≈ 5	
$7p^2\,{}^3P$	4.07		
$7p\,6d$	4.2–4.6		
$7p^2\,{}^1S$	4.3		
$6d^2\,{}^3P$	5.0		

Prompted by the spin-polarization measurements of the Munster group for heavy metal targets. Bartschat and Scott (1984) have calculated low-energy (0–5 eV) cross sections for electron scattering by Tl in both the relativistic and nonrelativistic R-matrix formalism. These calculations reveal a wealth of resonance structure, usually closely associated in energy with excited states of neutral thallium. The energies of these structures and their proposed classifications are summarized in Table XXX. We note that a number of these features exist near the threshold of the $7s\,{}^2S_{1/2}$ state (3.283 eV) and may be responsible for the experimentally observed, steep, near-threshold rise of this cross section (Chen and Gallagher). It is also interesting to note that, although the structure exhibited in the theoretical excitation cross section for the $7s\,{}^2S_{1/2}$ state is more pronounced than the experimental result, the absolute magnitudes of the two cross sections are similar, and some of the shape differences may be explained by the experimental energy resolution.

In a recent experiment, Kaussen *et al.* (1987) measured the spin polarization of electrons elastically scattered from thallium in the energy region from 6 to 12 eV with a particular emphasis on the influence of resonances. They found no effects that they could attribute to resonances, although the energy resolution in these experiments was only about 0.5 eV.

The energies and widths of the Tl^- resonances, together with their proposed classifications, where appropriate, are shown in Table XXX.

5. Copper

The ground $3d^{10}4s^2\,{}^1S$ state of Cu^- is bound with an electron affinity of 1.226 eV (Hotop *et al.*, 1973; Hotop

and Lineberger, 1975). To our knowledge, at the time of writing, there have been no experiments, either photodetachment or electron scattering, aimed at revealing structure due to resonances in Cu^-. The only information on such states comes from a number of calculations (Scheibner *et al.*, 1987; Scheibner and Hazi, 1988) using the nonrelativistic R-matrix technique.

Scheibner *et al.* calculated low-energy (0–8 eV) electron-scattering cross sections of relevance to the kinetics of the copper-vapor laser discharge. Specifically, they calculated total elastic-scattering cross sections and total excitation cross sections for the $3d^{10}4p$ and $3d^94s^2$ excited states of copper, which are the upper and lower lasing levels, respectively. They used the wave functions of Msezane and Henry (1986), which include coupling between the ground ^2S state and the $3d^{10}4p$, $3d^94s^2$, and $3d^{10}4d$ excited states, as their target wave function and treated the scattering process in the R-matrix approach. They found a wealth of resonance structure in each of the elastic and excitation cross sections. The dominant structure in the elastic channel is a low-energy shape resonance at about 0.3 eV, which they classified as $3d^{10}4s4p\ ^3P^\circ$ and which appears to be a typical b resonance. The barrier-height model of Kurtz and Jordan predicts a value of 0.33 eV for this state. Other resonances are found at 0.5 eV ($3d^{10}4s4p\ ^1P^\circ$), $\approx$2.0 eV ($3d^{10}4s4d\ ^1D$), 2.3 eV ($3d^94s^24p\ ^{1,3}P^\circ$), 3.5 eV ($3d^{10}4p^2\ ^1D$), and 4.2 eV ($3d^{10}4p4d\ ^3F^\circ$).

These resonances, particularly the $3d^{10}4s4p$, $3d^94s^24p\ ^{1,3}P^\circ$, and $3d^{10}4p^2\ ^1D + 3d^{10}4p4d\ ^3F^\circ$, significantly enhance the cross sections for low-energy elastic scattering and excitation of the $3d^94s^2$ and $3d^{10}4p$ states, respectively. Indeed, the $^{1,3}P^\circ$ resonances increase the value of the calculated near-threshold cross section for the $3d^94s^2$ state by an order of magnitude over previous estimates, a result that may have implications for the modeling of copper-vapor lasers.

Scheibner and Hazi (1988, 1989) have also calculated cross sections for photodetachment of Cu^- between 1.0 and 5.5 eV and find evidence for resonances of ^1P character which can be excited from the $Cu^-\ ^1S$ ground state by photoabsorption. In particular the total photodetachment cross section shows a strong resonance at about 1.9 eV due to the $3d^{10}4s4p\ ^1P^\circ$ shape resonance and a weak structure at about 4.25 eV due to the $3d^94s^24p\ ^1P^\circ$ shape resonance. They note that the more dominant of these two structures, that at 1.9 eV, should be easily accessible in a laser photodetachment experiment at around 660 nm. Whilst the lack of experimental effort in copper, both for electron scattering and laser photodetachment, is perhaps understandable given the experimental difficulties involved in producing controlled copper vapour beams, it is clear that further experiments in both areas would be desirable.

6. Aluminum, gallium, and indium

Once again there has been very little experimental work with these group-IIB atoms and, to our knowledge, no theoretical calculations. Shimon and co-workers have measured optical excitation functions for several $4s$ and $3d$ levels of aluminum (Shimon, Nepiĭpov, and Zapesochnyĭ, 1975), for a large number of *ns*, *np*, and *nd* excited states of gallium (Shimon, Nepiĭpov, Golodovsky, and Golovchak, 1975), and for 17 *ns*, *np*, and *nd* ($n = 5,6,7$) spectral lines in indium (Shimon and Nepiĭpov, 1974). The excitation functions for many of these levels show structures that are probably due to negative-ion resonances, although no discussion is given. It is not possible to give accurate energies for any of these possible negative-ion states.

V. RESONANCE STATES OF DOUBLY CHARGED NEGATIVE IONS

There has long been an interest in the existence, or otherwise, of short-lived excited states of multiply charged negative ions. The initial impetus for this interest came from the experimental studies of Walton *et al.* (1971) on electron detachment of the negative hydrogen ion. They measured the absolute electron-impact detachment cross section of H^- from threshold (0.75 eV) to 30 eV and found a large structure in the detachment cross section at about 14.2 eV. They offered no firm explanation for this structure, which had a typical resonance profile and which represented a variation in the cross section of more than 30%. They did speculate that it might be a H^{2-} resonance or a feature associated with the opening of the double detachment threshold at 14.35 eV.

Following these experiments, Taylor and Thomas (1972), using the stabilization method, found evidence for a resonance with a dominant configuration $2s^2\ 2p$ at an energy of 14.8 eV, and indications of a further stabilization point at higher energies.

In a subsequent series of experiments in the same apparatus, but under experimental conditions specifically designed to improve the signal to background and test for experimental artifacts, Peart and Dolder (1973) confirmed the earlier observation of the structure at 14.2 eV and found evidence for an additional resonance at even higher energies, 17.2 eV above the H^- ground state. Both experiments were conducted using a merged electron-H^- ion-beam apparatus, although for the second the intersection angle of the two beams was reduced from 20° to 10° in order to increase the interaction path length and provide kinematically more favorable operating conditions for the electron source.

This observation prompted a closer investigation by Thomas (1974) of the earlier stabilization calculation. He found that the wave function for the higher-energy structure was predominantly (60%) $(2p)^3$ and that stabilization occurred at 17.26 eV, in good agreement with the experiment.

The experimental observations of these structures are indeed very persuasive, a consequence both of their size with respect to the background detachment cross section

and of the independence of their occurrence on the energies of the incident merged beams. The large, lower-energy structure could be associated with the breakup threshold at 14.35 eV. There is particular interest in the higher feature, as its occurrence would apparently violate a theorem due to Simon (1973), which indicates that resonances cannot exist at energies greater than the threshold for total breakup of the system. Some mechanisms that might reconcile the experimental data with Simon's theorem have been put forward by Nuttall (1979). However, to the extent that a stabilization calculation is to be viewed as an approximation to the resonance wave function, the results of Taylor and Thomas do appear to violate the theorem, and they may thus have to be discounted. To our knowledge, there have been no other theoretical calculations that have revealed these features, nor has any subsequent experiment been reported.

The possibility of doubly charged negative-ion resonances has also been raised in the case of oxygen by the experiments of Peart *et al.* (1979a, 1979b). Electron-impact detachment cross sections of C^- and O^- were measured in a crossed-beam apparatus for incident electron energies between ~ 5 and 40 eV. Two structures were observed in the detachment cross section of O^-, at electron energies of 19.5 and 26.5 eV: they appear as dips of about 10% of the total cross section (which is $\sim 6\times 10^{-16}$ cm^2), with widths of the order of 2 eV. The size of the features is greater than, but comparable to, the statistical fluctuations in the experimental data. We are not aware of theoretical investigations of these structures, nor of subsequent experimental work. Hofmann *et al.* (1989) made some rough estimates of the energy of a hypothetical O^{2-} $2s^2 2p^6$ resonance that could be responsible for electron-stimulated desorption of O from metal surfaces; they gave a somewhat lower energy of ~ 10 eV. A Hartree-Fock calculation of the energy of O^{2-} by Clementi and McLean (1964) gave an energy of 8.3 eV above O^-, which correlation effects were estimated to reduce to about 6 eV. Subsequent Hartree-Fock calculations by Prat (1972), Huzinaga and Hart-Davis (1973), and Delgado-Barrio and Prat (1975) reduced these energies by 1 eV or so. Although this approximation is unrealistic in forcing all $2p$ electrons to occupy the same orbital, and probably has a larger error than when applied to singly charged negative ions, the results suggest that the O^{2-} $2s^2 2p^6$ resonance would not lie near the features observed by Peart *et al.*

VI. SYSTEMATIC VARIATION OF RESONANCE PROPERTIES AMONG THE ELEMENTS

At present, only hydrogen and the noble gases exhibit *series* of resonances that are sufficiently long to admit classification in terms of *channel* quantum numbers analogous to those that describe Rydberg series of neutral atoms and positive ions. Moreover, it is not particularly useful to view a negative-ion resonance of a given spectroscopic configuration as the first member of an *isoelectronic* sequence (e.g., Ne^- $2p^5 3s^2$, Na^{**} $2p^5 3s^2$, Mg^+ $2p^5 3s^2, \ldots$), since the properties of subsequent members are largely governed by the long-range Coulomb potential. Thus, in trying to place the properties of negative-ion resonances in some broader context, we are more or less restricted to take a view along *isoionic* sequences (e.g., Na^- $2p^6 3s^2$, Ne^- $2p^5 3s^2$, F^- $2p^4 3s^2, \ldots$). Such sequences typically involve significant variation of the grandparent and parent configurations. Although this makes it difficult to make unique associations of resonances in different elements, it is nevertheless possible to draw some qualitative conclusions regarding systematic behavior.

We shall discuss the analysis of *a*, *b*, and *c* features along these lines; it will be seen that these features display a remarkable degree of commonality between elements, which can be interpreted in terms of a two-electron complex weakly bound to a positive-ion core. The resonance level structures in these cases closely track those of their parent or grandparent states.

A more detailed isoionic correspondence can be made between the $1s\,nln'l'$ resonances of He^- and the $nln'l'$ resonances of H^-, in terms of the $(KT)^A$ coupling scheme. A detailed elucidation of this correspondence has been made by Watanabe and Le Dourneuf (1990). It is successful because of the compact nature of the $1s$ orbital of He^+, which provides highly effective screening of one unit of nuclear charge, and otherwise interacts with outer electrons (to lowest order) via a spherically symmetric exchange interaction which is fairly weak due to the small overlap of the excited electrons with the core. Helium resonances are distinct in this regard from those of the heavier noble gases below the ionization limit. In the heavier noble gases, the grandparent ion states are separated by energies that are comparable to the characteristic binding energies of resonances. In addition, the $np^5\ ^2P^\circ_{3/2}$ grandparent core state possesses a permanent electric quadrupole moment, whose associated long-range interaction can mix the orbital angular momentum of the outer electrons. It may be noted that, except for S states, the spectrum of singly excited He is very similar to that of H, if viewed from the ionization limit: the largest quantum defect of $1s\,nl$ states with $l\neq 0$ is ~ 0.07, and the largest term splitting is ~ 0.25 eV. Thus, to the extent that the spectrum of excited He looks like a "replicated" hydrogen spectrum, it is reasonable to suppose that the doubly excited spectra of the negative ions will be similar. It is conceivable that the spectrum of Li^- would also fit this general pattern, and a qualitative similarity between adiabatic potential curves for H^- and Li^- has been noted by Lin (1983c). It seems likely that the $(KT)^A$ scheme will be less applicable to the categorization of the resonances of heavier atoms, for which the structure of parent and grandparent states plays a dominant role.

The last part of this section describes briefly some regularities in broad shape resonances observed in the total

cross sections for electron scattering by the noble gases. The main scientific value of this discussion is the association of these resonances with the phenomenon of "shell collapse" in neutral atoms and positive ions, in which the d and f orbitals undergo a transition from Rydberg to valence character.

A. The *a* resonances

The a features occur prominently in systems with tightly bound, open-shell residual ion cores, such as the halogens and the noble gases. The most striking characteristic of these states is the degree to which their energies reflect the structure of the core: in Ne^- and Ar^-, for example, the splitting of the a pair is identical, to within experimental uncertainty, to the fine-structure splitting of the $np^5\ ^2P^\circ$ core; for Kr the two intervals differ by about 20%. These results were of great historical importance in motivating the "grandparent model" description and for validating the spectroscopic identification of these resonances as an $ns^2\ ^1S$ electron pair bound to the core: the fine structure of such a resonance should simply reflect that of the residual core. It turns out that the properties of the a resonances depend only weakly on the residual core, so that it is appropriate to view them as members of a family which contains the ground states of the alkali negative ions.

The spectroscopic designation $ns^2\ ^1S$ evokes a picture of two equivalent electrons outside a positively charged core, but this is a simplistic description. We recall that the simplest negative-ion state, the ground state of H^-, is called $1s^2$ for convenience; but it takes only 0.75 eV to remove the first electron from H^-, and 13.6 eV to remove the second. This great disparity in binding energies is reflected in the charge distribution that can be determined by accurate calculations; the ground state is seen to be more accurately characterized by $1s'1s''$, where $1s'$ is similar to the $1s$ orbital of H, and $1s''$ is very diffuse. A similar picture applies to the alkali negative ions. Figure 55(a) shows the valence probability distribution of the valence electron of Na $3s$, as computed in the HF approximation, and the two electrons of Na^- "$3s^2$", as computed in a four-state MCHF approximation that is discussed below; Fig. 55(b) shows the difference of these distributions. The additional electron in Na^- is distributed about the periphery of the ground state of Na and does not appreciably affect the probability distribution near the $2p^6$ core.

Another manifestation of this phenomenon is seen in Figs. 56(a)–56(d), which show a sequence of MCHF results for the nominally isoelectronic ground states of Na^- and Mg. These calculations use wave-function expansions of the form

$$\Psi = 1s^2 2s^2 2p^6 \sum_k a_k \phi_k^2 \tag{39}$$

with the orbitals ϕ_k introduced in the order indicated on the figure. Thus the two-state calculation involves self-consistent determination of the amplitudes and orbitals associated with $3s^2$ and $3p^2$ configurations that share a common Ne-like core; the three-state, the same for $3s^2$, $3p^2$, $3d^2$; and so on up to the 12 configurations indicated. The electron affinity (resp., ionization potential) is determined from the difference between the total energy of the state and the Hartree-Fock energy of Na (resp., Mg^+) $1s^2 2s^2 2p^6 3s$. The interaction of the valence electrons with the core is treated at the mean-field level in both the $3s$ and $3s^2$ states, and, as can be seen from the results, correlation between the two valence electrons is pretty much accounted for; thus the principal error in the binding energies should derive from correlation between the core and valence electrons. As indicated in the figures, this residual error is of the order of a few meV for Na^-, and 100 meV for Mg. This is consistent with the view of the second valence electron in Na^- being very diffuse and thus having a much weaker interaction with the core

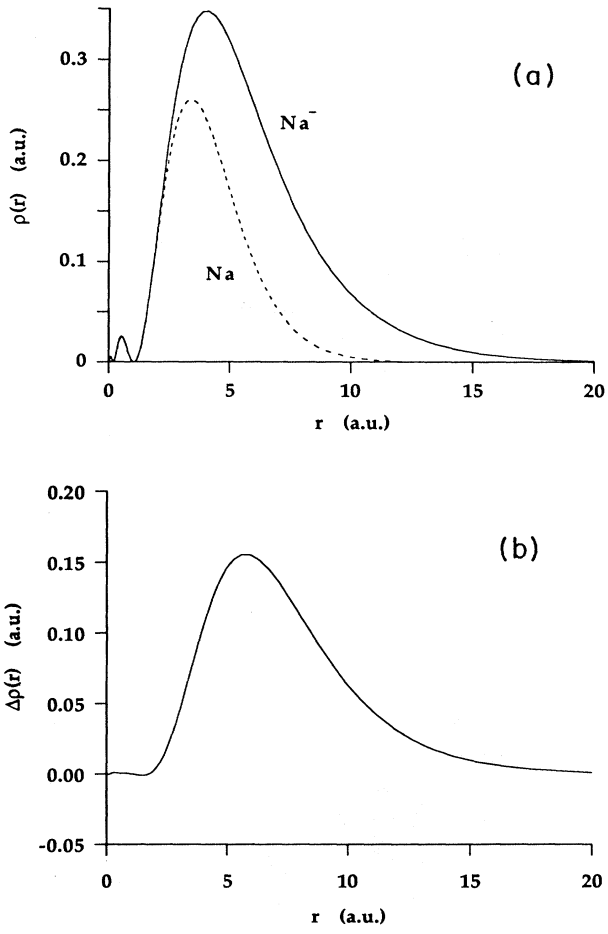

FIG. 55. Comparison of calculated charge densities for Na and Na^-: (a) Charge densities as computed in the Hartree-Fock and MCHF approximations (present work); contributions from the Ne-like core, which are nearly identical in both cases, are neglected. (b) The difference $\rho(Na^-) - \rho(Na)$ of the two curves in (a).

than its counterpart in Mg. Calculations by this method of the electron affinities of the other alkalis give similar results; i.e., they are much more accurate than would be estimated from the errors in the ionization potentials of their isoelectronic counterparts. A similar observation presumably applies to calculations of the bound b states of the alkaline earths, discussed in Sec. VI.B; these have yielded electron affinities of 40 meV or less, a value which would lie within the range of error for calculations of a neutral species, but which may very well be more accurate because of the diffuse nature of the orbitals involved.

We shall now show that it is natural to view the a resonances, which are encountered in the noble gases, halogens, and other miscellaneous systems, as members of a family that is exemplified by the ground state of the nearest alkali negative ion. Figure 57 shows the amplitudes of the principal configurations that result from MCHF calculations, analogous to those described in the preceding paragraph, for resonances in C^- through Na^- with the nominal classification $1s^2 2s^2 2p^q 3s^2$. The computed binding energies of these resonances (with respect to the appropriate $2p^q 3s$ parent state) are in reasonable accord with known experimental data, as is discussed in the separate element-specific sections of this paper. The associated charge distributions are found to be similar to those depicted in Fig. 55, except that there is a regular contraction of the outer orbitals with increasing atomic number.

It is thus evident that, at this level of description, the a resonances of this isoionic sequence have essentially the same configurational composition as that of the ground state of Na^-. As they are found to be relatively insensitive to the nature of the residual ion core, which varies significantly within this sequence, it is appropriate to visualize them as a characteristic two-electron complex bound by the Coulomb field of the core. On the surface, this is a confirmation of the grandparent description of these resonances. Note, however, that in light of Fig. 55, these states can also be plausibly described in terms of an excess electron loosely attached to a parent state of the neutral atom. Thus a suitable coupling scheme for these resonances is expressed by the grandparent model, but their dynamics reflect some influence of the parent state. This will be seen to be the case for the b resonances as well.

The basic composition of the a resonances also does not vary greatly along the noble-gas column of the periodic table. Table XXXI shows the makeup of the a

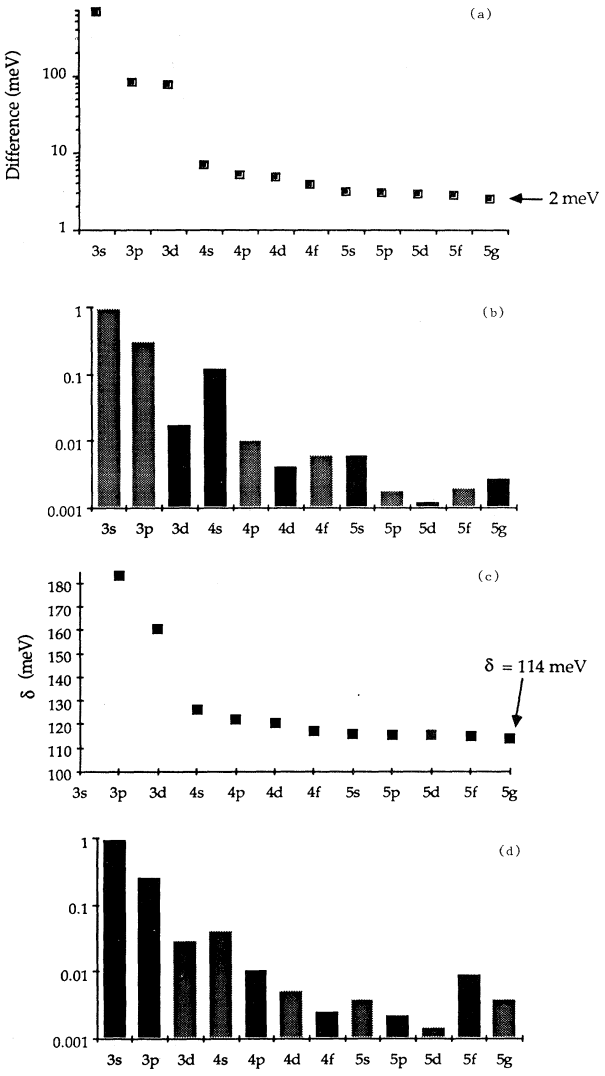

FIG. 56. Comparison of calculations for Na and Mg: (a) Electron affinity of the ground state of Na vs number of states in the MCHF expansion. (b) Amplitudes of the $(nl)^2$ configurations in the 12-state MCHF calculation of the ground state of Na^-, on logarithmic scales. Relative sign of the amplitude is indicated by shading. (c) Ionization potential of the ground state of Mg, as in (a). (d) Expansion of the ground state of Mg, as in (b).

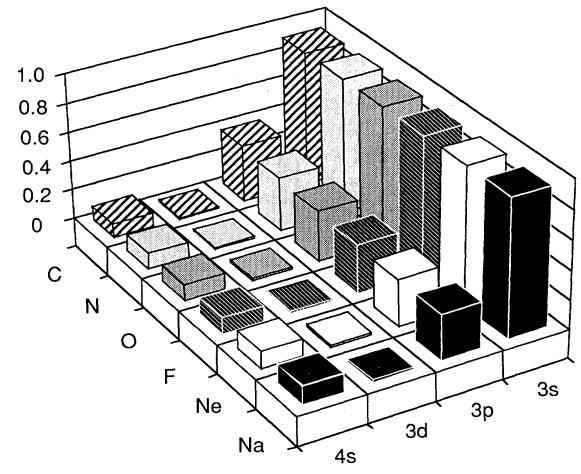

FIG. 57. Amplitudes of leading configurations in MCHF calculations for the a resonances of C^- through Ne^-, and the ground state of Na^-, with the dominant configuration being $1s^2 2s^2 2p^q 3s^2$. Only the ground term of the $2p^q$ grandparent configuration is included in each case; however, similar results are obtained for all terms of this configuration.

TABLE XXXI. Amplitudes of configurations obtained in nonrelativistic MCHF calculations of a resonances of Kr^- and Xe^-. n = principal quantum number of p-shell vacancy; $n_q = n + q$.

State	Kr^- ($n=4$)	Xe^- ($n=5$)
$np^5n_1s^2$	0.924	0.913
$np^5n_1p^2(^1S)$	0.347	0.362
$np^5n_2s^2$	−0.106	−0.097
$np^5nd(^3P^\circ)n_1s$	0.086	0.128
$np^5nd(^1P^\circ)n_1s$	0.008	0.007
$np^5n_1sn_2s(^3S)$	0.062	0.063
$np^5n_1p^2(^3P)$	−0.015	−0.018
$np^5n_1p^2(^1D)$	0.049	0.068
$np^5nd^2(^1S)$	−0.019	−0.020
$np^5nd^2(^3P)$	−0.001	−0.0003
$np^5nd^2(^1D)$	−0.002	−0.004

resonances of Kr^- and Xe^-, as computed at the same level of approximation as those described above. The energy (eV) of a_1 above the ground state in each case is

	Kr^-	Xe^-
Experimental	9.472	7.878
Calculated	9.484	7.900

Some systematic variations do appear in this description, such as the increased importance of the p^5sd configuration for the heavier atoms.

In Table XXXII we show the binding energies of experimentally known a states of the alkalis, noble gases, and halogens, as referred to the appropriate parent state of highest multiplicity (the $^2P^\circ_{3/2}$ and ^1D grandparent core states for the heavy noble gases and halogens, respectively, are exhibited because these are the only two that are known unambiguously for all elements of the family; however, similar results are obtained for other grandparent states where they are known). Although the ground state of H^- is somewhat different from the other a states, particularly with respect to having a lower degree of angular correlation, we have included it for purposes of general reference. The $2s^2$ states of H^- and He^- are usually classified in terms of the $(K,T)^A$ scheme or its equivalents (Watanabe, 1982; Lin, 1986), but we believe they fit the general pattern for a resonances as well.

TABLE XXXII. Binding energies (in meV) of a states of alkalis, noble gases, and halogens, expressed relative to the appropriate parent states of highest multiplicity (from experimental values cited in the tables of Sec. IV and Moore, 1971).

H^- $1s^2\,^1S$ 0.7542		
Li^- $1s^22s^2\,^1S$ 0.618	He^- $1s2s^2(^1S)$ 0.651	H^- $2s^2\,^1S$ 0.643
Na^- $2p^63s^2\,^1S$ 0.548	Ne^- $2p^5(^2P^\circ_{3/2})3s^2(^1S)$ 0.527	F^- $2p^4(^1D)3s^2(^1S)$ 0.516
K^- $3p^64s^2\,^1S$ 0.501	Ar^- $3p^5(^2P^\circ_{3/2})4s^2(^1S)$ 0.478	Cl^- $3p^4(^1D)4s^2(^1S)$ 0.459
Rb^- $4p^65s^2\,^1S$ 0.486	Kr^- $4p^5(^2P^\circ_{3/2})5s^2(^1S)$ 0.470	Br^- $4p^4(^1D)5s^2(^1S)$ 0.560
Cs^- $5p^66s^2\,^1S$ 0.472	Xe^- $5p^5(^2P^\circ_{3/2})6s^2(^1S)$ 0.455	I^- $5p^4(^1D)6s^2(^1S)$ 0.440

Effects of configuration interaction with the continuum, which have been neglected so far in this discussion, exhibit no real regularity among diverse elements, as they are highly sensitive to the positions of thresholds and the number of open channels. For example, the experimentally determined widths of the lowest a resonance in the heavy noble gases (a_1, associated with the $^2P^\circ_{3/2}$ state of the core) vary by an order of magnitude between Ne^- and Xe^-, but always lie below the first excitation threshold of the neutral atom and are thus fairly narrow ($\Gamma < 10$ meV). The a_2 resonance, in contrast, lies below the first threshold in Ne^- and Ar^-, but crosses over it in Kr^-, where it exhibits a significant branching ratio for decay into excited states of Kr. In Xe^-, a_2 apparently interacts so strongly with the Xe* $5p^5(^2P^\circ_{3/2})6s[2,1]$ channels that it is difficult to discern clearly in most experiments. Of the halogens, only Cl^- is known to have all the a resonances that would be associated with alternative states of the grandparent core, though this may be due to the limited volume of experimental information rather than to any fundamental reason. Evidence for a states outside the alkalis, noble gases, and halogens is sporadic.

B. The *b* resonances

The b resonances are prominent features in electron scattering by the noble gases, lying just above the lowest (a) resonances. Read *et al.* (1976) gave them the spectroscopic classification $np^5[(n+1)s\,(n+1)p\,^3P^\circ]$, based on the fact that the $np^5(n+1)s^2$ states were accounted for by the a resonances, and that $^3P^\circ$ external coupling should give a lower energy than $^1P^\circ$. This assignment is consistent with results of calculations for electron scattering by Ne (Noro *et al.*, 1979; Clark and Taylor, 1982) and by Ar (Ojha *et al.*, 1982); we are not aware of calculations for Kr or Xe. These resonances appear particularly strongly in various excitation spectra of the $np^5(n+1)s$ configuration (e.g., metastable atom yield, ultraviolet photon yield, and differential electron excitation functions). This shows that they have a significant branching ratio for autodetachment into states of this configuration, and so they might be regarded as shape resonances built upon such states. This view was taken by Clark and Buckman (1987), who demonstrated a strong correspondence between the b resonance in Ne^- and the low-energy p-wave shape resonances in Na^- and Mg^-. We believe that a number of resonances in other elements fit this general pattern and have accordingly designated them b states. Similar to the case of the a resonances, it seems that most states of neutral atoms with

one or two electrons in a valence s orbital (i.e., effective quantum number $n^* \sim 2$) are able to support p-wave shape resonances. The existence of such a resonance depends upon the coupling between the s and p electrons, but this existence apparently is not sensitive to the nature of the residual ion core. However, the actual resonance energy does not depend upon the residual core, and, in fact, in heavier atoms, it appears that some of the b resonances actually become bound with respect to their parent states.

We review briefly the arguments of Clark and Buckman (1987) regarding the correspondence between the b resonances of Ne^- and Na^-. As discussed in Sec. IV.C.1, the existence of a shape resonance in the $3s\varepsilon p\ ^3P^\circ$ channel of Na^- is well established. Phase shifts for both $^3P^\circ$ (crosses) and $^1P^\circ$ (squares) $3s\varepsilon p$ channels of Na^-, as computed by Sinfailam and Nesbet (1973), are depicted in Fig. 58; the $^3P^\circ$ phase shift exhibits the characteristic behavior of a near-threshold resonance. We now think of electron scattering by Ne* $2p^5 3s$ as being analogous to electron scattering by Na $2p^6 3s$. The thin lines in this figure depict the three eigenphases for electron scattering by Ne in overall ^2S symmetry at collision energies below the $2p^5 3p$ thresholds [the three open channels are $2p^6\varepsilon s$, $2p^5 3s(^3P^\circ)\varepsilon' p$, $2p^5 3s(^1P^\circ)\varepsilon'' p$]. One of these eigenphases exhibits a resonance near the Ne $2p^5 3s(^3P^\circ)$ threshold and tracks the $Na^-\ ^3P^\circ$ phase shift fairly closely; another follows the $Na^-\ ^1P^\circ$ phase shift; the third belongs to a predominantly $2p^6\varepsilon s$ channel that has no counterpart in the Na^- system. We thus see that the two scattering eigenchannels for Ne^- that are associated with the $2p^5 3s$ target states are characterized by essentially the same dynamics as $^3P^\circ$ and $^1P^\circ$, eigenchannels of Na^-, and they should thus be labeled $2p^5(3s\varepsilon p\ ^{3,1}P^\circ)\ ^2S$. This coupling scheme was inferred directly by Clark and Taylor (1982) from an analysis of the eigenvectors of the scattering matrix. The b resonance of Ne^- apparently has the same origin as the low-energy resonance of Na^-, which is universally regarded as a straightforward shape resonance in the $^3P^\circ$ channel. This interpretation is strengthened by viewing the p-wave phase shifts for electron scattering by Mg, which appear as a thick line on Fig. 58. This resonance involves *three* electrons in the valence shall (i.e., $3s^2\varepsilon p$), rather than two as for Ne^- and Na^-, yet it has a similar character. The correspondence between the $3s\varepsilon p\ ^3P^\circ$ state of Na^- and the $3s^2\varepsilon p\ ^2P^\circ$ state of Mg^- can perhaps be understood at the Hartree-Fock level, in that the $3s$-εp exchange potential has the same (attractive) coefficient for these two terms, whereas $3s\varepsilon p$ $^1P^\circ$ coupling is characterized by a repulsive exchange interaction (Clark and Buckman, 1987). As we have discussed in Secs. IV.C and IV.G, the energies of the Na^- and Mg^- b resonances are comparable to the height of the barrier structure created by the repulsive centrifugal potential and the attractive potential due to polarization of the target atom by the incident electron. Since the Ne $2p^5 3s$ states have polarizabilities comparable to that of Na $2p^6 3s$, the same argument applies. The absence of a resonance in the $^1P^\circ$ channel, which would have long-range interactions identical to those in the $^3P^\circ$ channel, presumably is due to the repulsive exchange interaction at short range, which does not support a standing wave inside the barrier. A recent paper by Bentley (1991) presents an alternative view, in which the exchange interaction effectively extends beyond the distance of the barrier, due to the diffuse nature of the $3s$ orbital.

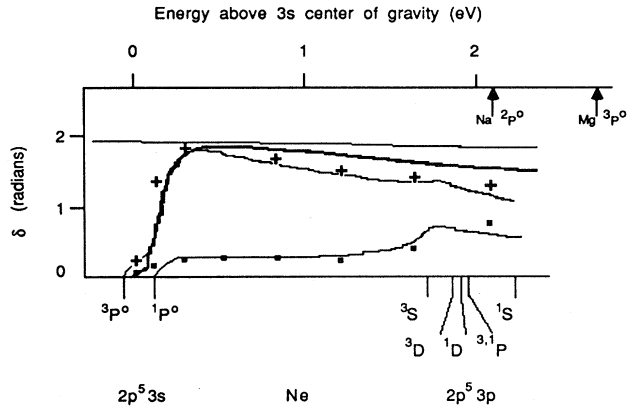

FIG. 58. Calculated eigenphases for electron scattering by Ne, Na, and Mg, as a function of collision energy with respect to the center of gravity of the $3s$ configuration (i.e., the ground states of Na and Mg, and the $2p^5 3s$ excited configuration of Ne). Thin lines are from Clark and Taylor (1981): eigenphases for e + Ne, ^2S symmetry, open channels being $2p^6\varepsilon s$, $2p^5 3s(^3P^\circ)\varepsilon' p$, and $2p^5 3s(^1P^\circ)\varepsilon'' p$. Crosses and points are from Sinfailam and Nesbet (1973): e + Na, respectively, $^3P^\circ$ and $^1P^\circ$ symmetry, open channels being $2p^6 3s\varepsilon p\ ^3P^\circ$ and $2p^6 3s\varepsilon p\ ^1P^\circ$. Bold line is from Kurtz and Jordan (1981): e + Mg, $^2P^\circ$ symmetry, open channel being $2p^6 3s^2\varepsilon p$. The energies of states in the $3p$ configurations are indicated for each atom; for Ne and Na, as calculated in the LS-coupling approximation; and for Mg, experimental value.

These results indicate that the grandparent model does indeed give the appropriate coupling scheme for the excited two-electron complex and that the dynamics of this complex, if viewed from the appropriate perspective, are not highly sensitive to the nature of the residual ion core. This is similar to our findings for the a resonances discussed in the previous section. However, as is also the case for the a resonances, the actual mechanism for resonance formation appears to be associated with a *parent* state: in particular, the polarization potential of the $2p^q 3s$ target. Indeed, the appearance of the b resonance in elastic electron scattering by the Ne* $2p^5 3s\ ^3P^\circ$ metastable state, as computed by the multichannel approach just described (Taylor *et al.*, 1985), is quite similar to that of the older single-channel calculations of Robinson (1969), which are based upon a simple one-electron potential. We thus feel that it is proper to characterize the b features as shape resonances with an $sp\ ^3P^\circ$ external coupling scheme. Krause and Berry (1986) show conditional probability distributions derived from two-electron wave functions for the b resonances of all alkalis, as com-

puted by diagonalization in a finite basis; these exhibit a great deal of similarity.

The invocation of an external coupling scheme provides a description that clashes with the usual distinction made between shape and Feshbach resonances, since the thresholds of excited states are defined within the parent (i.e., target) coupling scheme. In the case of Ne^-, the b resonance lies above all the Ne* $2p^5 3s\ ^3P^\circ$ states and has a significant branching ratio for autodetaching to them, so it could be regarded unambiguously as a shape resonance associated with those states. On the other hand, it is bound with respect to Ne* $2p^5 3s\ ^1P^\circ$ and might also therefore be described as a Feshbach resonance associated with this state (an analogous statement is true for all the heavier noble gases). Indeed, as indicated in the caption to Fig. 59, the transformation between external and target coupling schemes gives

$$2p^5(3s\varepsilon p\ ^3P^\circ)=\frac{\sqrt{3}}{2}2p^5 3s(^1P^\circ)\varepsilon p+\frac{1}{2}2p^5 3s(^3P^\circ)\varepsilon p\ ,$$
$$2p^5(3s\varepsilon p\ ^1P^\circ)=\frac{-\sqrt{3}}{2}2p^5 3s(^3P^\circ)\varepsilon p+\frac{1}{2}2p^5 3s(^1P^\circ)\varepsilon p\ , \quad (40)$$

so that in the target coupling scheme the b resonance appears to be associated primarily with the $2p^5 3s(^1P^\circ)$ channel, and a Feshbach identification would superficially appear to be appropriate. This ambiguity

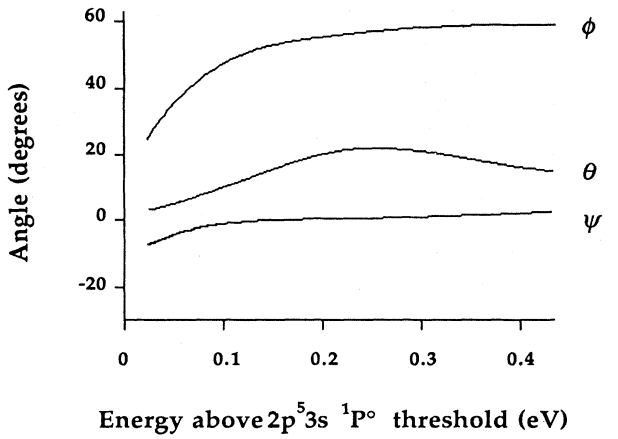

FIG. 59. Euler angles describing the transformation between target channels and eigenchannels for electron scattering by Ne in overall ^2S symmetry, in the vicinity of the b resonance (Clark and Taylor, 1982). The three open target channels at these energies are $2p^5 3s(^3P^\circ)\varepsilon' p$, $2p^5 3s(^1P^\circ)\varepsilon'' p$, and $2p^6\varepsilon s$. These are to be visualized as the x, y, and z axes of a Cartesian reference frame; the three Euler rotations take this frame to the corresponding x'', y'', z'' frame of eigenchannels, the eigenphases of which are shown in Fig. 2. The x'' axis represents the eigenchannel of the b resonance; the y'' axis, the eigenchannel which opens at the $2p^5 3s(^1P^\circ)$ threshold; and the z'' axis, the eigenchannel with a nearly constant phase shift. The sequence of Euler rotations is ϕ about the z axis $(x,y\rightarrow x',y')$, θ about the y' axis, and ψ about the z' axis. The key feature of this figure is that $\phi\sim 60^\circ$ is the angle for recoupling the two excited-state channels to form $2p^5(3s\varepsilon p\ ^3P^\circ)$ and $2p^5(3s\varepsilon p\ ^1P^\circ)$.

appears to underlie the discussion during the early 1980s (Bhatia and Temkin, 1981; Chung, 1981; Junker, 1982a; Komninos *et al.*, 1983) of the shape vs Feshbach nature of the $1s2s2p\ ^2P^\circ$ resonance of He^-. For example, Junker (1982a) performed a single-channel calculation of p-wave scattering by He $1s2s\ ^3S$ and found no shape resonance, whereas a two-channel calculation $[1s2s(^1S)2p+1s^2\varepsilon p]$ gave a resonance below the He $1s2s\ ^1S$ threshold. However, the transformation between target and external coupling schemes in this case happens to be identical to that given above (Komninos *et al.*, 1983), so that Junker's single-channel calculation was done in predominantly $1s2s\varepsilon p(^1P^\circ)$ external coupling, which should not give rise to a low-energy shape resonance. It should be noted that Robinson's (1969) early single-channel calculation of electron scattering by He $1s2s$ gave a p-wave shape resonance; in this work no specific angular momentum coupling scheme was used, the electron-atom interaction being represented by (effectively) the average-of-configuration approximation (plus a polarization potential), which would be closer to $^3P^\circ$ than to $^1P^\circ$ external coupling. We thus feel that the original interpretation of the $^2P^\circ$ feature as a shape resonance (Oberoi and Nesbet, 1973; Fon *et al.*, 1978) is essentially correct, if it be understood within the context of the external coupling scheme. We believe that the $^2P^\circ$ state of He^- fits the general pattern of the b resonances of the noble gases, alkalis, and alkaline earths and that, in particular, it should be similar to the b state of Li^-, which has yet to be observed.

The external coupling scheme for the b resonances implies the existence of multiplet structure in negative ions with open-shell grandparent cores, due to coupling of the triplet pair to the core. Such multiplets are clearly seen in the excitation spectra of Ar, Kr, and Xe, but as of yet no details of their quantum numbers are known.

The mechanism that gives rise to b shape resonances could as well produce stable bound states if the potential were sufficiently attractive inside the barrier. This appears to be the case for Ca^-, as discussed in Sec. IV.G. The discovery that the b resonance in Ca^- is, in fact, a stable bound state has given rise to speculation that the heavier alkaline earths Sr^-, Ba^-, and Ra^- will have stable bound states as well. Calculations indicating that these ions do have bound ns^2np states have been performed in several independent approximations. Vosko *et al.* (1989), using a density-functional formalism, find bound states of all these ions. Froese Fischer (1989) finds stable states of Sr^- and Ba^- in a nonrelativistic MCHF calculation with some relativistic energy corrections; she did not investigate Ra^-. Kim and Greene (1989) use a three-electron R-matrix method with electron-core interactions represented by a model potential and find stable states in all ions. Johnson *et al.* (1989) apply many-body perturbation theory and find stable states of Ca^-, Sr^-, and Ba^-. Gribakin *et al.* (1990) achieve similar results using a Dyson equation. Cowan and Wilson (1991) use a relativistic Hartree-Fock equation supple-

mented by a correlation potential derived from density-functional theory and get bound states of all ions. Fuentealba *et al.* (1990), on the other hand, report configuration-interaction calculation in which a pseudopotential is employed to approximate the effects of core-valence correlation; they believe that their approach strongly suggests that Sr^- and Ba^- are bound, but the approach is inconclusive regarding Ca^-, since the estimated uncertainties in the computed binding energy are comparable to its magnitude. Rotated-coordinate Hartree-Fock calculations by Bentley (1990) yield positive-energy *b* resonances of Ca^-, Sr^-, and Ba^-. Garwan *et al.* (1990) have detected long-lived states of all of these ions in accelerator mass spectrometry. At present we know of no experimental determination of the electron affinities of Sr and Ba.

The electron affinity of the alkaline earths is found to increase with increasing atomic number in all these approximations (with the exception of Ra), including that of Bentley, which gives negative electron affinities in all cases. It should be noted that the theoretical affinities are all relatively small, less than 200 meV, and are comparable in size to the errors that occur in the most accurate calculations that can be performed for heavy atoms at the present time. The reliability of these calculations is thus open to question. However, we note that *ab initio* calculations of the binding energies of negative ions have been found to be substantially more accurate than calculations at the same level of approximation for the binding energies of isoelectronic states of neutral atoms, as shown for the *a* resonances in the previous section. This presumably derives from the fact that in these cases the additional electron occupies a diffuse orbital attached to the neutral atom, so that the effects of virtual core excitation are reduced in comparison to those in the neutral. This circumstance, and the consensus of independent calculations, lend credibility to the belief that the heavy alkaline earths form stable negative ions. Although this issue has not been settled decisively by experiment, it is difficult to think of other states (e.g., metastables) that could account for the long-lived Sr^- and Ba^- ions observed in accelerator mass spectrometry (Kilius *et al.*, 1989; Garwan *et al.*, 1990).

Several qualitative pictures have been proposed to explain why the *b* resonance becomes bound in the heavier alkaline earths. These consist primarily of descriptions of the effective potential for a *p* electron, which becomes more attractive as the atomic number increases. This has been demonstrated in the context of the Hartree-Fock approximation (Froese Fischer, 1989), as well as for the effective long-range potential that consists of the centrifugal and polarization terms (Kim and Greene, 1989) as in Eq. 34. Kim and Greene, in particular, suggest that the electron affinity is correlated with the polarizability of the neutral atom, with greater polarizability being associated with stronger binding. This picture is intuitively appealing, and it is true that both the electron affinity and the polarizability increase from Ca to Ba. However, the electron affinity also increases in the Hartree-Fock approximation (Bentley, 1990), which accounts only for the mean atomic field. It is instructive to make a quantitative comparison of the results of a fully correlated approach, such as that of Kim and Greene, with those of the Hartree-Fock method.

Figure 60 depicts the difference of electron affinities of the alkaline earths, as computed by Kim and Greene and by Bentley, and shows their polarizabilities on a different scale. It is apparent that for Ca, Sr, and Ba the *correlation energy*, as represented by this difference, is relatively constant, whereas the polarizability changes by 60%. Thus, although the Hartree-Fock method gives values of the electron affinity that are wrong, their error is sensibly constant for the heavier alkalis; i.e., it is much smaller than the change in the electron affinities. Therefore we believe that the increase in binding energy of the *b* state along this sequence reflects the greater attractiveness of the short-range electron-core interaction, rather than the effect of increasing polarizability.

In light of the correspondence between the *b* resonances of the alkalis and the alkaline earths described above, it is possible that the heavier alkalis (K, Rb, and Cs) would also have bound *b* states. We are unaware of any direct experimental evidence for such states, such as might derive from photodetachment measurements. Electron transmission experiments are not conclusive, but they suggest the presence of resonances in K^- and Rb^-. All calculations of which we are aware of the K^- and Rb^- *b* states give shape resonances. For Cs^-, on the other hand, there are disparate experimental and theoretical results, but the most recent calculations (Froese Fischer and Chen, 1989; Greene, 1990) indicate that the *b* state is bound, although by an energy that is comparable to an optimistic estimate of the uncertainties in the calculations. We note that the dipole polarizabilities of the heavier alkalis are at least 50% larger than those of

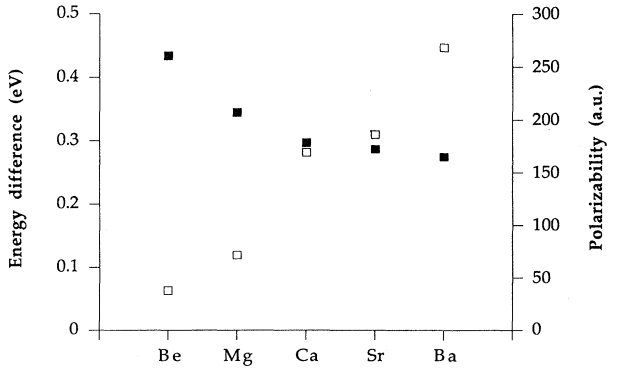

FIG. 60. Differences in eV between the electron affinities of the alkaline earths as computed by Kim and Greene (1989) and by Bentley (1990), shown as open squares. The affinities of Kim and Greene are always larger. Polarizabilities in a.u. of the alkaline earths are shown as solid squares. From Miller and Bederson (1977).

their neighboring alkaline earths. Thus the lack of binding in K^- and Rb^- vs Ca^- and Sr^- indicates that the long-range electron-atom interaction does not play a critical role in stabilizing the *b* resonance; apparently, the increase in the short-range attraction in the alkaline earths vs the alkalis is responsible for binding. Such an increase obviously takes place in the simple self-consistent-field model described above, since the increase in nuclear charge between the alkali and the alkaline earth is only partially screened by the additional valence electron.

The group-IIB elements Zn, Cd, and Hg all exhibit *b*-type resonances, as discussed in Sec. IV.H. There is no indication, from either experiment or theory, that the *b* state should become bound in any of these elements, in contrast to the case of group IIA.

One interesting feature of the bound *b* states in heavy atoms is that their fine-structure splitting can become comparable to their binding energies. As noted in Sec. IV.C.5, Greene (1990) finds all levels of Cs^- $6s6p\ ^3P^\circ$ to be bound, but the highest-lying ($J=2$) is only bound by 10 meV; Thumm and Norcross (1991), who find these states all to be unbound, also obtain fine-structure intervals that are comparable to the resonance energies. A calculation by Vosko *et al.* (1991) for Yb^-, on the other hand, gives a bound state for the $J=1/2$ level of the *b* state $4f^{14}6s^26p$, but finds the $J=3/2$ level to be unbound by about 10 meV. Litherland *et al.* (1991) have observed a long-lived state of Yb^-, but their technique does not provide a spectroscopic identification of this state. Dzuba *et al.* (1991) calculate Ra $7s^27p\ ^2P^\circ_{1/2}$ to be bound by 150 meV, but find the $^2P^\circ_{3/2}$ state to be unbound by about 18 meV. It is thus possible that both bound and resonant *b* states will be found in heavy atoms. As noted by Dzuba *et al.* (1991), this could provide a mechanism for efficient spin polarization of low-energy electrons.

C. The *c* resonances

Unlike the *a* and *b* resonances, which have an unambiguous presence in a variety of negative ions, the *c* features have a well-defined character, in our view, only in the noble gases. The *c* states have traditionally been viewed as the other *LS* term of the configuration that describes the *b* resonance as an $nsnp\ ^1P^\circ$ electron pair. This identification derives from the grandparent model, and it has been supported in the case of Ne^- by the eigenchannel analysis of Clark and Taylor (1982). Given the analogy with Na^- described in the previous section, there are, indeed, strong reasons to believe that the external coupling scheme provides an appropriate description of the eigenchannels for electron scattering by Ne at total collision energies near the lowest excited states. Nevertheless, the structure apparent in Fig. 58 in the externally coupled $^1P^\circ$ channel near the $3p$ thresholds does not exhibit the usual behavior of a resonance, in which the phase increases by π. This may be due to its proximity to the thresholds, at which new channels open. A similar observation applies to Na and K, in which a rapid increase in the phase shift in the $^1P^\circ$ channel begins just below the first excitation threshold of the neutral atom (Sinfailam and Nesbet, 1973). In Cu, on the other hand, Scheibner *et al.* (1987) report a fully developed $3d^{10}4s4p\ ^1P^\circ$ resonance well below the $3d^{10}4p$ threshold. From these calculations it is not clear that the feature labeled *c* in Fig. 33 should be called a resonance. The metastable excitation cross sections obtained in these calculations are in reasonably good agreement with experiment (Taylor *et al.*, 1985).

In electron scattering by Ar, on the other hand, Ojha *et al.* (1982) find a broad ($\Gamma\sim 1$ eV) resonance in the $^2F^\circ$ channel at about 1 eV above the $3p^54s$ threshold, which they identify as the *c* feature. Such a resonance can only be associated with a ^1D or ^3D external coupling scheme. Ojha *et al.* attribute it to a combination of $3p^54s3d\,(^1D)$ and $3p^54p^2(^1D)$ resonances, the presence of two resonances being inferred from a kink in the $^2F^\circ$ eigenphase sum (though the eigenphase sum increases only by π). No such resonance behavior is seen in the $^2P^\circ$ channel, which would also be expected to contain resonances with *D* external coupling. The agreement of the calculated metastable excitation cross section with that observed by Brunt *et al.* (1977c) is reasonably good, though the strength of the *b* feature relative to *c* may be slightly high.

Clark and Taylor make no mention of a resonance in the $^2P^\circ$ or $^2F^\circ$ channels in Ne in this energy region, so that it is either not present or too broad to be distinguished clearly. We note that a resonance of this type ought to be present in the *d*-wave partial cross section for elastic scattering by the metastable state. Earlier calculations by Robinson (1969) of elastic electron scattering by metastable rare gases, using a modified Hartree-Fock-Slater potential plus a polarization potential, exhibit *d*-wave resonances for Ar, Kr, and Xe at energies between 1 and 3 eV; Ne does not support a *d*-wave resonance in this approximation. The cross sections for elastic and inelastic scattering by Ne $2p^53s\ ^3P^\circ$ and $^1P^\circ$ computed by Taylor *et al.* (1985) show no *d*-wave resonance. The absence of such a resonance in Ne is consistent with results for the total scattering cross section of the ground state which we discuss in Sec. VI.D.

In view of these results, we believe that the *c* features in the heavier noble gases may warrant different classifications from those originally proposed by Brunt *et al.*: they may be better described by $ns\varepsilon d\ ^1D$ or ^3D external coupling schemes. Measurements of the differential angular cross sections for electron scattering from the metastable states could help clarify this matter.

D. Higher-energy shape resonances in the heavier noble gases

The total cross sections for electron scattering by the heavier noble gases exhibit resonance structures in the vicinity of 10–20 eV, the systematic behavior of which can be related to the order of filling of electron shells in the

periodic table. Figure 61 shows the cross sections for electron scattering by Ne, Ar, Kr, and Xe at energies between 1 and 300 eV. The Ne curve is featureless on this scale, whereas Ar and Kr display peaks at 10–15 eV, and Xe shows two discernible structures.

The structure in the Ar cross section is due to the d-wave shape resonance that has been discussed in Sec. II.B.1. This resonance may be viewed as a manifestation of a double-well structure in an effective electron-atom potential, as described by Rau and Fano (1968). Let the interaction between electron and atom be approximated by a local potential $U(r)=-Z_{\rm eff}(r)/r$, where $Z_{\rm eff}(r)$ can be regarded as the charge of the nucleus, Z, screened by the net electronic charge within a sphere of radius r about the nucleus (effects of exchange and correlation do not affect this picture in a qualitative way). It is clear that $Z_{\rm eff}(r)\to Z$ as $r\to 0$, and (for a neutral atom) $Z_{\rm eff}(r)\to 0$ as $r\to\infty$; in the transition between these two limits, we expect rapid changes in $Z_{\rm eff}(r)$ as r traverses the regions in which electron shells are localized. The net potential acting upon the electron in this picture is $V_{\rm eff}(r)=-Z_{\rm eff}(r)/r+l(l+1)/2r^2$. For a neutral atom, $Z_{\rm eff}(r)\approx 0$ for $r>5a_0$; so, as a d electron moves from large r in towards the atom, it encounters the rising centrifugal potential barrier. As it enters the atom, it becomes subject to the attractive potential $-Z_{\rm eff}(r)/r$, which shows sudden decreases as subsequent electron shells are penetrated; as $r\to 0$ the centrifugal potential becomes dominant. If Z is sufficiently large, the centrifugal repulsion can be overcome in the interior of the atom, and $V_{\rm eff}(r)$ will exhibit an inner well behind the centrifugal barrier. The depth of this well increases with Z and eventually becomes sufficient to support a state that is localized in the inner region. For the d wave, this occurs around $Z=21$ (scandium), at the beginning of the transition-metal sequence; for the f wave, it happens near $Z=57$ (lanthanum), heralding the onset of the lanthanide elements. For values of Z that are just short of the critical value, the inner potential well is not quite deep enough to hold a bound state. We therefore expect shape resonances to occur in the appropriate partial wave for elements with Z somewhat smaller than the critical value.

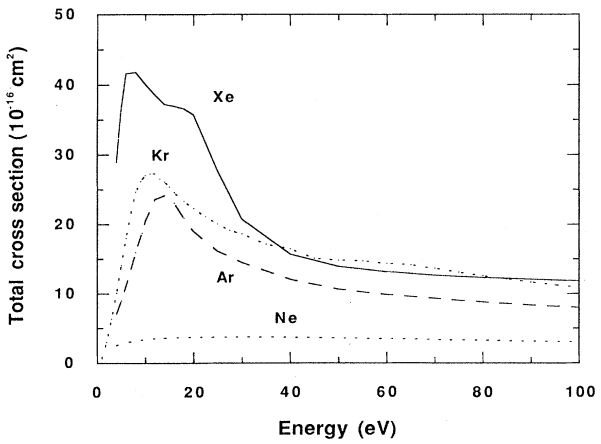

FIG. 61. Total cross section for electron scattering from Ne, Ar, Kr, and Xe between 1 and 300 eV. Experimental data are from Dababneh *et al.* (1980), Nickel *et al.* (1985), and Buckman and Lohmann (1987).

A similar phenomenon occurs when the inner well becomes sufficiently deep to hold a *second* (or third, etc.) localized state, such as the $4d$, $5d$, $6d$, or $5f$ states. Thus Kr exhibits a d-wave shape resonance similar to that of Ar. Note that the peak value of the cross sections for Kr and Ar is similar to what one would expect from the unitarity limit for elastic scattering in a d-wave resonance:

$$\sigma=\frac{4\pi}{k^2}(2l+1)=1.8\times 10^{-15}\ \text{cm}^2\ ,$$

$$\text{for } E=1 \text{ Rydberg},\ l=2\ . \quad (41)$$

Xe exhibits two features: a d-wave resonance around 7 eV and an f-wave resonance around 20 eV. The f-wave resonance is associated with the impending collapse of the $4f$ orbital. It occurs in a straightforward single-configuration description: A continuum Hartree-Fock calculation (present work), for example, gives a resonance energy of 27 eV and a width of 14 eV; a rotated-coordinate calculation (Bentley, 1989), which incorporates effects of core relaxation, yields $E=22.3$ eV, $\Gamma=9.6$ eV. The unitarity limit for the maximum cross section for a pure f-wave resonance with these parameters is also of the order of 2×10^{-15} cm^2. Radon would presumably also exhibit a double-resonance structure similar to that of Xe, associated with the localization of the $6d$ and $5f$ orbitals.

The energies and widths of these resonances are consistent with results of the independent-electron model applied to a plausible atomic potential, so it is reasonable to view them as garden-variety shape resonances. Note, however, that they straddle the ionization limits of the target atoms and so are capable, in principle, of interacting with multiply excited negative-ion resonances. This aspect does not appear to have been investigated extensively to date.

It is likely that similar shape resonances will be found in the heavier halogens. For example, simple continuum Hartree-Fock calculations (present work) give resonances in all LS terms of Cl^- $3p^5\varepsilon d$ (Fig. 62). Except for the $^1P^\circ$ term, their energies and widths are comparable to those of the d-wave resonance in Ar. The exceptional behavior of the $^1P^\circ$ term derives from a strongly repulsive p-d dipole exchange interaction, which has been discussed extensively in the context of photoabsorption (Hansen, 1980). We know of no experimental data on shape resonances in the halogens.

We now discuss the nature of the c features in the noble gases in light of the preceding remarks. Supposing the d-wave resonance in electron scattering by Ar $3p^6$ to be attributable to a double-well structure in an effective one-electron potential, we consider the implications for

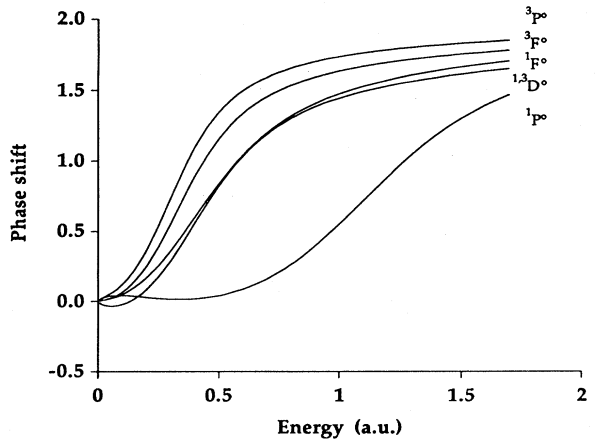

FIG. 62. Phase shifts for d-wave scattering by Cl, $3p^5$, as computed in the continuum Hartree-Fock approximation (present work), labeled by an LS term. The $^1D°$ and $^3D°$ phase shifts are identical in this approximation.

d-wave scattering by Ar $3p^5 4s$, viewed in the most elementary way. The promotion of a $3p$ electron to a $4s$ orbital results in reduced screening of the nuclear charge and also dramatically increases the polarizability of the target (making it comparable to Ar $3p^6 4s$). Both effects will increase the attraction of the atomic potential. Thus the existence of a d-wave shape resonance in scattering by Ar $3p^6$ almost certainly leads to a d-wave resonance in scattering by Ar $3p^5 4s$, though at lower incident electron energies. This is consistent with the results of Robinson (1969). Thus the information depicted in Fig. 61 tends to substantiate the view that the c features in Kr, Ar, and Xe derive from a different mechanism than that applicable to Ne. Their similarity in the metastable excitation spectra may simply be due to the fact that they are all low-energy shape resonances built upon an excited state of the target.

The photoabsorption spectra of the noble gases exhibit broad features that are attributable to shape resonances in the d and f waves, and analogous features are observed in the neighboring alkalis and alkaline earths (Connerade *et al.*, 1987). Thus we may expect to find counterparts of the noble-gas d- and f-wave shape resonances in electron scattering by the alkalis and alkaline earths. If atomic polarizabilities are neglected, the effective potentials for these systems are similar to those of their neighboring noble gases, and shape resonances ought to occur with the same pattern, i.e., none for Li, Be, Na, and Mg; d wave for K, Ca, Rb, and Sr; and d and f wave for Cs and Ba. However, these systems are much more polarizable than the noble gases, and they also possess numerous low-lying excited states that may complicate this simple picture. The calculations of Kurtz and Jordan (1981) show that the addition of a polarization potential does induce a d-wave resonance in Mg, though not in Be; in Ca, a d-wave resonance is apparent even in the static-exchange approximation, and the inclusion of polarizability dramatically reduces its energy and width. Results for the alkalis are complicated by effects of channel interaction: the d-wave phase shifts begin to exhibit resonance behavior near the $^2P°$ thresholds (Sinfailam and Nesbet, 1973). Calculations by Burke and Mitchell (1973) and Scott *et al.* (1984a, 1984b) yield a low-energy $^3F°$ shape resonance in Cs^-, which appears to involve a significant admixture of $6s\varepsilon f$ and $6p5d$ configurations.

ACKNOWLEDGMENTS

It is a pleasure to acknowledge the many colleagues who sent details of their recent (and not so recent) work in this area in response to our solicitations. Many people have also helped in achieving the final form of this manuscript by providing extensive comment and criticism. We thank, in particular but not exclusively, Chris Greene, Ravi Rau, Ugo Fano, Doug Heddle, David Norcross, and Michael Brunger for their careful reading of the manuscript and for their helpful comments. S.J.B. wishes to thank the members of the Electron Scattering Group at the University of Manchester, particularly Frank Read, George King, and Peter Hammond, for both introducing him to this subject and sharing their insight with him.

We are both indebted to our respective institutions. The Australian National University and the National Institute of Standards and Technology, for providing travel funds and expenses to both of us over the extended period of preparation of this article. It would not have been possible without this support.

REFERENCES

The acronym ICPEAC, which appears often in this list of references, denotes the International Conference on the Physics of Electronic and Atomic Collisions.

Relevant reviews since 1973

Biondi, M. A., A. Herzenberg, and C. E. Kuyatt, 1979, "Resonances in atoms and molecules," Phys. Today **32**, 44.

Fano, U., 1983a, "Dynamics of resonant states," *Atomic Physics, Vol. 8,* edited by I. Lindgren and S. Svanberg (Plenum, New York), p. 5.

Fano, U., 1983b, "Correlations of two excited electrons," Rep. Prog. Phys. **46**, 97.

Fano, U., and A. R. P. Rau, 1986, *Atomic Collisions and Spectra* (Academic, New York).

Golden, D. E., 1978, "Resonances in electron atom and molecule scattering," Adv. At. Mol. Phys. **14**, 1.

Heddle, D. W. O., 1976, "Resonances in optical excitation functions," Contemp. Phys. **17**, 443.

Heideman, H. G. M., 1985, "Electron correlation effects in electron-atom collisions," in *Fundamental Processes in Atomic Collision Physics,* edited by H. Kleinpoppen, J. S. Briggs, and H. O. Lutz (Plenum, New York), p. 521.

Ho, Y. K., 1983, "The method of complex coordinate rotation

and its application to atomic collision processes," Phys. Rep. **99**, 1.
Hotop, H., and W. C. Lineberger, 1975, "Binding energies in atomic negative ions," J. Phys. Chem. Ref. Data **4**, 539.
Lin, C. D., 1986, "Doubly excited states, including new classification schemes," Adv. At. Mol. Phys. **22**, 77.
Macek, J., and S. Watanabe, 1987, "Wannier theory of two electron resonances," Comments At. Mol. Phys. **19**, 313.
Read, F. H., 1981, "Correlation effects in electron-atom scattering," *Atomic Physics, Vol. 7,* edited by D. Kleppner and F. M. Pipkin (Plenum, New York), p. 429.
Read, F. H., 1982, "A new class of atomic states: The 'Wannier-ridge' resonances," Aust. J. Phys. **35**, 475.
Read, F. H., 1983, "Electron-atom scattering: The state of the experiments," Phys. Scr. **27**, 103.
Rost, J. M., and J. S. Briggs, 1991, "Saddle structure of the three-body Coulomb problem; symmetries of doubly-excited states and propensity rules for transitions," J. Phys. B **24**, 4293.
Williams, J. F., 1978, "The spectroscopy of atomic compound states," in *Progress in Atomic Spectroscopy, Part B,* edited by W. Hanle and H. Kleinpoppen (Plenum, New York), p. 1031.

General references

Aberth, W., and J. R. Peterson, 1967, Rev. Sci. Instrum. **38**, 745.
Aguilar, J., and J. M. Combes, 1971, Commun. Math. Phys. **22**, 269.
Aksela, S., M. Karras, M. Pessa, and E. Souninen, 1970, Rev. Sci. Instrum. **41**, 351.
Albert, K., C. Christian, T. Heindorff, E. Reichert, and S. Schön, 1977, J. Phys. B **10**, 3733.
Aleksakhin, I. S., A. A. Borovik, V. P. Sarodub, and I. I. Shafranosh, 1979, Opt. Spektrosk. **46**, 1125 [Opt. Spectrosc. (USSR) **46**, 636 (1979)].
Aleksakhin, I. S., I. I. Garga, I. P. Zapesochnyĭ, and V. P. Starodub, 1973, Opt. Spektrosk. **34**, 1053 [Opt. Spectrosc. (USSR) **34**, 611 (1974)].
Aleksakhin, I. S., I. P. Zapesochnyĭ, I. I. Garga, and V. P. Starodub, 1974, Opt. Spektrosk. **37**, 20 [Opt. Spectrosc. (USSR) **37**, 10 (1974)].
Alekshakhin, I. S., and V. A. Zayats, 1974, Opt. Spektrosk. **36**, 1229 [Opt. Spectrosc. (USSR) **36**, 717 (1974)].
Allan, M., 1989, J. Electron Spectrosc. Relat. Phenom. **48**, 219.
Allis, W. P., and P. M. Morse, 1931, Z. Phys. **70**, 567.
Altick, P. L., 1985, J. Phys. B **18**, 1841.
Amusia, M. Ya., and N. Cherepkov, 1975, Case Stud. At. Phys. **5**, 47.
Andersen, L. H., J. P. Bangsgaard, and J. Sørensen, 1986, Phys. Rev. Lett. **57**, 1558.
Andrick, D., 1973, Adv. At. Mol. Phys. **9**, 207.
Andrick, D., 1979, J. Phys. B **12**, L175.
Andrick, D., and H. Bader, 1984, J. Phys. B **17**, 4549.
Andrick, D., and H. Ehrhardt, 1966, Z. Phys. **192**, 99.
Andrick, D., H. Ehrhardt, and M. Eyb, 1968, Z. Phys. **214**, 388.
Andrick, D., M. Eyb, and M. Hofmann, 1972, J. Phys. B **5**, L15.
Andrick, D., and L. Langhans, 1975, J. Phys. B **8**, 1245.
Andrick, D., L. Langhans, F. Linder, and G. Seng, 1975, *Electronic and Atomic Collisions, Abstracts of Papers,* IX ICPEAC, Seattle, 1975, edited by J. S. Risley and R. Geballe (University of Washington, Seattle), Vol. 2, p. 833.
Aspromallis, G., C. A. Nicolaides, and D. R. Beck, 1986, J. Phys. B **19**, 1713.
Aspromallis, G., C. A. Nicolaides, and Y. Komninos, 1985, J. Phys. B **18**, L545.
Bader, H., 1986, J. Phys. B **19**, 2177.
Bae, Y. K., and J. R. Peterson, 1985, Phys. Rev. A **32**, 1917.
Bae, Y. K., and J. R. Peterson, 1986, in *Electronic and Atomic Collisions, Invited Papers,* XIV ICPEAC, Palo Alto, 1985, edited by D. C. Lorents, W. E. Meyerhof, and J. R. Peterson (North-Holland, Amsterdam), p. 799.
Bae, Y. K., J. R. Peterson, A. S. Schlachter, and J. W. Stearns, 1985, Phys. Rev. Lett. **54**, 789.
Bain, R. A., J. N. Bardsley, B. R. Junker, and C. V. Sukumar, 1974, J. Phys. B **7**, 2189.
Balslev, E., and J. M. Combes, 1971, Commun. Math. Phys. **22**, 280.
Baranger, E., and E. Gerjuoy, 1958, Proc. Phys. Soc. London **72**, 362.
Bardsley, J. N., and B. R. Junker, 1972, J. Phys. B **5**, L178.
Bartschat, K., 1985, J. Phys. B **18**, 2519.
Bartschat, K., and P. G. Burke, 1986, J. Phys. B **19**, 1231.
Bartschat, K., and N. S. Scott, 1984, J. Phys. B **17**, 3787.
Bartschat, K., N. S. Scott, K. Blum, and P. G. Burke, 1984, J. Phys. B **17**, 269.
Bass, A. D., P. Hammond, S. J. Buckman, G. C. King, and F. H. Read, 1988, in *Electronic and Atomic Collisions, Abstracts of Contributed Papers,* XV ICPEAC, Brighton, UK, 1987, edited by J. Geddes, H. B. Gilbody, A. E. Kingston, C. J. Latimer, and H. R. J. Walters (North-Holland, Amsterdam), p. 220.
Batelaan, H., J. Van Eck, and H. G. M. Heideman, 1991, J. Phys. B **24**, 5151.
Bates, D. R., and B. L. Moiseiwitsch, 1955, Proc. Phys. Soc. London Sect. A **68**, 540.
Bauschlicher, C. W., Jr., S. R. Langhoff, and P. R. Taylor, 1989, Chem. Phys. Lett. **158**, 245.
Baxter, J. A., J. Comer, P. J. Hicks, and J. W. McConkey, 1979, J. Phys. B **12**, L355.
Beck, D., 1987, private communication cited by Pegg *et al.* (1987).
Behringer, K., and P. Thoma, 1978, Phys. Rev. A **17**, 1408.
Bentley, M., 1989, private communication.
Bentley, M., 1990, Phys. Rev. A **42**, 1192.
Bentley, M., 1991, Phys. Rev. A **44**, 5414.
Berk, A., A. K. Bhatia, B. R. Junker, and A. Temkin, 1986, Phys. Rev. A **34**, 4591.
Berrington, K. A., P. G. Burke, K. Butler, M. J. Seaton, P. J. Storey, K. T. Taylor, and Yu Yan, 1987, J. Phys. B **20**, 6379.
Berrington, K. A., P. G. Burke, and W. D. Robb, 1975, J. Phys. B **8**, 2500.
Berrington, K. A., P. G. Burke, and A. L. Sinfailam, 1975, J. Phys. B **8**, 1459.
Bethge, K., E. Heinecke, and H. Baumann, 1966, Phys. Lett. **23**, 542.
Bhatia, A. K., and A. Temkin, 1974, Phys. Rev. A **8**, 2184; **10**, 458(E).
Bhatia, A. K., and A. Temkin, 1981, Phys. Rev. A **23**, 3361.
Blatt, J. M., and J. D. Jackson, 1949, Phys. Rev. **76**, 18.
Boesten, L., 1985, J. Phys. E **18**, 232.
Bogdanova, I. P., and V. D. Marusin, 1971, Opt. Spectrosc. (USSR) **31**, 184.
Bolduc, E., and P. Marmet, 1973, Can. J. Phys. **51**, 2108.
Bolduc, E., J. J. Quemener, and P. Marmet, 1971, Can. J. Phys. **49**, 3095.
Bolduc, E., J. J. Quemener, and P. Marmet, 1972, J. Chem. Phys. **57**, 1957.

Borst, W. L., 1969, Phys. Rev. **181**, 257.
Boulay, M., and P. Marchand, 1982, Can. J. Phys. **60**, 855.
Broad, J. T., and W. P. Reinhardt, 1976, Phys. Rev. A **14**, 2159.
Brunger, M. J., S. J. Buckman, and P. J. O. Teubner, 1987, private communication.
Brunt, J. N. H., G. C. King, and F. H. Read, 1976, J. Phys. B **9**, 2195.
Brunt, J. N. H., G. C. King, and F. H. Read, 1977a, J. Phys. B **10**, 433.
Brunt, J. N. H., G. C. King, and F. H. Read, 1977b, J. Electron Spectrosc. Relat. Phenom. **12**, 221.
Brunt, J. N. H., G. C. King, and F. H. Read, 1977c, J. Phys. B **10**, 1289.
Brunt, J. N. H., G. C. King, and F. H. Read, 1977d, J. Phys. B **10**, 3781.
Brunt, J. N. H., F. H. Read, and G. C. King, 1977e, J. Phys. E **10**, 134.
Bryant, H. C., 1980, in *Electronic and Atomic Collisions,* Proceedings of the XIth ICPEAC, Kyoto, 1979, edited by N. Oda and K. Takayanagi (North-Holland, Amsterdam), p. 145.
Bryant, H. C., 1986, in *Advances in Laser Science—1,* edited by W. C. Stwalley and M. Lapp (American Institute of Physics, New York), p. 389.
Bryant, H. C., K. B. Butterfield, D. A. Clark, C. A. Frost, J. B. Donahue, P. A. M. Gram, M. E. Hamm, R. W. Hamm, and W. W. Smith, 1981, in *Atomic Physics 7,* edited by D. Kleppner and F. M. Pipkin (Plenum, New York), p. 29.
Bryant, H. C., D. A. Clark, K. B. Butterfield, C. A. Frost, H. Sharifian, H. Tootoonchi, J. B. Donahue, P. A. M. Gram, M. E. Hamm, R. W. Hamm, J. C. Pratt, M. A. Yates, and W. W. Smith, 1983, Phys. Rev. A **27**, 2889.
Bryant, H. C., B. D. Dieterle, J. Donahue, H. Sharifian, H. Tootoonchi, D. M. Wolfe, P. A. M. Gram, and M. A. Yates-Williams, 1977, Phys. Rev. Lett. **38**, 228.
Buckman, S. J., P. Hammond, G. C. King, and F. H. Read, 1983b, J. Phys. B **16**, 4219.
Buckman, S. J., P. Hammond, F. H. Read, and G. C. King, 1983a, J. Phys. B **16**, 4039.
Buckman, S. J., G. C. King, and F. H. Read, 1981, *Electronic and Atomic Collisions, Abstracts of Contributed Papers,* XII ICPEAC, Gatlinburg, 1981, edited by S. Datz (North-Holland, Amsterdam), Vol. 1, p. 200.
Buckman, S. J., and B. Lohmann, 1987, J. Phys. B **20**, 5807.
Buckman, S. J., and D. S. Newman, 1987, J. Phys. B **20**, L711.
Bui, T. D., 1977, Can. J. Phys. **55**, 742.
Bui, T. D., and A. D. Stauffer, 1975, Can. J. Phys. **53**, 1615.
Bunge, A. V., and C. F. Bunge, 1984, Phys. Rev. A **30**, 2179.
Bunge, C. F., M. Galan, R. Jáuregui, and A. V. Bunge, 1982, Nucl. Instrum. Methods **202**, 299.
Burke, P. G., 1968, Adv. At. Mol. Phys. **4**, 173.
Burke, P. G., K. A. Berrington, M. Le Dourneuf, and Vo Ky Lan, 1974, J. Phys. B **7**, L531.
Burke, P. G., J. W. Cooper, and S. Ormonde, 1969, Phys. Rev. **183**, 245.
Burke, P. G., and J. F. B. Mitchell, 1973, J. Phys. B **6**, L161.
Burke, P. G., S. Ormonde, and W. Whitaker, 1967, Proc. Phys. Soc. London **92**, 319.
Burke, P. G., and A. J. Taylor, 1966, Proc Phys. Soc. London **88**, 549.
Burke, P. G., and A. J. Taylor, 1969, J. Phys. B **2**, 869.
Burrow, P. D., 1967, Phys. Rev. **158**, 65.
Burrow, P. D., 1985, "A Bibliography of Studies in Electron Transmission Spectroscopy" (unpublished). See Jordan, K. D., and P. D. Burrow, 1987, Chem. Rev. **87**, 557.
Burrow, P.D., 1992, private communication.
Burrow, P. D., and J. Comer, 1975, J. Phys. B **8**, L92.
Burrow, P. D., J. A. Michejda, 1974, *Proceedings of the International Symposium on Electron and Photon Interactions with Atoms, University of Stirling,* Abstracts, edited by H. Kleinpoppen (Stirling University), p. 50.
Burrow, P. D., J. A. Michejda, and J. Comer, 1976, J. Phys. B **9**, 3225.
Burrow, P. D., and G. J. Schulz, 1969, Phys. Rev. Lett. **22**, 1271.
Bydin, Yu. F., 1967, Zh. Eksp. Teor. Fiz. Pis'ma **6**, 857 [Sov. Phys. JETP Lett. **6**, 297 (1967)].
Callaway, J., 1978, Phys. Lett. A **68**, 315.
Callaway, J., 1982, Phys. Rev. A **26**, 199.
Callaway, J., 1990, J. Phys. B **23**, 751.
Callaway, J., and A. R. P. Rau, 1978, J. Phys. B **11**, L289.
Cavagnero, M., 1984, Phys. Rev. A **30**, 1169.
Chamberlain, G. E., 1967, Phys. Rev. **155**, 46.
Chamberlain, G., S. J. Smith, and D. W. O. Heddle, 1964, Phys. Rev. Lett. **12**, 647.
Chase, R. L., and H. P. Kelly, 1972, Phys. Rev. A **6**, 2150.
Chen, S. T., and A. Gallagher, 1976, Phys. Rev. A **14**, 593.
Chen, S. T., and A. Gallagher, 1977, Phys. Rev. A **15**, 888.
Christensen-Dalsgaard, B. L., 1984, Phys. Rev. A **29**, 470.
Christensen-Dalsgaard, B. L., 1985, J. Phys. B **18**, L407.
Christensen-Dalsgaard, B. L., 1988, J. Phys. B **21**, 2539.
Chrysos, M., Y. Komninos, Th. Mercouris, and C. A. Nicolaides, 1990, Phys. Rev. A **42**, 2634.
Chrysos, M., Y. Komninos, and C. A. Nicolaides, 1992, J. Phys. B **25**, 1977.
Chung, K. T., 1972, Phys. Rev. A **6**, 1809.
Chung, K. T., 1979, Phys. Rev. A **20**, 1743.
Chung, K. T., 1981, Phys. Rev. A **23**, 1079.
Chutjian, A., 1979, Rev. Sci. Instrum. **50**, 347.
Clark, C. W., 1984, in *Electron Correlation Effects and Negative Ions,* edited by T. Andersen (Aarhus University, Aarhus, Denmark), p. 49.
Clark, C. W., 1986, in *Advances in Laser Science—1,* edited by W. C. Stwalley and M. Lapp (American Institute of Physics, New York), p. 379.
Clark, C. W., and S. J. Buckman, 1987, J. Opt. Soc. Am. B **4**, 815.
Clark, C. W., and C. H. Greene, 1980, Phys. Rev. A **21**, 1786.
Clark, C. W., and K. T. Taylor, 1982, J. Phys. B **15**, L213.
Clark, D. A., H. C. Bryant, K. B. Butterfield, C. A. Frost, J. B. Donahue, P. A. M. Gram, M. E. Hamm, R. W. Hamm, and W. W. Smith, 1980, Bull. Am. Phys. Soc. **25**, 1137.
Clementi, E., and A. D. McLean, 1964, Phys. Rev. **133**, A419.
Cohen, S., H. C. Bryant, C. J. Harvey, J. E. Stewart, K. B. Butterfield, D. A. Clark, J. B. Donahue, D. W. MacArthur, G. Comtet, and W. W. Smith, 1987, Phys. Rev. A **36**, 4728.
Comtet, G., C. J. Harvey, J. E. Stewart, H. C. Bryant, K. B. Butterfield, D. A. Clark, J. B. Donahue, P. A. M. Gram, D. W. MacArthur, V. Yuan, W. W. Smith, and S. Cohen, 1987, Phys. Rev. A **35**, 1547.
Connerade, J. P., J. M. Esteva, and R. C. Karnatak, 1987, Eds., *Giant Resonances in Atoms, Molecules, and Solids* (Plenum, New York).
Connerade, J. P., W. R. S. Garton, M. W. D. Mansfield, and M. A. P. Martin, 1976, Proc. R. Soc. London, Ser. A **350**, 47.
Cooper, J. W., U. Fano, and F. Prats, 1963, Phys. Rev. Lett. **10**, 538.
Cowan, R. D., N. L. S. Martin, and M. Wilson, 1988, J. Phys. B **21**, L1.

Cowan, R. D., and M. Wilson, 1991, Phys. Scr. **43**, 244.
Cross, J. D., F. H. Read, and E. A. Riddle, 1967, J. Sci. Instrum. **44**, 993.
Crossley, R. J. S., 1964, Proc. Phys. Soc. London **83**, 375.
Cunningham, D. L., and A. K. Edwards, 1973, Phys. Rev. A **8**, 2960.
Cunningham, D. L., and A. K. Edwards, 1974, Phys. Rev. Lett. **32**, 915.
Cvejanovic, S., J. Comer, and F. H. Read, 1974, J. Phys. B **7**, 468.
Cvejanovic, S., and F. H. Read, 1974, J. Phys. B **7**, 1180.
Dababneh, M. S., W. E. Kauppila, J. P. Downing, F. Laperriere, V. Pol, J. H. Smart, and T. S. Stein, 1980, Phys. Rev. A **22**, 1872.
Dahl, D. A., and J. E. Delmore, 1988, The SIMION PC/PS2 User's Manual, V4.0.
Damburg, R. J., and M. K. Gailitis, 1963, Proc. Phys. Soc. London **82**, 192.
Dassen, H. W., R. Gomez, G. C. King, and J. W. McConkey, 1983, J. Phys. B **16**, 1481.
Delâge, A., D. Roy, and J. D. Carette, 1977, J. Phys. B **10**, 1487.
Delgado-Barrio, G., and R. F. Prat, 1975, Phys. Rev. A **12**, 2288.
de Prunelé, E., 1991, Phys. Rev. A **44**, 90.
De Vreugd, C., R. W. Wijnaendts van Resandt, J. B. Delos, and J. Los, 1982a, Chem. Phys. **68**, 261.
De Vreugd, C., R. W. Wijnaendts van Resandt, J. B. Delos, and J. Los, 1982b, Chem. Phys. **68**, 275.
Dmitrieva, I. K., and G. I. Plindov, 1988, J. Phys. B **21**, 3055.
Dmitrieva, I. K., and G. I. Plindov, 1989, J. Phys. B **22**, 1297.
Dmitrieva, I. K., and G. I. Plindov, 1990, J. Phys. B **23**, 693.
Donnelly, R. A., and J. Simons, 1980, J. Chem. Phys. **73**, 2858.
Doolen, G. D., J. Nuttall, and R. W. Stagat, 1974, Phys. Rev. A **10**, 1612.
Dulieu, O., 1989, Z. Phys. D **13**, 17.
Dulieu, O., and C. Le Sech, 1987, Europhys. Lett. **3**, 975.
Düweke, M., N. Kirchner, E. Reichert, and E. Staudt, 1973, J. Phys. B **6**, L208.
Düweke, M., N. Kirchner, E. Reichert, and S. Schön, 1976, J. Phys. B **9**, 1915.
D'yachkov, L. G., O. A. Golubev, G. A. Kobzev, and A. N. Vargin, 1978, J. Quant. Spectrosc. Radiat. Transfer **20**, 175.
D'yachkov, L. G., G. A. Kobzev, and G. É. Norman, 1973, Zh. Eksp. Teor. Fiz. **65**, 1399 [Sov. Phys. JETP **38**, 697 (1974)].
Dzuba, V. A., V. V. Flambaum, G. F. Gribakin, and D. P. Sushkov, 1991, Phys. Rev. A **44**, 2823.
Edlén, B., 1960, J. Chem. Phys. **33**, 98.
Edwards, A. K., 1975a, in *The Physics of Electronic and Atomic Collisions,* edited by J. S. Risley and R. Geballe (University of Washington, Seattle), p. 790.
Edwards, A. K., 1975b, Phys. Rev. A **12**, 1830.
Edwards, A. K., 1976, Phys. Rev. A **13**, 1654.
Edwards, A. K., and D. L. Cunningham, 1973, Phys. Rev. A **8**, 168.
Edwards, A. K., and D. L. Cunningham, 1974a, Phys. Rev. A **9**, 1011.
Edwards, A. K., and D. L. Cunningham, 1974b, Phys. Rev. A **10**, 448.
Edwards, A. K., J. S. Risley, and R. Geballe, 1971, Phys. Rev. A **3**, 583.
Ehlers, V. J., and A. Gallagher, 1973, Phys. Rev. A **7**, 1573.
Ehrhardt, H., L. Langhans, F. Linder, and H. S. Taylor, 1968, Phys. Rev. **173**, 222.
Ehrhardt, H., and K. Willmann, 1967, Z. Phys. **203**, 1.
Eland, J. H. D., 1978, J. Phys. E **11**, 969.
Elander, N., C. Carlsund, P. Krylstedt, and P. Winkler, 1989, in *Resonances,* edited by E. Brandäs and N. Elander (Springer-Verlag, Berlin), p. 383.
Elford, M. T., 1980, Aust. J. Phys. **33**, 251.
England, J. P., and M. T. Elford, 1991, private communication.
Esaulov, V. A., 1981, J. Phys. B **14**, 1303.
Esaulov, V. A., 1986, Ann. Phys. (Paris) **11**, 493.
Eyb, M., 1968, Diplomarbeit (Universität Freiburg).
Eyb, M., 1976, J. Phys. B **9**, 101.
Eyb, M., and H. Hofmann, 1975, J. Phys. B **8**, 1095.
Ezra, G. S., and R. S. Berry, 1982, Phys. Rev. A **25**, 1513.
Ezra, G. S., and R. S. Berry, 1983a, Phys. Rev. A **28**, 1974.
Ezra, G. S., and R. S. Berry, 1983b, Phys. Rev. A **28**, 1989.
Ezra, G. S., K. Richter, G. Tanner, and D. Wintgen, 1991, J. Phys. B **24**, L413.
Fabrikant, I. I., 1974, J. Phys. B **7**, 91.
Fabrikant, I. I., 1980, J. Phys. B **13**, 603.
Fabrikant, I. I., 1982, Opt. Spectrosc. (USSR) **53**, 131.
Fabrikant, I. I., 1986, J. Phys. B **19**, 1527.
Fano, U., 1980, J. Phys. B **13**, L519.
Fano, U., and J. W. Cooper, 1965, Phys. Rev. **138**, A400.
Fano, U., and A. R. P. Rau, 1985, Comments At. Mol. Phys. **16**, 241.
Fayeton, J., D. Dhuicq, and M. Barat, 1978, J. Phys. B **11**, 1267.
Feagin, J. M., 1984, J. Phys. B **17**, 2433.
Feagin, J. M., and J. S. Briggs, 1986, Phys. Rev. Lett. **57**, 984.
Feagin, J. M., and J. S. Briggs, 1988, Phys. Rev. A **37**, 4599.
Feagin, J. M., and J. Macek, 1984, J. Phys. B **17**, L245.
Feagin, J. M., J. Macek, and A. F. Starace, 1985, Phys. Rev. A **32**, 3219.
Fedorov, V. L., and A. P. Mezentsev, 1965, Opt. Spectrosc. (USSR) **19**, 5.
Feigerle, C. S., R. R. Corderman, and W. C. Lineberger, 1981, J. Chem. Phys. **74**, 1513.
Feigerle, C. S., D. T. Pierce, A. Seiler, and R. J. Celotta, 1984, Appl. Phys. Lett. **44**, 866.
Feldman, D., R. Rackwitz, E. Heinicke, and H. J. Kaiser, 1973, Phys. Lett. A **45**, 404.
Feshbach, H., 1962, Ann. Phys. (NY) **19**, 287.
Field, D., D. W. Knight, G. Mrotzek, J. Randell, S. L. Lunt, J. B. Ozenne, and J. P. Ziesel, 1991, Meas. Sci. Technol. **2**, 757.
Field, D., G. Mrotzek, D. W. Knight, S. L. Lunt, and J. P. Ziesel, 1988, J. Phys. B **21**, 171.
Fink, J., and E. Kisker, 1980, Rev. Sci. Instrum. **51**, 918.
Fock, V. A., 1958, K. Nor. Vidensk. Selsk. Forh. **31**, 138.
Fon, W. C., K. A. Berrington, P. G. Burke, and A. E. Kingston, 1978, J. Phys. B **11**, 325.
Fon, W. C., K. A. Berrington, P. G. Burke, and A. E. Kingston, 1989, J. Phys. B **22**, 3939.
Frankowski, K., and C. L. Pekeris, 1966, Phys. Rev. **146**, 46.
Freitas, L. C. G., K. A. Berrington, P. G. Burke, A. Hibbert, A. E. Kingston, and A. L. Sinfailam, 1984, J. Phys. B **17**, L303.
Frey, P., F. Freyer, and H. Hotop, 1978, J. Phys. B **11**, L589.
Frey, P., M. Lawen, F. Breyer, H. Klar, and H. Hotop, 1982a, Z. Phys. A **304**, 155.
Frey, P., M. Lawen, F. Breyer, H. Klar, and H. Hotop, 1982b, Z. Phys. A **306**, 185.
Froese Fischer, C., 1978, *The Multiconfiguration Hartree-Fock Method for Atoms* (Wiley, New York).
Froese Fischer, C., 1989, Phys. Rev. A **39**, 963.
Froese Fischer, C., and D. Chen, 1989, J. Mol. Struct. **199**, 61.
Froese Fischer, C., J. B. Lagowski, and S. H. Vosko, 1987, Phys. Rev. Lett. **59**, 2263.

Frye, D., and L. Armstrong, Jr., 1986, Phys. Rev. A **34**, 1682.
Fuentealba, P., A. Savin, H. Stoll, and H. Preuss, 1990, Phys. Rev. A **41**, 1238.
Fukuda, H., N. Koyama, and M. Matsuzawa, 1987, J. Phys. B **20**, 2959.
Fung, A. C., and J. J. Matese, 1972, Phys. Rev. A **5**, 22.
Gadzuk, J. W., and C. W. Clark, 1989, J. Chem. Phys. **91**, 3174.
Gailitis, M., and R. Damburg, 1963, Zh. Eksp. Teor. Fiz. **44**, 1644 [Sov. Phys. JETP **17**, 1107 (1963)].
Gallagher, A. C., and G. York, 1974, Rev. Sci. Instrum. **45**, 662.
Garga, I. I., I. S. Aleksakhin, V. P. Starodub, and I. P. Zapesochnyĭ, 1974, Opt. Spektrosk. **37**, 843 [Opt. Spectrosc. (USSR) **37**, 482 (1974)].
Garwan, M. A., L. R. Kilius, A. E. Litherland, M.-J. Nadeau, and X.-L. Zhao, 1990, Nucl. Instrum. Methods Phys. Res. B **52**, 512.
Gehenn, W., and E. Reichert, 1972, Z. Phys. **254**, 28.
Gehenn, W., and E. Reichert, 1977, J. Phys. B **10**, 3105.
Gibson, J. R., and K. T. Dolder, 1969, J. Phys. B **2**, 741.
Glockler, G., 1934, Phys. Rev. **46**, 111.
Golden, D. E., 1978, Ad. At. Mol. Phys. **14**, 1.
Golden, D. E., and H. W. Bandel, 1965, Phys. Rev. **138**, A14.
Golden, D. E., N. G. Koepnick, and L. Fornari, 1972, Rev. Sci. Instrum. **43**, 1249.
Golden, D. E., F. D. Schowengerdt, and J. Macek, 1974, J. Phys. B **7**, 478.
Golden, D. E., and A. Zecca, 1970, Phys. Rev. A **1**, 241.
Gram, P. A. M., J. C. Pratt, M. A. Yates-Williams, H. C. Bryant, J. B. Donahue, H. Sharifian, and H. Tootoonchi, 1978, Phys. Rev. Lett. **40**, 107.
Granneman, E. H. A., and M. J. Van der Wiel, 1983, in *Handbook on Synchrotron Radiation, Vol. 1,* edited by E.-E. Koch (North-Holland, Amsterdam), p. 367.
Greene, C. H., 1980a, Phys. Rev. Lett. **44**, 869.
Greene, C. H., 1980b, Phys. Rev. A **22**, 149.
Greene, C. H., 1980c, J. Phys. B **13**, L39.
Greene, C. H., 1990, Phys. Rev. A **42**, 1405.
Greene, C. H., and C. W. Clark, 1984, Phys. Rev. A **30**, 2161.
Gribakin, G. F., B. V. Gul'tsev, V. K. Ivanov, and M. Yu. Kuchiev, 1990, J. Phys. B **23**, 4505.
Grisenti, R., and A. Zecca, 1982, Rev. Sci. Instrum. **53**, 9.
Grissom, J. T., W. R. Garrett, and R. N. Compton, 1969, Phys. Rev. Lett. **23**, 1011.
Grivet, P., 1972, *Electron Optics,* 2nd ed. (Pergamon, Oxford).
Grouard, J. P., V. A. Esaulov, R. I. Hall, J. L. Montmagnon, and Vu Ngoc Tuan, 1986, J. Phys. B **19**, 1483.
Gutzwiller, M. C., 1990, *Chaos in Classical and Quantum Mechanics* (Springer, New York).
Hahn, Y., T. F. O'Malley, and L. Spruch, 1962, Phys. Rev. **128**, 932.
Hamm, M. E., R. W. Hamm, J. Donahue, P. A. M. Gram, J. C. Pratt, M. A. Yates, R. D. Bolton, D. A. Clark, H. C. Bryant, C. A. Frost, and W. W. Smith, 1979, Phys. Rev. Lett. **43**, 1715.
Hammond, P., 1982, Ph.D. thesis (University of Manchester).
Hammond, P., F. H. Read, S. Cvejanovic, and G. C. King, 1985, J. Phys. B **18**, L141.
Hammond, P., F. H. Read, and G. C. King, 1984, J. Phys. B **17**, 2925.
Hanne, G. F., V. Nickich, and M. Sohn, 1985, J. Phys. B **18**, 2037.
Hansen, J. E., 1977, J. Opt. Soc. Am. **67**, 754.
Hansen, J. E., 1980, Phys. Scr. **21**, 510.
Hanstorp, D., P. Devynck, W. G. Graham, and J. R. Peterson, 1989, Phys. Rev. Lett. **63**, 368.
Harris, P. G., *et al.*, 1990, Phys. Rev. Lett. **65**, 309.
Harris, P. G., H. C. Bryant, A. H. Monagheghi, R. A. Reeder, C. Y. Tang, J. B. Donahue, and C. R. Quick, 1990, Phys. Rev. A **42**, 6443.
Harting, E., and F. H. Read, 1976, *Electrostatic Lenses* (Elsevier, Amsterdam).
Hazi, A. U., 1978, J. Phys. B **11**, L259.
Hazi, A. U., 1979, Phys. Rev. A **19**, 920.
Hazi, A. U., and K. Reed, 1981, Phys. Rev. A **24**, 2269.
Heber, O., I. Gertner, I. Ben-Itzhak, and B. Rosner, 1988, Phys. Rev. A **38**, 4504.
Heddle, D. W. O., 1969, J. Phys. E **2**, 1046.
Heddle, D. W. O., 1971a, J. Phys. E **4**, 589.
Heddle, D. W. O., 1971b, J. Phys. E **4**, 981.
Heddle, D. W. O., 1975, J. Phys. B **8**, L33.
Heddle, D. W. O., 1976a, Contemp. Phys. **17**, 443.
Heddle, D. W. O., 1976b, in *Electron and Photon Interactions with Atoms,* edited by H. Kleinpoppen and M. R. C. McDowell (Plenum, New York), p. 671.
Heddle, D. W. O., 1977, Proc. R. Soc. London Ser. A **352**, 441.
Heddle, D. W. O., 1978, J. Phys. B **8**, L711.
Heddle, D. W. O., 1991, *Electrostatic Lens Systems* (Adam Hilger–IOP Publishing, Bristol).
Heddle, D. W. O., R. G. W. Kessing, and J. M. Kurepa, 1973, Proc. R. Soc. London Ser. A **334**, 135.
Heddle, D. W. O., R. G. W. Keesing, and J. M. Kurepa, 1974, Proc. R. Soc. London Ser. A **337**, 435.
Heddle, D. W. O., R. G. W. Keesing, and A. Parkin, 1977, Proc. R. Soc. London Ser. A **352**, 419.
Heddle, D. W. O., R. G. W. Keesing, and R. D. Watkins, 1974, Proc. R. Soc. London Ser. A **337**, 443.
Heddle, D. W. O., and N. Papadovassilakis, 1984, J. Phys. E **17**, 599.
Heideman, H. G. M., 1988, in *Multiphoton Processes,* edited by S. J. Smith and P. L. Knight (Cambridge University Press, Cambridge, England), p. 272.
Heideman, H. G. M., G. Nienhuis, and T. van Ittersum, 1974, J. Phys. B **7**, L493.
Heindorff, T., J. Hofft, and P. Dabkiewicz, 1976, J. Phys. B **9**, 89.
Heindorff, T., J. Hofft, and E. Reichert, 1973, J. Phys. B **6**, 477.
Heinicke, E., and H. Baumann, 1969, Nucl. Instrum. Methods **74**, 229.
Heinicke, E., H. J. Kaiser, R. Rackwitz, and D. Feldmann, 1974, Phys. Lett. A **50**, 265.
Henry, R. J. W., P. G. Burke, and A. L. Sinfailam, 1969, Phys. Rev. **178**, 218.
Herrick, D. R., 1983, Adv. Chem. Phys. **52**, 1.
Herrick, D. R., M. E. Kellman, and R. D. Poliak, 1980, Phys. Rev. A **22**, 1517.
Herrick, D. R., and O. Sinagnoğlu, 1975, Phys. Rev. A **11**, 97.
Herzenberg, A., 1988, in *Electron-Molecule Scattering and Photoionization,* edited by P. G. Burke and J. B. West (Plenum, New York), p. 187.
Hicks, P. J., J. Comer, S. Cvejanović, and F. H. Read, 1973, *Electronic and Atomic Collisions, Abstracts of Papers,* VIII ICPEAC, Beograd, 1973, edited by B. C. Čobić and M. V. Kurepa (Institute of Physics, Beograde, Yugoslavia), Vol. 2, p. 513.
Hicks, P. J., S. Cvejanovic, J. Comer, F. H. Read, and J. M. Sharp, 1974, Vacuum **24**, 573.
Hicks, P. J., S. Daviel, B. Wallbank, and J. Comer, 1980, J. Phys. E **13**, 713.
Hicks, P. J., S. Daviel, B. Wallbank, and J. Comer, 1982, Nucl.

Instrum. Methods **195**, 323.
Hiraoka, H., R. K. Nesbet, and L. W. Walsh, Jr., 1977, Phys. Rev. Lett. **39**, 130.
Ho, Y. K., 1977, J. Phys. B **10**, L373.
Ho, Y. K., 1986, Phys. Rev. A **34**, 148.
Ho, Y. K., 1989, J. Phys. B **23**, L71.
Ho, Y. K., 1990, Phys. Rev. A **41**, 1492.
Ho, Y. K., 1992, Phys. Rev. A **45**, 4402.
Ho, Y. K., and J. Callaway, 1986, Phys. Rev. A **34**, 130.
Hoffman, A., X. Guo, J. T. Yates, Jr., J. W. Gadzuk, and C. W. Clark, 1989, J. Chem. Phys. **90**, 5793.
Hose, G., and H. S. Taylor, 1983, Phys. Rev. Lett. **51**, 947.
Hotop, H., R. A. Bennett, and W. C. Lineberger, 1973, J. Chem. Phys. **58**, 2373.
Hotop, H., and W. C. Lineberger, 1975, J. Phys. Chem. Ref. Data **4**, 539.
Hotop, H., and W. C. Lineberger, 1985, J. Phys. Chem. Ref. Data **14**, 731.
Huard, D., P. Marmet, and E. Bolduc, 1978, Can. J. Phys. **56**, 82.
Huetz, A., F. Gresteau, R. I. Hall, and J. Mazeau, 1980, J. Chem. Phys. **72**, 5297.
Huetz, A., and J. Mazeau, 1981, J. Phys. B **14**, L591.
Huetz, A., and J. Mazeau, 1983, J. Phys. B **16**, 2577.
Hunt, J., and B. L. Moiseiwitsch, 1970, J. Phys. B **3**, 892.
Hutt, P. K., 1975, J. Phys. B **8**, L88.
Hutt, P. K., and B. H. Bransden, 1974, J. Phys. B **7**, 2223.
Huzinaga, S., and A. Hart-Davis, 1973, Phys. Rev. A **8**, 1734.
Imhof, R. E., A. Adams, and G. C. King, 1976, J. Phys. E **9**, 138.
Ishihara, T., and T. C. Foster, 1974, Phys. Rev. A **9**, 2350.
Johnson, C. T., P. G. Burke, and A. E. Kingston, 1987, J. Phys. B **20**, 2553.
Johnson, H. R., and F. Rohrlich, 1959, J. Chem. Phys. **30**, 1608.
Johnson, W. R., J. Sapirstein, and S. A. Blundell, 1989, J. Phys. B **22**, 2341.
Johnston, A. R., 1983, Ph.D. thesis (University of Nebraska).
Johnston, A. R., and P. D. Burrow, 1979, Bull. Am. Phys. Soc. **24**, 1189.
Johnston, A. R., and P. D. Burrow, 1982, J. Phys. B **15**, L745.
Johnston, A. R., G. A. Gallup, and P. D. Burrow, 1989, Phys. Rev. A **40**, 4770.
Jongerius, H. M., 1961, Philips Res. Rep. Suppl. No. 2.
Jost, K., 1979a, J. Phys. E **12**, 1001.
Jost, K., 1979b, J. Phys. E **12**, 1006.
Jost, K., P. G. F. Bisling, F. Eschen, M. Felsmann, and L. Walther, 1983, in *Electronic and Atomic Collisions—Abstracts of Contributed Papers,* edited by J. Eichler, W. Fritsch, I. V. Hertel, N. Stolterfoht, and U. Wille (North-Holland, Amsterdam), p. 91.
Jost, K., and B. Ohnemus, 1979, Phys. Rev. A **19**, 641.
Jung, K., 1980, in *Electronic and Atomic Collisions, Invited Papers,* XI ICPEAC, Kyoto, 1979, edited by N. Oda and K. Takayanagi (North-Holland, Amsterdam), p. 787.
Jung, K., Th. Antoni, R. Müller, K.-H. Kochem, and H. Ehrhardt, 1982, J. Phys. B **15**, 3535.
Junker, B. R., 1982a, Adv. At. Mol. Phys. **18**, 207.
Junker, B. R., 1982b, J. Phys. B **15**, 4495.
Jureta, J., S. Cvejanovic, J. N. H. Brunt, and F. H. Read, 1978, J. Phys. B **11**, L347.
Kaiser, H. J., E. Heinicke, H. Baumann, and K. Bethge, 1971, Z. Phys. **243**, 46.
Karstensen, F., and H. Köster, 1971, Astron. Astrophys. **13**, 116.
Karule, E., 1965, *Riga Conference on Atomic Collisions* (Trudy Inst. Fiz. Akad. Nauk. Latv. SSR **3**, 1 [JILA translation No. 3 (1966)].
Karule, E., 1972, J. Phys. B **5**, 2051.
Kaufman, M., 1963, Astrophys. J. **137**, 1296.
Kaulakys, B., 1982, J. Phys. B **17**, L719.
Kaussen, F., H. Geesmann, G. F. Hanne, and J. Kessler, 1987, J. Phys. B **20**, 151.
Kazakov, S. M., A. I. Korotkov, and O. B. Shpenik, 1980, Zh. Eksp. Teor. Fiz. **78**, 1687 [Sov. Phys. JETP **51**, 847 (1980)].
Kazakov, S. M., and O. V. Khristoforov, 1982, Zh. Eksp. Teor. Fiz. **82**, 1772 [Sov. Phys. JETP **55**, 1023 (1982)].
Kazakov, S. M., and O. V. Khristoforov, 1985, Sov. Phys. Tech. Phys. **30**, 476.
Keesing, R. G. W., 1977, Proc. R. Soc. London Ser. A **352**, 429.
Kellman, M. E., and D. R. Herrick, 1980, Phys. Rev. A **22**, 1536.
Kennerly, R. E., R. A. Bonham, and M. McMillan, 1979, J. Chem. Phys. **70**, 2039.
Kennerly, R. E., R. J. van Brunt, and A. C. Gallagher, 1981, Phys. Rev. A **23**, 2430.
Kilius, L. R., M. A. Garwan, A. E. Litherland, M.-J. Nadeau, J. C. Rucklidge, and X.-L. Zhao, 1989, Nucl. Instrum. Methods Phys. Res. B **40**, 745.
Kim, L., and C. H. Greene, 1989, J. Phys. B **22**, L175.
Kisker, E., 1972a, Phys. Lett. A **38**, 79.
Kisker, E., 1972b, Phys. Lett. A **41**, 173.
Kisker, E., 1982, Rev. Sci. Instrum. **53**, 114.
Klar, H., 1986a, Phys. Rev. Lett. **57**, 66.
Klar, H., 1986b, Few Body Sys. **1**, 123.
Klar, H., 1987a, J. Opt. Soc. Am. B **4**, 788.
Klar, H., 1987b, Comments At. Mol. Phys. **19**, 171.
Klar, H., and M. Klar, 1980, J. Phys. B **13**, 1057.
Klar, H., P. Zoller, and M. V. Fedorov, 1985, Acta Phys. Austriaca **57**, 157.
Klemperer, O., and M. E. Barnett, 1971, *Electron Optics* (Cambridge University, Cambridge, England).
Knoop, F. W. E., and H. H. Brongersma, 1970, Chem. Phys. Lett. **5**, 450.
Koch, L., T. Heindorff, and E. Reichert, 1984, Z. Phys. A **316**, 127.
Komninos, Y., G. Aspromallis, and C. A. Nicolaides, 1983, Phys. Rev. A **27**, 1865.
Komninos, Y., M. Chrysos, and C. A. Nicolaides, 1987, J. Phys. B **20**, L791.
Komninos, Y., M. Chrysos, and C. A. Nicolaides, 1988, Phys. Rev. A **38**, 1365.
Korotkov, A. I., 1970, Opt. Spectrosc. (USSR) **28**, 347.
Koschmieder, H., V. Raible, and H. Kleinpoppen, 1973, Phys. Rev. A **8**, 3182.
Koyama, N., H. Fukuda, T. Motoyama, and M. Matsuzawa, 1986, J. Phys. B **19**, L331.
Koyama, N., A. Takafuji, and M. Matsuzawa, 1989, J. Phys. B **22**, 553.
Krause, H. F., S. G. Johnson, and S. Datz, 1977, Phys. Rev. A **15**, 611.
Krause, J. L., and R. S. Berry, 1986, Comments At. Mol. Phys. **18**, 91.
Krylstedt, P., N. Elander, and E. Brändas, 1988, J. Phys. B **21**, 3969.
Krylstedt, P., M. Rittby, N. Elander, and E. Brändas, 1987, J. Phys. B **20**, 1295.
Kurepa, M. V., M. D. Tasic, and J. J. Kurepa, 1974, J. Phys. E **7**, 940.

Kurtz, H. A., and K. D. Jordan, 1981, J. Phys. B **14**, 4361.
Kurtz, H. A., and Y. Öhrn, 1979, Phys. Rev. A **19**, 43.
Kuyatt, C. E., and J. A. Simpson, 1967, Rev. Sci. Instrum. **38**, 103.
Kuyatt, C. E., J. A. Simpson, and S. R. Mielczarek, 1965, Phys. Rev. **138**, A385.
Langendam, P. J. K., and M. J. Van der Wiel, 1978, J. Phys. B **11**, 3603.
Langhans, L., 1978, J. Phys. B **11**, 2361.
Langmuir, I., 1921, Phys. Rev. **17**, 339.
Le Dourneuf, M., 1976, These de Doctorat d'État (Université Paris).
Le Dourneuf, M., 1978, in *Electronic and Atomic Collisions, Invited Papers and Progress Reports,* Xth ICPEAC, Paris, 1977, edited by G. Watel (North-Holland, Amsterdam), p. 143.
Le Dourneuf, M., and Vo Ky Lan, 1977a, J. Phys. B **10**, L97.
Le Dourneuf, M., and Vo Ky Lan, 1977b, in *États atomiques et moléculaires couplés a un continuum atomes et molécules hautment excités,* Colloques Internationaux du C.N.R.S. no. 273 (CNRS, Paris), p. 235.
Le Dourneuf, M., Vo Ky Lan, and P. G. Burke, 1977, Comments At. Mol. Phys. **7**, 1.
Le Dourneuf, M., and S. Watanabe, 1984, *10e Colloque sur la Physique des Collisions Atomiques et Electroniques, Aussois, Conferences Invitees* (CNRS, Paris), p. 65.
Le Dourneuf, M., and S. Watanabe, 1990, J. Phys. B **23**, 3205.
Lee, N., and A. K. Edwards, 1975, Phys. Rev. A **11**, 1768.
Leep, D., and A. Gallagher, 1976, Phys. Rev. A **13**, 148.
Lefaivre, D., and P. Marmet, 1975, Int. J. Mass Spectrom. Ion Phys. **18**, 153.
Lin, C. D., 1974, Phys. Rev. A **10**, 1986.
Lin, C. D., 1975, Phys. Rev. Lett. **35**, 1150.
Lin, C. D., 1981, Phys. Rev. A **23**, 1585.
Lin, C. D., 1982a, Phys. Rev. A **25**, 76.
Lin, C. D., 1982b, Phys. Rev. A **25**, 1535.
Lin, C. D., 1983a, Phys. Rev. A **28**, 99.
Lin, C. D., 1983b, Phys. Rev. A **28**, 1876.
Lin, C. D., 1983c, J. Phys. B **16**, 723.
Lin, C. D., 1983d, Phys. Rev. Lett. **51**, 1348.
Lin, C. D., 1984, Phys. Rev. A **29**, 1019.
Lin, C. D., 1986, Adv. At. Mol. Phys. **22**, 77.
Lin, C. D., 1987, Comments At. Mol. Phys. **19**, 89.
Lin, C. D., and S. Watanabe, 1987, Phys. Rev. A **35**, 4499.
Lipsky, L., R. Anania, and M. J. Conneely, 1977, At. Data Nucl. Data Tables **20**, 127.
Litherland, A. E., L. R. Kilius, M. A. Garwan, M-J. Nadeau, and X.-L. Zhao, 1991, J. Phys. B **24**, L233.
Liu, C.-R., and A. F. Starace, 1989, Phys. Rev. Lett. **62**, 407.
MacArthur, D. W., K. B. Butterfield, D. A. Clark, J. B. Donahue, P. A. M. Gram, H. C. Bryant, C. J. Harvey, and G. Comtet, 1985, Phys. Rev. A **32**, 1921.
Macek, J., 1966, Phys. Rev. **146**, 50.
Macek, J., 1967, Phys. Rev. **160**, 170.
Macek, J., 1968, J. Phys. B **1**, 831.
Macek, J., 1970, Phys. Rev. A **2**, 1101.
Macek, J., and A. K. Edwards, 1982, Phys. Rev. A **25**, 881.
Macek, J., and J. M. Feagin, 1985, J. Phys. B **18**, 2161.
Makarewicz, J., 1989, J. Phys. B **22**, L235.
Mandl, A., and H. A. Hyman, 1973, Phys. Rev. Lett. **31**, 417.
Marchand, P., and J. Cardinal, 1979, Can. J. Phys. **57**, 1624.
Maria, H. J., J. L. Meeks, P. Hochmann, J. F. Arnett, and S. P. McGlynn, 1973, Chem. Phys. Lett. **19**, 309.
Marriott, R., and M. Rotenberg, 1968, Phys. Rev. Lett. **21**, 722.
Martin, W. C., J. Sugar, and J. L. Tech, 1972, Phys. Rev. A **6**, 2022.
Martin, W. C., and R. Zalubas, 1979, J. Phys. Chem. Ref. Data **8**, 817.
Martin, W. C., and R. Zalubas, 1980, J. Phys. Chem. Ref. Data **9**, 1.
Martinez, G., and M. Sancho, 1983, J. Phys. E **16**, 625.
Martinez, G., M. Sancho, and F. H. Read, 1983, J. Phys. E **16**, 631.
Massey, H. S. W., 1976, *Negative Ions,* 3rd ed. (Cambridge University Press, Cambridge, England).
Matese, J. J., 1974, Phys. Rev. A **10**, 454.
Matese, J. J., S. P. Rountree, and R. J. W. Henry, 1972, Phys. Rev. A **7**, 846.
Matese, J. J., S. P. Rountree, and R. J. W. Henry, 1973, Phys. Rev. A **8**, 2965.
Mazeau, J., F. Gresteau, R. I. Hall, and A. Huetz, 1978, J. Phys. B **11**, L557.
Mazeau, J., F. Gresteau, R. I. Hall, G. Joyez, and J. Reinhardt, 1973, J. Phys. B **6**, 862.
McCurdy, C. W., J. G. Lauderdale, and R. C. Mowrey, 1981, J. Chem. Phys. **75**, 1835.
McCurdy, C. W., T. N. Rescigno, E. R. Davidson, and J. G. Lauderdale, 1980, J. Chem. Phys. **73**, 3268.
McCutchen, C. W., 1958, Phys. Rev. **112**, 1848.
McGowan, J. W., J. F. Williams, and E. K. Curley, 1969, Phys. Rev. **180**, 132.
McMillan, M. R., and J. H. Moore, 1980, Rev. Sci. Instrum. **51**, 944.
McNutt, J. F., and C. W. McCurdy, 1983, Phys. Rev. A **27**, 132.
Mercouris, T., and C. A. Nicolaides, 1991, J. Phys. **24**, L557.
Miller, T. M., B. B. Aubrey, P. N. Eisner, and B. Bederson, 1970, Bull. Am. Phys. Soc. **15**, 416.
Miller, T. M., and B. Bederson, 1977, Adv. At. Mol. Phys. **13**, 1.
Mishra, M., O. Goscinski, and Y. Öhrn, 1983, J. Chem. Phys. **79**, 5505.
Mishra, M., H. A. Kurtz, O. Goscinski, and Y. Öhrn, 1983, J. Chem. Phys. **79**, 1896.
Mitchell, P., J. A. Baxter, J. Comer, and P. J. Hicks, 1980, J. Phys. B **13**, 4481.
Moiseiwitsch, B. L., 1965, in *Advances in Atomic and Molecular Physics, Vol. 1,* edited by D. R. Bates and I. Estermann (Academic, New York), p. 61.
Mølmer, K., and K. Taulbjerg, 1988, J. Phys. B **21**, 1739.
Molof, R. W., H. L. Schwartz, T. M. Miller, and B. Bederson, 1974, Phys. Rev. A **10**, 1131.
Moore, C. E., 1970, *Selected Tables of Atomic Spectra: C I, C II, C III, ,C IV, C V, C VI,* NSRDS-NBS 3, Sec. 3 (U.S. GPO, Washington, D.C.).
Moore, C. E., 1971, *Atomic Energy Levels,* NSRDS-NBS 35, Vols. 1–3 (U.S. GPO, Washington D.C.).
Moore, C. E., 1975, *Selected Tables of Atomic Spectra: N I, N II, N III,* NSRDS-NBS 3, Sec. 5 (U.S. GPO, Washington, DC).
Moores, D. L., 1976, J. Phys. B **9**, 1329.
Moores, D. L., and D. W. Norcross, 1972, J. Phys. B **5**, 1482.
Moores, D. L., and D. W. Norcross, 1974, Phys. Rev. A **10**, 1646.
Morgan, J. D., III, 1986, Theor. Chim. Acta **69**, 181.
Morgan, L. A., M. R. C. McDowell, and J. Callaway, 1977, J. Phys. B **10**, 3297.
Msezane, A. Z., and R. J. W. Henry, 1986, Phys. Rev. A **33**, 1631.
Nakamura, Y., and J. Lucas, 1978a, J. Phys. D **11**, 325.
Nakamura, Y., and J. Lucas, 1978b, J. Phys. D **11**, 337.
Natali, S., D. DiChio, E. Uva, and C. E. Kuyatt, 1972, Rev. Sci.

Instrum. **43**, 80.
Neiger, M., 1973, 11 ICPIG Abs. **30A**, 474.
Neiger, M., 1975, Z. Naturforsch. Teil A **30**, 474.
Nesbet, R. K., 1975, Phys. Rev. A **12**, 444.
Nesbet, R. K., 1977, Adv. At. Mol. Phys. **13**, 315.
Nesbet, R. K., 1978, J. Phys. B **11**, L21.
Nesbet, R. K., 1980a, J. Phys. B **13**, L193.
Nesbet, R. K., 1980b, *Variational Methods in Electron-Atom Scattering Theory* (Plenum, New York).
Nesbet, R. K., 1982, private communication cited in Junker, 1982b.
Newman, D. S., M. Zubek, and G. C. King, 1985, J. Phys. B **18**, 985.
Neynaber, R. H., L. L. Marino, E. W. Rothe, and S. M. Trujillo, 1963, Phys. Rev. **129**, 2069.
Nickel, J. C., K. Imre, D. F. Register, and S. Trajmar, 1985, J. Phys. B **18**, 125.
Nicolaides, C. A., 1972, Phys. Rev. A **6**, 2078.
Nicolaides, C. A., G. Aspromallis, and D. R. Beck, 1989, J. Mol. Struct. **199**, 283.
Nicolaides, C. A., and Y. Komninos, 1987, Phys. Rev. A **35**, 999.
Nicolaides, C. A., Y. Komninos, and D. R. Beck, 1981, Chim. Chron. **10**, 35.
Nighan, W. L., and A. J. Postma, 1972, Phys. Rev. A **6**, 2109.
Norcross, D. W., 1971, J. Phys. B **4**, 1458.
Norcross, D. W., and D. L. Moores, 1972, in *Atomic Physics 3*, edited by S. J. Smith and G. K. Walters (Plenum, New York), p. 261.
Noro, T., F. Sasaki, and H. Tatewaki, 1979, J. Phys. B **12**, 2217.
Nuttall, J., 1972, communication cited in Bardsley and Junker, 1972.
Nuttall, J., 1979, Comments At. Mol. Phys. **9**, 15.
Oberoi, R. S., 1972, J. Phys. B **5**, 1120.
Oberoi, R. S., and R. K. Nesbet, 1973, Phys. Rev. A **8**, 2969.
Ojha, P. C., P. G. Burke, and K. T. Taylor, 1982, J. Phys. B **15**, L507.
Olmsted, J., A. S. Newton, and K. Street, 1965, J. Chem. Phys. **42**, 2321.
Ormonde, S., 1977, Phys. Rev. Lett. **38**, 690.
Ormonde, S., F. B. Kets, and H. G. M. Heideman, 1974, Phys. Lett. A **50**, 147.
Ormonde, S., K. Smith, B. W. Torres, and A. R. Davies, 1973, Phys. Rev. A **8**, 262.
Ott, W. R., J. Slater, J. Cooper, and G. Gieres, 1975, Phys. Rev. A **12**, 2009.
Ottley, T. W., and H. Kleinpoppen, 1975, J. Phys. B **8**, 621.
Palenius, H. P., 1968, Ark. Fys. **39**, 425.
Palenius, H. P., R. E. Huffman, J. C. Larrabee, and Y. Tanaka, 1978, J. Opt. Soc. Am. **68**, 1564.
Palmer, R. E., and P. J. Rous, 1992, Rev. Mod. Phys. **64**, 383.
Paske, W. C., S. Shadfar, S. R. Lorentz, N. C. Steph, and D. E. Golden, 1981, Rev. Sci. Instrum. **52**, 1296.
Pathak, A., P. G. Burke, and K. A. Berrington, 1989, J. Phys. B **22**, 2759.
Pathak, A., A. E. Kingston, and K. A. Berrington, 1988, J. Phys. B **21**, 2939.
Patterson, T. A., H. Hotop, A. Kasdan, D. W. Norcross, and W. C. Lineberger, 1974, Phys. Rev. Lett. **32**, 189.
Peart, B., and K. T. Dolder, 1973, J. Phys. B **6**, 1497.
Peart, B., R. A. Forrest, and K. T. Dolder, 1979a, J. Phys. B **12**, 847.
Peart, B., R. A. Forrest, and K. T. Dolder, 1979b, J. Phys. B **12**, 2735.
Pegg, D. J., J. S. Thompson, R. N. Compton, and G. D. Alton, 1987, Phys. Rev. Lett. **59**, 2267.
Peterkop, R., 1974, J. Phys. B **4**, 513.
Peterson, J. R., 1992, Aust. J. Phys. **45**, 293.
Peterson, J. R., Y. K. Bae, and D. L. Heustis, 1985, Phys. Rev. Lett. **55**, 692.
Peterson, J. R., M. J. Coggiola, and Y. K. Bae, 1983, Phys. Rev. Lett. **50**, 664.
Phillips, J. M., 1982, J. Phys. B **15**, 4259.
Phillips, J. M., and S. F. Wong, 1981, Phys. Rev. A **23**, 3324.
Pichanick, F. M. J., and J. A. Simpson, 1968, Phys. Rev. **168**, 64.
Pichou, F., A. Heutz, G. Joyez, M. Landau, and J. Mazeau, 1976, J. Phys. B **9**, 933.
Pople, J. A., and P. Schofield, 1957, Philos. Mag. **2**, 591.
Popp, H.-P., 1974, Vacuum **24**, 551.
Postma, A. J., 1969a, Physica **43**, 229.
Postma, A. J., 1969b, Physica **43**, 465.
Postma, A. J., 1969c, Physica **44**, 38.
Poulin, A., and D. Roy, 1978, J. Phys. E **11**, 35.
Prat, R. F., 1972, Phys. Rev. A **6**, 1735.
Quemener, J. J., C. Paquet, and P. Marmet, 1971, Phys. Rev. A **4**, 494.
Rabin, Y., and F. Rebentrost, 1982, Opt. Commun. **40**, 257.
Radojevic, V., H. P. Kelly, and W. R. Johnson, 1987, Phys. Rev. A **35**, 2117.
Radziemski, L. J., and V.Kaufman, 1969, J. Opt. Soc. Am. **59**, 424.
Raible, V., H. Koschmeider, and H. Kleinpoppen, 1974, J. Phys. B **7**, L14.
Raith, W., 1976, Adv. Mol. Phys. **12**, 281.
Ramsauer, C., 1921, Ann. Phys. (Leipzig) **66**, 546.
Rau, A. R. P., 1971, Phys. Rev. A **4**, 207.
Rau, A. R. P., 1983, J. Phys. B **16**, L699.
Rau, A. R. P., 1984a, Pramana **23**, 297.
Rau, A. R. P., 1984b, J. Phys. B **17**, L75.
Rau, A. R. P., 1984c, in *Atomic Physics* **9**, edited by R. S. Van Dyck, Jr., and E. N. Fortson (World Scientific, Singapore), p. 491.
Rau, A. R. P., 1986, in *Atoms in Unusual Situations*, edited by J.-P. Briand (Plenum, New York), p. 383.
Rau, A. R. P., 1991, Nucl. Instrum. Methods B **56**, 200.
Rau, A. R. P., and U. Fano, 1968, Phys. Rev. **167**, 7.
Read, F. H., 1974, private communication to H. G. M. Heideman.
Read, F. H., 1975, J. Phys. B **8**, 1034.
Read, F. H., 1977, J. Phys. B **10**, 449.
Read, F. H., 1982, Aust. J. Phys. **35**, 475.
Read, F. H., 1983, Phys. Scr. **27**, 103.
Read, F. H., 1990, J. Phys. B **23**, 951.
Read, F. H., A. Adams, and J. R. Soto-Montiel, 1971, J. Phys. E **4**, 625.
Read, F. H., J. N. H. Brunt, and G. C. King, 1976, J. Phys. B **9**, 2209.
Read, F. H., J. Comer, R. E. Imhof, J. N. H. Brunt, and E. Harting, 1974, J. Electron Spectrosc. Relat. Phenom. **4**, 293.
Reader, J., 1974, J. Opt. Soc. Am. **64**, 1017.
Reddish, T., B. Wallbank, and J. Comer, 1984, J. Phys. E **17**, 100.
Rehmus, P., and R. S. Berry, 1979, Chem. Phys. **38**, 257.
Reichert, E., 1986, private communication.
Reichert, E., and H. Deichsel, 1967, Phys. Lett. A **25**, 560.
Reinhardt, W. P., 1982, Annu. Rev. Phys. Chem. **33**, 223.
Rescigno, T. N., C. F. Bender, and B. V. McKoy, 1978, Phys.

Rev. A **17**, 645.
Rescigno, T. N., A. U. Hazi, and N. Winter, 1977, Phys. Rev. A **16**, 2488.
Rescigno, T. N., C. W. McCurdy, Jr., and A. E. Orel, 1978, Phys. Rev. A **17**, 1931.
Richter, K., and D. Wintgen, 1990, J. Phys. B **23**, L197.
Risley, J. S., 1972, Rev. Sci. Instrum. **43**, 95.
Risley, J. S., 1980, in *Electronic and Atomic Collisions,* Proceedings of the XIth ICPEAC, Kyoto, 1979, edited by N. Oda and K. Takayanagi (North-Holland, Amsterdam), p. 619.
Risley, J. S., A. K. Edwards, and R. Geballe, 1974, Phys. Rev. A **9**, 1115.
Risley, J. S., and R. Geballe, 1974, Phys. Rev. A **10**, 2206.
Robb, W. D., and R. J. W. Henry, 1977, Phys. Rev. A **16**, 2491.
Robinson, E. J., 1969, Phys. Rev. **182**, 196.
Rockwood, S. D., 1973, Phys. Rev. A **8**, 2348.
Rohr, K., and F. Linder, 1976, J. Phys. B **9**, 2521.
Romanyuk, N. I., O. B. Shpenik, and I. P. Zapesochnyĭ, 1980, Pis'ma Zh. Eksp. Teor. Fiz. **32**, 472 [JETP Lett. **32**, 452 (1980)].
Rost, J. M., and J. S. Briggs, 1988, J. Phys. B **21**, L233.
Rost, J. M., R. Gersbacher, K. Richter, J. S. Briggs, and D. Wintgen, 1991, J. Phys. B **24**, 2455.
Rountree, S. P., and R. J. W. Henry, 1972, Phys. Rev. A **6**, 2106.
Roy, D., and J.-D. Carette, 1974, J. Phys. B **7**, L536.
Roy, D., and J.-D. Carette, 1975, J. Phys. B **8**, L157.
Roy, D., A. Delâge, and J.-D. Carette, 1975a, Phys. Rev. A **12**, 45.
Roy, D., A. Delâge, and J.-D. Carette, 1975b, J. Phys. E **8**, 109.
Roy, D., A. Delâge, and J.-D. Carette, 1976, J. Phys. B **9**, 1923.
Roy, D., A. Delâge, and J.-D. Carette, 1978a, J. Phys. B **11**, 895.
Roy, D., A. Delâge, and J.-D. Carette, 1978b, J. Phys. B **11**, 4059.
Sadeghpour, H. R., 1991, Phys. Rev. A **43**, 5821.
Sadeghpour, H. R., and C. H. Greene, 1990, Phys. Rev. Lett. **65**, 313.
Saelee, H. T., and J. Lucas, 1979, J. Phys. D **12**, 1275.
Sanche, L., and P. D. Burrow, 1972, Phys. Rev. Lett. **29**, 1639.
Sanche, L., and G. J. Schulz, 1972a, Phys. Rev. A **5**, 1672.
Sanche, L., and G. J. Schulz, 1972b, Phys. Rev. A **6**, 69.
Sanche, L., and G. J. Schulz, 1972c, Phys. Rev. A **6**, 2500.
Sar-El, H. Z., 1970, Rev. Sci. Instrum. **41**, 561.
Sawada, T., J. E. Purcell, and A. E. S. Green, 1971, Phys. Rev. A **4**, 193.
Sawey, P. M. J., K. A. Berrington, P. G. Burke, and A. E. Kingston, 1990, J. Phys. B **23**, 4321.
Schaefer, III, H. F., and F. E. Harris, 1968, Phys. Rev. Lett. **23**, 1561.
Schaefer, III, H. F., R. A. Klemm, and F. E. Harris, 1969, J. Chem. Phys. **51**, 4643.
Scheibner, K. F., and A. U. Hazi, 1988, Phys. Rev. A **38**, 539.
Scheibner, K. F., and A. U. Hazi, 1989, in *Electronic and Atomic Collisions, Abstracts of Contributed Papers,* XVI ICPEAC, New York, edited by A. Dalgarno *et al.* (North-Holland, Amsterdam), p. 27.
Scheibner, K. F., A. U. Hazi, and R. J. W. Henry, 1987, Phys. Rev. A **35**, 4869.
Schowengerdt, F. D., and D. E. Golden, 1974, Rev. Sci. Instrum. **45**, 391.
Schulz, G. J., 1958, Phys. Rev. **112**, 150.
Schulz, G. J., 1963, Phys. Rev. Lett. **10**, 104.
Schulz, G. J., 1973a, Rev. Mod. Phys. **45**, 378.
Schulz, G. J., 1973b, Rev. Mod. Phys. **45**, 423.
Schulz, G. J., and R. E. Fox, 1957, Phys. Rev. **106**, 1179.
Scott, N. S., K. Bartschat, P. G. Burke, W. B. Eissner, and O. Nagy, 1984a, J. Phys. B **17**, L191.
Scott, N. S., K. Bartschat, P. G. Burke, O. Nagy, and W. B. Eissner, 1984b, J. Phys. B **17**, 3755.
Scott, N. S., K. L. Bell, P. G. Burke, and K. T. Taylor, 1982, J. Phys. B **15**, L627.
Scott, N. S., P. G. Burke, and K. Bartschat, 1983, J. Phys. B **16**, L361.
Scott, N. S., and K. T. Taylor, 1982, Comput. Phys. Commun. **25**, 347.
Seiler, G. J., R. S. Oberoi, and J. Callaway, 1971, Phys. Rev. A **3**, 2006.
Sharp, J. M., J. Comer, and P. J. Hicks, 1975, J. Phys. B **8**, 2512.
Sharpton, F. A., R. M. St. John, C. C. Lin, and F. E. Fajen, 1970, Phys. Rev. A **2**, 1305.
Shimon, L. L., and É. I. Nepiĭpov, 1974, Ukr. Fiz. Zh. **19**, 627.
Shimon, L. L., É. I. Nepiĭpov, and I. P. Zapesochnyĭ, 1972, Ukr. Fiz. Zh. **17**, 1955.
Shimon, L. L., E. I. Nepiĭpov, and I. P. Zapesochnyĭ, 1975, Ukr. Fiz. Zh. **20**, 229.
Shimon, L. L., É. I. Nepiĭpov, V. L. Golodovsky, and N. V. Golovchak, 1975, Ukr. Fiz. Zh. **20**, 233.
Shpenik, O. B., V. V. Souter, A. N. Zavilopulo, I. P. Zapesochnyĭ, and E. É. Kontrosh, 1975, Zh. Eksp. Teor. Fiz. **69**, 48 [Sov. Phys. JETP **42**, 23 (1976)].
Shpenik, O. B., I. P. Zapesochnyĭ, E. É. Kontrosh, É. I. Nepiĭpov, N. I. Romanyuk, and V. V. Sovter, 1979, Zh. Eksp. Teor. Fiz. **76**, 846 [Sov. Phys. JETP **49**, 426 (1979)].
Shpenik, O. B., I. P. Zapesochnyĭ, V. V. Sovter, E. É. Kontrosh, and A. N. Zavilopulo, 1973, Zh. Eksp. Teor. Fiz. **65**, 1797 [Sov. Phys. JETP **38**, 898 (1974)].
Siegert, A. J. F., 1939, Phys. Rev. **56**, 750.
Simon, B., 1972, Commun. Math. Phys. **27**, 1.
Simon, B., 1973, Ann. Math. **97**, 247.
Simon, B., 1974, Math. Ann. **207**, 133.
Simpson, J. A., 1964, in *Atomic Collision Processes,* Proceedings of the III ICPEAC, London, 1963, edited by M. R. C. McDowell (North-Holland, Amsterdam), p. 128.
Simpson, J. A., and U. Fano, 1963, Phys. Rev. Lett. **11**, 158.
Simpson, J. A., M. G. Menendez, and S. R. Mielczarek, 1966, Phys. Rev. **150**, 76.
Sinanoğlu, O., and D. R. Herrick, 1975, J. Chem. Phys. **62**, 886.
Sinfailam, A. L., and W. E. Baylis, 1981, J. Phys. B **14**, 559.
Sinfailam, A. L., and R. K. Nesbet, 1972, Phys. Rev. A **6**, 2118.
Sinfailam, A. L., and R. K. Nesbet, 1973, Phys. Rev. A **7**, 1987.
Sinfailam, L. T., 1980, Aust. J. Phys. **33**, 261.
Sinfailam, L. T., 1981, J. Phys. B **14**, L437.
Slater, J. C., 1960, *Quantum Theory of Atomic Structure, Vol. II* (McGraw-Hill, New York).
Slater, J., F. H. Read, S. E. Novick, and W. C. Lineberger, 1978, Phys. Rev. A **17**, 201.
Slevin, J., and W. Sterling, 1981, Rev. Sci. Instrum. **52**, 1780.
Smit, C., and H. M. Fijnaut, 1965, Phys. Lett. **19**, 121.
Smith, W. W., C. Harvey, J. E. Stewart, H. C. Bryant, K. B. Butterfield, D. A. Clark, J. B. Donahue, P. A. M. Gram, D. MacArthur, G. Comtet, and T. Bergeman, 1985, in *Atomic Excitation and Recombination in External Fields,* edited by M. H. Nayfeh and C. W. Clark (Gordon and Breach, New York), p. 211.
Smith. A. J., P. J. Hicks, F. H. Read, S. Cvejanovic, G. C. M. King, J. Comer, and J. M. Sharp, 1974, J. Phys. B **7**, L499.

Spence, D., 1974, Phys. Rev. A **10**, 1045.
Spence, D., 1975a, J. Phys. B **8**, L42.
Spence, D., 1975b, Phys. Rev. A **12**, 721.
Spence, D., 1977, Phys. Rev. A **15**, 883.
Spence, D., 1980, J. Phys. B **13**, 1611.
Spence, D., 1981, J. Phys. B **14**, 129.
Spence, D., and P. D. Burrow, 1979, J. Phys. B **12**, L179.
Spence, D., and W. A. Chupka, 1974, Phys. Rev. A **10**, 71.
Spence, D., and M. Inokuti, 1974, J. Quant. Spectrosc. Radiat. Transfer **14**, 953.
Spence, D., and T. Noguchi, 1975, J. Chem. Phys. **63**, 505.
Stamatovic, A., and G. J. Schulz, 1968, Rev. Sci. Instrum. **39**, 1752.
Stamatovic, A., and G. J. Schulz, 1970, Rev. Sci. Instrum. **41**, 423.
Starodub, V. P., I. S. Aleksahkin, I. I. Garga, and I. P. Zapesochnyĭ, 1973, Opt. Spektrosk. **35**, 1037 [Opt. Spectrosc. (USSR) **35**, 603 (1973)].
Steckelmacher, W., 1973, J. Phys. E **6**, 1061.
Stefanov, B., 1978, J. Phys. B **11**, L249.
Stewart, R. F., C. Laughlin, and G. A. Victor, 1974, Chem. Phys. Lett. **29**, 353.
Stoicheff, B. P., D. C. Thompson, and E. Weinberger, 1981, in *Spectral Line Shapes,* Proceedings of the 5th International Conference, Berlin, edited by B. Wende (de Gruyter, Berlin), p. 1071.
Swanson, N., R. J. Celotta, and C. E. Kuyatt, 1976, in *Electron and Photon Interactions with Atoms,* edited by H. Kleinpoppen and M. R. C. McDowell (Plenum, New York), p. 661.
Swanson, N., J. W. Cooper, and C. E. Kuyatt, 1973, Phys. Rev. A **8**, 1825.
Taylor, A. J., and P. G. Burke, 1967, Proc. Phys. Soc. London **92**, 336.
Taylor, H. S., 1970, Adv. Chem. Phys. **18**, 91.
Taylor, H. S., and L. D. Thomas, 1972, Phys. Rev. Lett. **28**, 1091.
Taylor, K. T., C. W. Clark, and W. C. Fon, 1985, J. Phys. B **18**, 2967.
Taylor, K. T., and D. W. Norcross, 1986, Phys. Rev. A **34**, 3878.
Tech, J. L., 1963, J. Res. Nat. Bur. Stand. A **67**, 505.
Temkin, A., and A. K. Bhatia, 1985, in *Autoionization: Recent Developments and Applications,* edited by A. Temkin (Plenum, New York), p. 1.
Temkin, A., A. K. Bhatia, and J. N. Bardsley, 1972, Phys. Rev. A **5**, 1663.
Thomas, G. E., and F. E. Vogelsberg, 1971, Rev. Sci. Instrum. **42**, 161.
Thomas, L. D., 1974, J. Phys. B **7**, L97.
Thomas, L. D., and R. K. Nesbet, 1975a, Phys. Rev. A **12**, 2369.
Thomas, L. D., and R. K. Nesbet, 1975b, Phys. Rev. A **12**, 2378.
Thomas, L. D., R. S. Oberoi, and R. K. Nesbet, 1974, Phys. Rev. A **10**, 1605.
Thumm, U., and D. W. Norcross, 1991, Phys. Rev. Lett. **67**, 3495.
Valin, M., and P. Marmet, 1975, J. Phys. B **8**, 2593.
Van Blerkom, J. K., 1970, J. Phys. B **3**, 932.
van den Brink, J. P., 1990, private communication to Batelaan *et al.*
van der Burgt, P. J. M., and H. G. M. Heideman, 1985, J. Phys. B **18**, L755.
van der Burgt, P. J. M., J. van Eck, and H. G. M. Heideman, 1985a, J. Phys. B **18**, 999.
van der Burgt, P. J. M., J. van Eck, and H. G. M. Heideman, 1985b, J. Phys. B **18**, L171.
van der Burgt, P. J. M., J. van Eck, and H. G. M. Heideman, 1986, J. Phys. B **19**, 2015.
Veillette, P., and P. Marchand, 1974, Can. J. Phys. **52**, 930.
Veillette, P., and P. Marchand, 1975, Int. J. Mass Spect. Ion Phys. **18**, 165.
Veillette, P., and P. Marchand, 1976, Can. J. Phys. **54**, 1208.
Visconti, P. J., J. A. Slevin, and K. Rubin, 1971, Phys. Rev. A **3**, 1310.
Vosko, S. H., J. A. Chevary, and I. L. Mayer, 1991, J. Phys. B **24**, L225.
Vosko, S. H., J. B. Lagowski, and I. L. Mayer, 1989, Phys. Rev. A **39**, 446.
Walker, D. W., 1975, J. Phys. B **8**, L161.
Wallbank, B., S. Daviel, J. Comer, and P. Hicks, 1983, J. Phys. B **16**, 3065.
Walton, D. S., B. Peart, and K. T. Dolder, 1971, J. Phys. B **4**, 1343.
Wannier, G. J., 1953, Phys. Rev. **90**, 817.
Warner, C. D., G. C. King, P. Hammond, and J. Slevin, 1986, J. Phys. B **19**, 3297.
Warner, C. D., P. M. Rutter, and G. C. King, 1990, J. Phys. B **23**, 93.
Watanabe, S., 1982, Phys. Rev. A **25**, 2074.
Watanabe, S., 1986, J. Phys. B **19**, 1577.
Watanabe, S., U. Fano, and C. H. Greene, 1984, Phys. Rev. A **29**, 177.
Watanabe, S., and C. H. Greene, 1980, Phys. Rev. A **22**, 158.
Watanabe, S., and M. Le Dourneuf, 1990, J. Phys. B **23**, 3205.
Watanabe, S., M. Le Dourneuf, and L. Pelamourgues, 1982, J. Phys. (Paris) Colloq. **43**, C2-223.
Watanabe, S., and C. D. Lin, 1987, Phys. Rev. A **36**, 511.
Weingartshofer, A., J. K. Holmes, J. Sabbagh, and S. Chin, 1983, J. Phys. B **16**, 1805.
Weingartshofer, A., K. Willmann, and E. M. Clarke, 1974, J. Phys. B **7**, 79.
Weiss, A. W., 1968, Phys. Rev. **166**, 70.
Weiss, A. W., and M. Krauss, 1970, J. Chem. Phys. **52**, 4363.
Wendoloski, J. J., and W. P. Reinhardt, 1978, Phys. Rev. A **17**, 195.
Weyhreter, M., B. Barzick, and F. Linder, 1983, in *Electronic and Atomic Collisions, Abstracts of Contributed Papers,* XIII ICPEAC, Berlin, 1983, edited by J. Eichler, W. Fritsch, I. V. Hertel, N. Stolterfoht, and U. Wille (North-Holland, Amsterdam), p. 78.
Wijesundera, W. P., I. P. Grant, and P. H. Norrington, 1992a, Phys. B **25**, 2143.
Wijesundera, W. P., I. P. Grant, and P. H. Norrington, 1992b, J. Phys. B **25**, 2165.
Wilden, D. G., P. J. Hicks, and J. Comer, 1977, J. Phys. B **10**, 1477.
Williams, J. F., 1976a, in *Electron and Photon Interactions with Atoms* (Plenum, New York).
Williams, J. F., 1976b, J. Phys. B **9**, 1519.
Williams, J. F., 1985, in *Electronic and Atomic Collisions, Abstracts of Contributed Papers,* XIV ICPEAC, Palo Alto, 1985, edited by M. J. Coggiola, D. L. Huestis, and R. P. Saxon (North-Holland, Amsterdam), p. 181.
Williams, J. F., 1988, J. Phys. B **21**, 2107.
Williams, J. F., and J. W. McGowan, 1968, Phys. Rev. Lett. **21**, 719.
Williams, J. F., and B. A. Willis, 1974, J. Phys. B **7**, L61.

Wintgen, D., K. Richter, and G. Tanner, 1992, Chaos **2**, 19.
Wolcke, A., K. Bartschat, K. Blum, H. Borgmann, G. F. Hanne, and J. Kessler, 1983, J. Phys. B **16**, 639.
Wong, S.-F., 1981, *XII ICPEAC Satellite Symposium,* Goddard Space Flight Center; and private communication.
Yuan, J., and Z. Zhang, 1989, J. Phys. B **22**, 2751.
Zapesochnyĭ, I. P., L. L. Shimon, and É. I. Nepiĭpov, 1973, Ukr. Fiz. Zh. **18**, 1301.
Zapesochnyĭ, I. P., and O. B. Shpenik, 1966, Zh. Eksp. Teor. Fiz. **50**, 890 [Sov. Phys. JETP **23**, 592 (1966)].
Zapesochnyĭ, I. P., V. V. Sovter, O. B. Shpenik, and A. N. Zavilopulo, 1974, Dokl. Akad. Nauk SSSR **214**, 1288 [Sov. Phys. Dokl. **19**, 77 (1974)].
Zetner, P. W., W. B. Westerveld, G. C. King, and J. W. McConkey, 1986, J. Phys. B **19**, 4205.
Zollweg, R. J., 1969, J. Chem. Phys. **50**, 4251.
Zubek, M., and G. C. King, 1987, J. Phys. B **20**, 1135.
Zubek, M., and G. C. King, 1990, J. Phys. B **23**, 561.